JPSS SST Products

Alexander Ignatov, John Stroup, Yury Kihai, Xingming Liang, Boris Petrenko, Prasanjit Dash, Irina Gladkova, Marouan Bouali, Karlis Mikelsons, John Sapper, Feng Xu, Xinjia Zhou

NOAA; CIRA; GST Inc; CUNY

JPSS SST Team

Name	Affiliation	Funding	Tasks
Ignatov	STAR	NOAA	Lead, JPSS Algorithm & Cal/Val
Stroup, Kihai, Dash, Liang, Petrenko, Xu, Bouali, Zhou, Gladkova, Mikelsons	STAR/CIRA STAR/STG STAR/GST STAR/GST	JPO, NOAA ORS, GOES-R, NASA	Monitoring , VAL, comparison of SSTs (SQUAM), Radiances (MICROS), in Situ SSTs (*i*Quam) Users support; ~~IDPS SST code,~~ ACSPO code and products (L2, L3); Match ups w/iQuam; Destriping and other L1b fixes; Algorithms improvements: Clear-Sky Mask, SST
May, Cayula, McKenzie, Willis	NAVO	Navy, NJO	NAVO SEATEMP SST & Cal/Val VIIRS Cloud Mask evaluation in IDPS and comparisons with NAVO Cloud Mask
Minnett Kilpatrick	U. Miami	JPO, U. Miami	Uncertainty & instrument analyses; RTM; VAL vs. drifters & radiometers; skin to sub-skin conversion; high-latitude and full swath focus
Arnone Fargion	USM/NRL UCSD	NJO, USM	SST Algorithm Analyses, SST improvements at slant view zenith angles/swath edge; SST consistency from multiple passes
LeBorgne Roquet	Meteo France	EUMETSAT	Processing VIIRS and Cal/Val using O&SI SAF heritage; Comparisons with AVHRR/SEVIRI

Acknowledgements

- ACSPO Users
  - NOAA: CRW, NOS, CW, geo-polar blend, NCDC
  - (Inter)national Users – CMC, BoM, UK MO, JMA, DMII, JPL
- JPSS Program – Mitch Goldberg, Kathryn Schontz, Bill Sjoberg
- NASA SNPP Project Scientist – Jim Gleason
- NOAA NDE Team – Tom Schott, Dylan Powell, Bonnie Reed
- JPSS DPA – Eric Gottshall, Janna Feeley, Bruce Gunther
- VIIRS SDR & GSICS – Changyong Cao, Frank DeLuccia, Jack Xiong, Mark Liu, Fuzhong Weng
- NESDIS/STAR JPSS Team – Ivan Csiszar, Lihang Zhou, Paul DiGiacomo, many others
- NOAA CRTM Team – Yong Han, Yong Chen, Mark Liu

VIIRS SST Products

IDPS – NOAA Interface Data Processing Segment (IDPS)

- ✓ Official NPOESS SST EDR, Now owned by NOAA JPSS PO
- ✓ Developed by NGAS; Operational at Raytheon; archived at NOAA CLASS
- ✓ Jan 2014: JPO recommends to "discontinue the IDPS EDR, concentrate on ACSPO sustainment, development, and Cal/Val"
- ✓ IDPS will be phased out as soon as ACSPO SST is archived at JPL/NODC

ACSPO – NOAA Advanced Clear-Sky Processor for Ocean (ACSPO)

- ✓ NOAA heritage SST system
- ✓ Operational with global AVHRR 4km-GAC & 1km-FRAC
- ✓ Terra/Aqua MODIS & S-NPP VIIRS – experimental Jan'2012
- ✓ SNPP VIIRS – operational Mar 2014, GDS2 archival at JPL/NODC underway

NAVO – SEATEMP

- ✓ Builds on NAVO AVHRR & NOAA pre-ACSPO heritage
- ✓ Transitioned from NOAA to NAVO in 1994, "Shared Processing Agreement"
- ✓ Operational with S-NPP since Mar 2013
- ✓ GDS2 archived at JPL/NODC since May 2013

Objective & Methodology

- **Objective:** **Compare ACSPO and NAVO SSTs to advise users on the specifics of the two products**

- **Methodology:** **Compare ACSPO/NAVO SST domain & performance against two global reference SSTs**
  - **L4 SST (Canadian Met Centre CMC0.2 Analysis. Note that VIIRS data are not assimilated in CMC0.2)**
  - ***in situ* SST (QCed drifting buoys in iQuam *www.star.nesdis.noaa.gov/sod/sst/iquam/*)**

Data: one representative day of global data – 23 April 2014 – in SST Quality Monitor (SQUAM)
www.star.nesdis.noaa.gov/sod/sst/squam/

NIGHT: ACSPO L2 minus CMC L4
23 April 2014

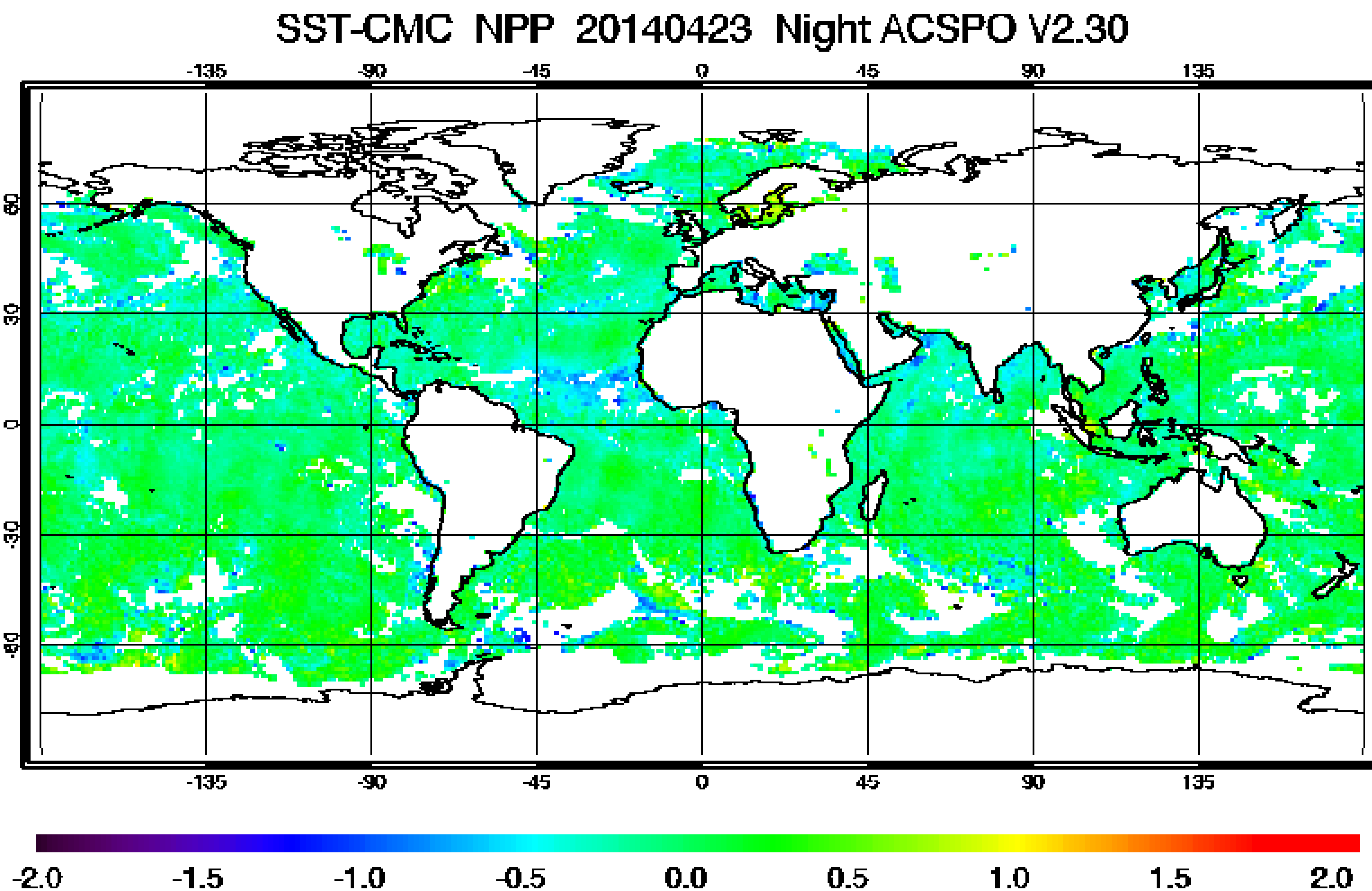

- ***Delta close to zero as expected***
- ***Cold spots – Residual Cloud/Aerosol leakages***

NIGHT: NAVO L2 minus OSTIA L4
23 April 2014

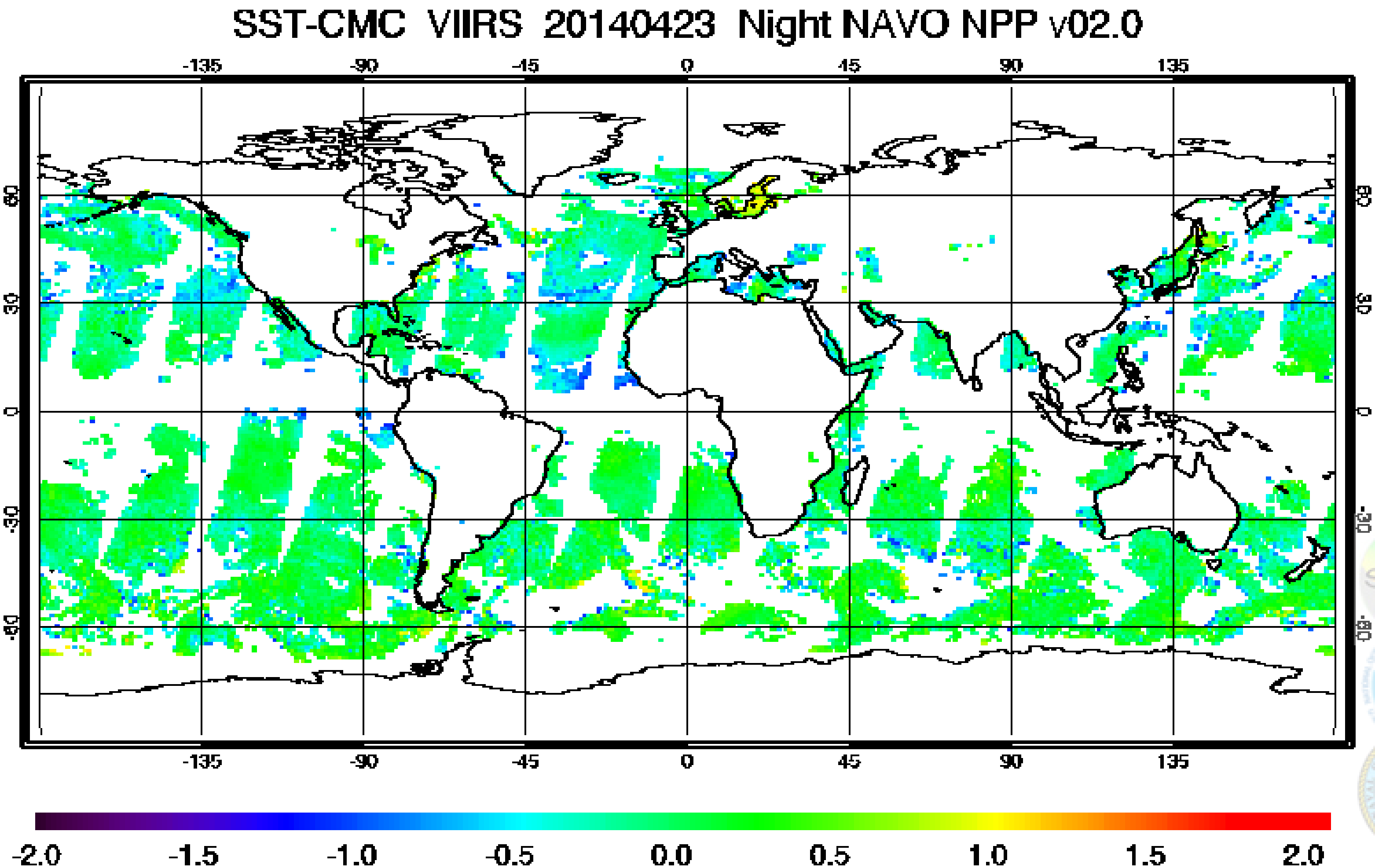

- ***Retrievals limited to VZA<54°***

NIGHT: ACSPO L2 minus CMC L4
23 April 2014

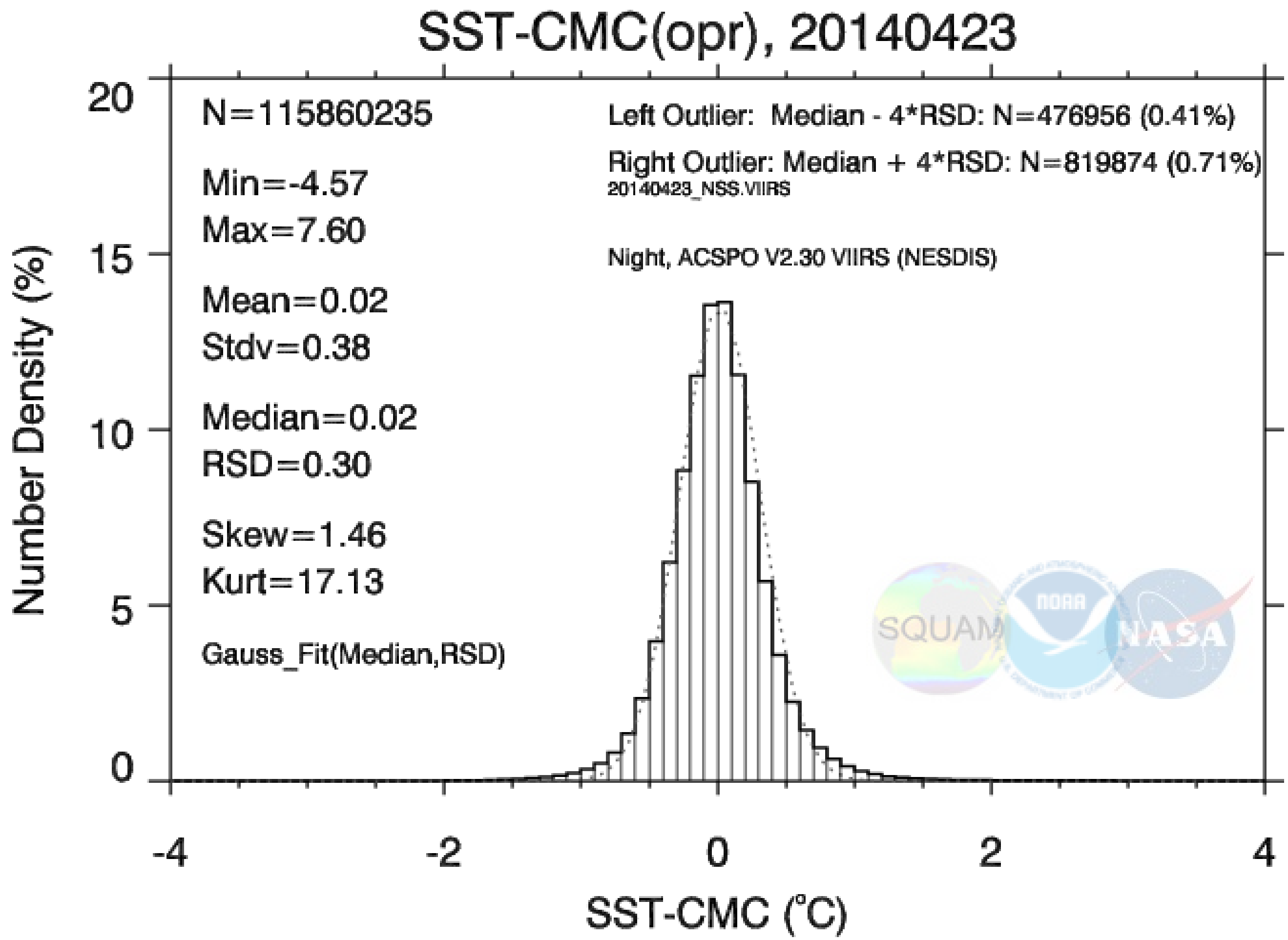

- ***Shape close to Gaussian***

NIGHT: NAVO L2 minus CMC L4
23 April 2014

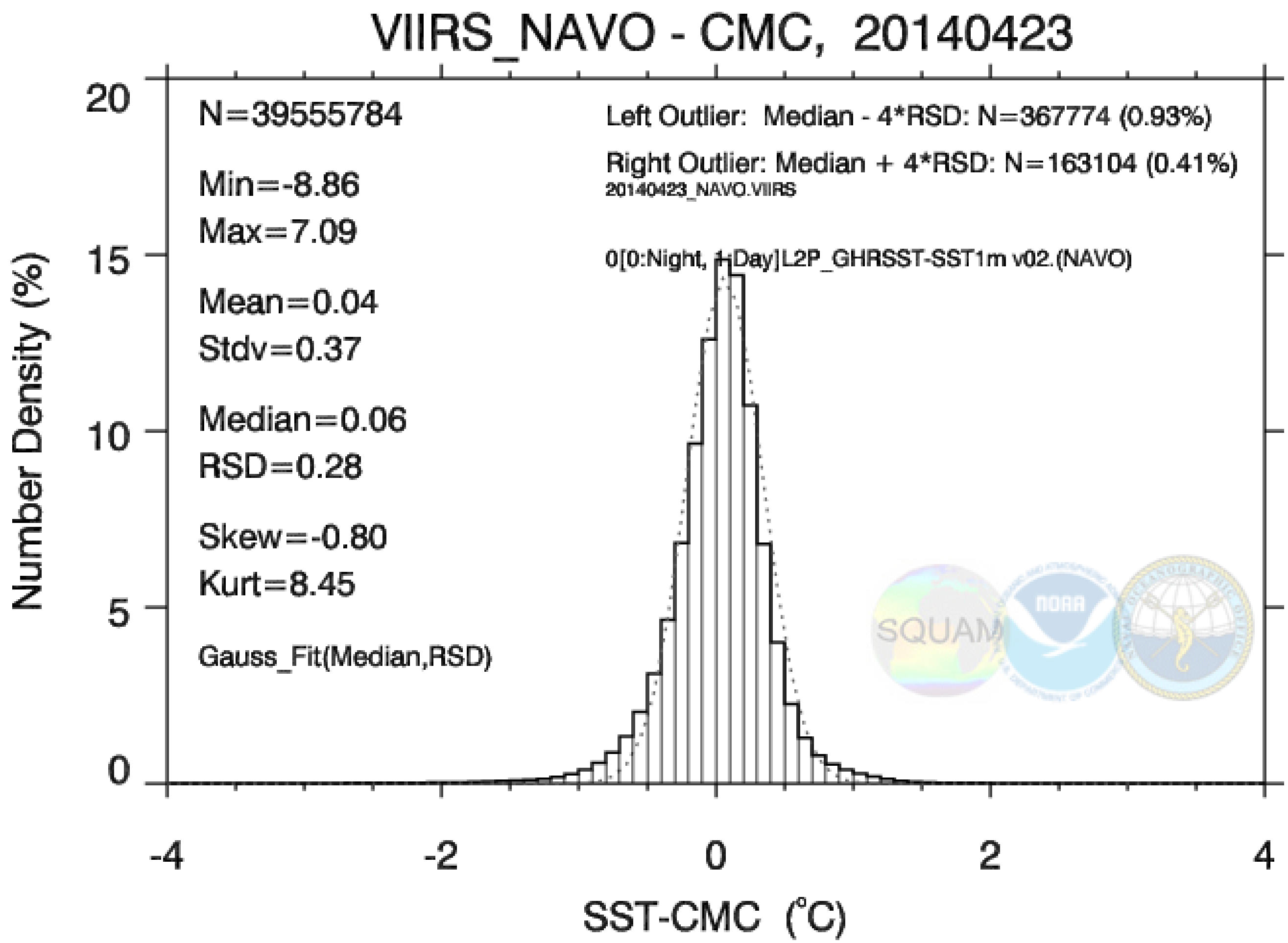

- ***Shape close to Gaussian***
- ***Domain smaller, STD slightly better***

NIGHT: ACSPO L2 minus *in situ* SST
23 April 2014

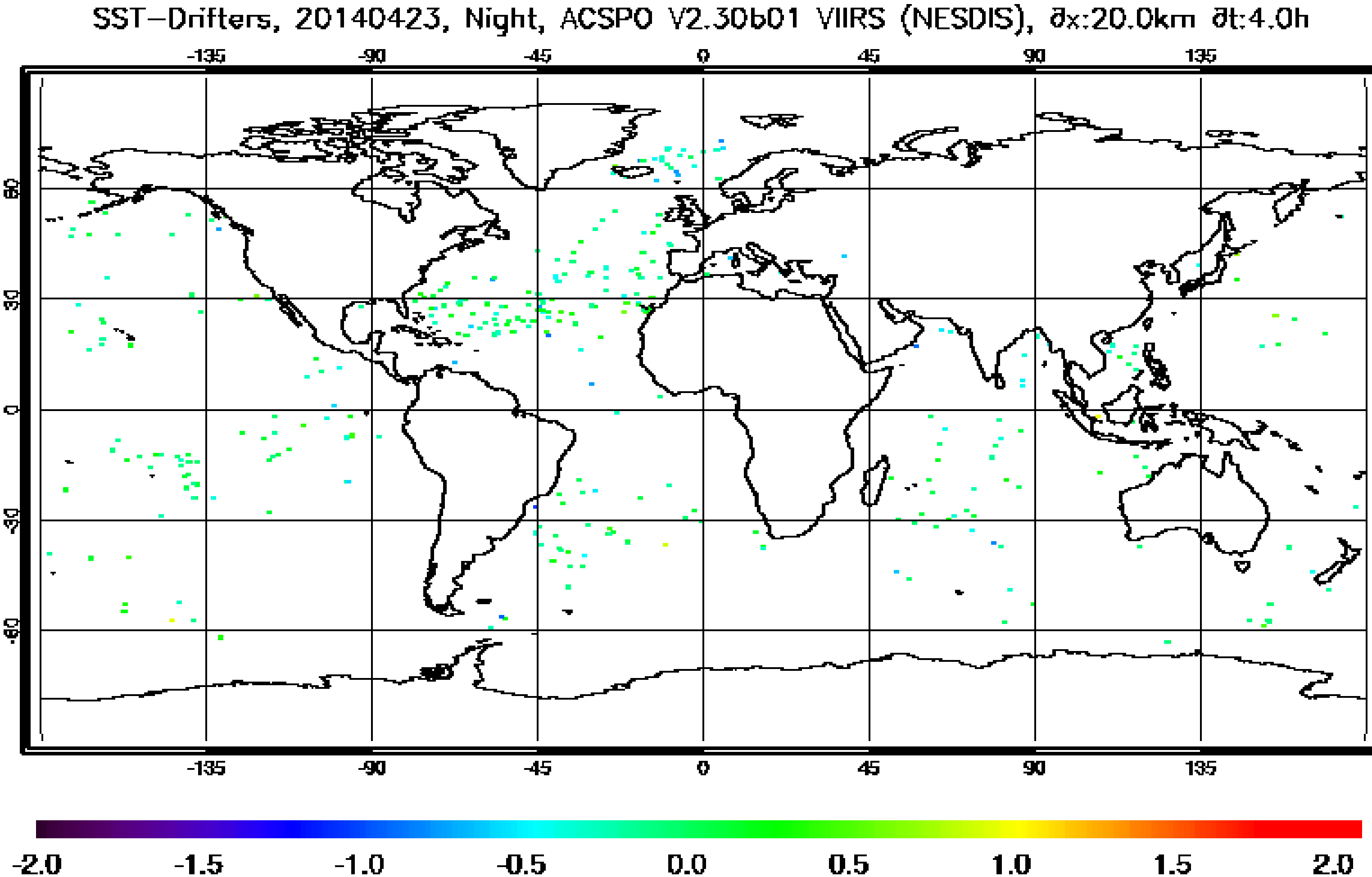

- ***Much sparser data coverage***
- ***Not fully representative of the globe***

NIGHT: NAVO L2 minus *in situ* SST
23 April 2014

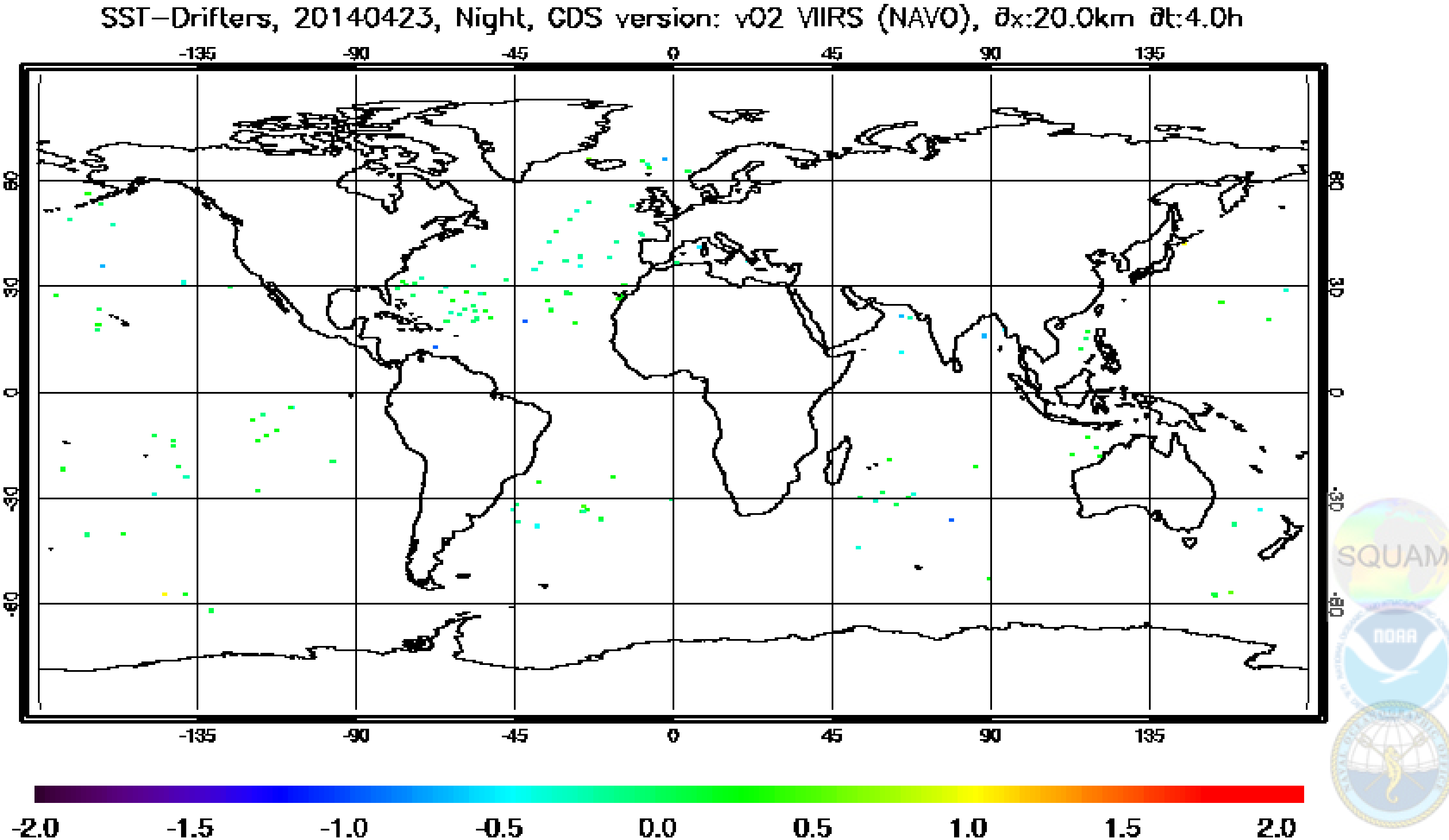

- ***Much sparser data coverage***
- ***Not fully representative of the globe***

NIGHT: ACSPO L2 minus *in situ* SST
23 April 2014

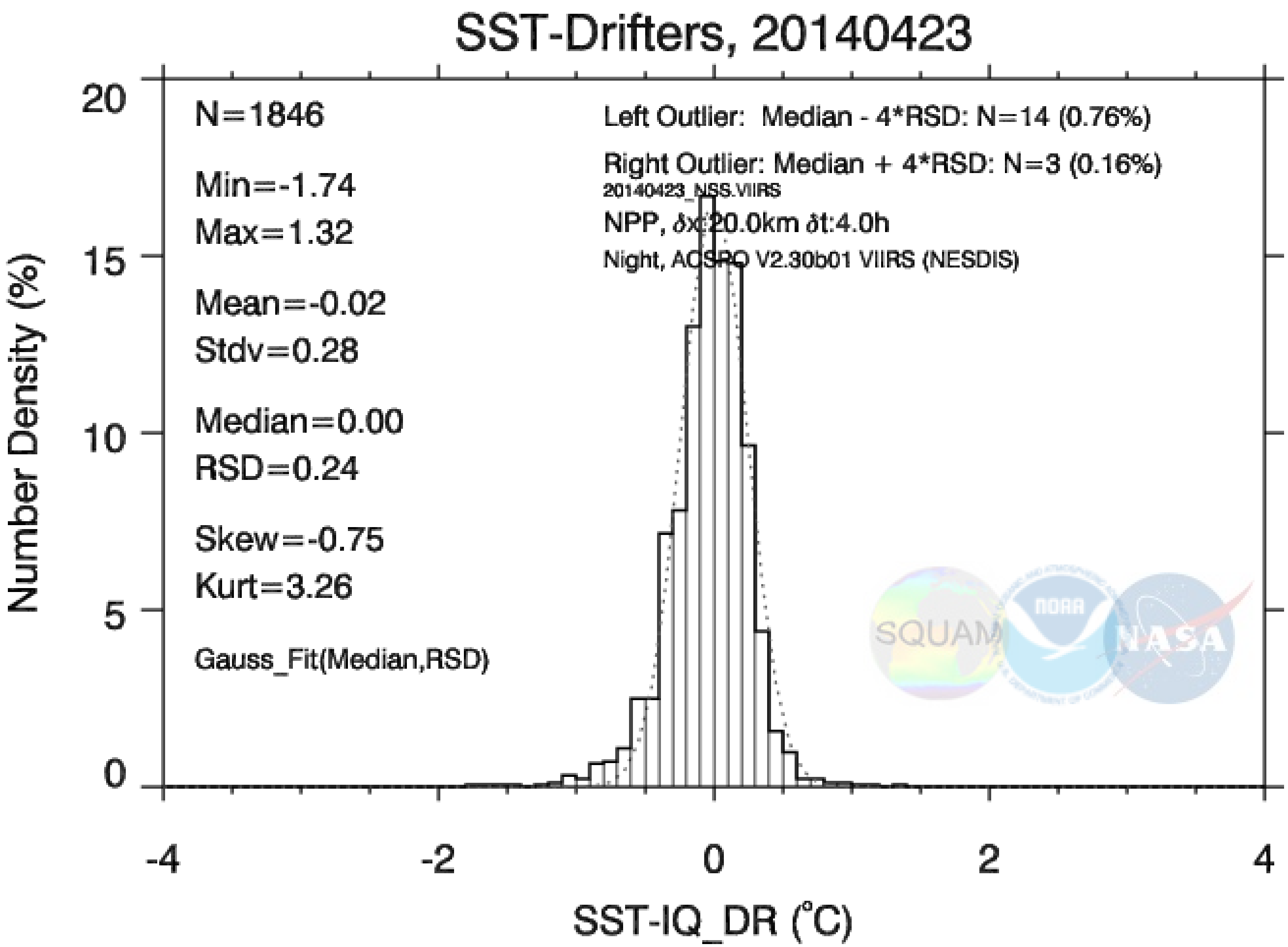

- ***Shape close to Gaussian – small cold tail***
- ***Performance Stats well within specs (Bias<0.2K, STD<0.6K)***

NIGHT: NAVO L2 minus *in situ* SST
23 April 2014

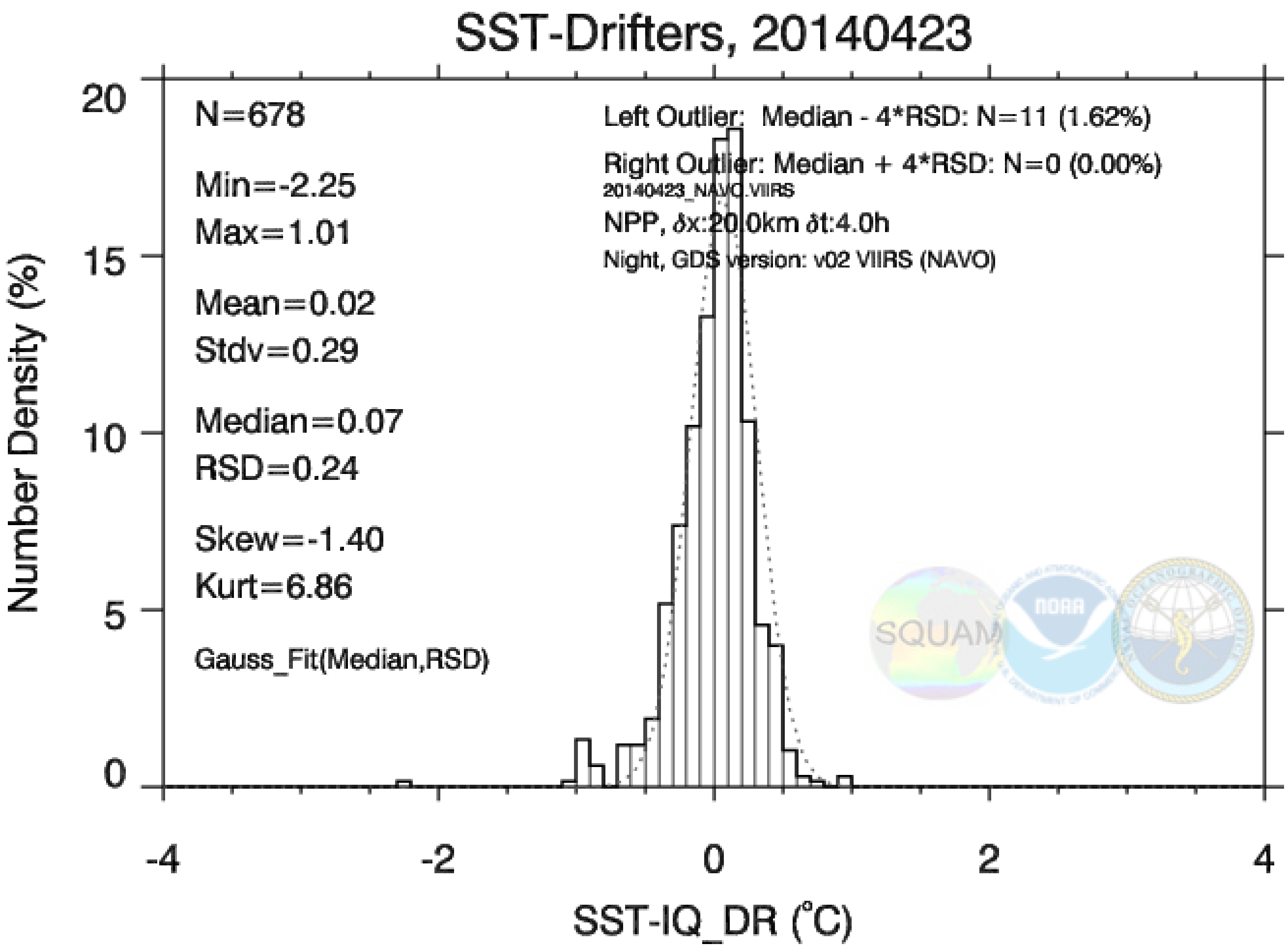

- ***Shape close to Gaussian – small cold tail***
- ***Performance Stats well within specs (Bias<0.2K, STD<0.6K)***

NIGHT – Summary

ΔT = "VIIRS minus CMC" SST (expected ~0)

	NOBS (%ACSPO)	Min/ Max	Mean/ STD	Med/ RSD
IDPS	116.8M (101%)	-13.1/+12.6	-0.04/0.46	-0.00/0.31
ACSPO	115.9M (100%)	- 4.6/+7.6	-0.02/0.38	-0.02/0.30
NAVO	39.5M (34%)	- 8.9/+7.1	+0.04/0.37	+0.06/0.28

- *IDPS: SST domain is +1% larger than ACSPO, All stats degraded*
- *NAVO: SST domain is factor of ×3 smaller than ACSPO, stats improved*

ΔT = "VIIRS minus in situ" SST (expected ~0)

	NOBS (%ACSPO)	Min/ Max	Mean/ STD	Med/ RSD
IDPS	2,082 (113%)	-2.9/+5.6	-0.06/0.43	-0.01/0.26
ACSPO	1,846 (100%)	-1.7/+1.3	-0.02/0.28	-0.00/0.24
NAVO	678 (37%)	-2.3/+1.0	+0.02/0.29	+0.07/0.24

- *IDPS: SST domain is +13% larger than ACSPO, All stats degraded*
- *NAVO: SST domain is factor of ×3 smaller than ACSPO, stats comparable*

DAY – Summary

ΔT = "VIIRS minus CMC" SST (expected ~0)

	NOBS (%ACSPO)	Min/ Max	Mean/ STD	Med/ RSD
IDPS	120.4M (100%)	- 28.7/+10.4	+0.20/0.77	+0.24/0.45
ACSPO	121.0M (100%)	- 5.4/+ 9.2	+0.29/0.59	+0.21/0.41
NAVO	41.3M (34%)	- 8.2/+ 7.5	+0.28/0.56	+0.22/0.40

- *IDPS: SST domain is comparable with ACSPO, All stats degraded*
- *NAVO: SST domain is factor of ×3 smaller than ACSPO, stats comparable*

ΔT = "VIIRS minus in situ" SST (expected ~0)

	NOBS (%ACSPO)	Min/ Max	Mean/ STD	Med/ RSD
IDPS	1,758 (105%)	-5.3/+2.7	-0.06/0.77	+0.10/0.48
ACSPO	1,680 (100%)	-1.4/+2.8	+0.07/0.42	+0.06/0.37
NAVO	510 (30%)	-1.2/+2.1	+0.12/0.35	+0.07/0.35

- *IDPS: SST domain is +5% larger than ACSPO, All stats degraded*
- *NAVO: SST domain is factor of ×3 smaller than ACSPO, stats improved*

ACSPO_V2.30b01_NPP_VIIRS_2014-01-18_1440-1450_20140314.174252_NAVO

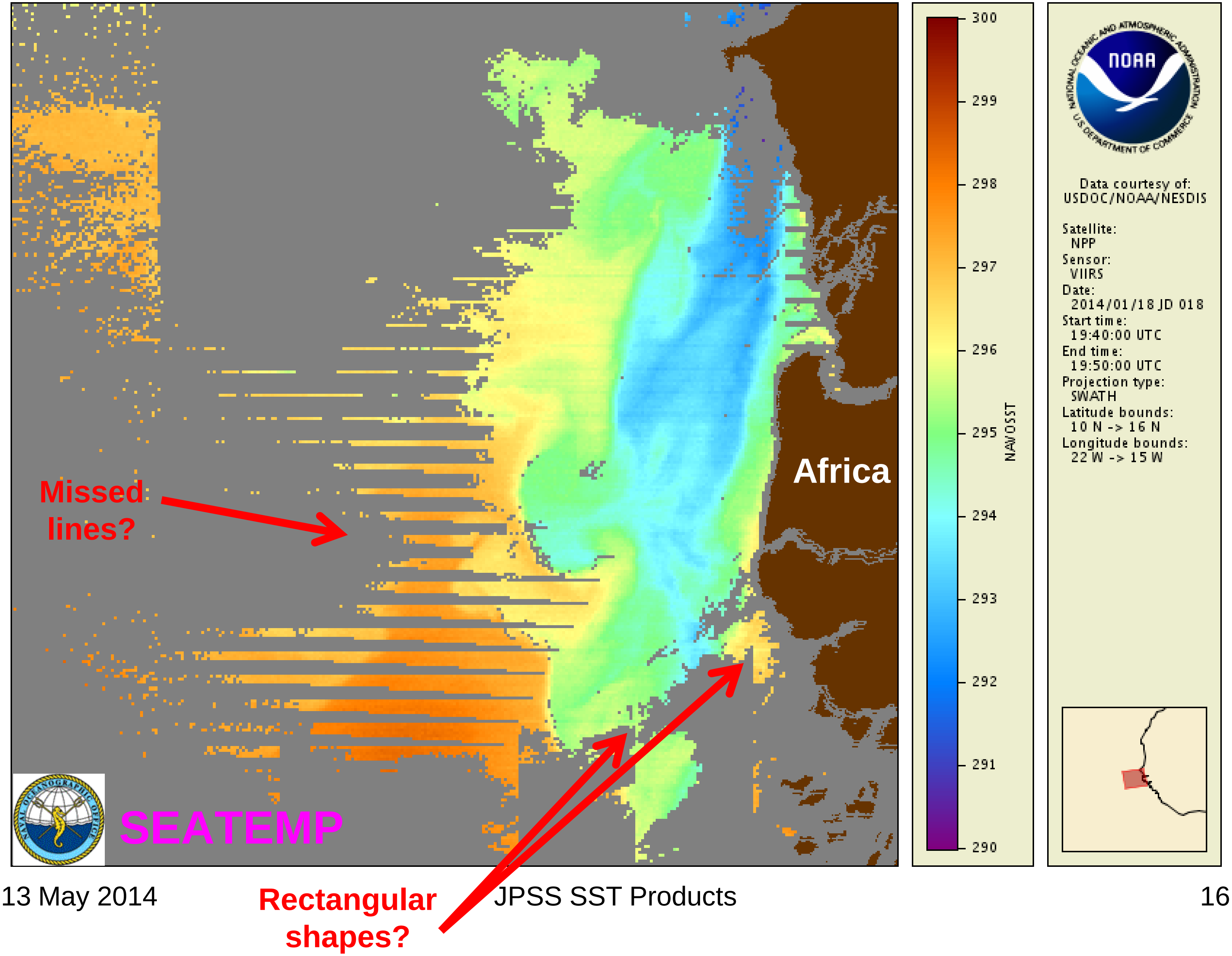

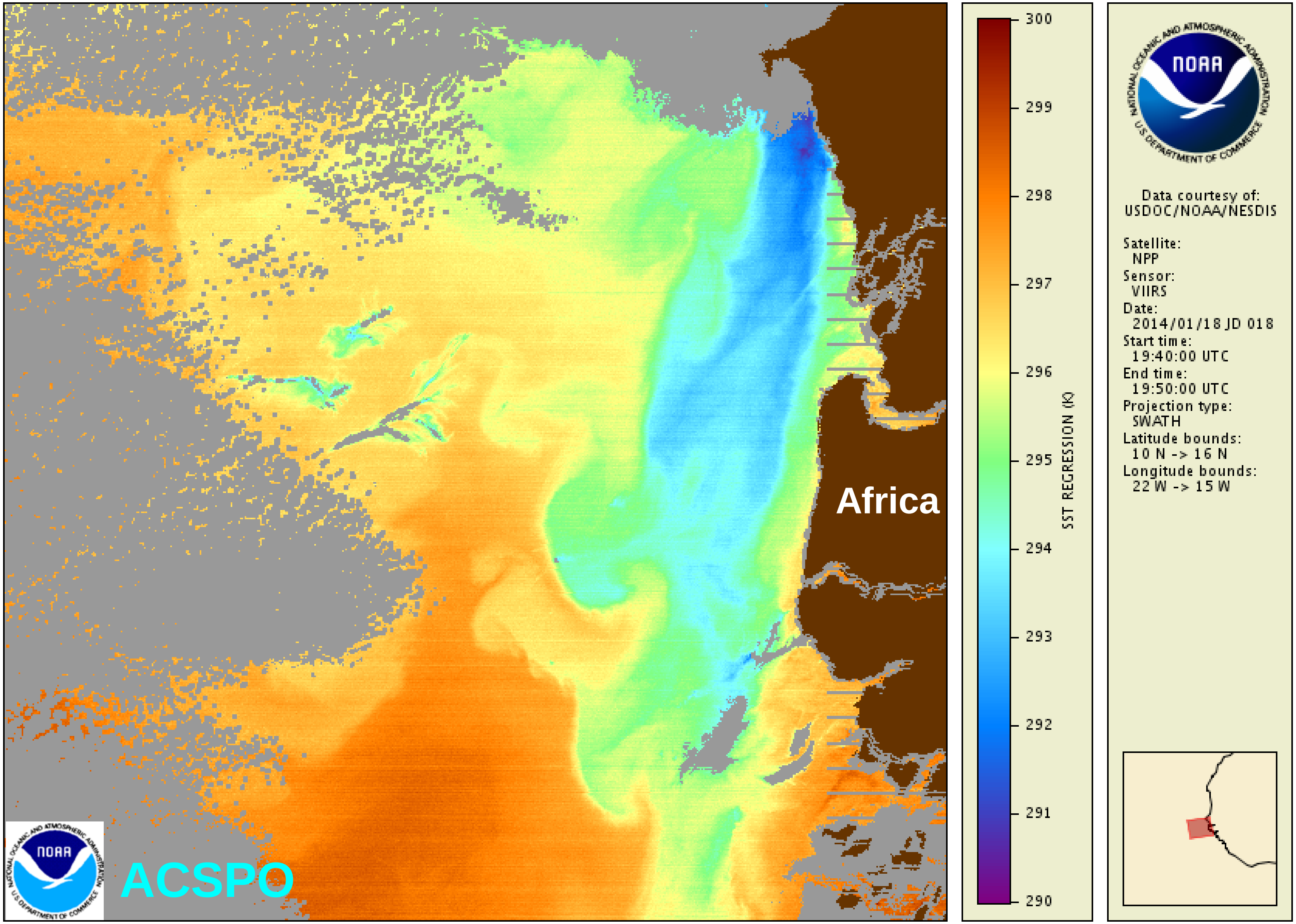

Africa
ACSPO
NOAA
300
299
298
297
296
295
294
293
292
291
290
SST REGRESSION (K)
Data courtesy of:
USDOC/NOAA/NESDIS
Satellite:
NPP
Sensor:
VIIRS
Date:
2014/01/18 JD 018
Start time:
19:40:00 UTC
End time:
19:50:00 UTC
Projection type:
SWATH
Latitude bounds:
10 N -> 16 N
Longitude bounds:
22 W -> 15 W

ACSPO_V2.30b01_NPP_VIIRS_2014-01-18_1810-1819_20140314.184153_NAVO

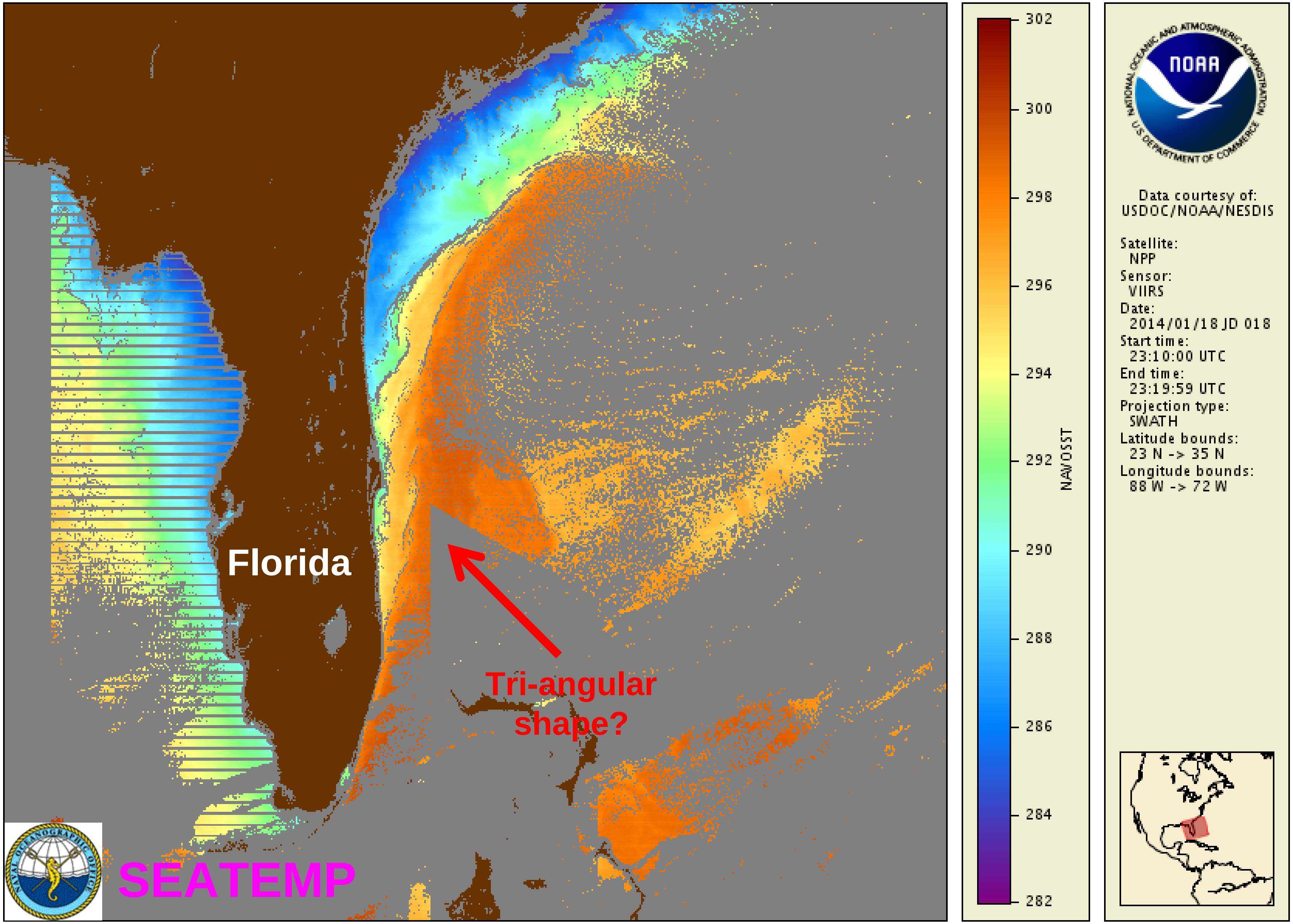

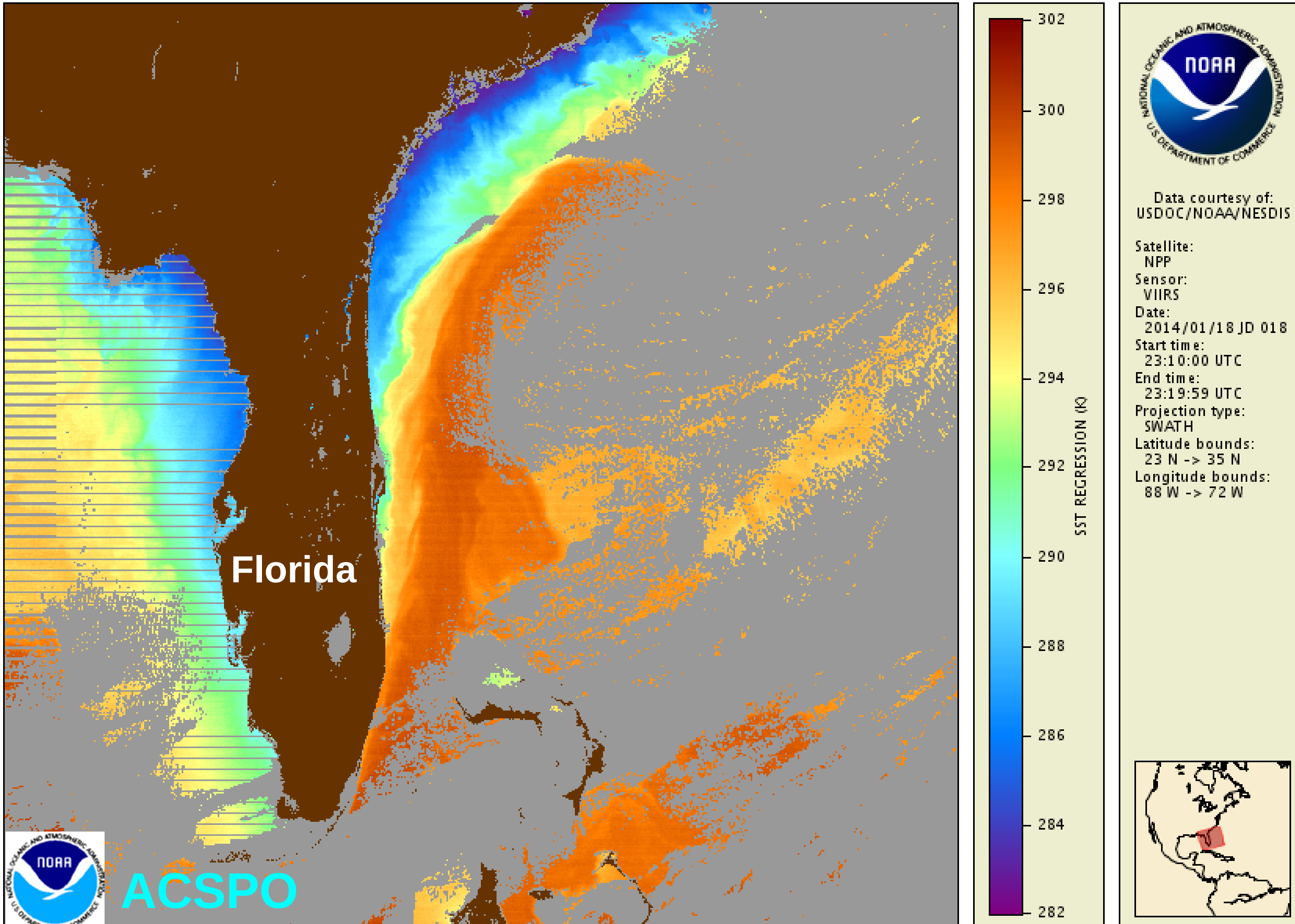
Florida
ACSPO
302
300
298
296
294
292
290
288
286
284
282
SST REGRESSION (K)
Data courtesy of:
USDOC/NOAA/NESDIS
Satellite:
NPP
Sensor:
VIIRS
Date:
2014/01/18 JD 018
Start time:
23:10:00 UTC
End time:
23:19:59 UTC
Projection type:
SWATH
Latitude bounds:
23 N -> 35 N
Longitude bounds:
88 W -> 72 W

ACSPO_V2.30b01_NPP_VIIRS_2014-01-18_2030-2039_20140314.192134_NAVO

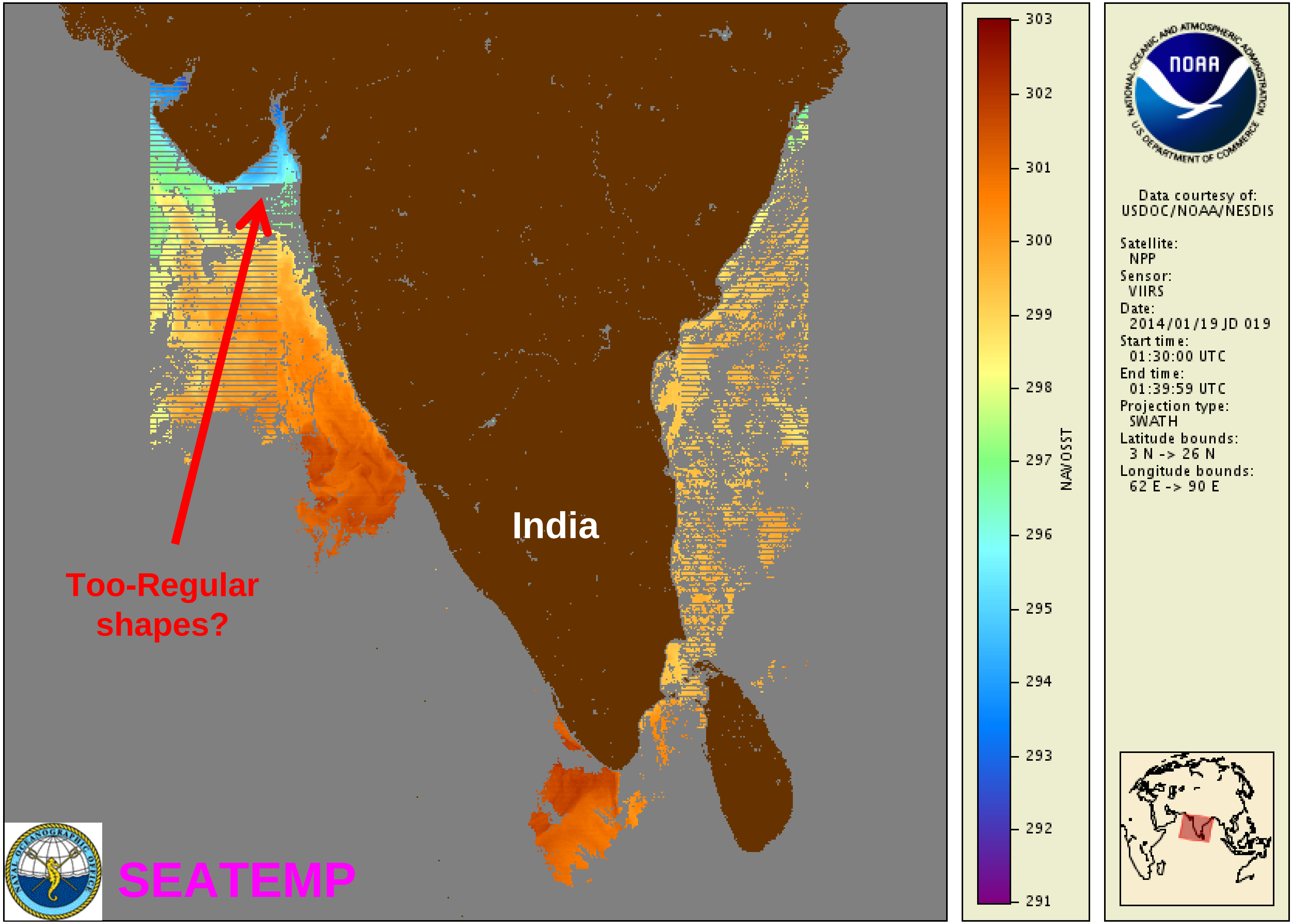

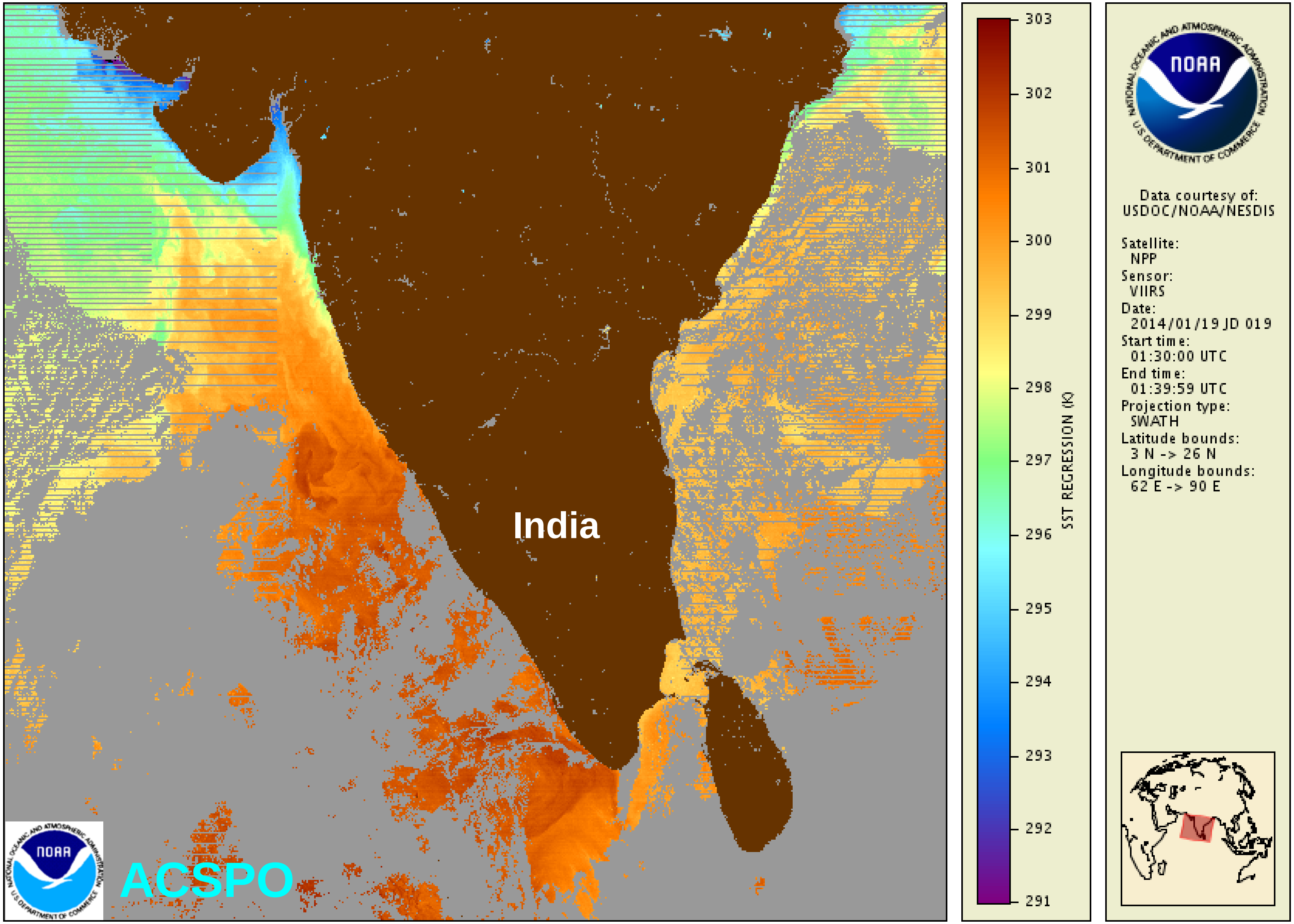
India
ACSPO
303
302
301
300
299
298
297
296
295
294
293
292
291
SST REGRESSION (K)
Data courtesy of:
USDOC/NOAA/NESDIS
Satellite:
NPP
Sensor:
VIIRS
Date:
2014/01/19 JD 019
Start time:
01:30:00 UTC
End time:
01:39:59 UTC
Projection type:
SWATH
Latitude bounds:
3 N -> 26 N
Longitude bounds:
62 E -> 90 E

ACSPO_V2.30b01_NPP_VIIRS_2014-01-18_0440-0450_20140314.145310_NAVO

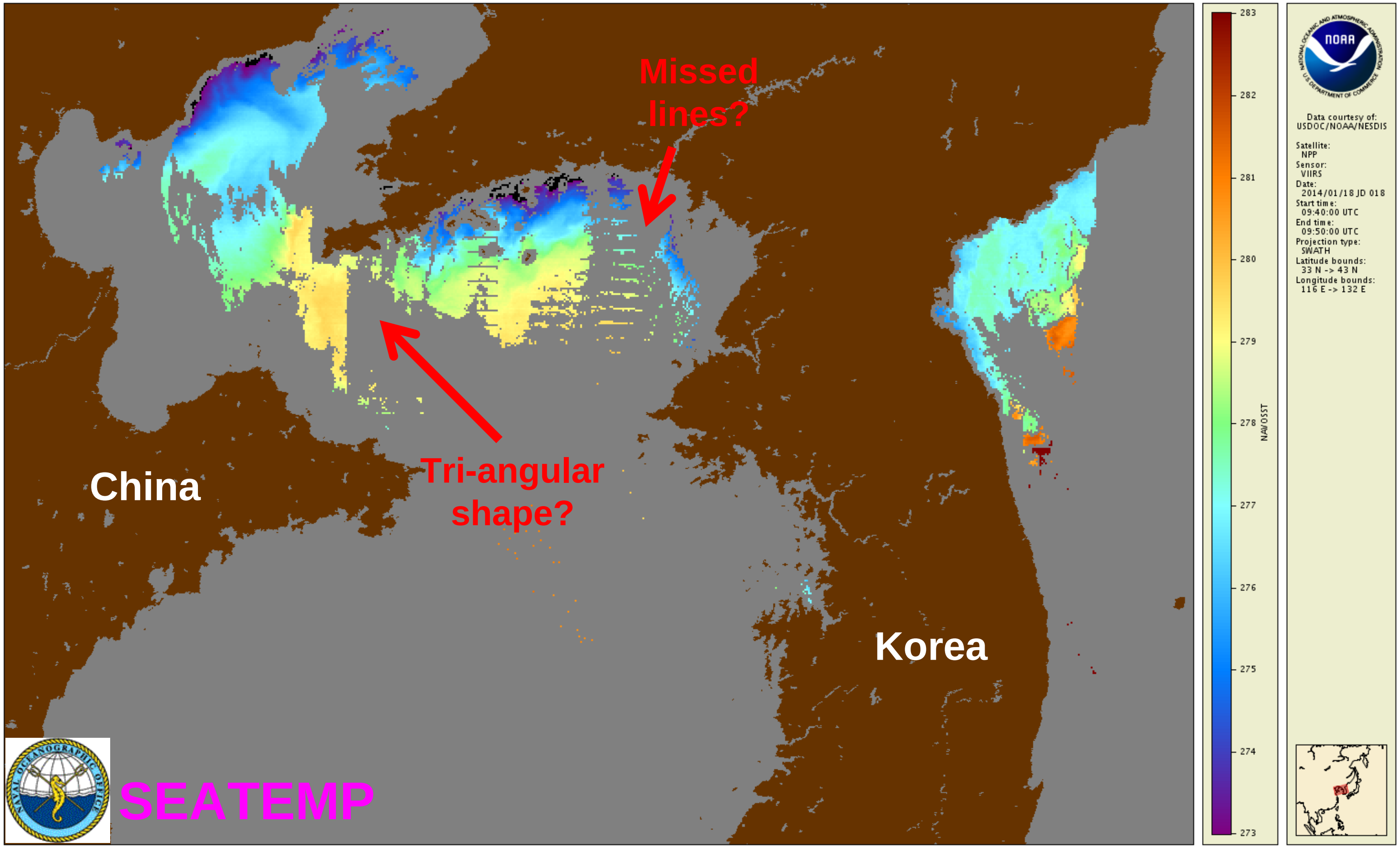

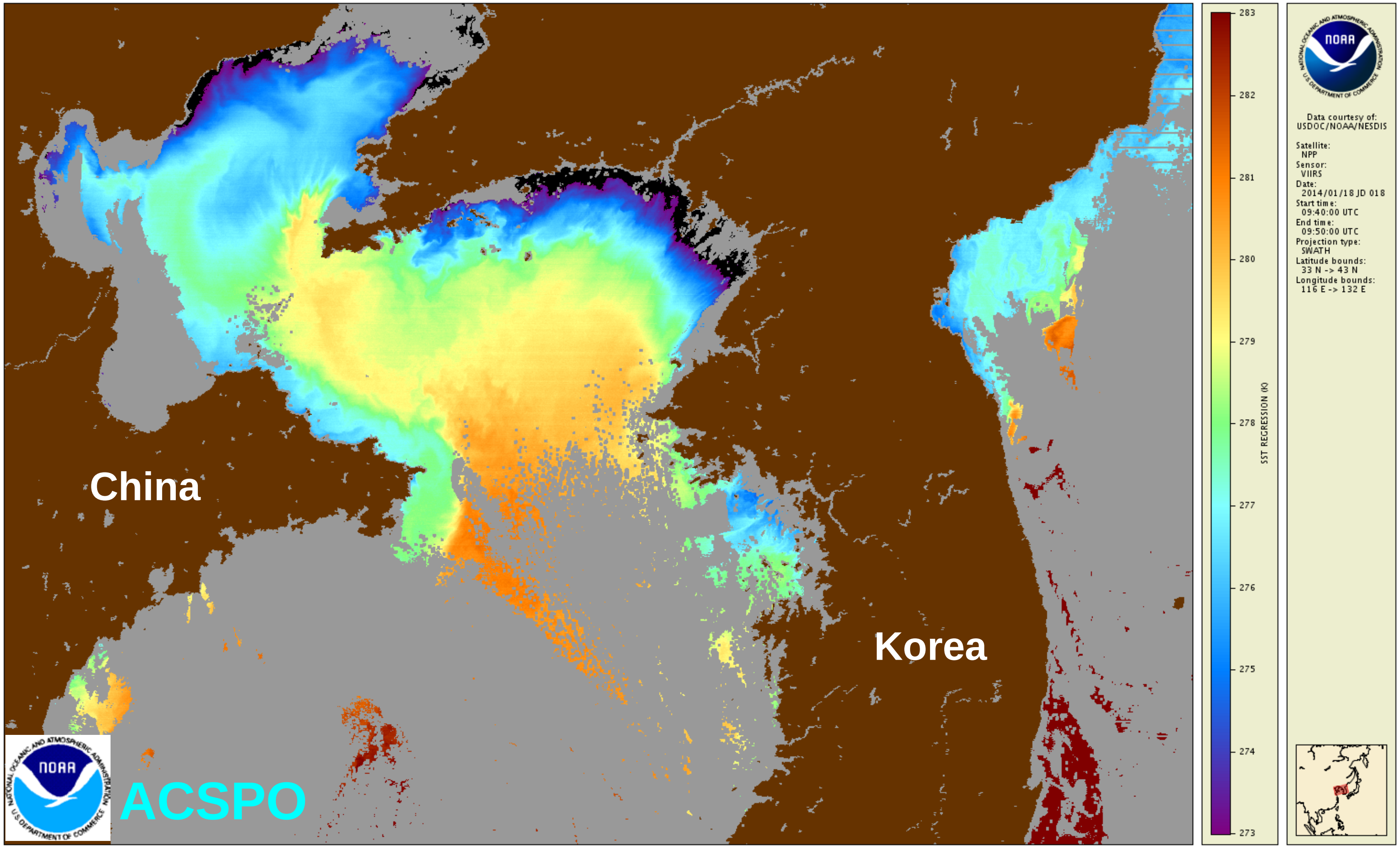
China
Korea
ACSPO
283
282
281
280
279
278
277
276
275
274
273
SST REGRESSION (K)
Data courtesy of:
USDOC/NOAA/NESDIS
Satellite:
NPP
Sensor:
VIIRS
Date:
2014/01/18 JD 018
Start time:
09:40:00 UTC
End time:
09:50:00 UTC
Projection type:
SWATH
Latitude bounds:
33 N -> 43 N
Longitude bounds:
116 E -> 132 E

Conclusion and Near-Future Work

ACSPO and NAVO are two VIIRS SST choices for users

- ✓ Both are GDS2, available (or shortly to be) via JPL/NODC
- ✓ ACSPO retrieval domain is larger than NAVO, by a factor of ~3, due to NAVO narrow swath VZA<54°, conservative cloud mask
- ✓ NAVO STDs are smaller than ACSPO by a narrow margin

Near-Term ACSPO tasks

- ✓ Work with users, solicit feedback, improve ACSPO
- ✓ Implement destriping operationally (Karlis Mikelsons)
- ✓ Pattern recognition ACSPO Clear-Sky Mask (Irina Gladkova)
- ✓ Focus on high-latitudes
- ✓ Focus on improved Quality Flags and Levels
- ✓ Generate L3 ACSPO product – many users requests
- ✓ Establish reprocessing and back-fill ACSPO VIIRS to Jan'2012

Environment Canada Environnement Canada

Canada

Some Early Results Assimilating ACSPO VIIRS L2P Datasets

Bruce Brasnett

Canadian Meteorological Centre

May, 2014

ACSPO VIIRS L2P Datasets

- Received courtesy of colleagues at STAR
- Two periods: 1 Jan. – 31 March, 2014 and 15 Aug. – 9 Sept. 2013
- Daily coverage is excellent with this product
- Experiments carried out assimilating VIIRS data only and VIIRS data in combination with other satellite products
- Rely on independent data from Argo floats to verify results
- Argo floats do not sample coastal regions or marginal seas

Coverage for 2014/02/01

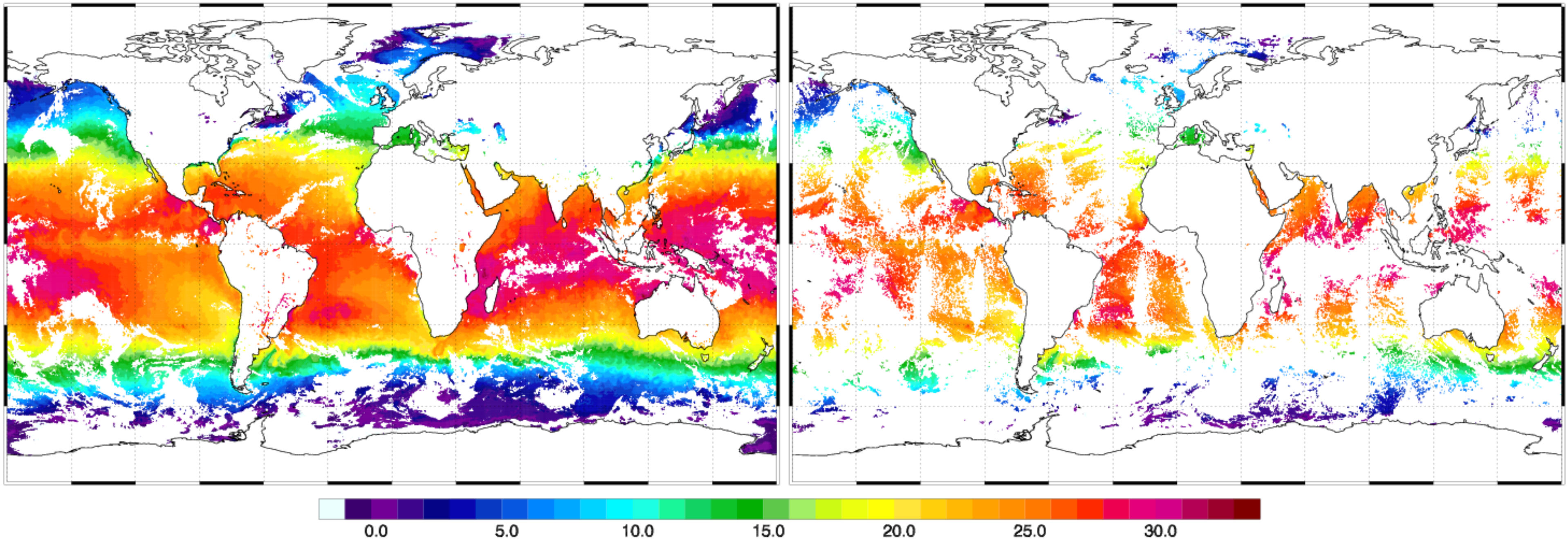

ACSPO VIIRS

NAVO AVHRR19

Coverage for 2013/09/01

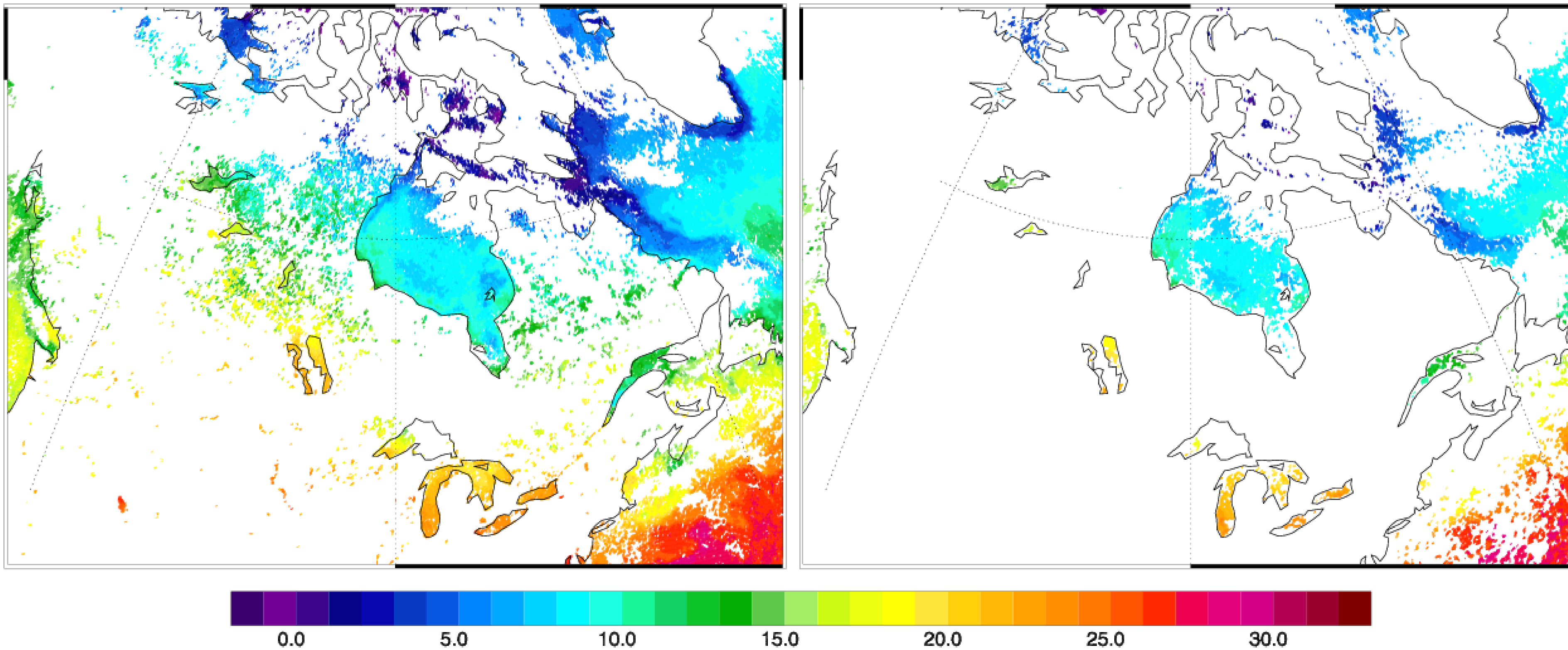

ACSPO VIIRS

NAVO AVHRR18 & 19
and Metop-A combined

Assessing utility of the ACSPO quality level flag

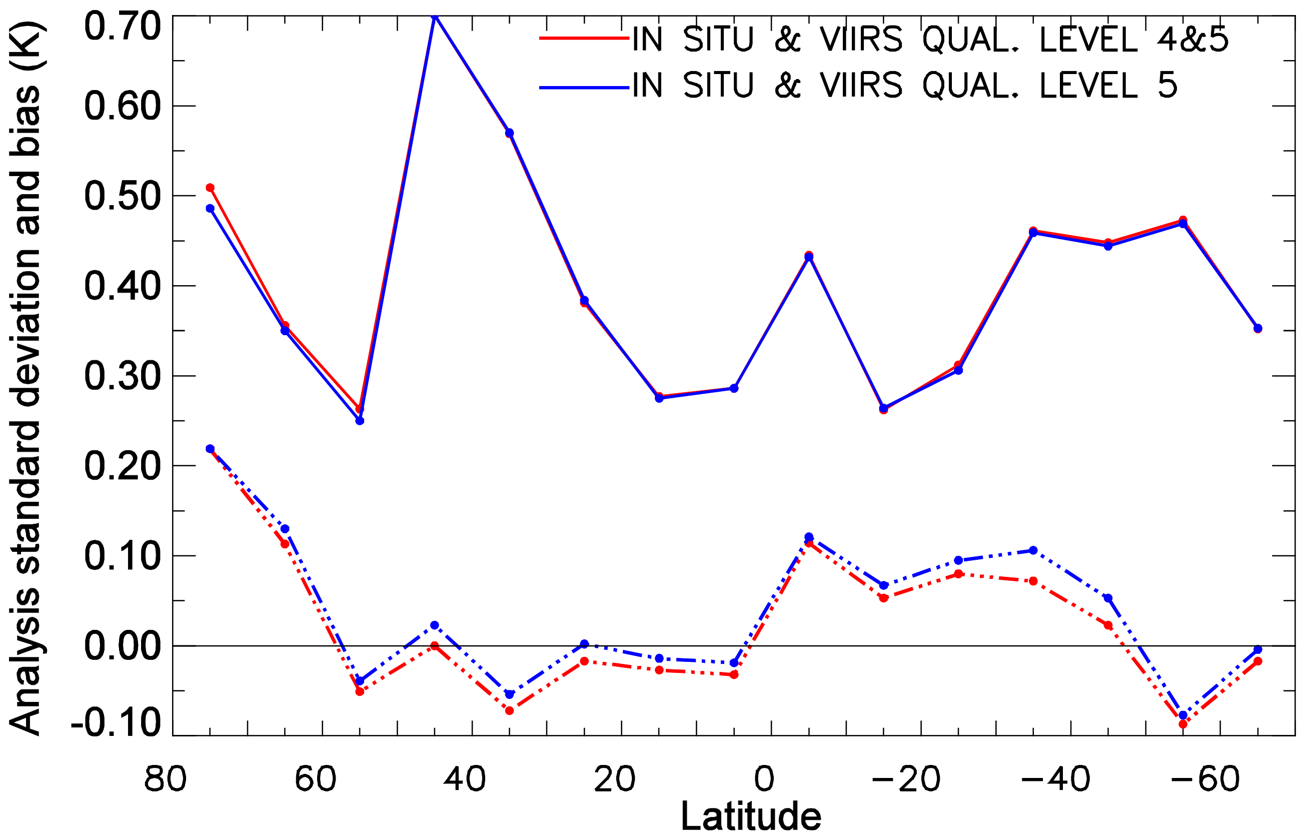

Including QL=4 leads to a small cold bias but does not affect the STD

Assessing utility of ACSPO SSES bias estimate

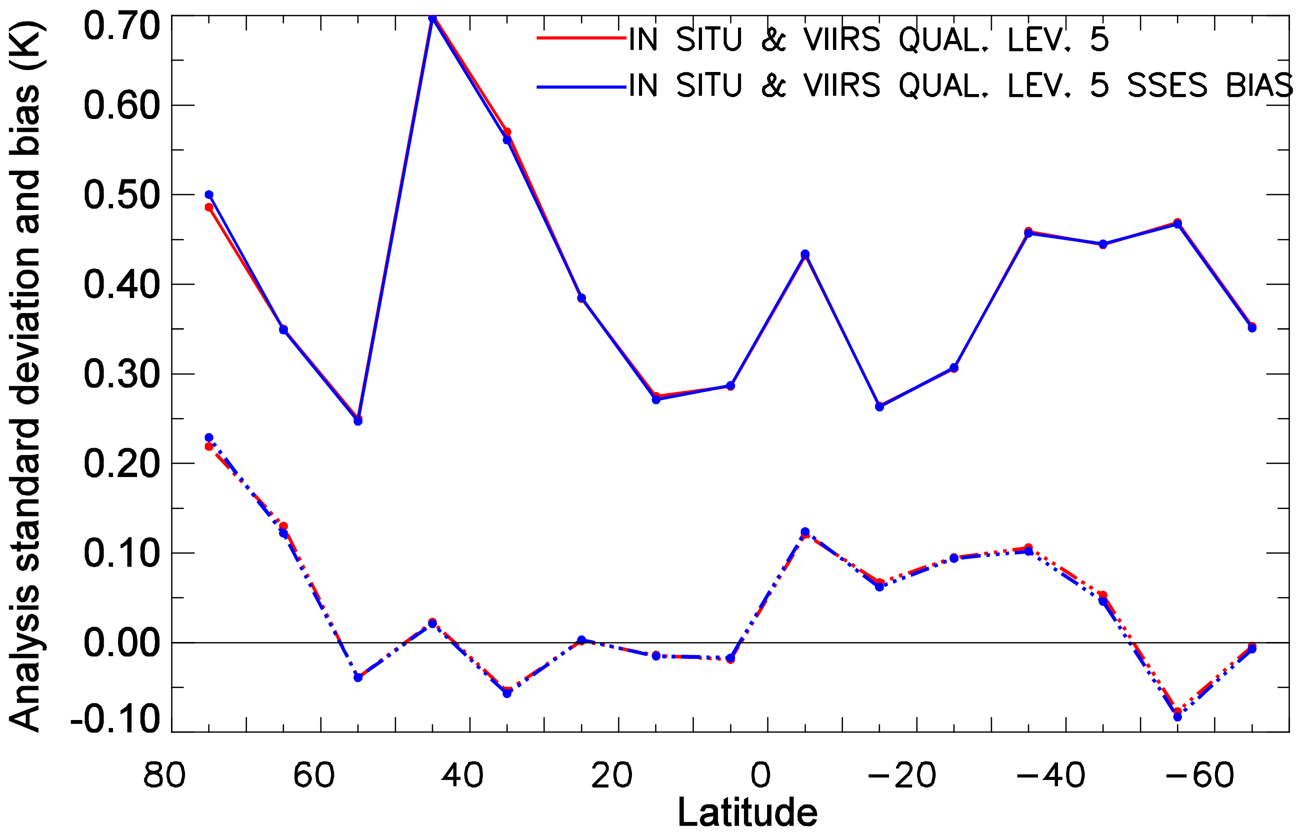

De-biasing VIIRS SST using ACSPO SSES bias does not affect assimilation

Assessing utility of screening daytime retrievals using L2P wind speeds

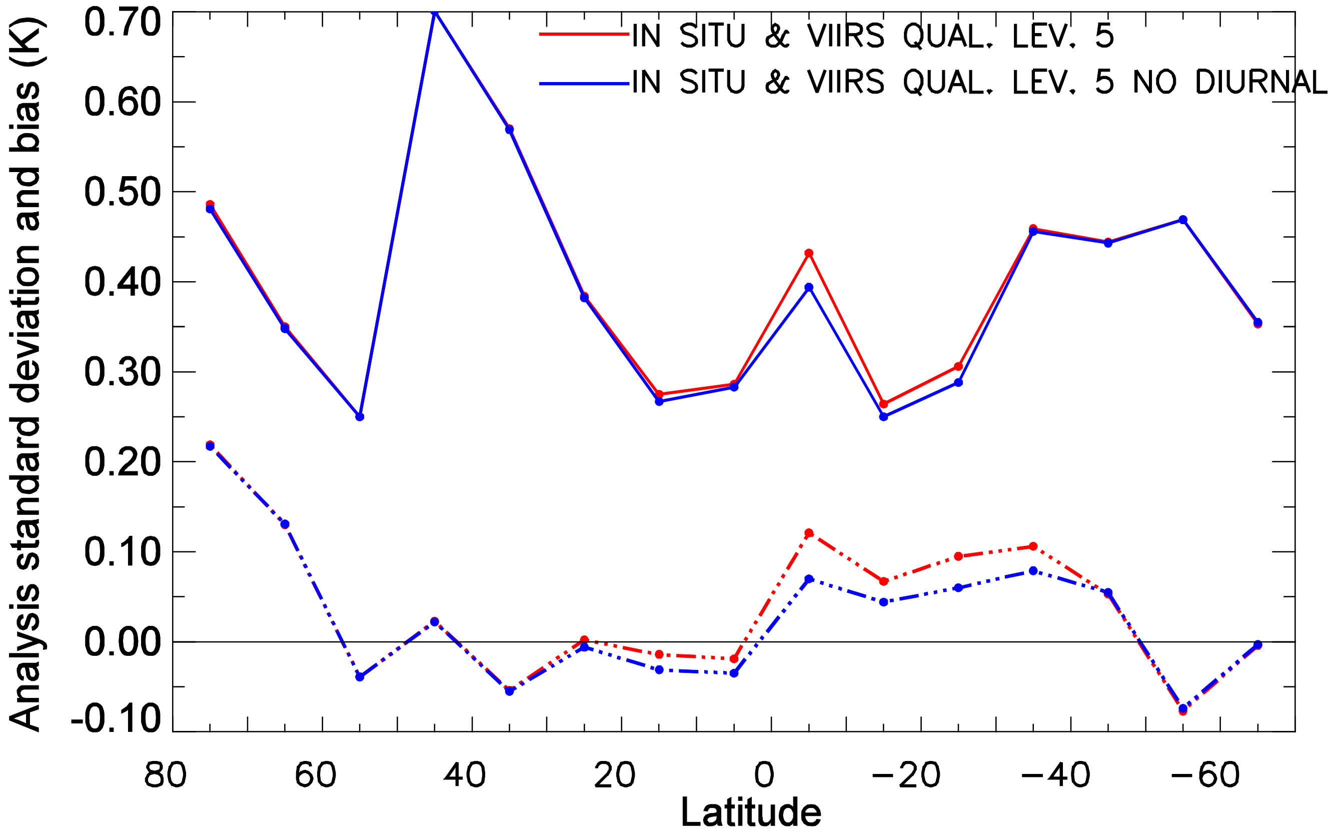

Using only daytime data with wind > 6m/s improves the assimilation

Assessing relative value of 2 VIIRS datasets: NAVO vs. ACSPO

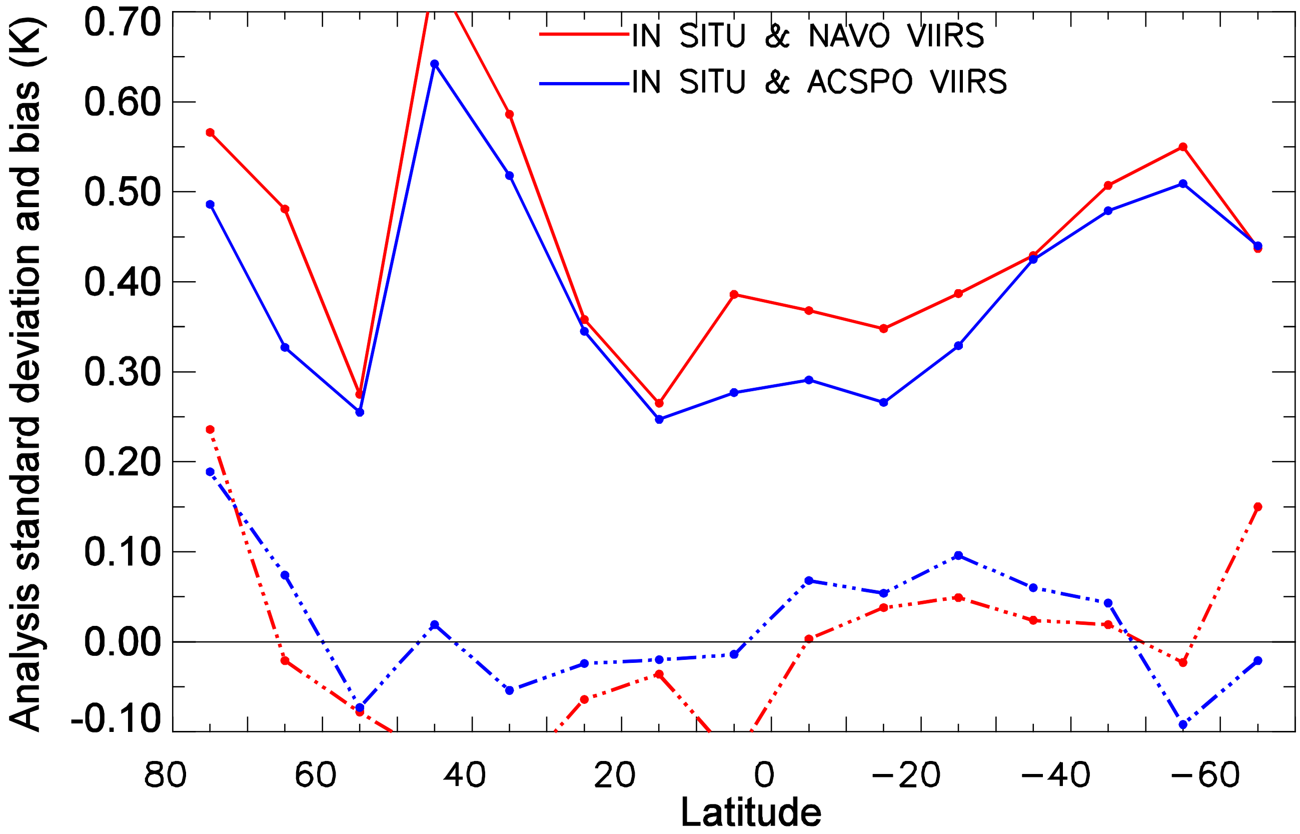

Using ACSPO instead of NAVO improves assimilation

Assessing the relative value of 3 datasets for January-March 2014

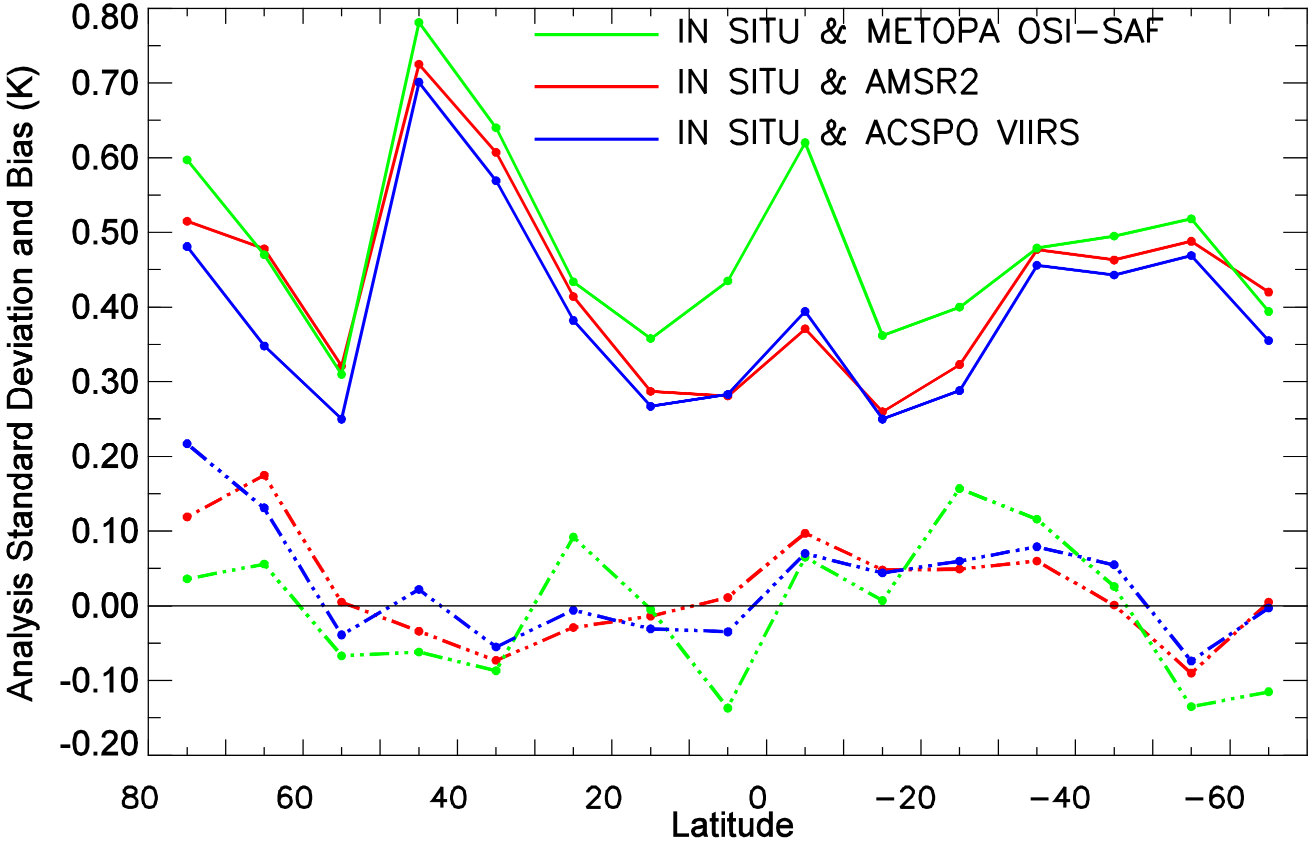

Using ACSPO improves STD in all LAT bands, except at 10°S

Assessing potential benefit of adding VIIRS to CMC analysis

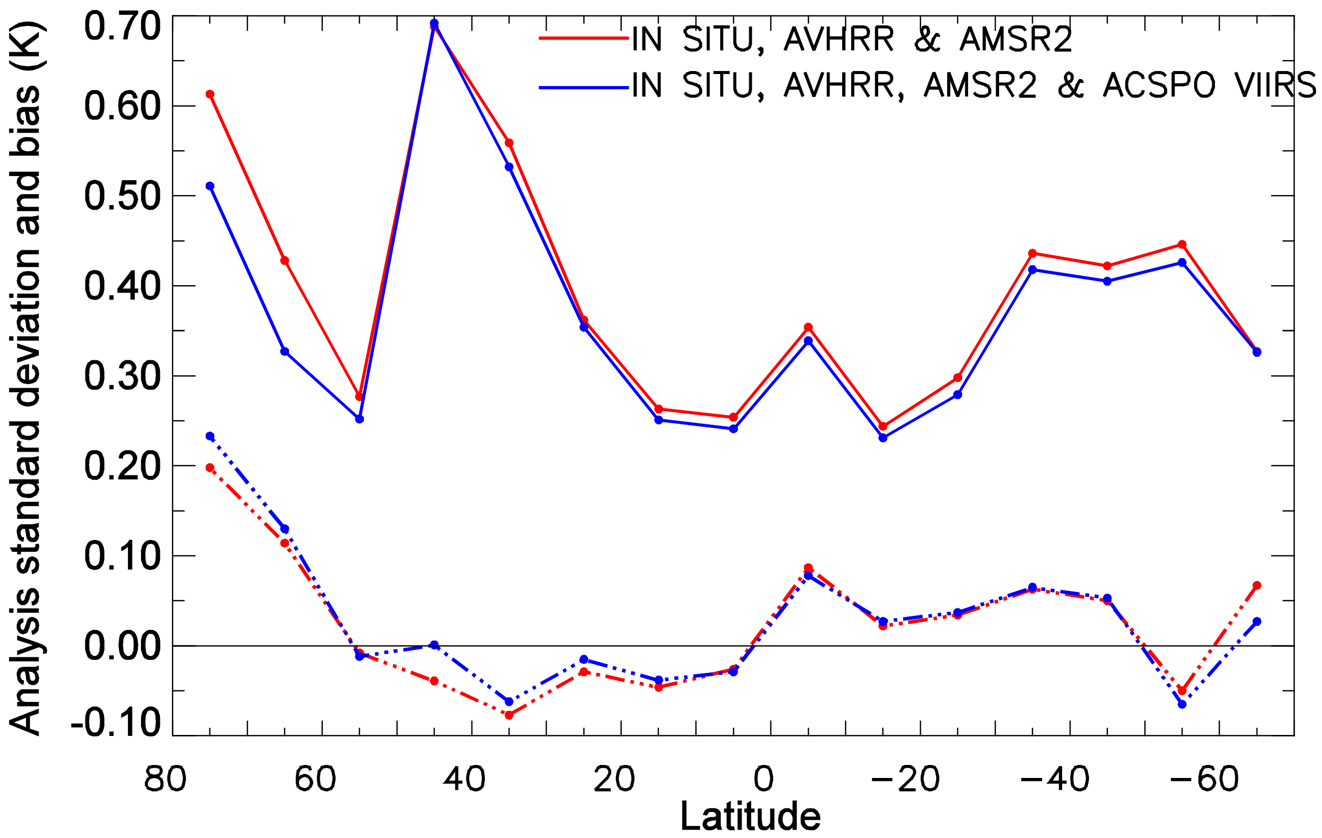

ACSPO improves assimilation in all LAT bands, except hi-lat North (high bias)

Summer Sample: Aug. 15- Sept. 9, 2013. VIIRS vs. NAVO AVHRR GAC

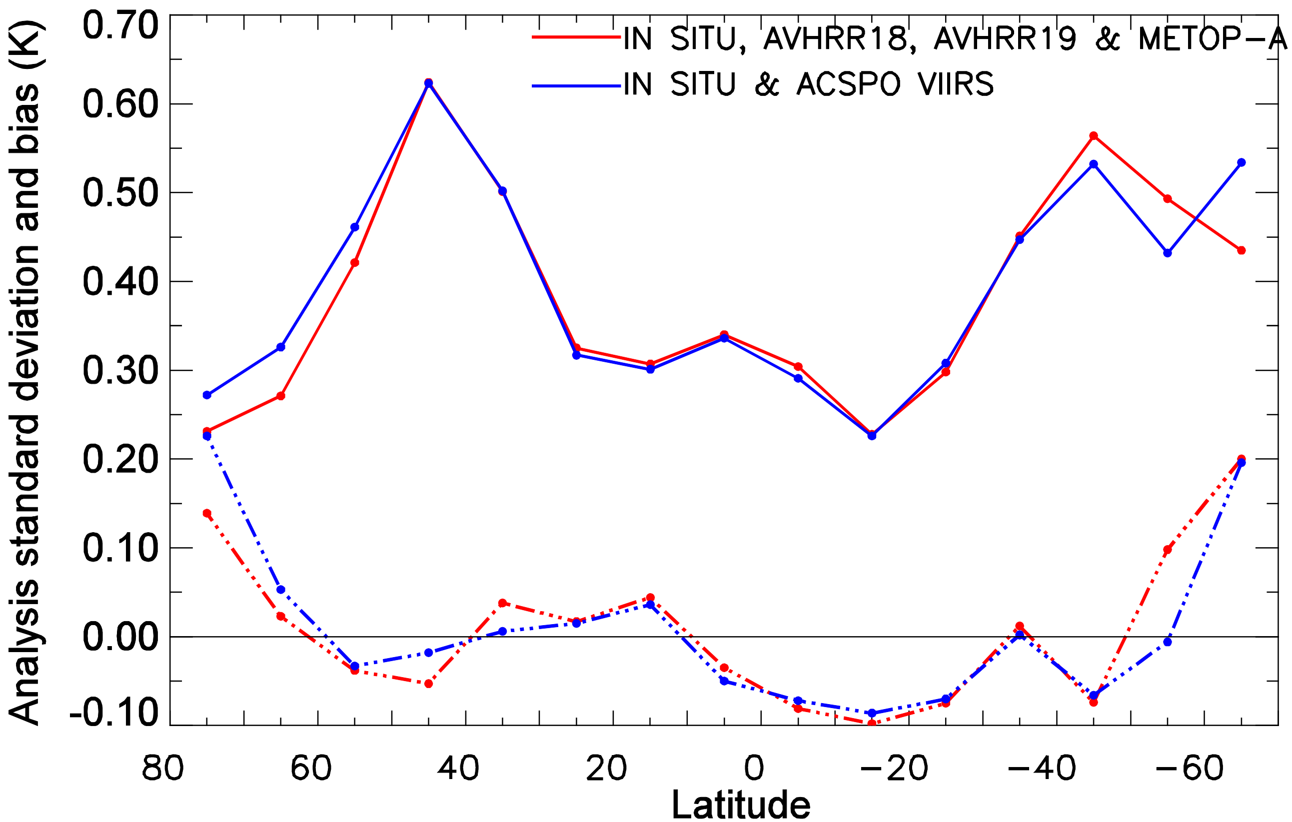

ACSPO VIIRS assimilation comparable to NAVO AVHRR, except at hi-lat

Summary

- ACSPO VIIRS L2P is an excellent product
- Based on the January – March sample, VIIRS contains more information than either the OSI-SAF MetOP-A or the RSS AMSR2 datasets
- L2P ancillary information: quality level flags and wind speeds are useful but experiment with SSES bias estimates was inconclusive
- Current plan at CMC is to assimilate ACSPO VIIRS L2P dataset when it becomes available

Assimilation of VIIRS SSTs and Radiances into Level 4 Analyses

Andy Harris
CICS/ESSIC/UMD
301-683-3349 Andy.Harris@noaa.gov
Jon Mittaz (UMD)
Robert Grumbine (NCEP/EMC/MMAB)
Mark Eakin (NOAA CRW)
Eileen Maturi (NESDIS/STAR)

5-km Blended SST Analysis

- **Produced daily from 24 hours of AVHRR & Geo-SST**
  - NOAA-19, MetOp-A (about to switch to MetOp-B)
  - GOES-E/W Imager
  - MTSAT-2 Imager
  - Meteosat-10 SEVIRI
  - VIIRS
  - [AMSR-2]
  - **Does not use buoy data**
- Multi-scale OI
  - Mimics Kalman Filter **(***Khellah et. al., 2005***)**
- **3 stationary priors**
  - Short, intermediate and long correlation lengths
  - Mimic non-stationary prior while preserving rigor
  - Interpolation of resultant analyses based data density
    - ➢ **Allows fine resolution where possible without introducing noise**

Separate Ocean Basins

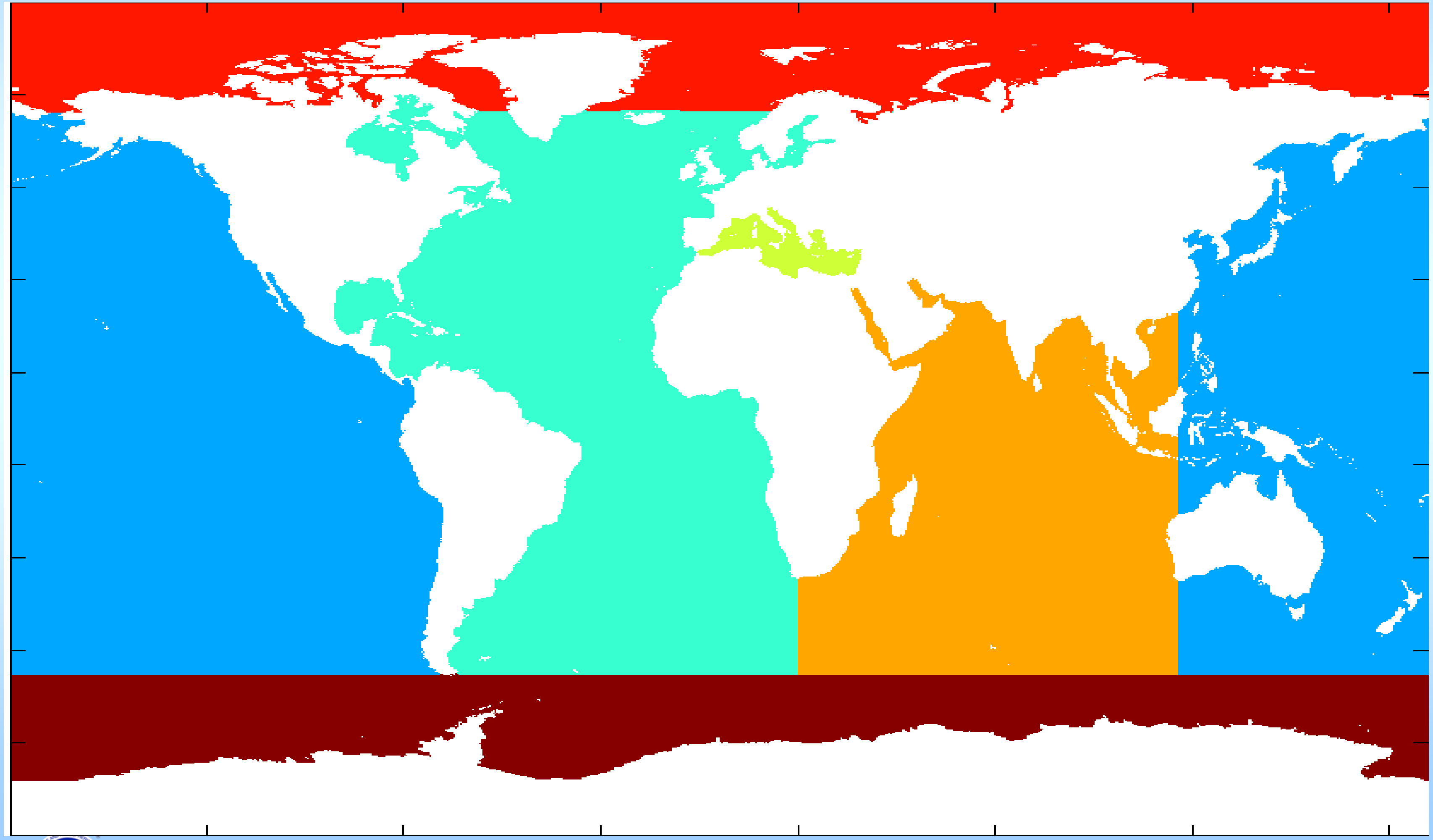

Data Coverage

Geostationary SST

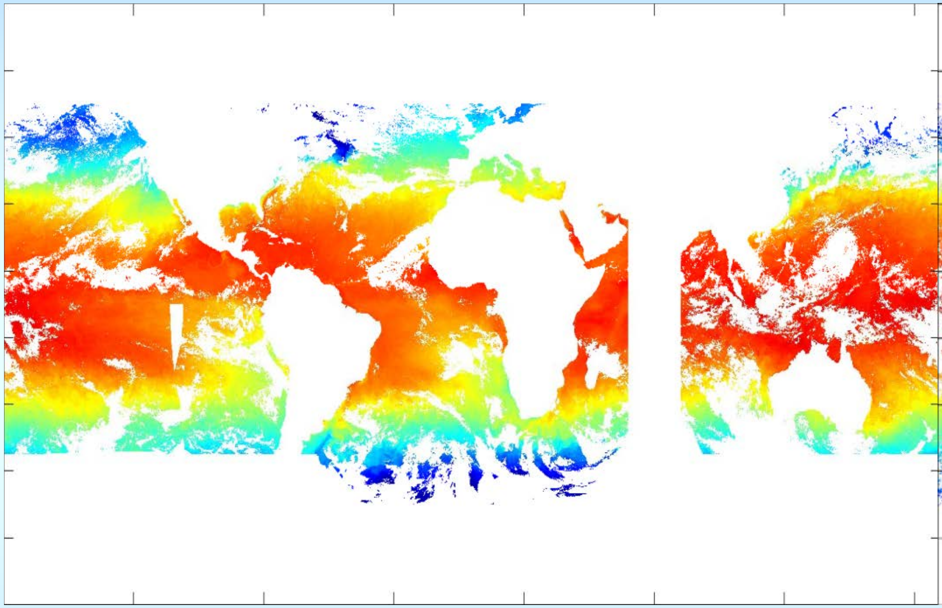

Polar-Orbiter SST

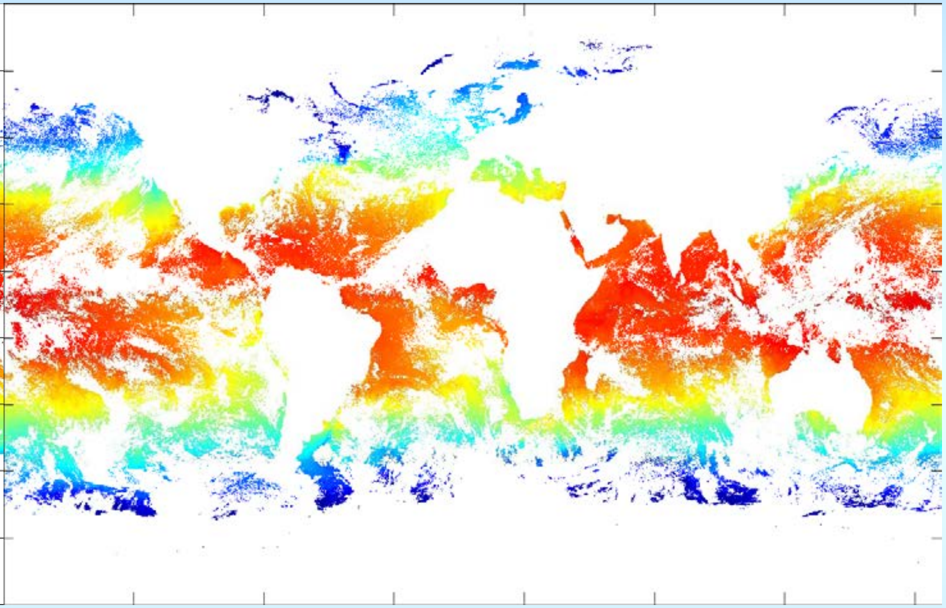

- **Geostationary data in particular provide lots of observations**
  - N.B. gap in coverage in Indian Ocean
- **Data-driven analysis**
  - Need to treat the input data “carefully”

Resolution difference

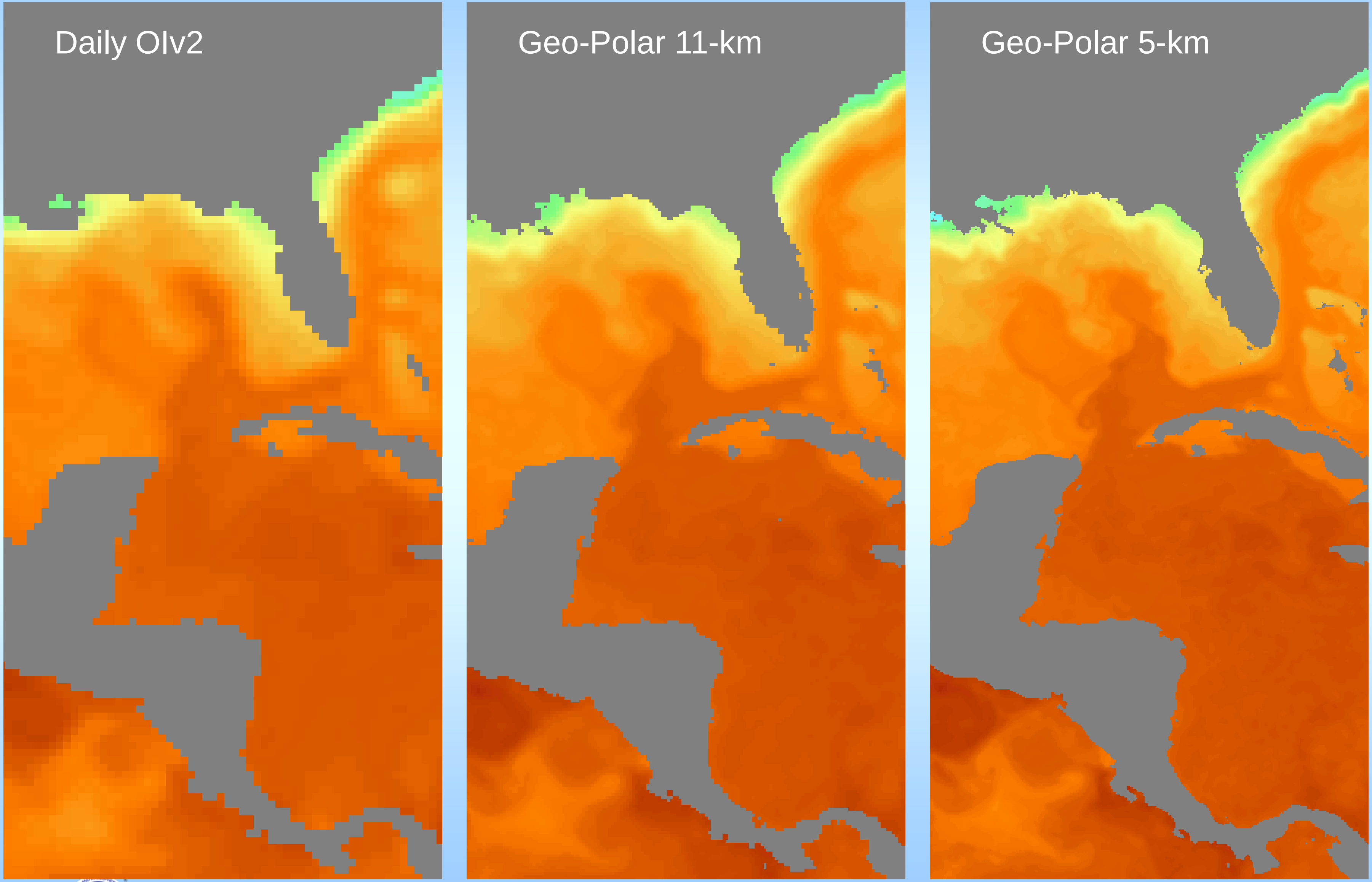

5-km Examples

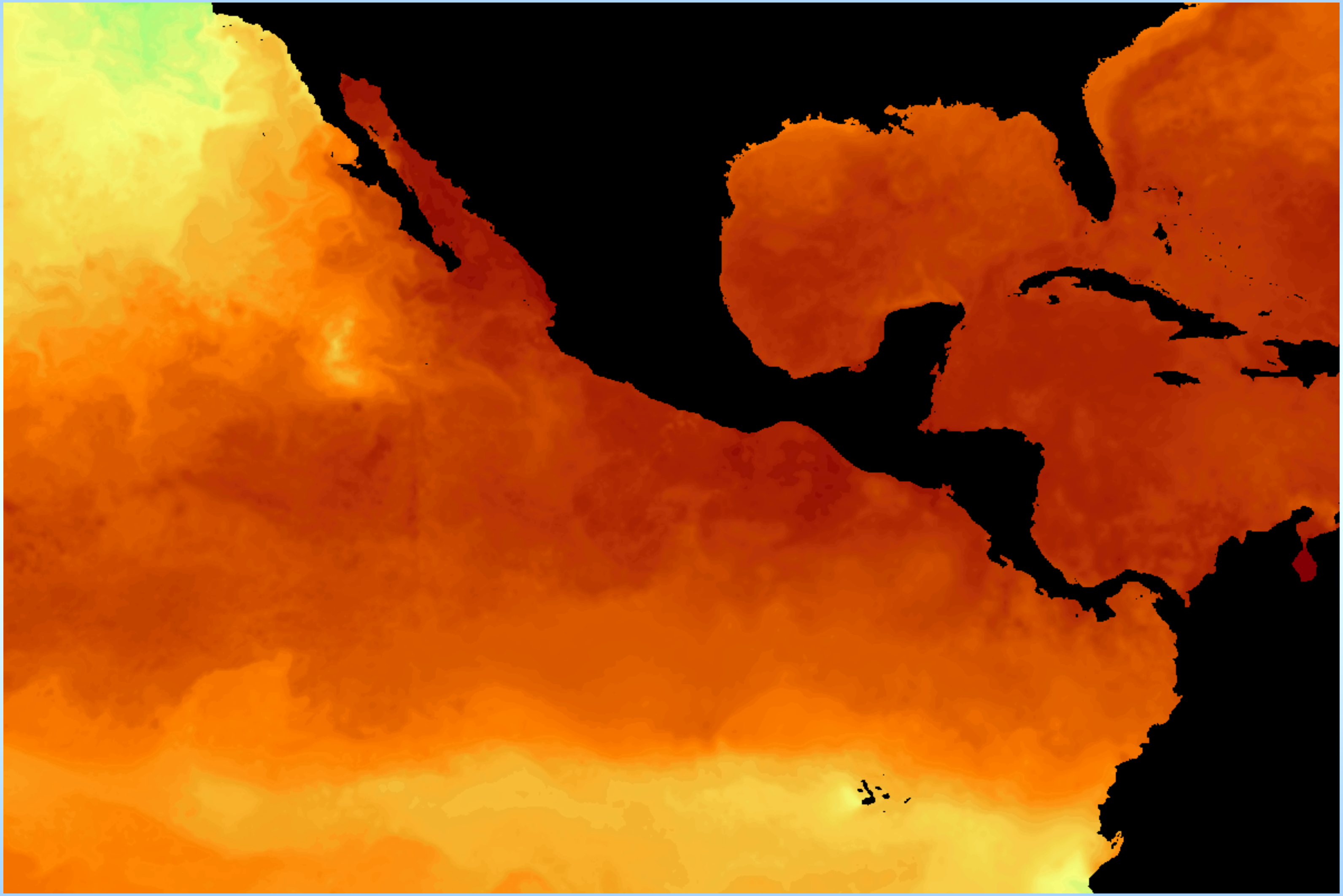

Day+night 5-km, Nov 1 – Dec 31, 2012

5-km Examples

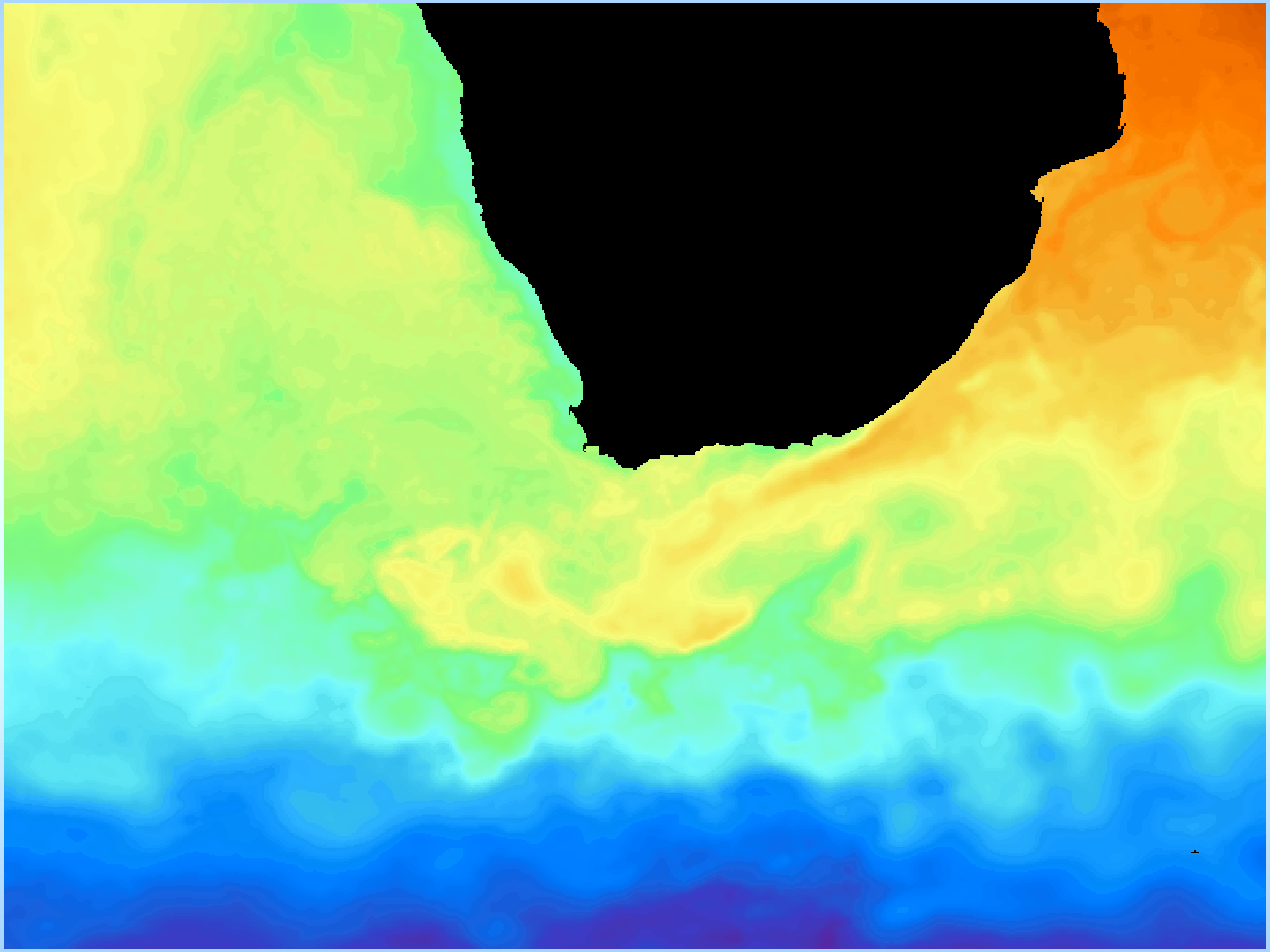

Day+night 5-km, Nov 1 – Dec 31, 2012

Key Results/Accomplishments

- VIIRS successfully incorporated into Geo-Polar Blended 5-km global SST analysis

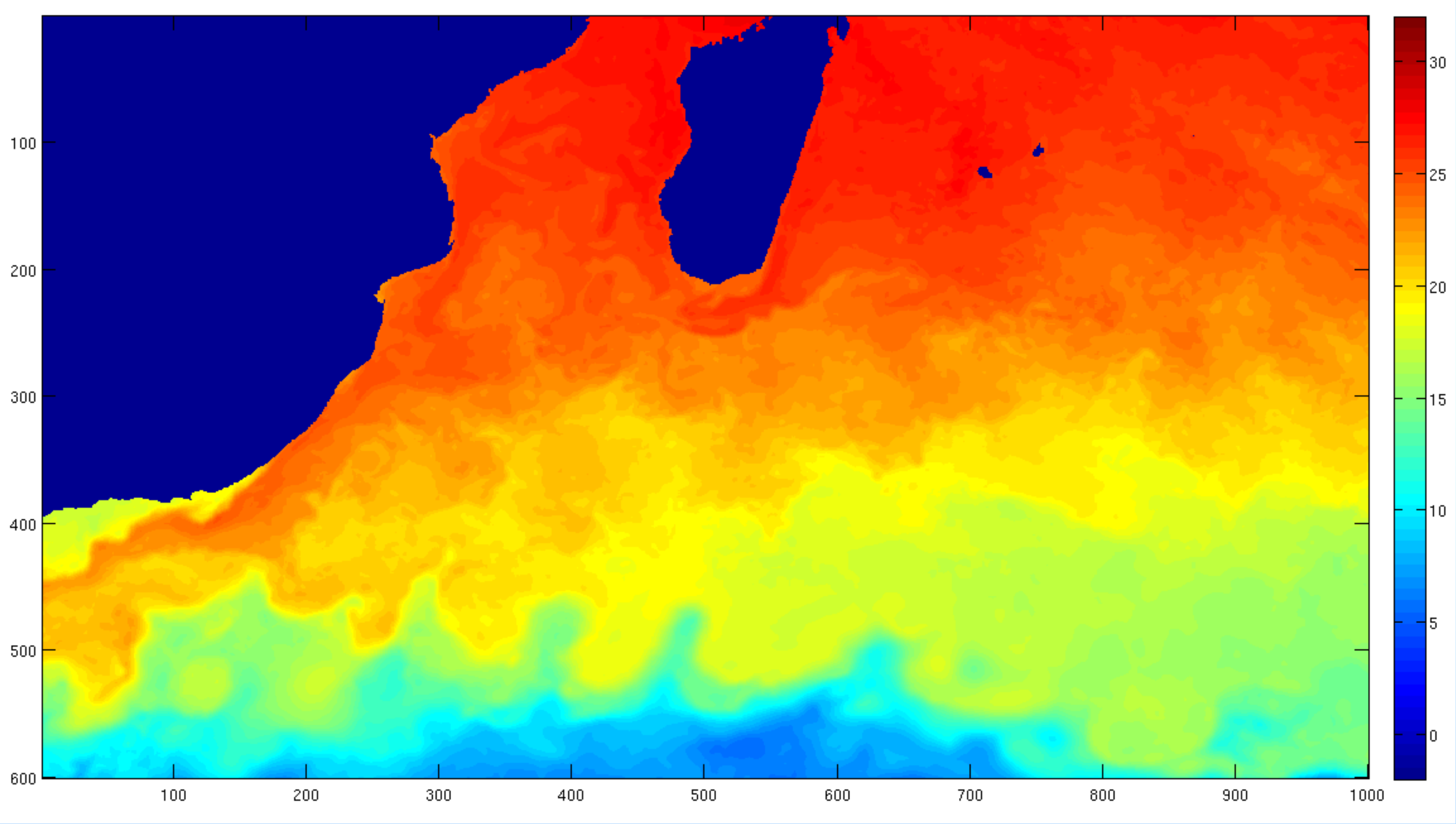

Super-Ob'd VIIRS SST data

Final SST analysis

Key Results/Accomplishments

- Coverage is improved w.r.t. MetOp AVHRR

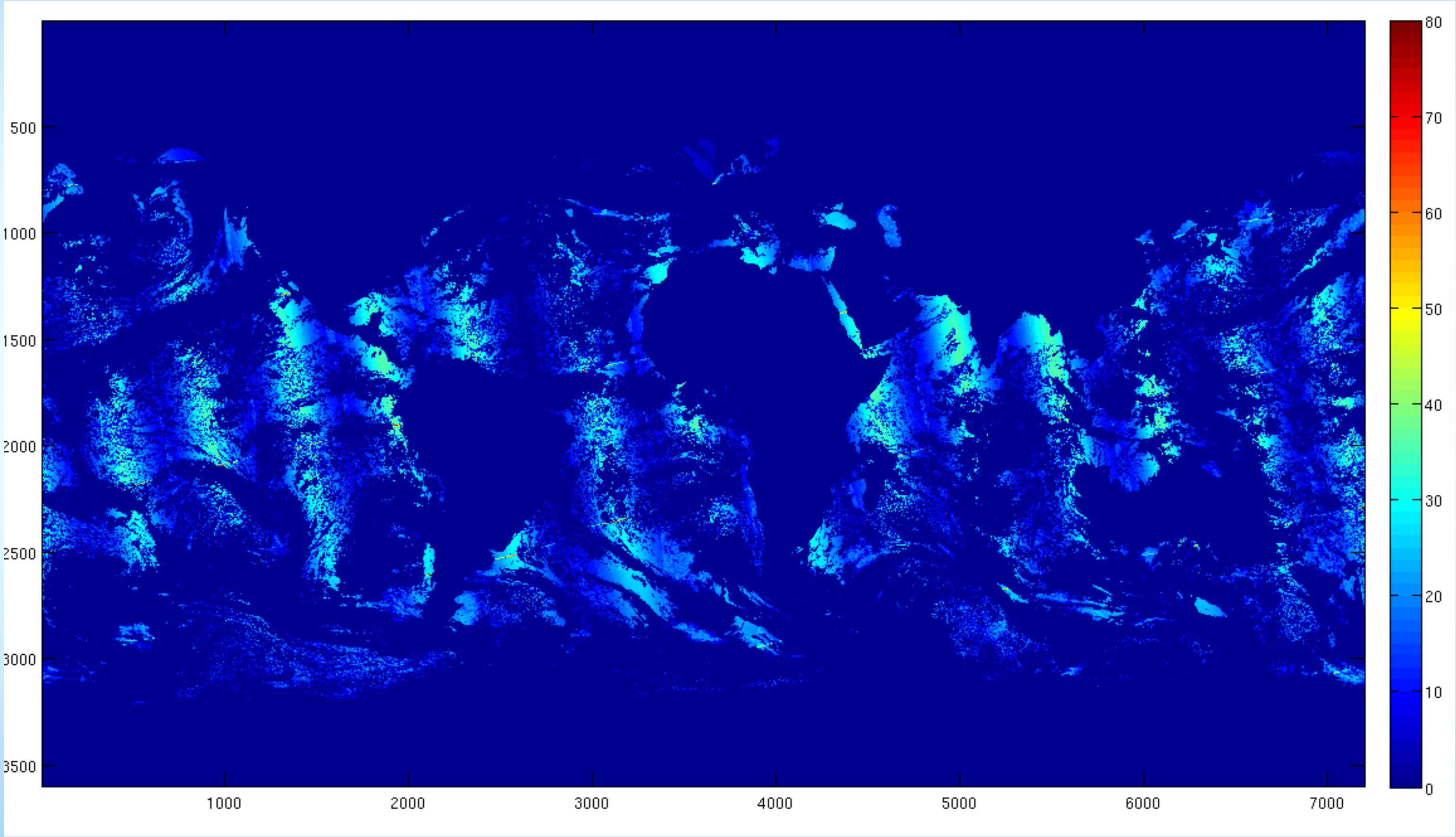

ACSPO AVHRR coverage

ACSPO VIIRS coverage

Key Results/Accomplishments

- Biases w.r.t. NCEP RTG_HR_SST indicate problem with the latter

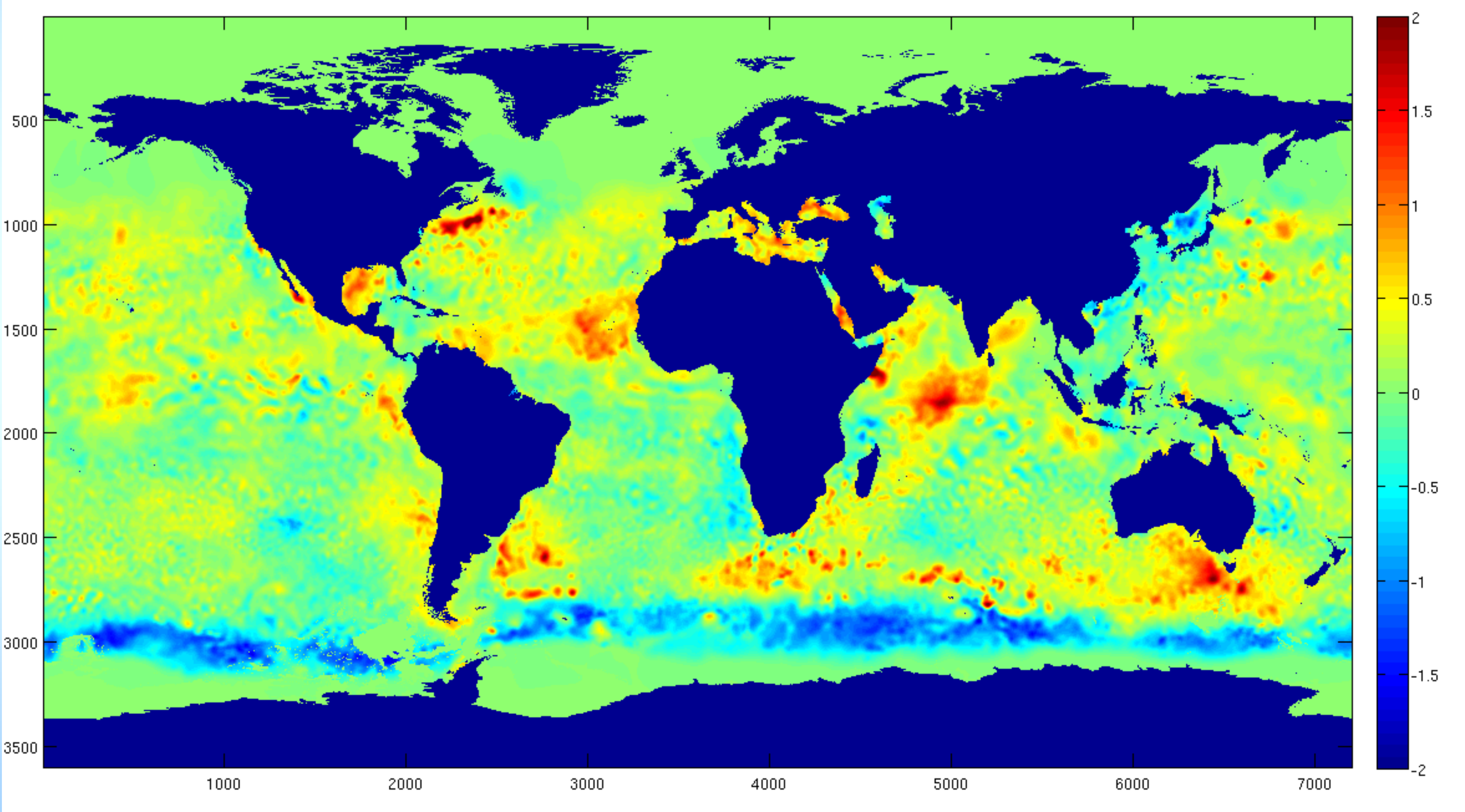

ACSPO VIIRS SST bias correction field

Key Results/Accomplishments

- Biases seems to be somewhat reduced w.r.t. RTG this year, but less *cf.* OSTIA SST analysis

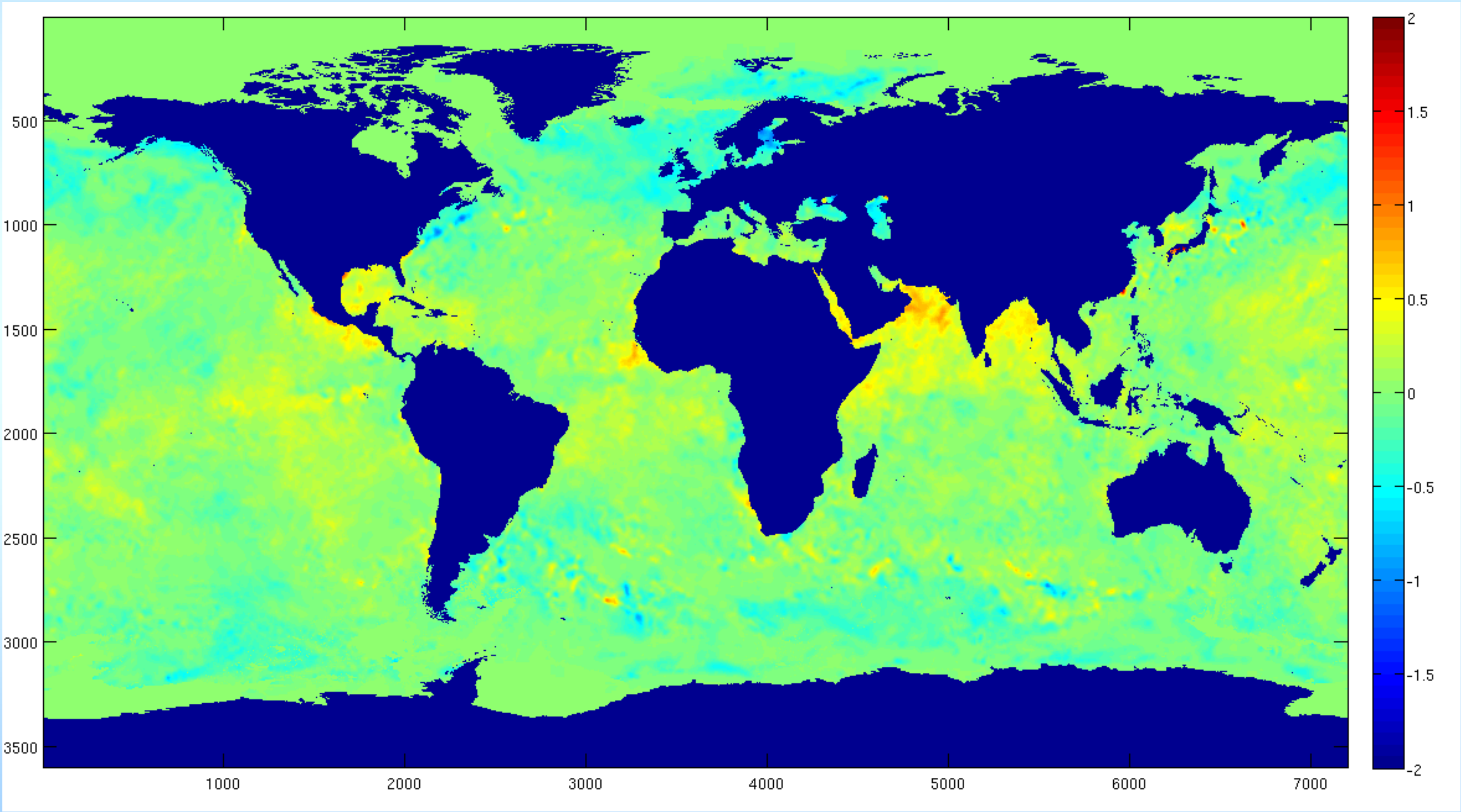

ACSPO VIIRS SST bias correction field w.r.t. OSTIA

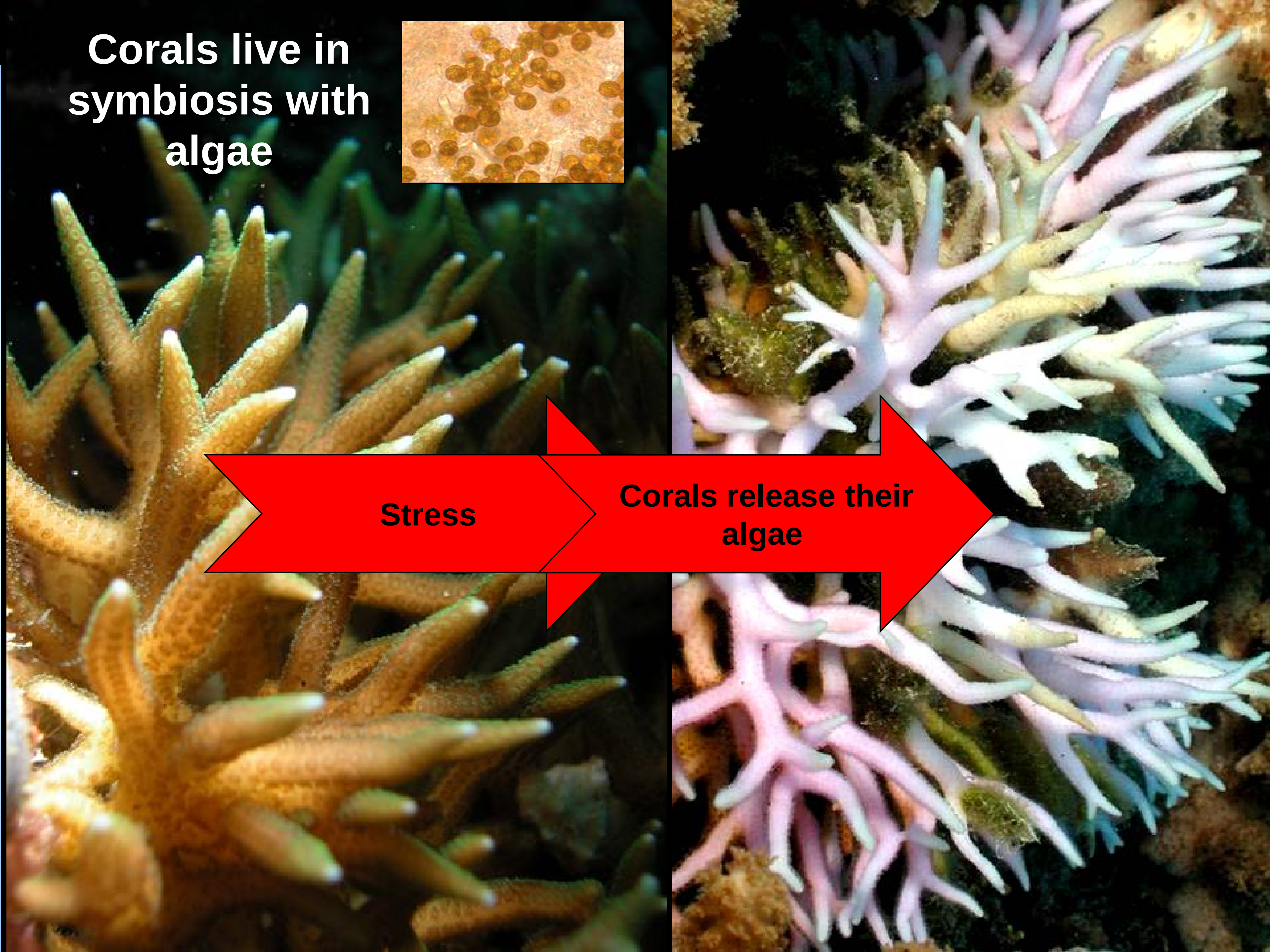
Corals live in symbiosis with algae
Stress
Corals release their algae

Thermal Stress Causes Mass Coral Bleaching

Thermal Stress Causes Mass Coral Bleaching

Thermal Stress Causes Mass Coral Bleaching and Mortality

Coral Reef Watch Products

"Coral Triangle"

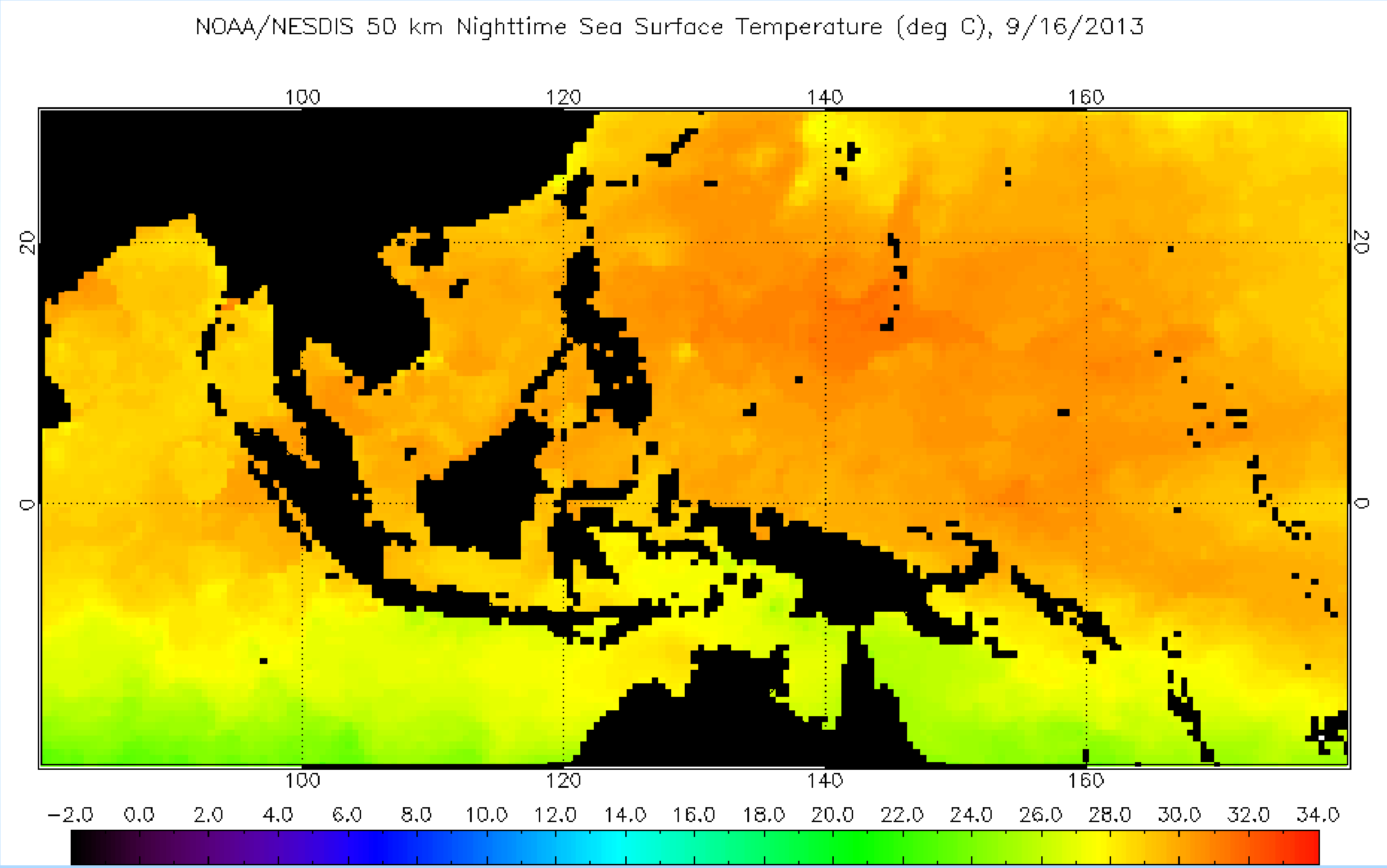

- **Current product uses 50-km AVHRR-only SST**

Coral Reef Watch Products

"Coral Triangle"

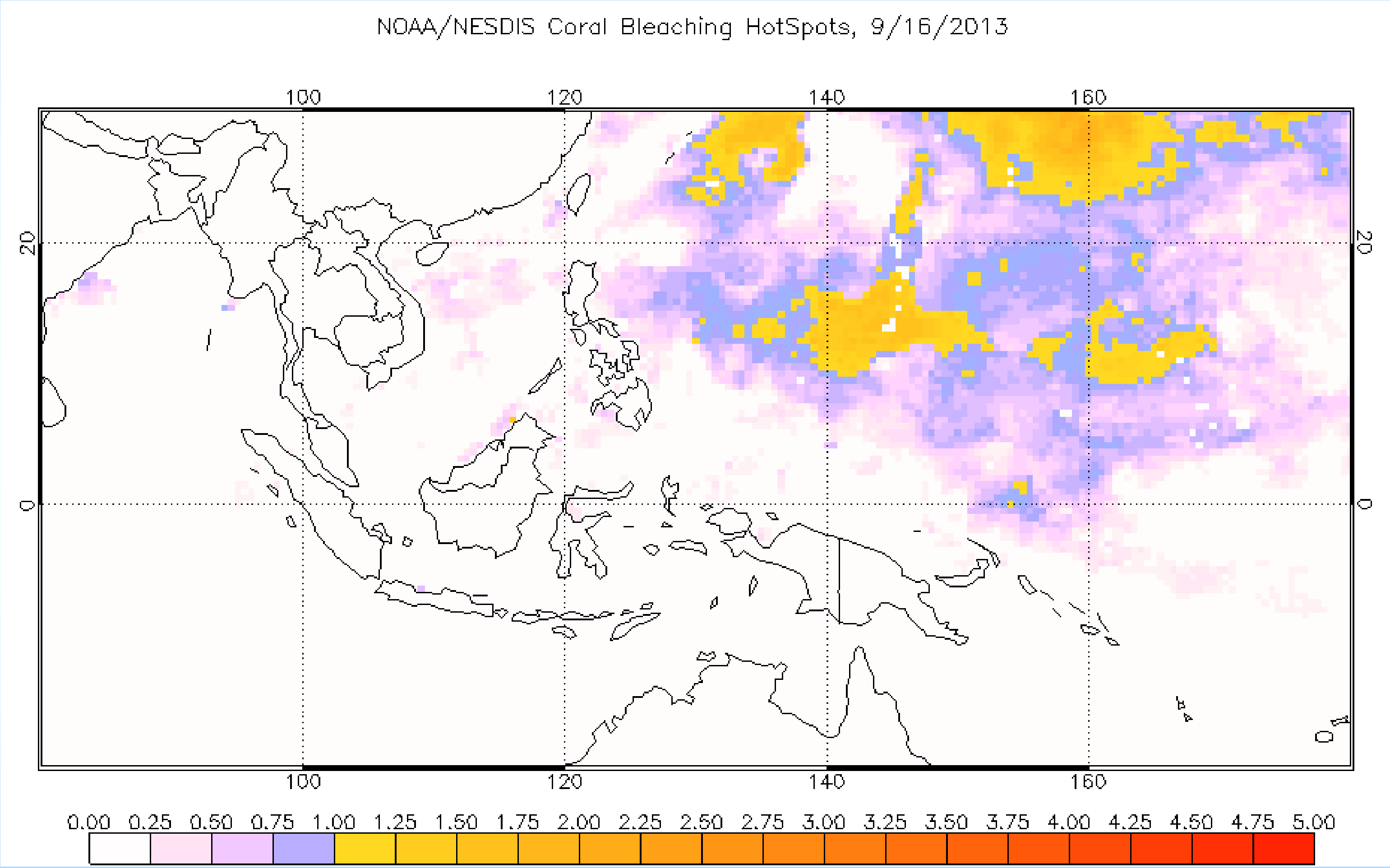

- **Hotspots are derived with respect to climatological threshold**

Coral Reef Watch Products

"Coral Triangle"

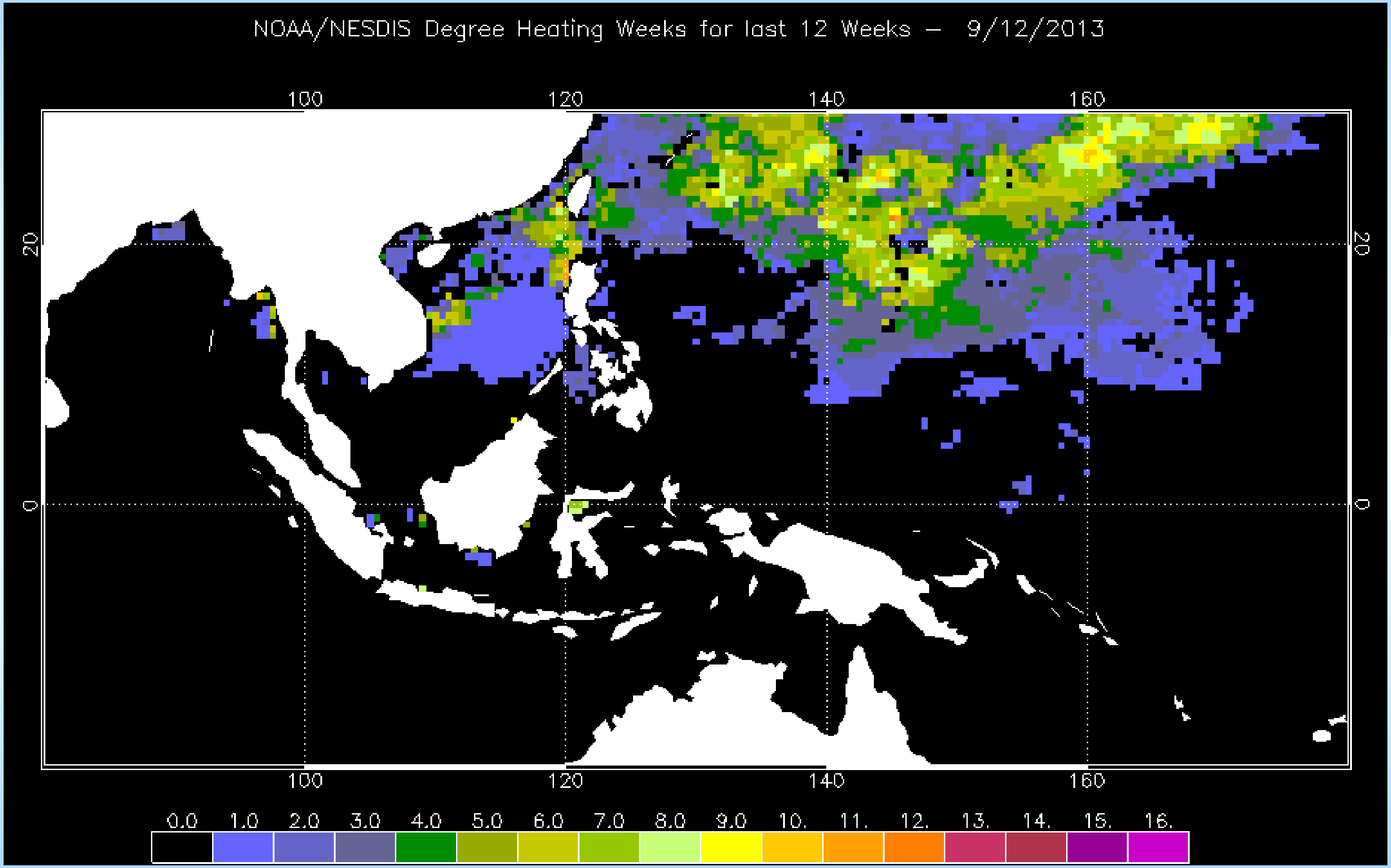

- **Accumulated thermal stress is predictor of bleaching risk**

Coral Reef Watch Products

"Coral Triangle"

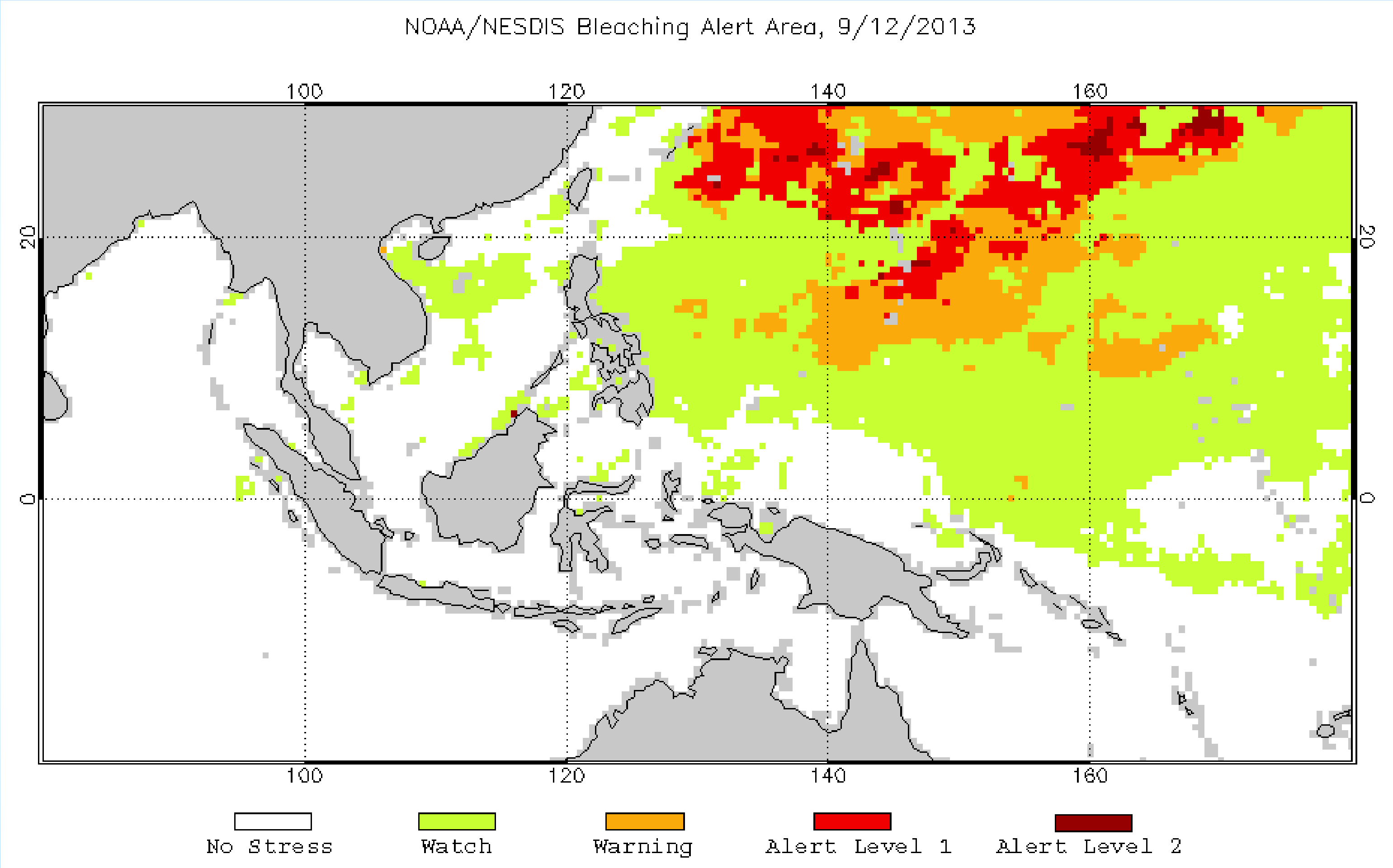

- **Bleaching risk alerts are issued**

CRW Products based on 5-km SST

"Coral Triangle"

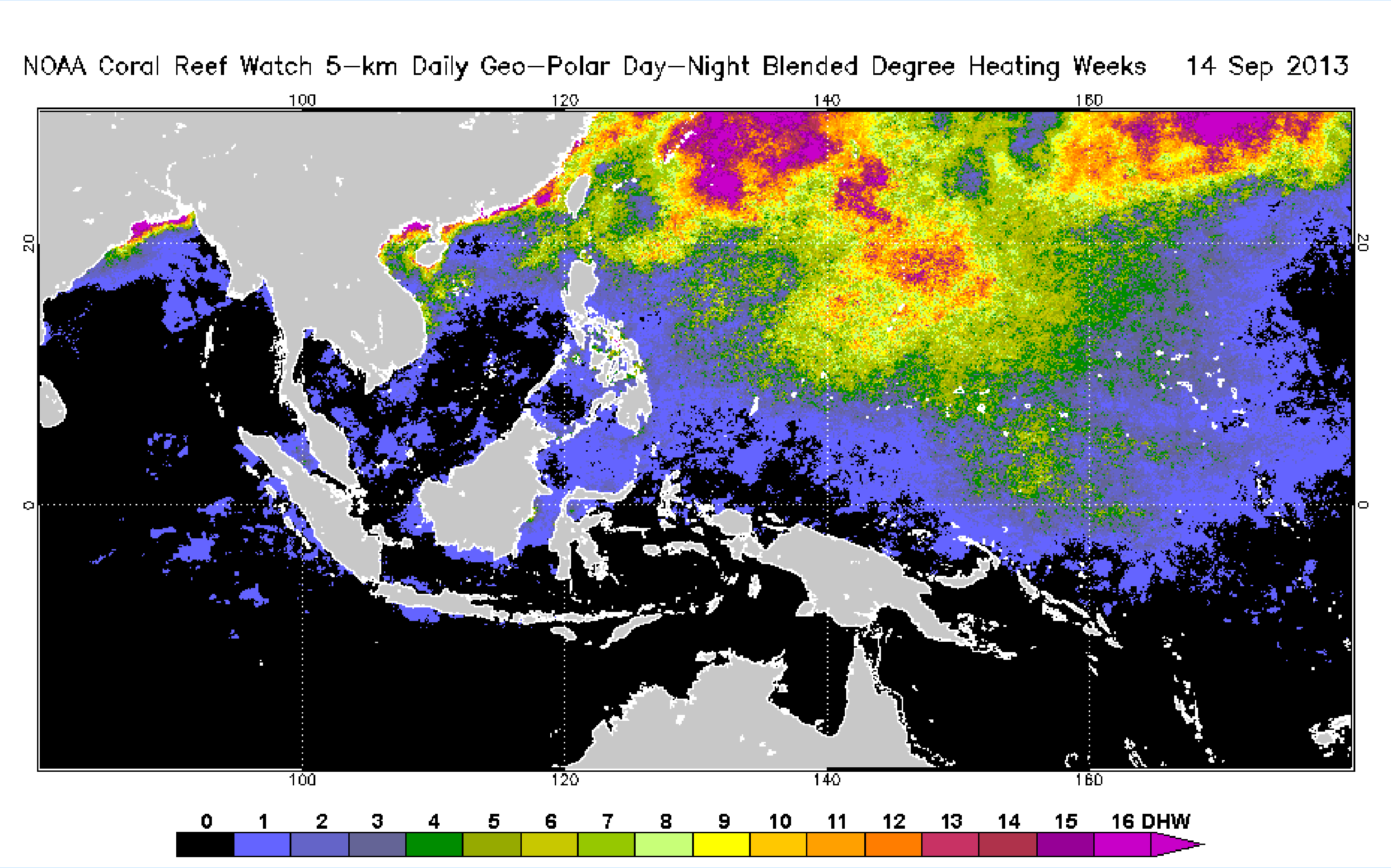

CRW Products – 5-km detail

"Coral Triangle"

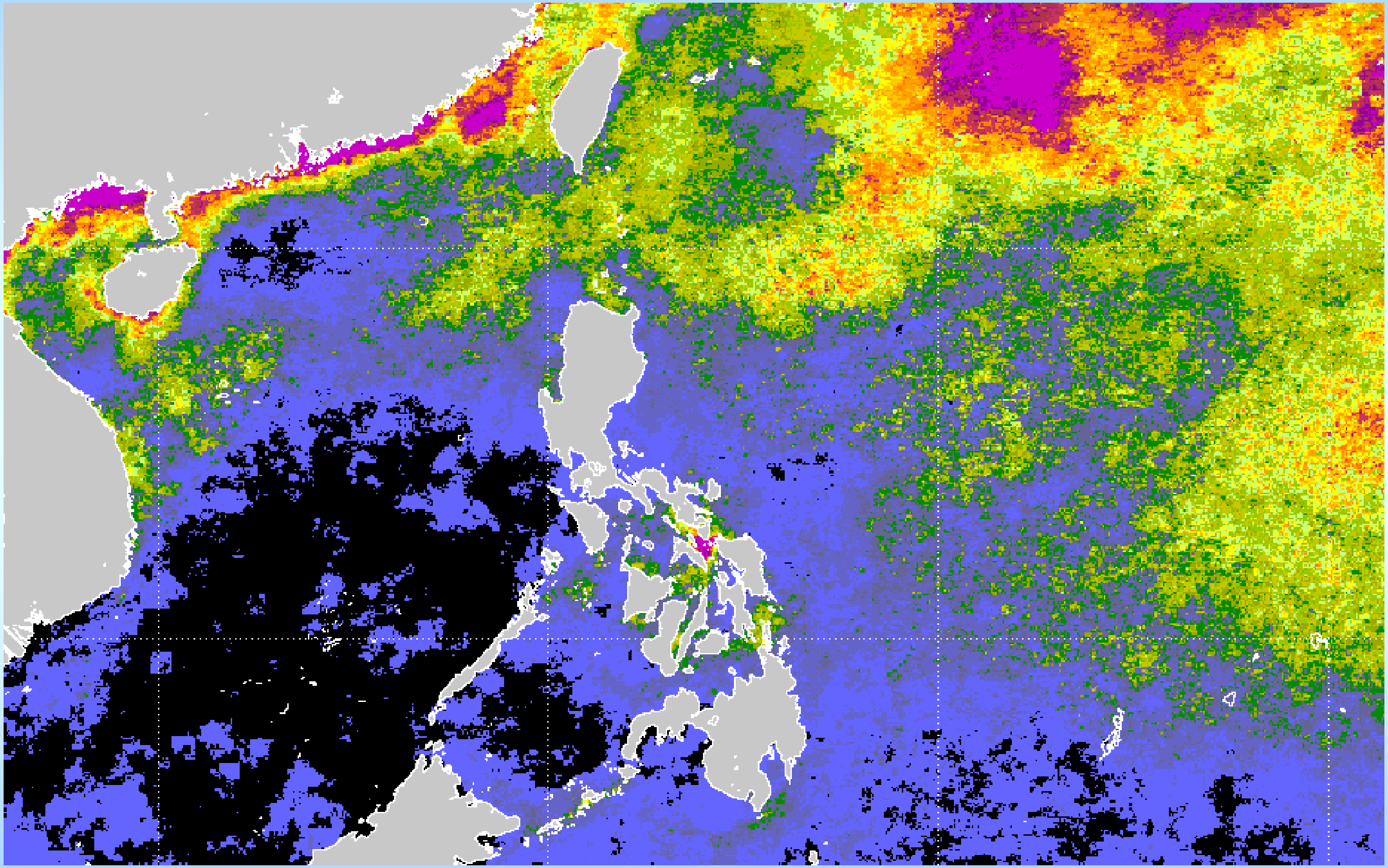

- **New analysis enables much greater precision, *e.g.* small fringing reefs**
- **However, <u>climatology is not derived from same dataset</u>**

CRW Products based on 5-km SST

"Coral Triangle"

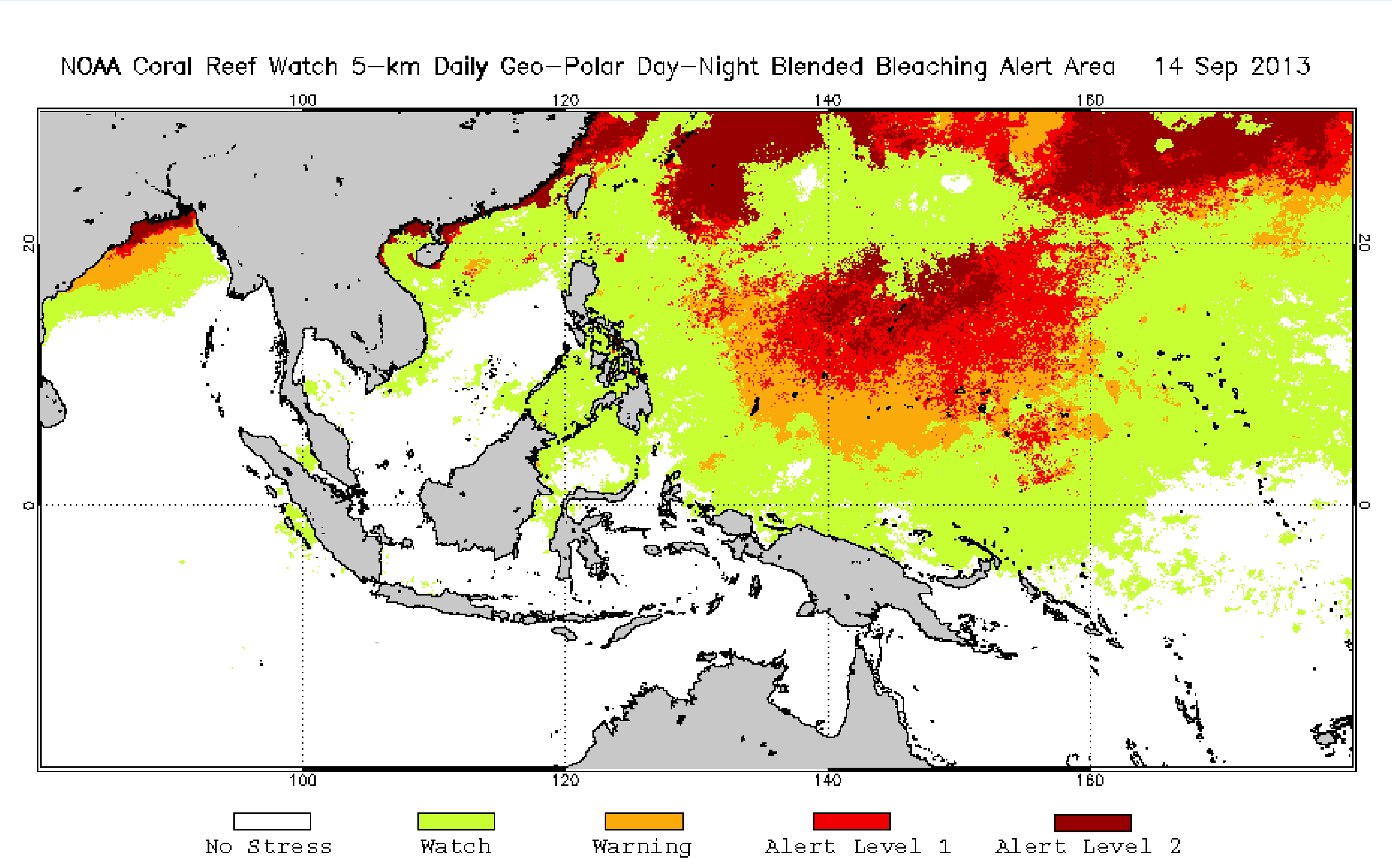

- **Strong bleaching alert for reefs in Guam & Mariana Islands – bleaching occurred in September 2013**

Next Phase of Project?

- Wish list for future VIIRS-related activities
  - Reprocessing (needed for many anomaly-based products)
  - High-resolution (1/80°) targeted regional analyses for CRW (and other users)
  - Investigate improved cloud detection for SST
  - Apply Physical Retrieval methodology to take full advantage of extra VIIRS channels and remove residual biases in SST product
    - ➢Modified Total Least Squares

Reprocessing

- Some <u>operational</u> products depend on anomalies w.r.t. a baseline
  - E.g. Coral Reef Watch
- Geo-Polar SST analysis September 2004 – present
  - Captures some major bleaching events
  - Sufficient to retune bleaching thresholds
  - **<u>Requires input data to be reprocessed as well</u>**
- Datasets
  - NOAA AVHRR (METOP, NOAA)
  - GOES-E/W (8, 10, 11, 12, 13, 15)
  - MTSAT-1R, MTSAT-2, GOES-9
  - Meteosat-8/9/10
  - Ancillary NWP
- Should be complete by August 2014

~200 TB

Recent update to Geo-SST

- Physical retrieval based on Modified Total Least Squares
- Improved bias and scatter *cf.* previous regression-based SST retrieval

GOES-13

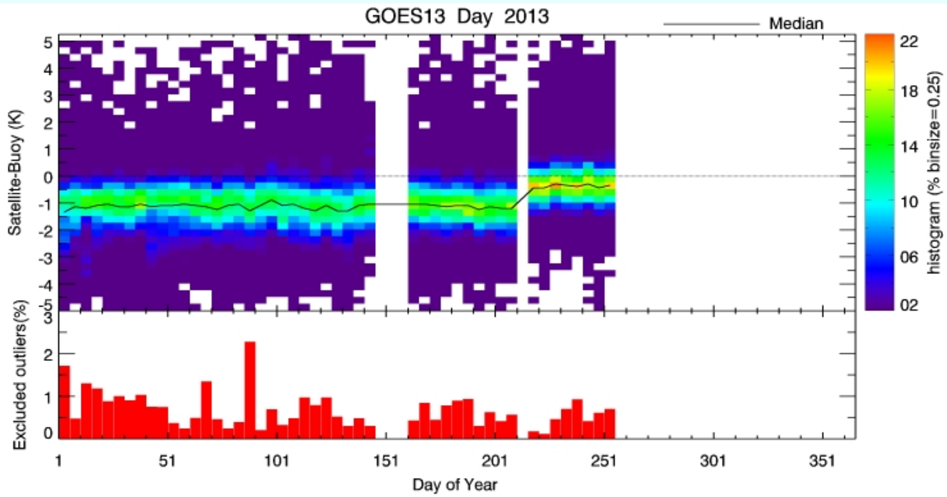

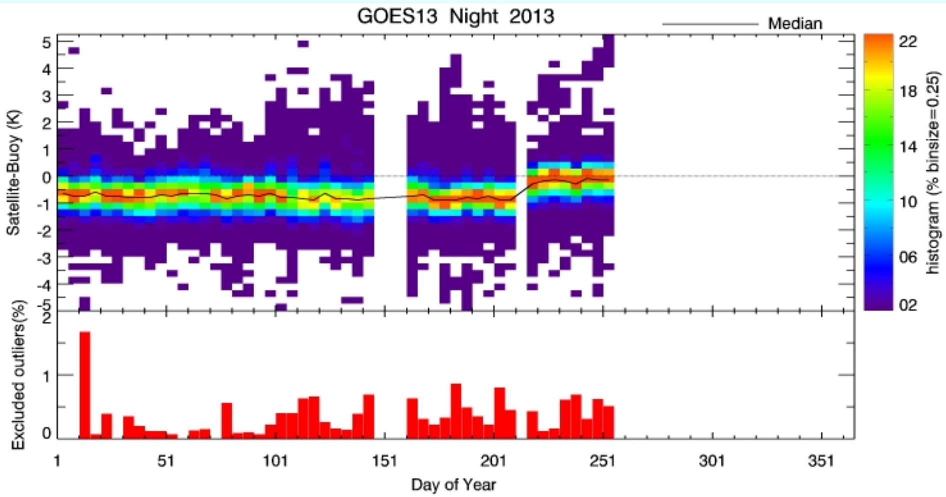

Daytime **Nighttime**

Recent update to Geo-SST

- Physical retrieval based on Modified Total Least Squares
- Improved bias and scatter *cf.* previous regression-based SST retrieval

GOES-15

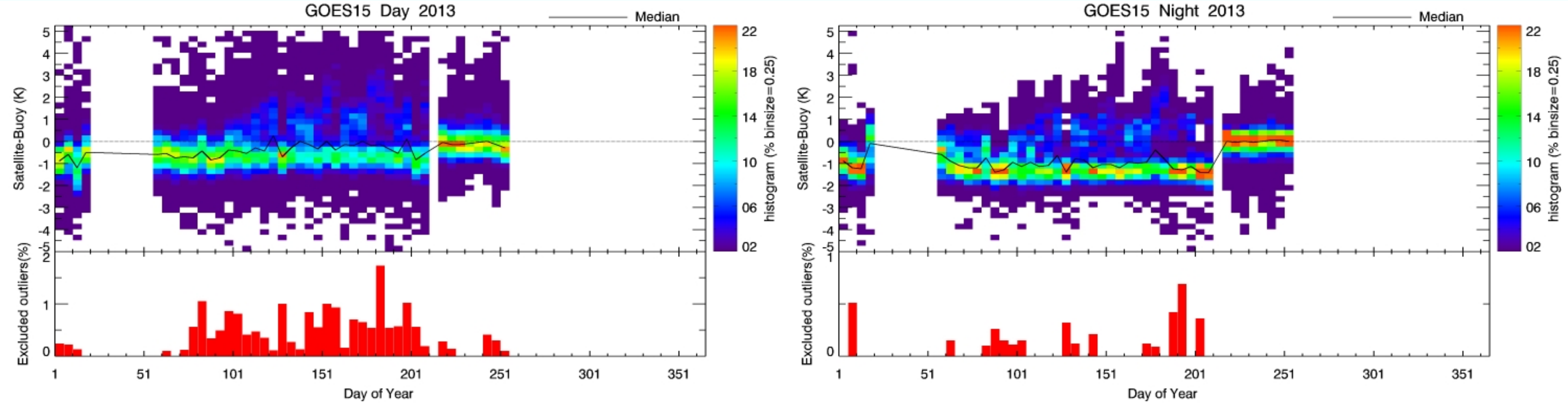

Daytime **Nighttime**

Summary of Product Accuracy: Geo-SST

GOES-15	GOES-13	MTSAT-2	Meteosat-10

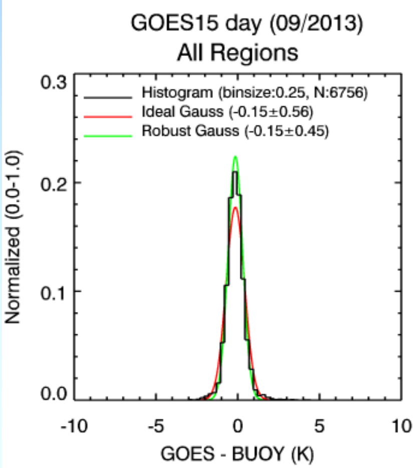

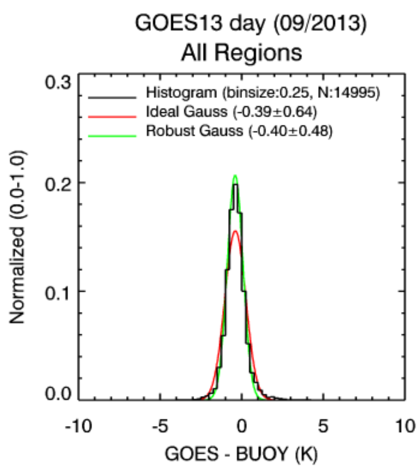

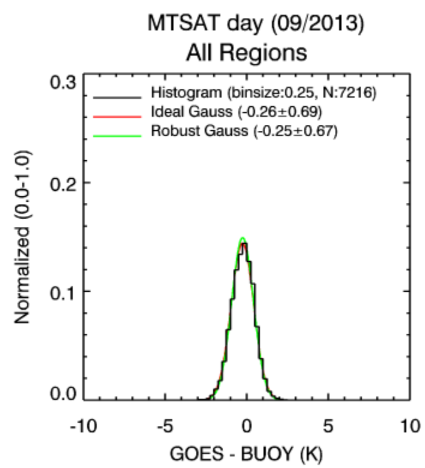

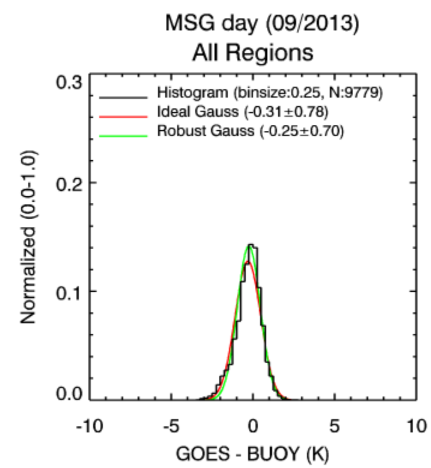

-0.15±0.56 (0.45)	-0.39±0.64 (0.48)	-0.26±0.69 (0.67)	-0.31±0.78 (0.70)

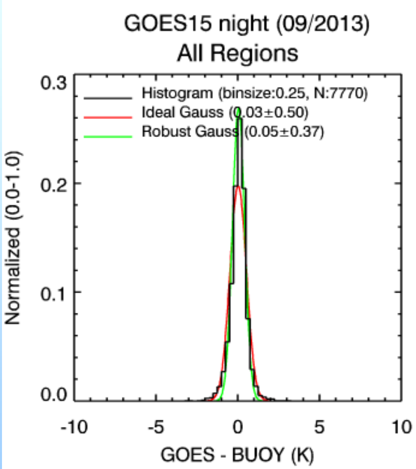

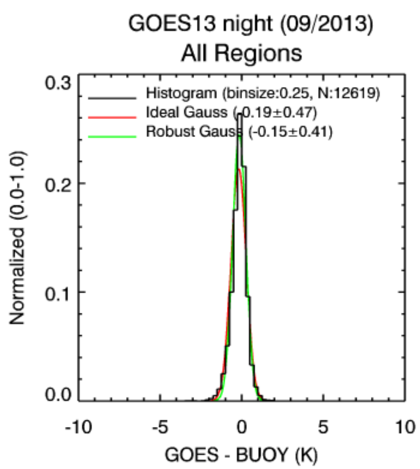

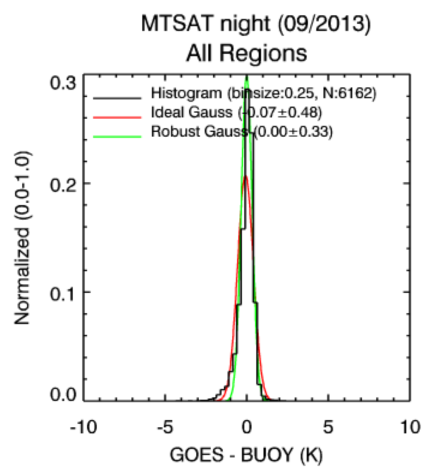

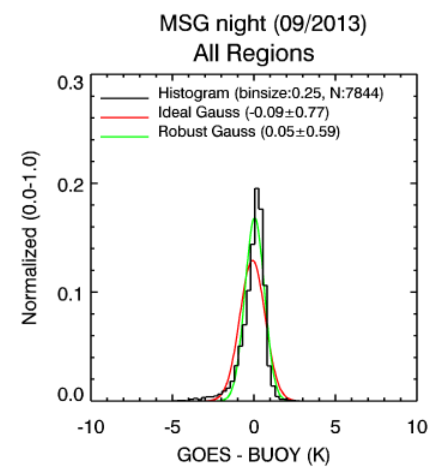

0.03±0.50 (0.37)	-0.19±0.47 (0.41)	-0.07±0.48 (0.33)	-0.09±0.77 (0.59)

Pattern Recognition Enhancements to ACSPO Clear-Sky Mask.

Irina Gladkova[1,2,3], Yury Kihai[1,2], Alexander Ignatov[1], Fazlul Shahriar[3,4], Boris Petrenko[1,2]

[1]NOAA/NESDIS/STAR,
[2]GST, Inc.,
[3]City College of New York, NOAA/CREST,
[4] Graduate Center of CUNY.

Motivation

- ACSPO Clear-Sky Mask (ACMS) employs comparisons of retrieved SST with L4 analyses, reflectance threshold tests and spatial uniformity tests.
- ACSM performs well on a global scale but tends to over-screen some highly dynamic areas (e.g., with strong currents, cold upwellings, eddies) as well as the coastal zones.
- These deficiencies cannot be completely eliminated by simple thresholds adjustment within ACSM without triggering massive cloud leakages.
- Visual analysis of SST field easily discriminates cloud leakages from cold SST anomalies

South Africa, 02/16/13

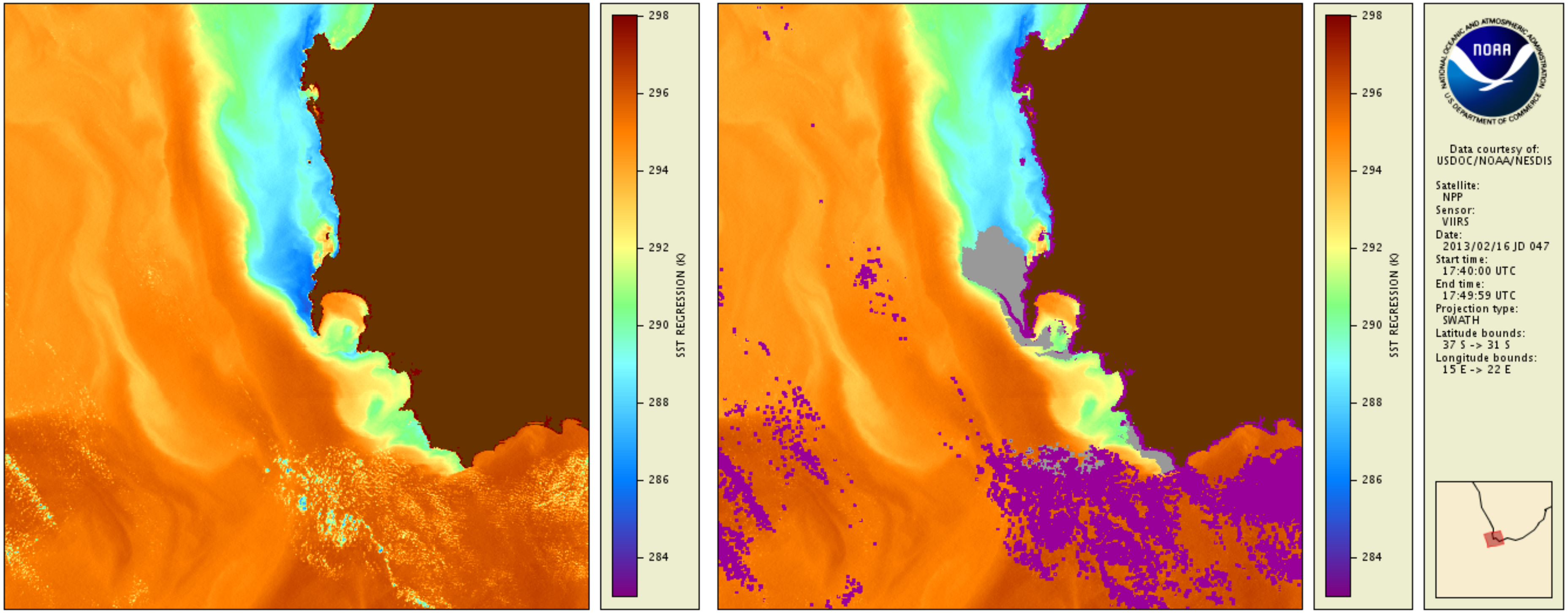

South Africa, 02/17/13

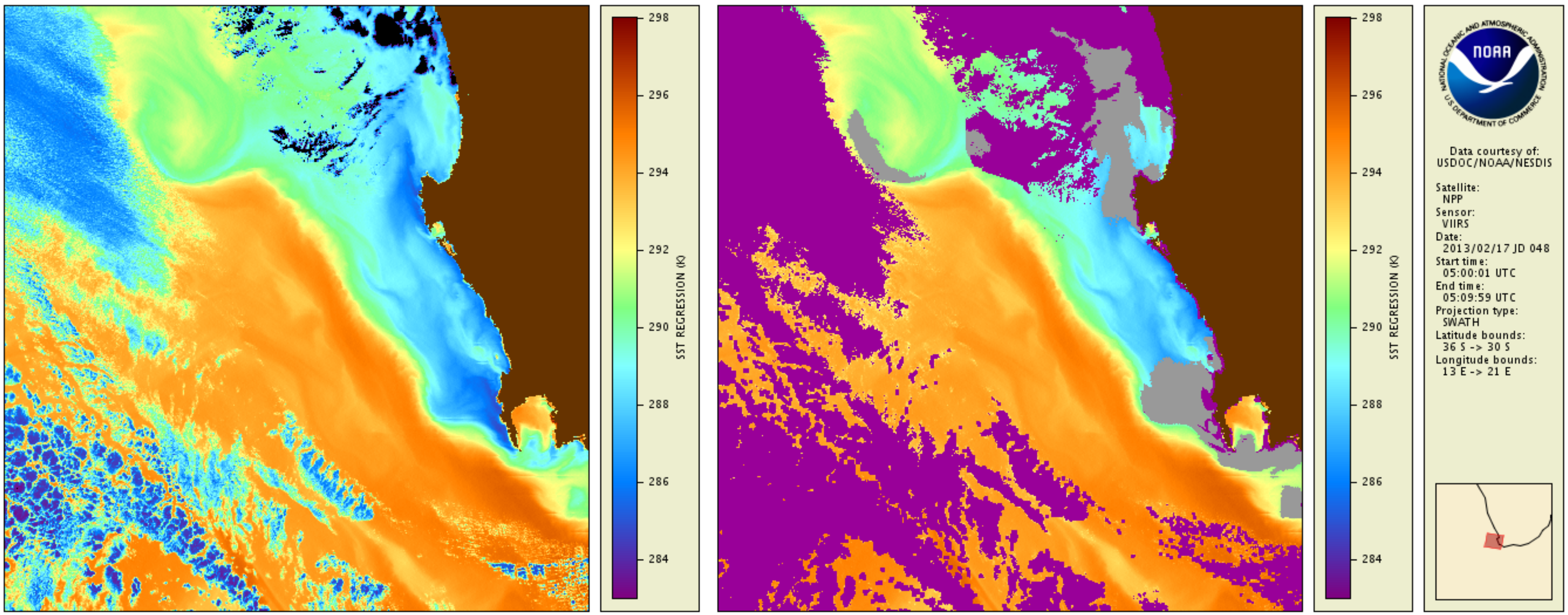

South Africa, 02/17/13

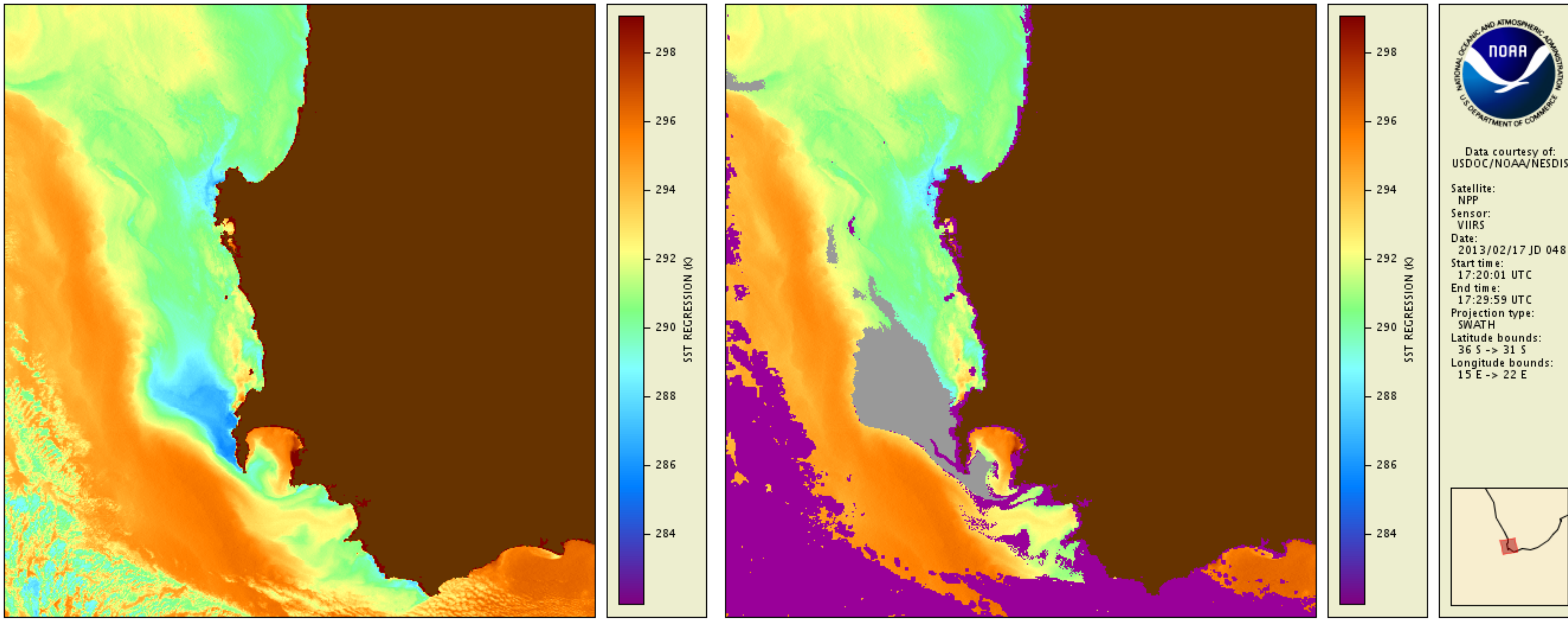

Types of misclassifications

Typical clear sky ocean regions misclassified by the ACSM :

- contiguous,
- with well-defined boundaries,
- typically located in the vicinity of ocean thermal fronts.

Existing image processing techniques:

- Segmentation;
- Morphological Procedures: erosion and dilation;
- Thermal Front Detection.

Human Perspective

- Human eye does not perceive absolute pixel values (i.e., SST values)
- It relies instead on local contrasts and ratios, which more directly correlate with gradients in an image.
- Difference between ocean and cloud patterns should be more pronounced in the SST gradient magnitude domain.

Gradient magnitude and angle

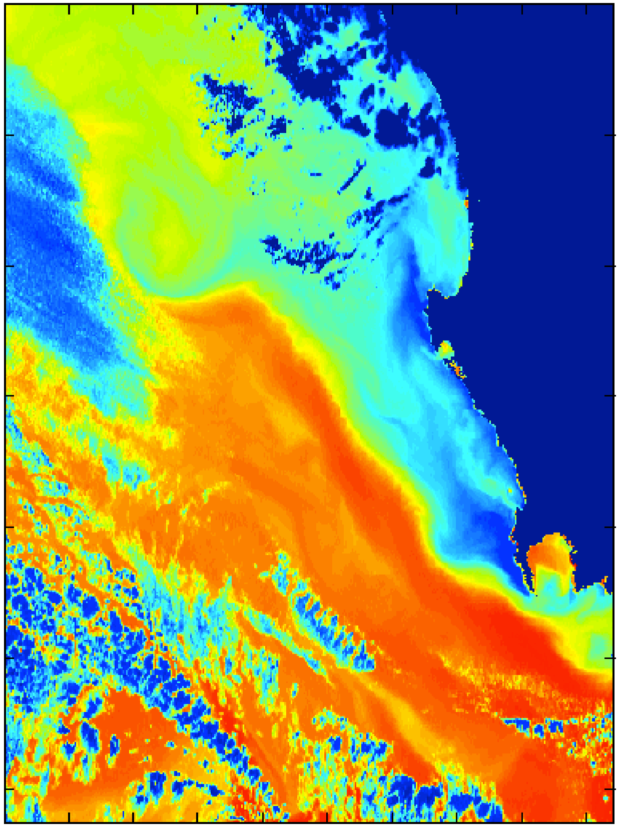

SST

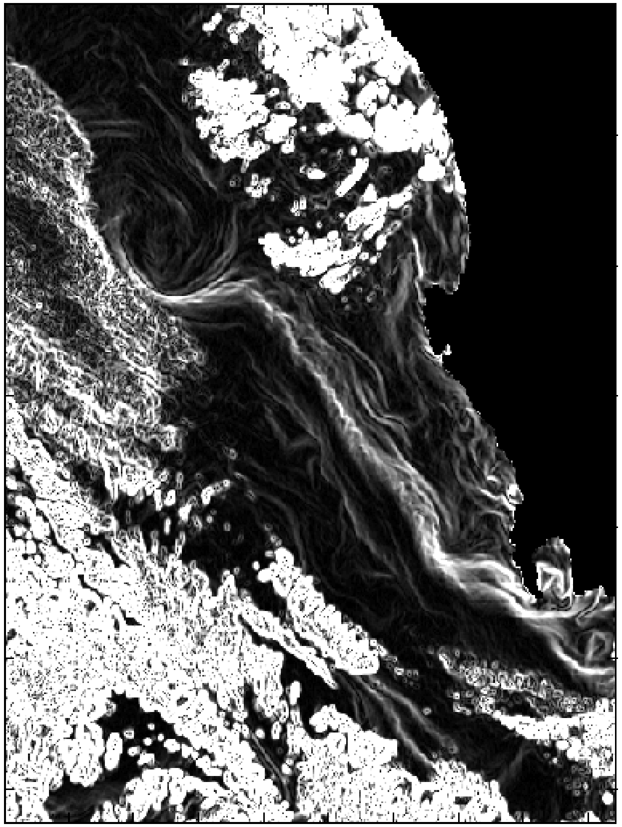

Gradient magnitude

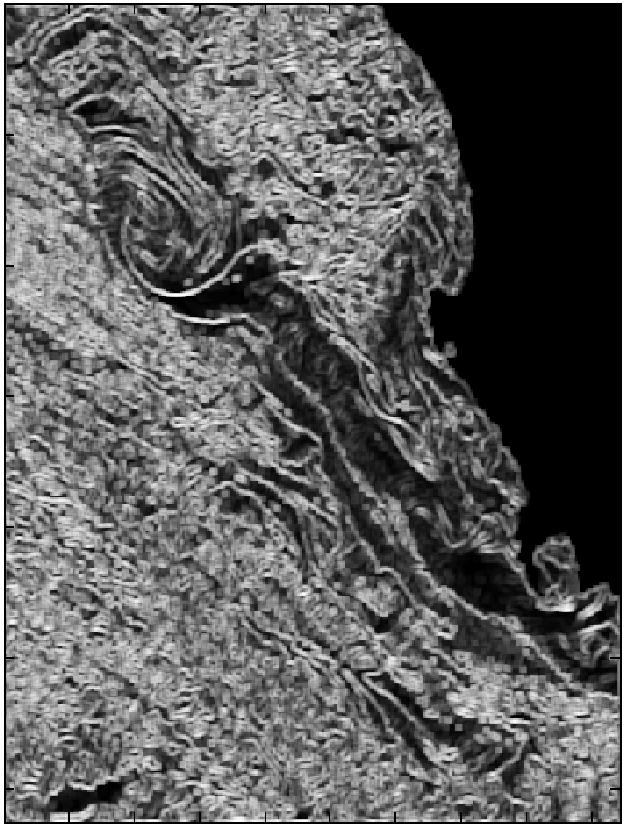

Gradient angle

Algorithm

Step 1: Identify Search Domain

Step 2: Determine SST gradient ridges

Step 3: Determine spatially connected cold SST regions

Step 4: Discard SST segments found in Step 3 that do not border the ridges found in Step 2

Step 5: Statistical Test

Steps

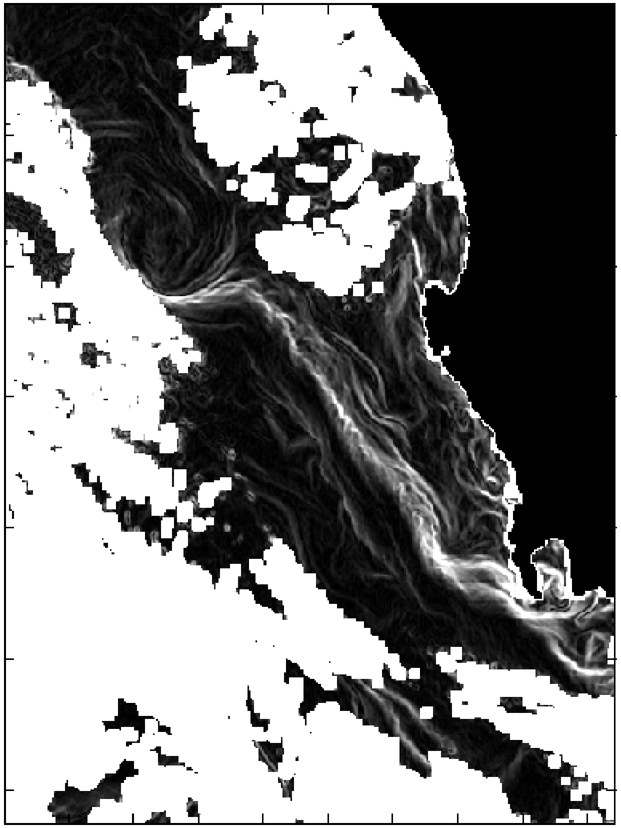

Search Space

SST Gradient Ridges

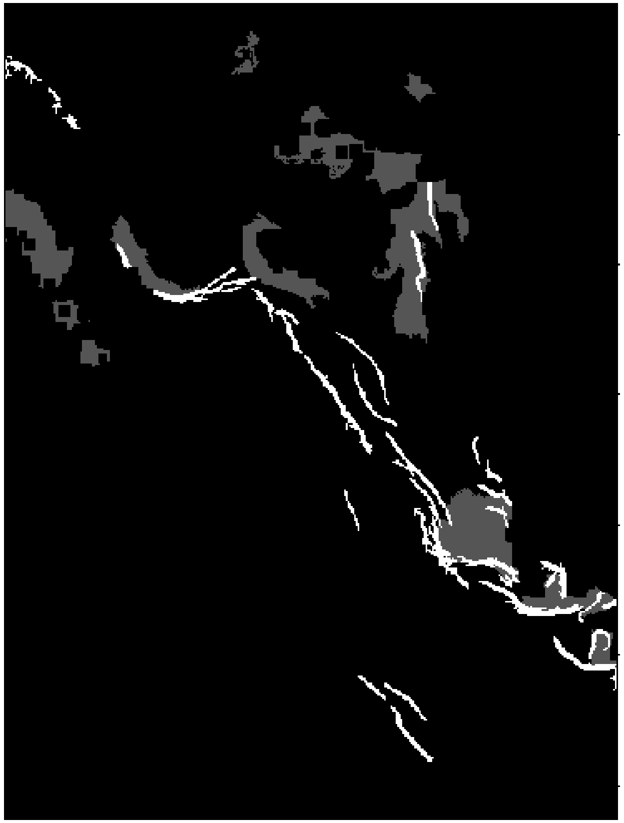

Segments bordering Ridges

Potentials and Limitations

Considered 2 sets of VIIRS data:

- 48 hand picked and cropped regions with typical clear sky misclassification
- 144 granules representing 1 day global observations

Results were visually inspected and analyzed;
Success rate is promising but more work is needed.

Gulf Stream, 05/10/13 (day)

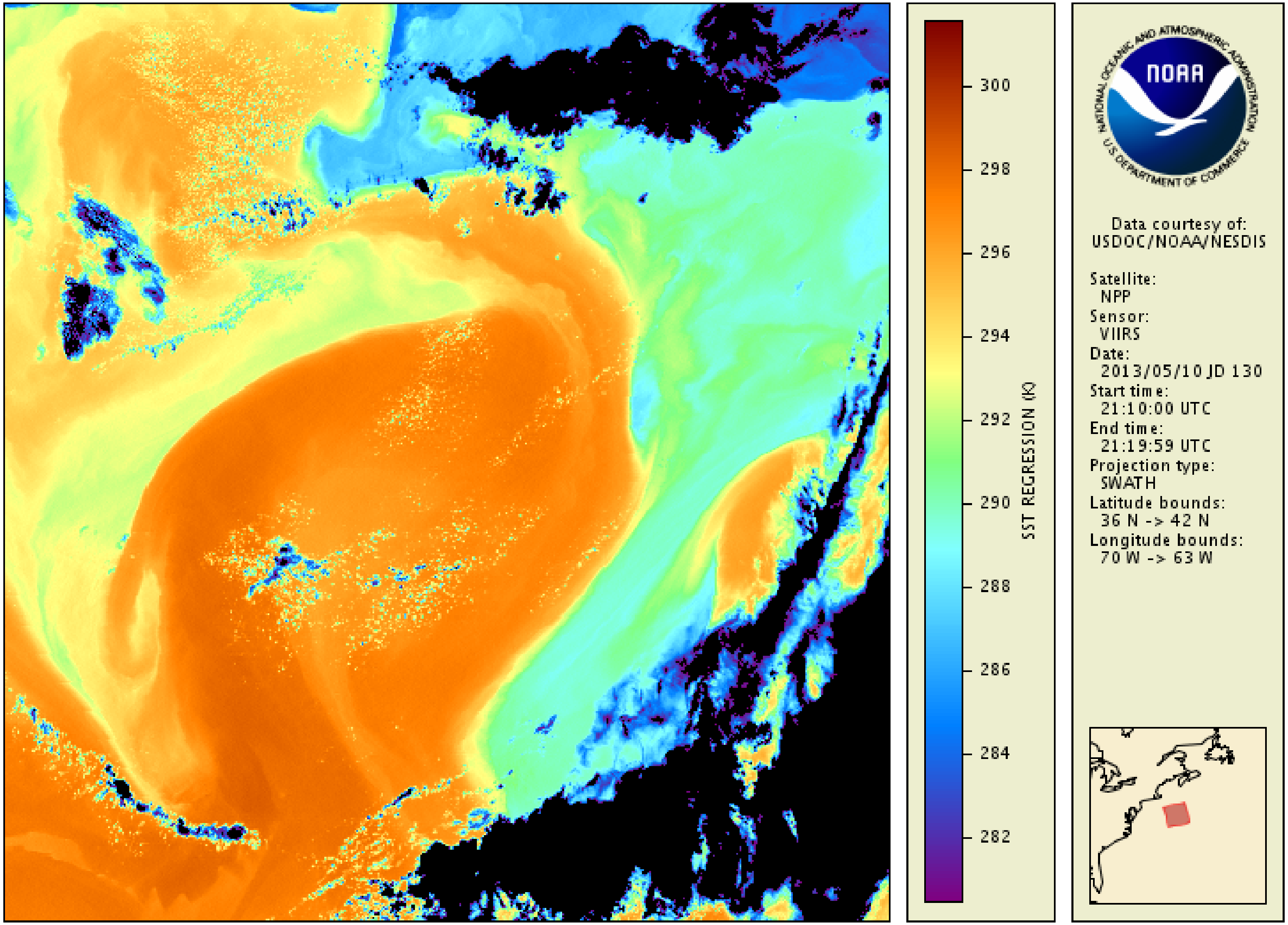

Gulf Stream, 05/10/13 (day)

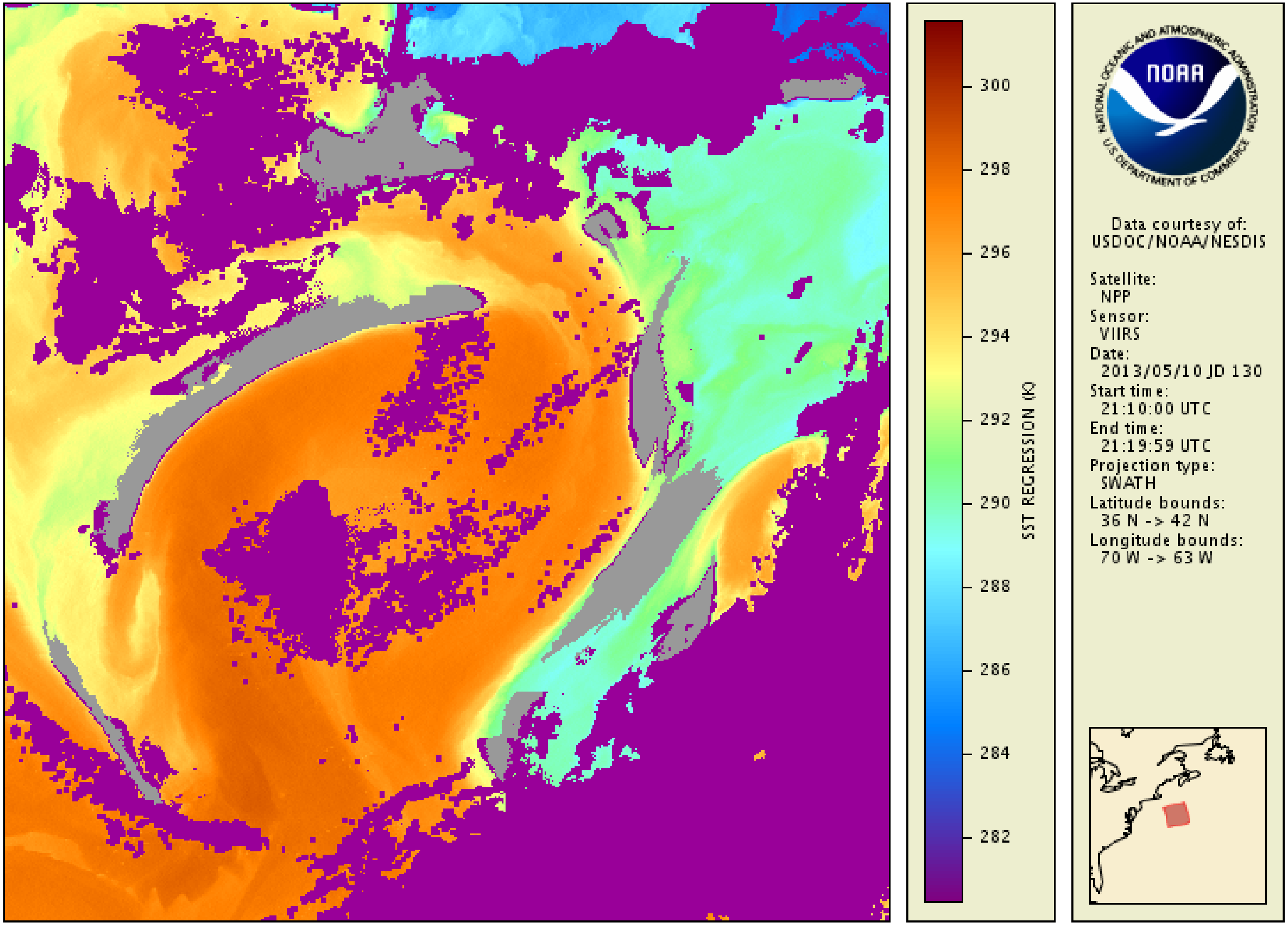

Gulf Stream, 02/16/13

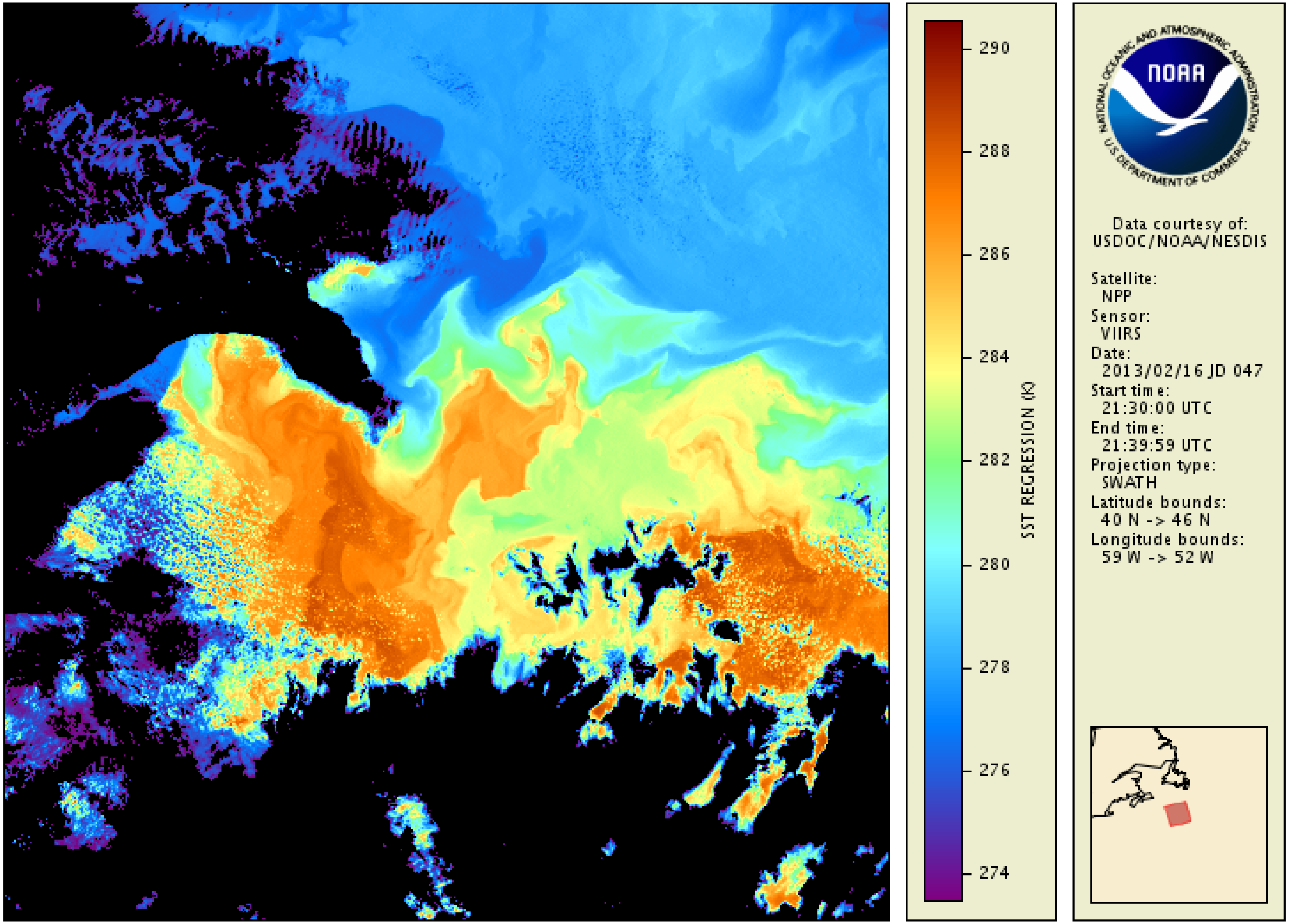

Gulf Stream, 02/16/13

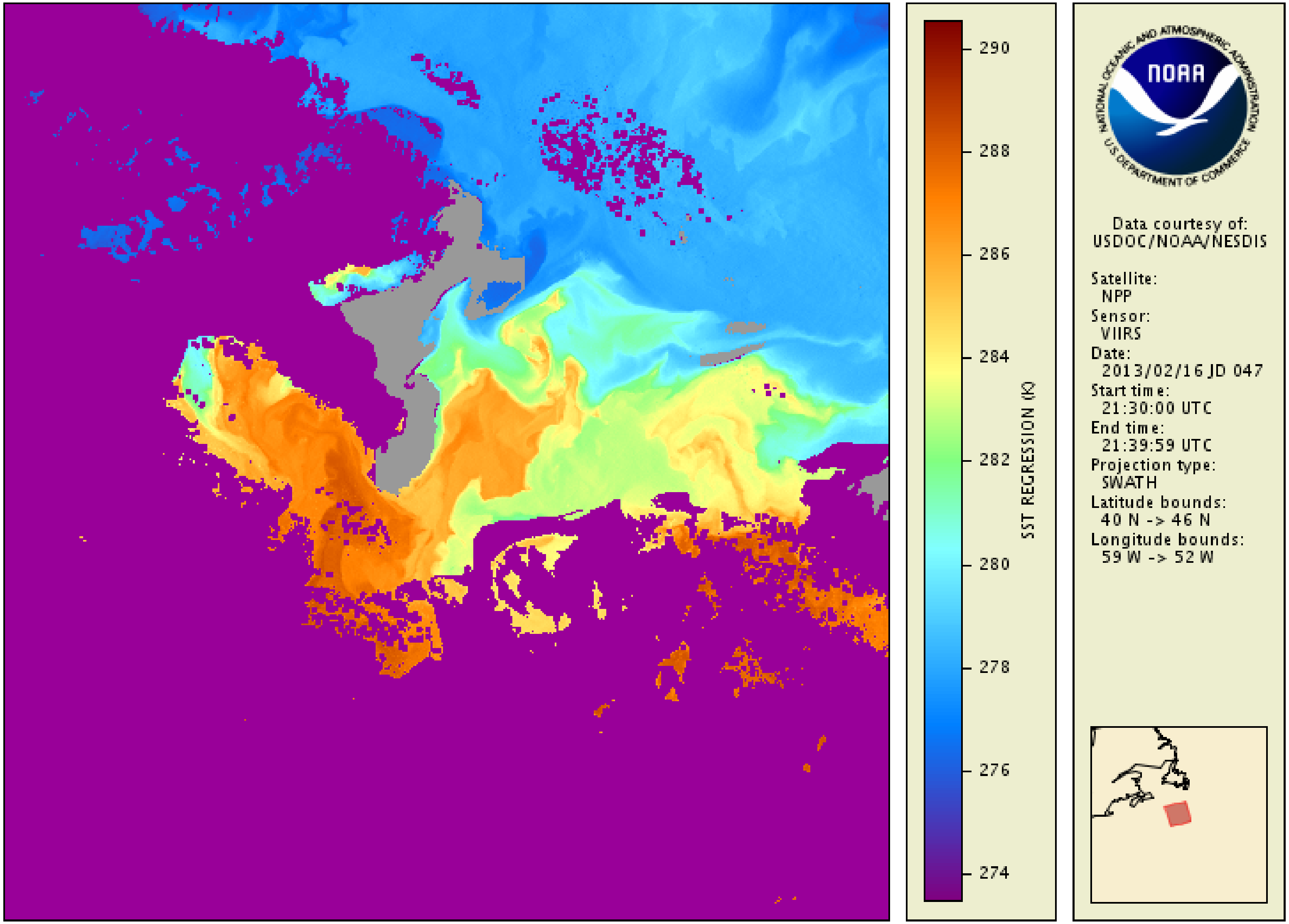

Gulf Stream, 02/17/13

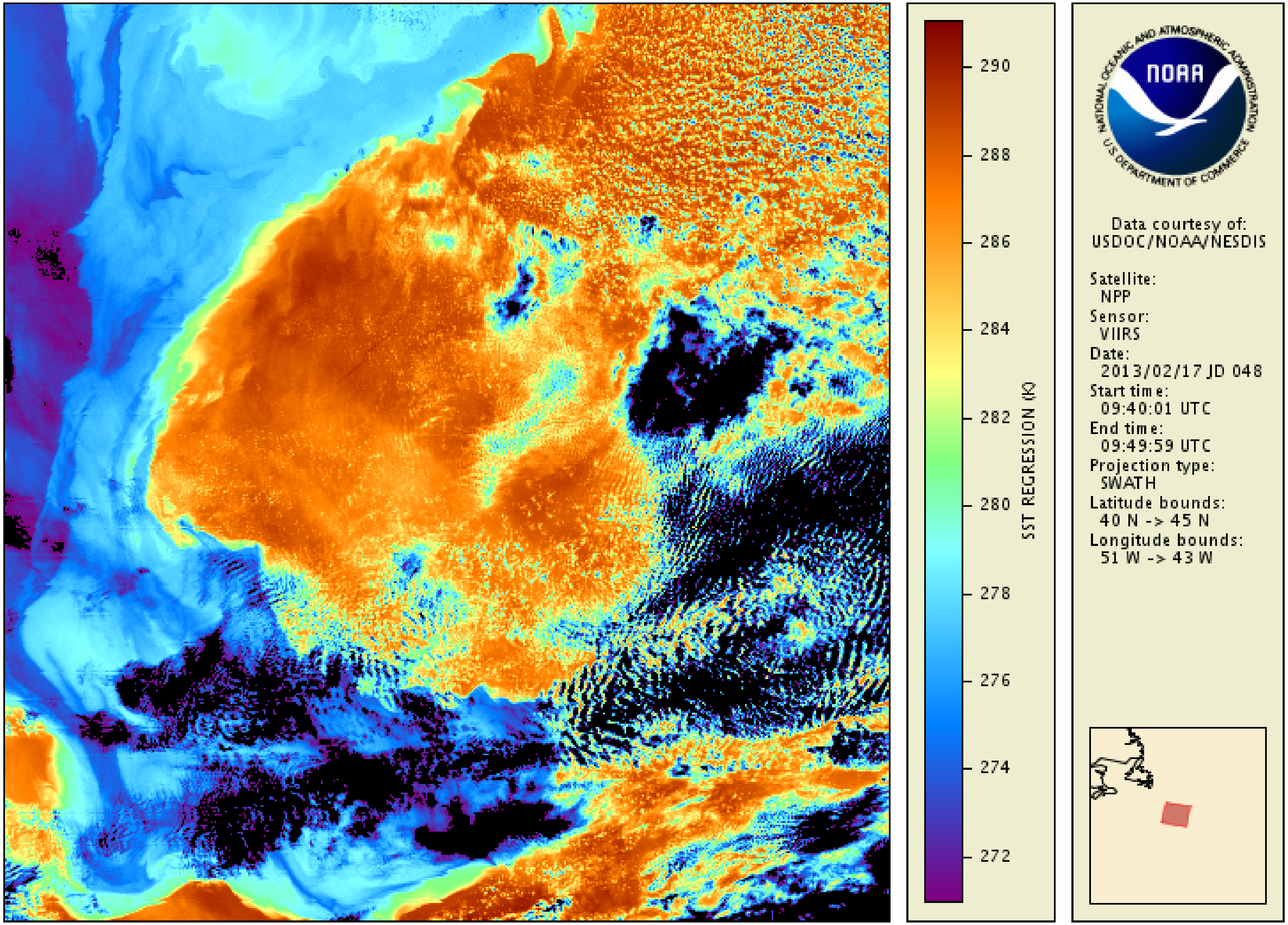

Gulf Stream, 02/17/13

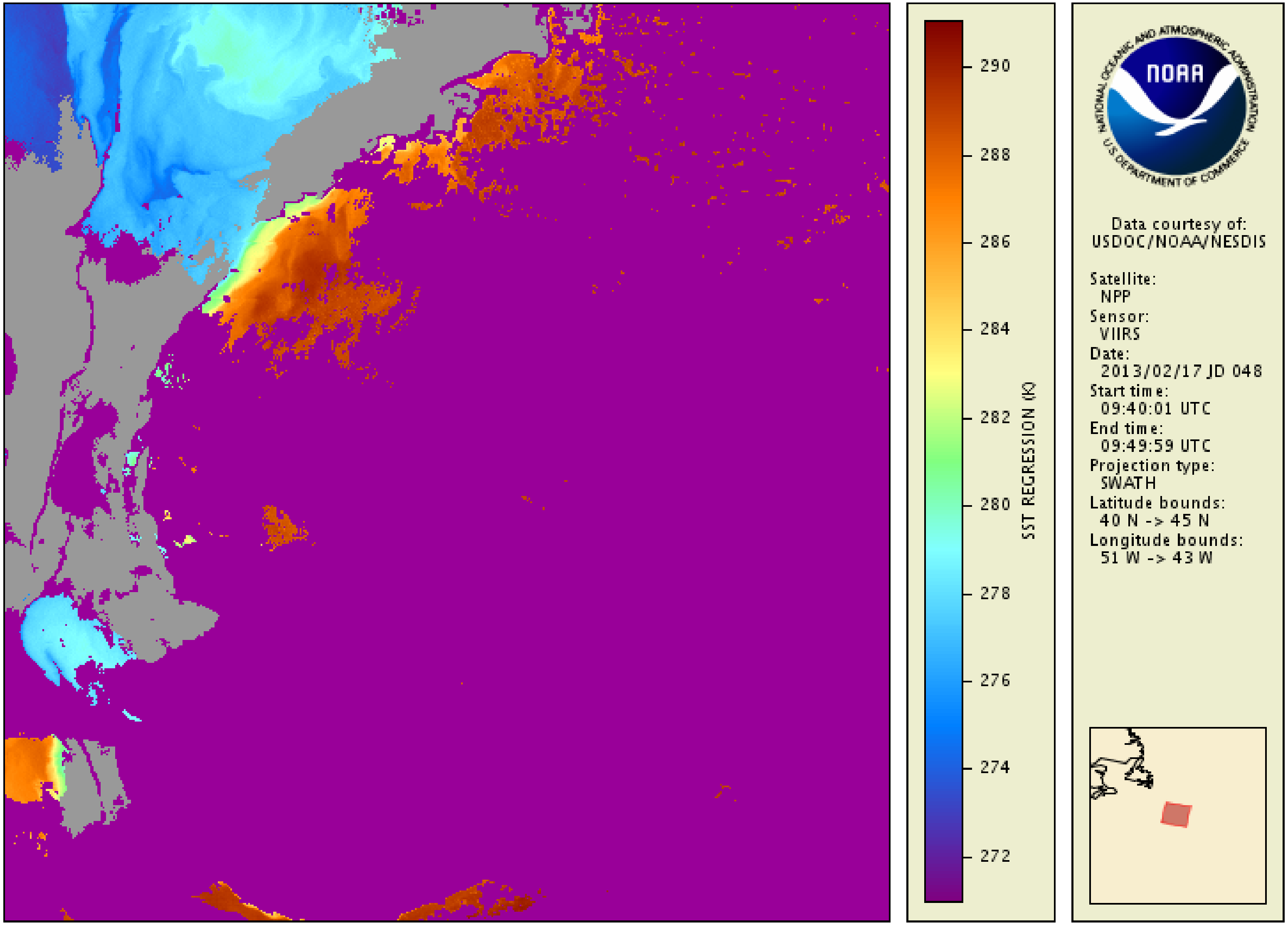

Gulf of Mexico, 02/17/13

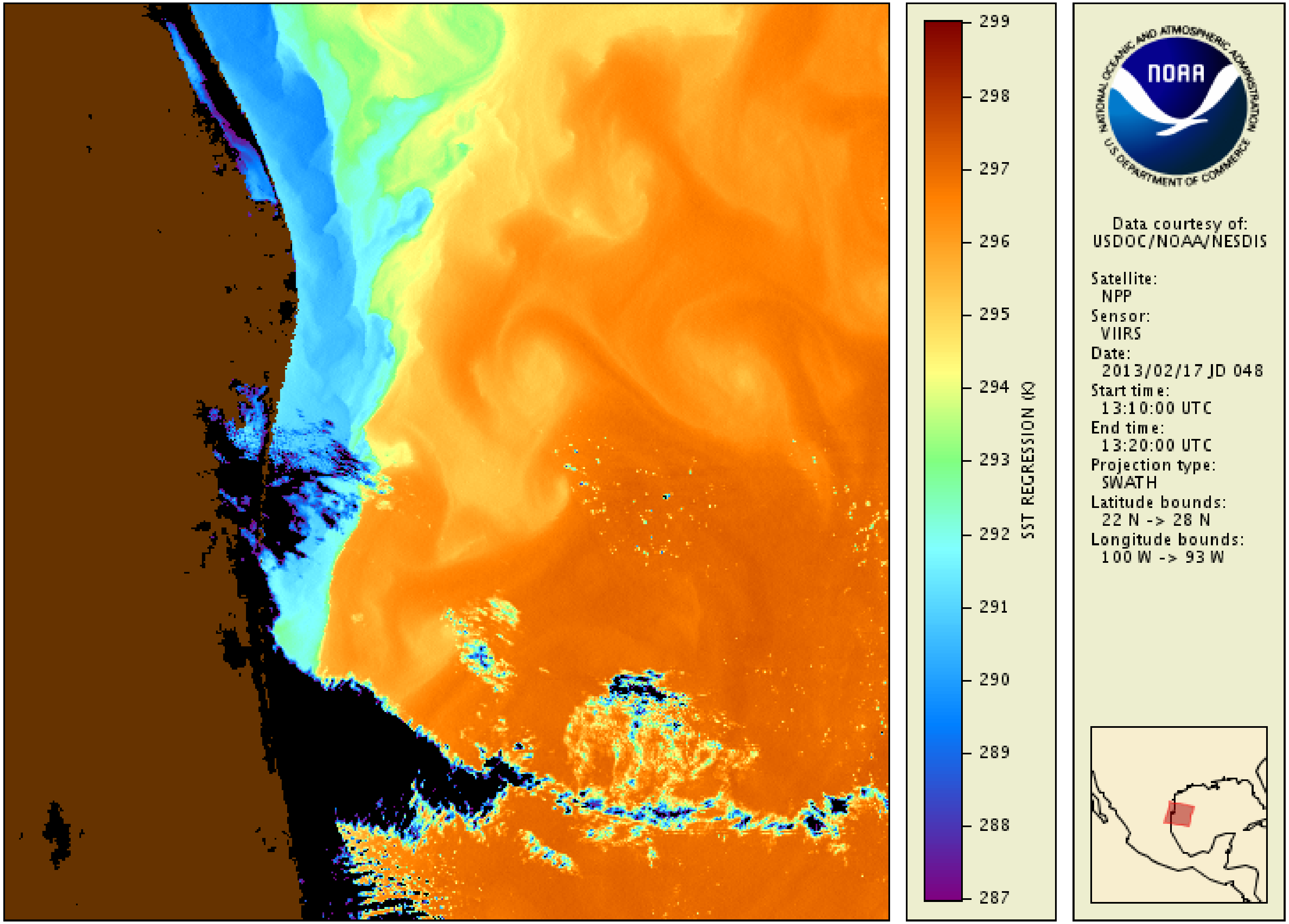

Gulf of Mexico, 02/17/13

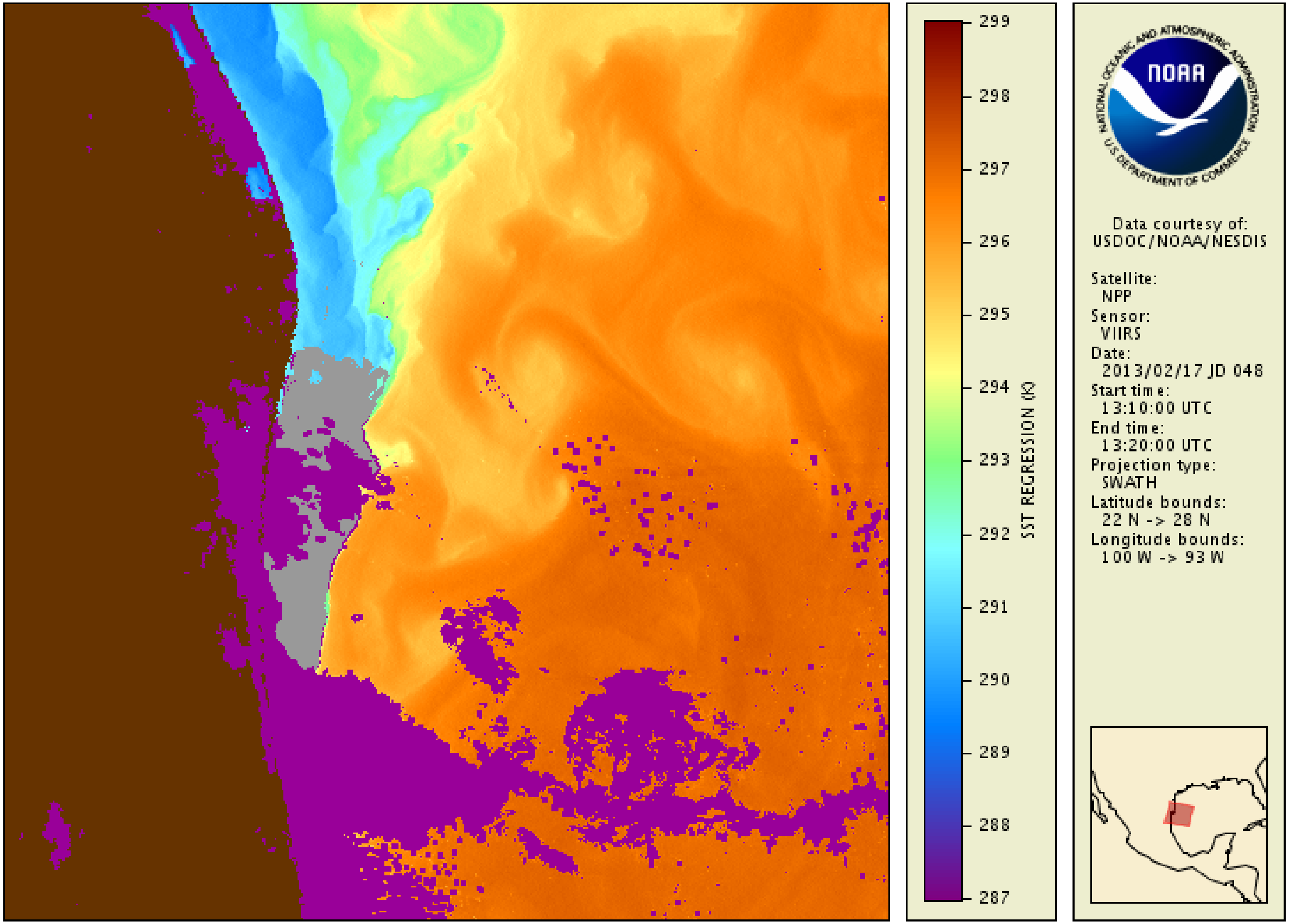

Great Lakes, 02/17/13

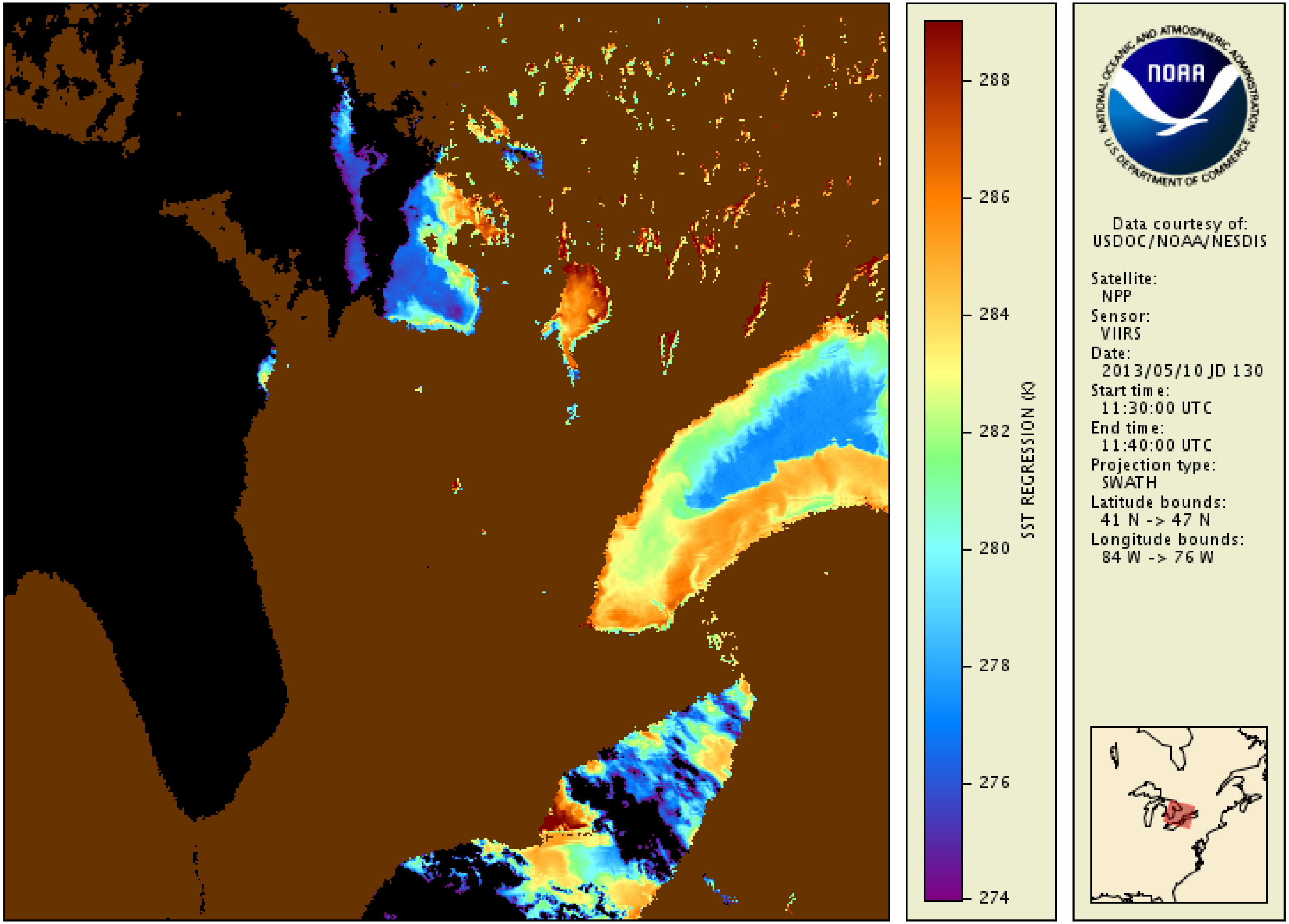

Great Lakes, 02/17/13

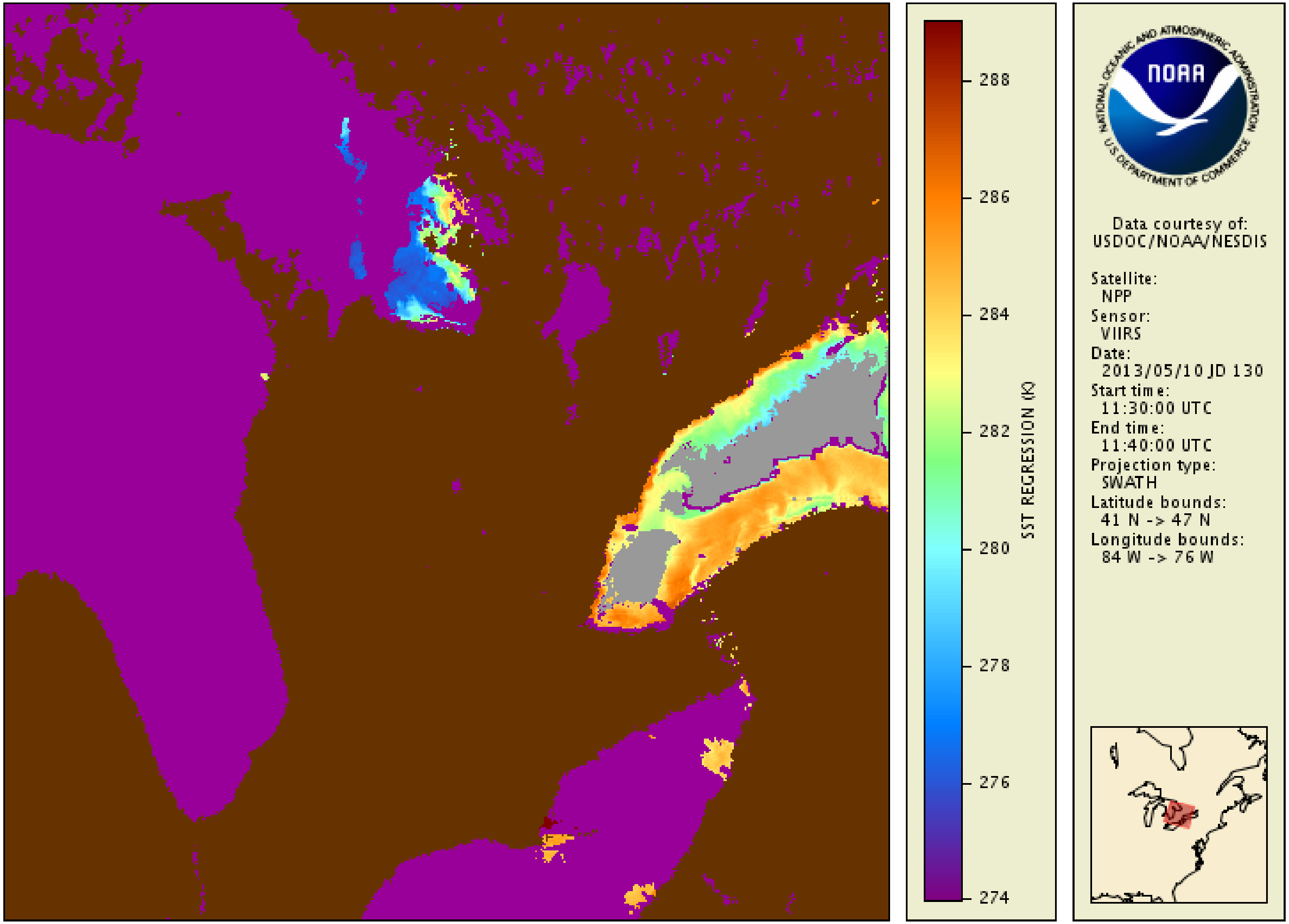

Uruguay, 05/05/13 (night)

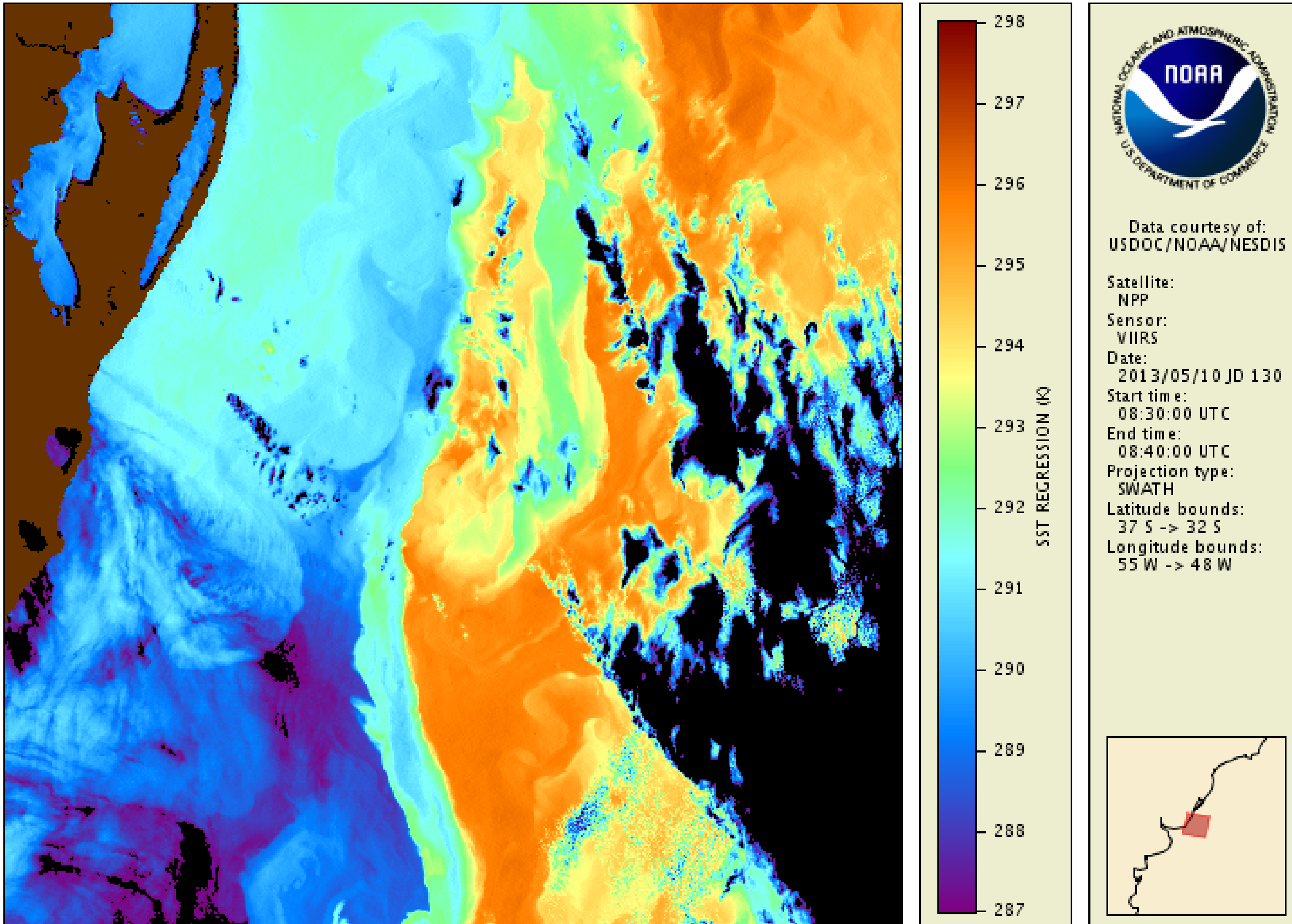

Uruguay, 05/05/13 (night)

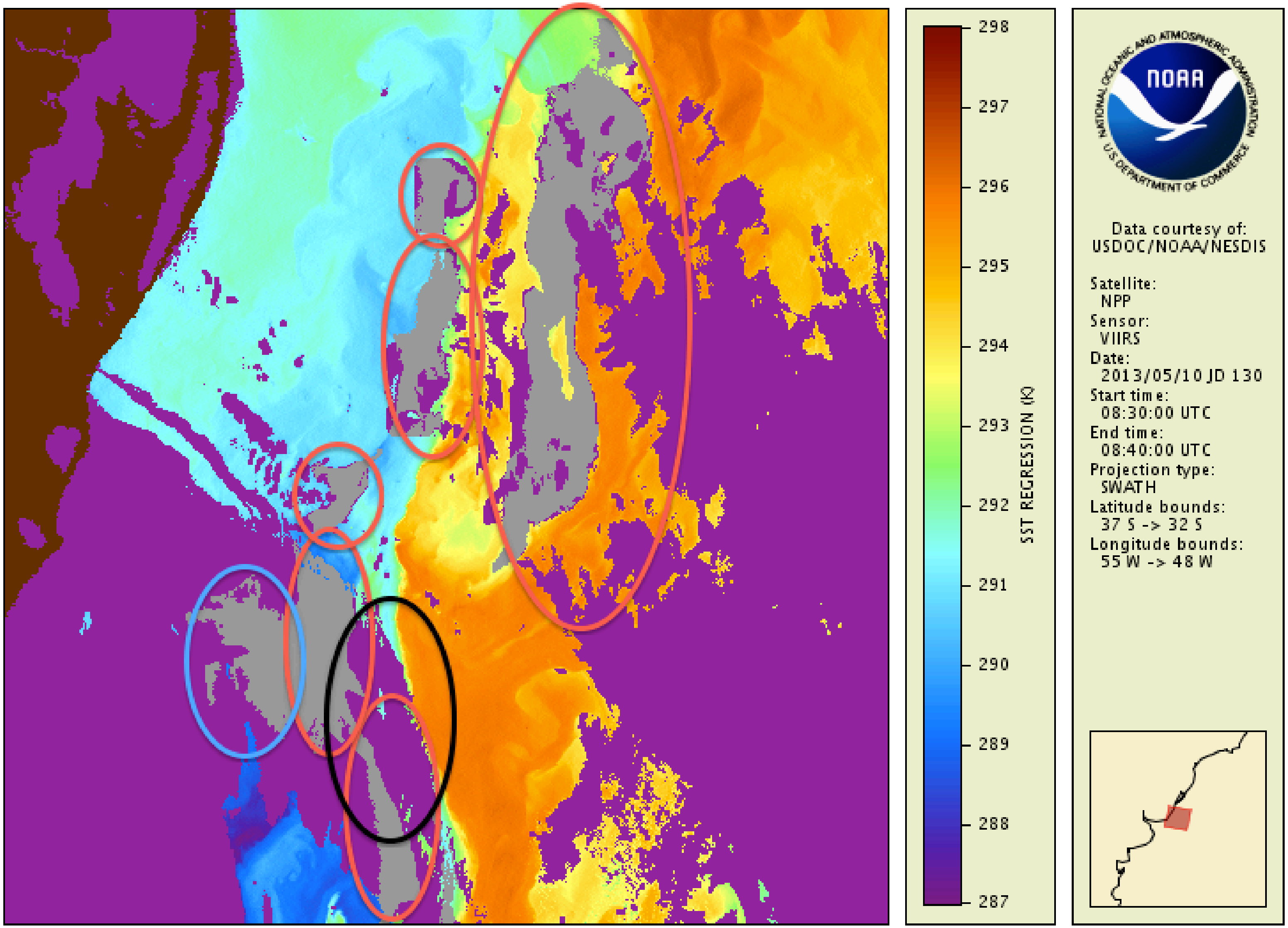

Pamlico Sound, 02/16/13 (night)

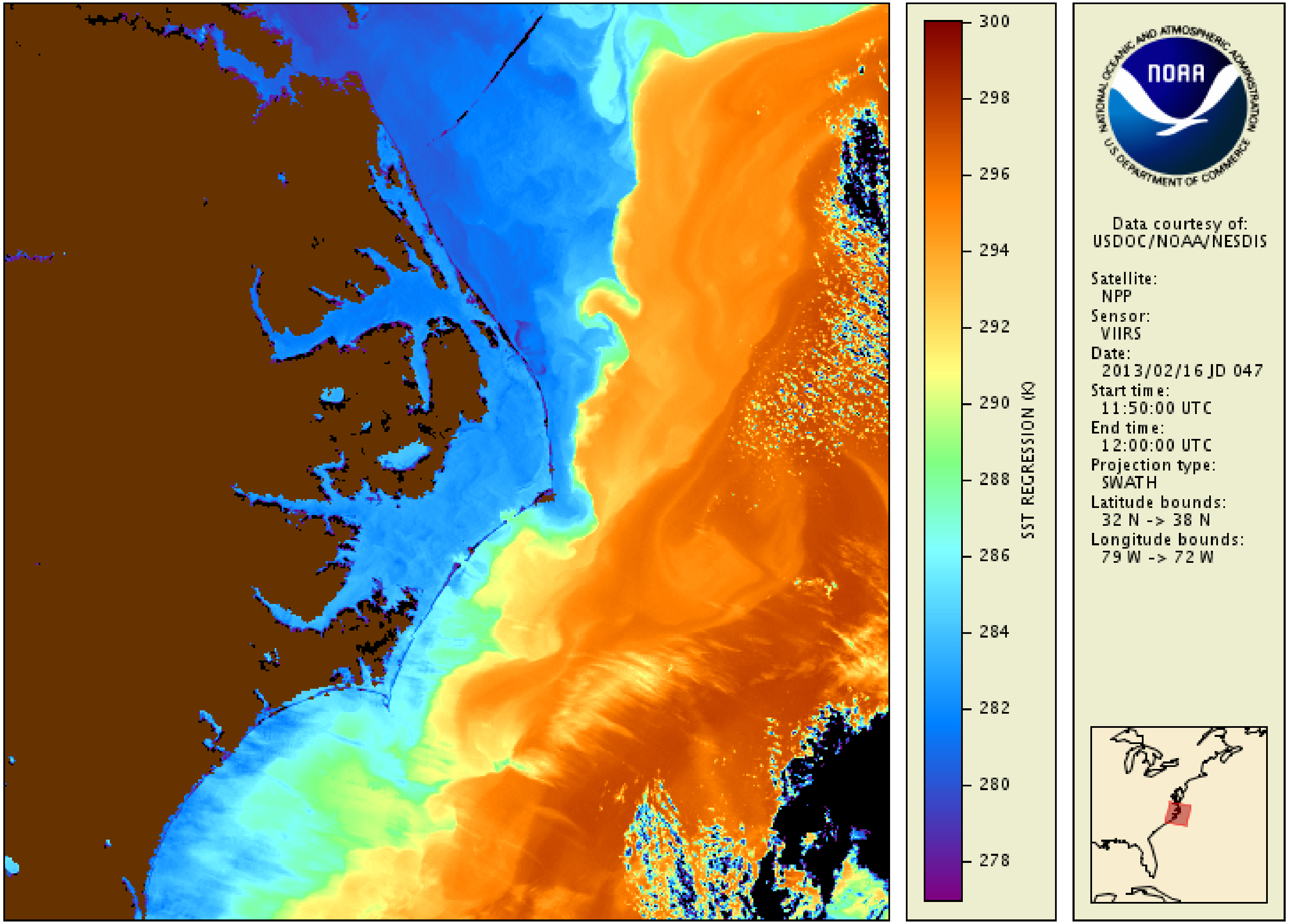

Pamlico Sound, 02/16/13 (night)

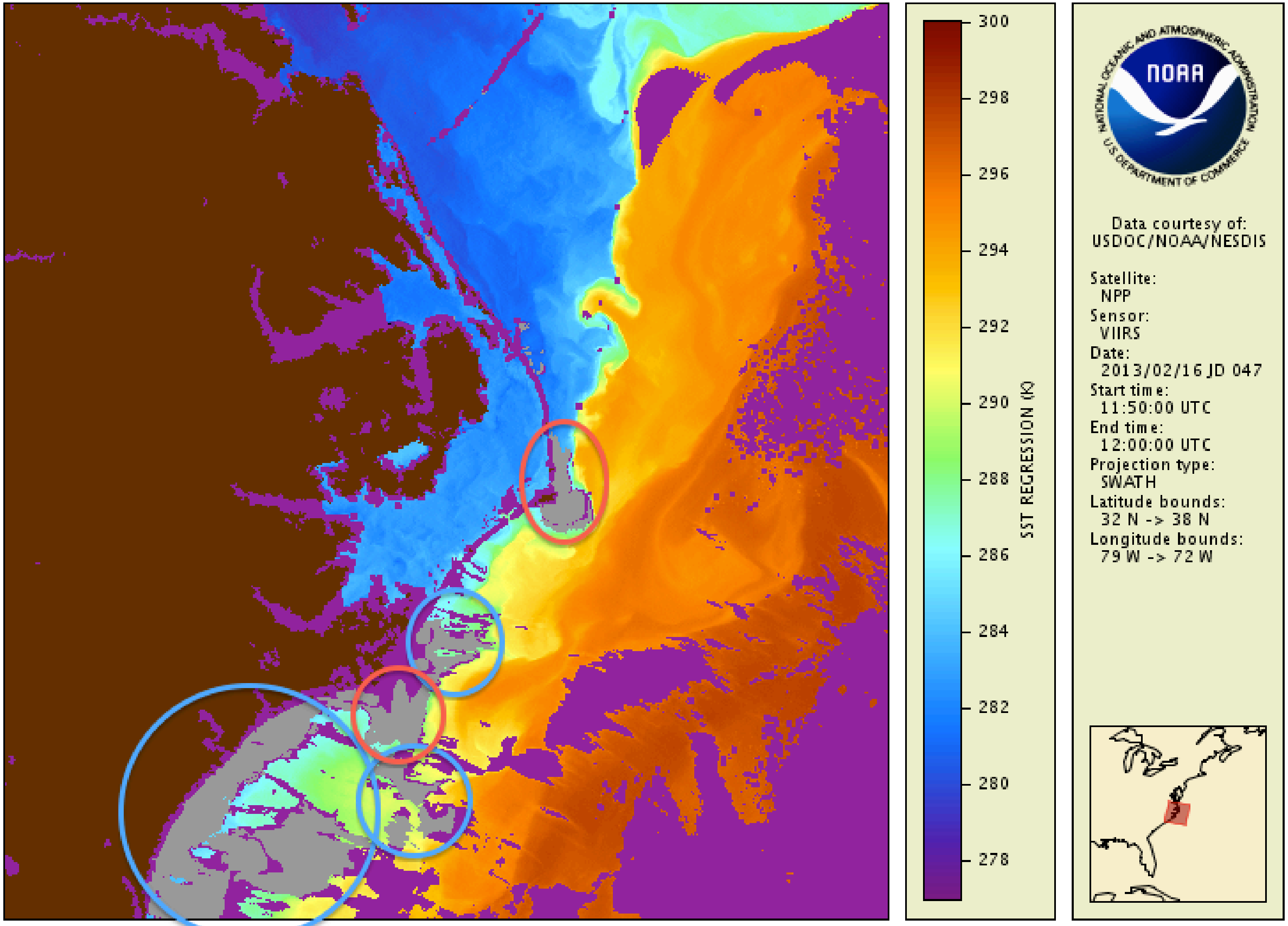

Conclusion

- A supplemental algorithm to the current ACSPO Clear-Sky Mask based on pattern recognition is being explored.
- Our preliminary analyses suggest that some of the limitations inherent to the current ACSM may be alleviated and SST coverage improved.
- The improvements are mostly noticeable in the areas interesting to ACSPO users, including dynamic areas of the ocean and coastal zones.
- Future work will include tuning the algorithm, with emphasis on resolving the remaining cloud leakages.

Destriping VIIRS brightness temperatures for SST

Karlis Mikelsons, Marouan Bouali, Alexander Ignatov, Yury Kihai

NOAA STAR, CSU CIRA, and GST Inc

STAR JPSS Annual Meeting
College Park, MD
May 14, 2014

Motivation: Example striping in nighttime VIIRS M12 BT

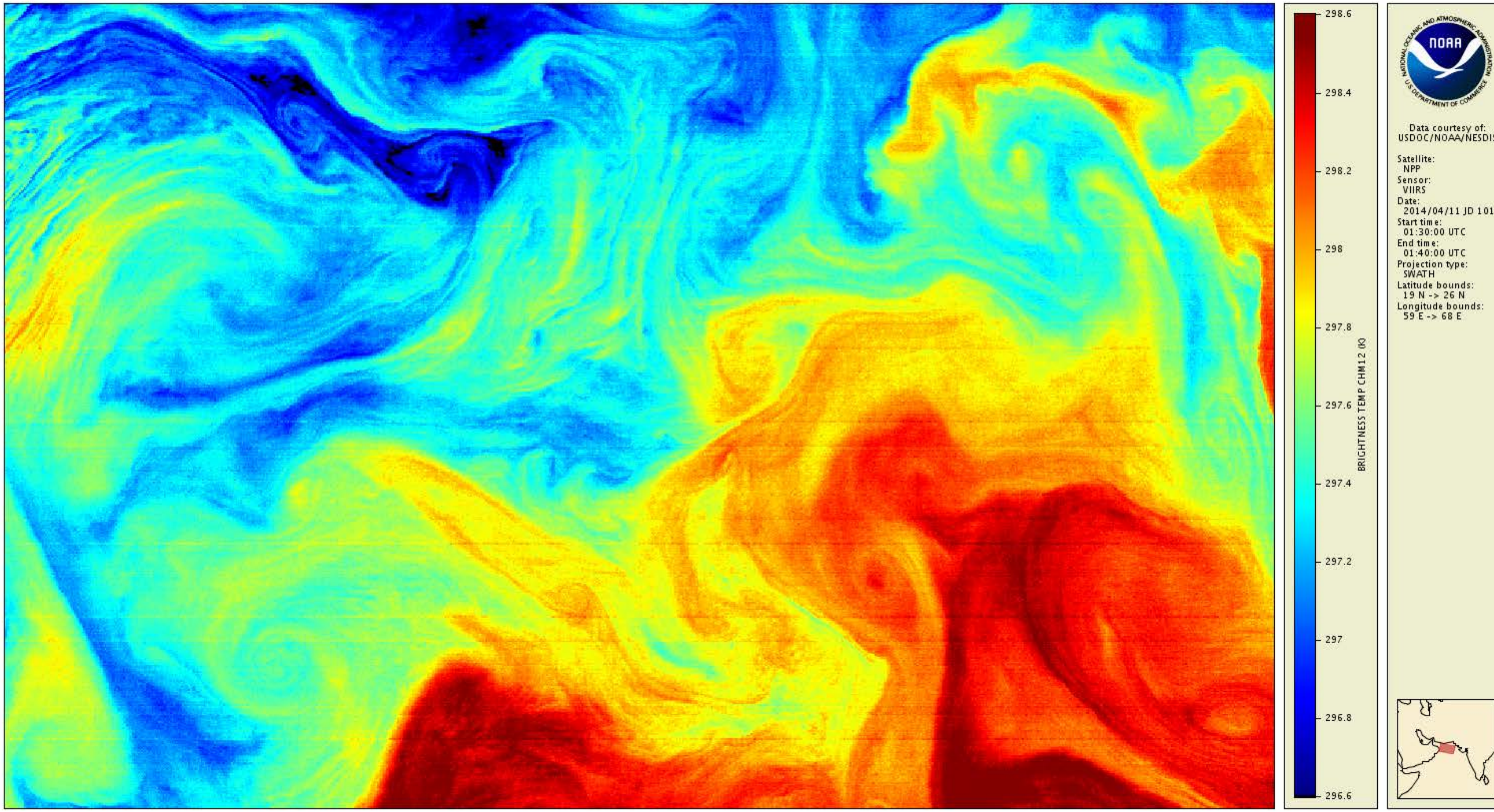

- Low amplitude
- Unidirectional artifact
- Strongly affects SST gradients

Destriping Method

- Start with striped image
- Calculate gradients
- Discard “y” gradients in striped, but otherwise smooth regions
- Poisson reconstruction (with DCT using FFT) yields approximate destriped image
- Split the original image into destriped and striped components

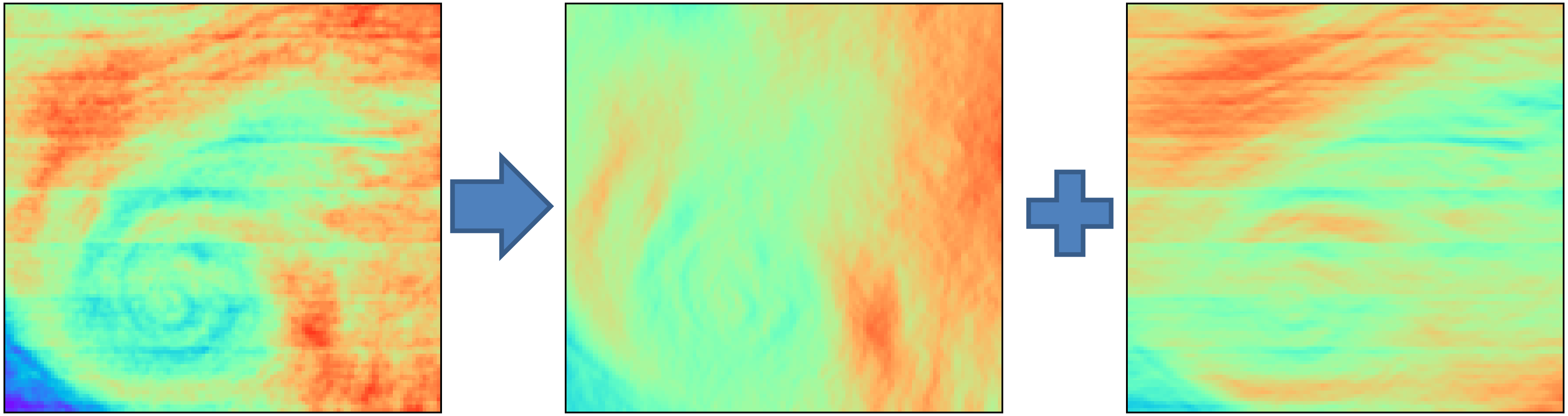

original image **destriped component** **residual striped component**

Algorithm: M. Bouali, A. Ignatov, *J. Atmos. Oceanic Technol.*, **31**, 150-163 (2014).

Destriping Method: Iterative refinement

- At each iteration, contribution to destriped image is extracted from residual striped component
- Repeat until destriped component contains (nearly) all useful information and residual is (nearly) reduced to stripes

residual striped component

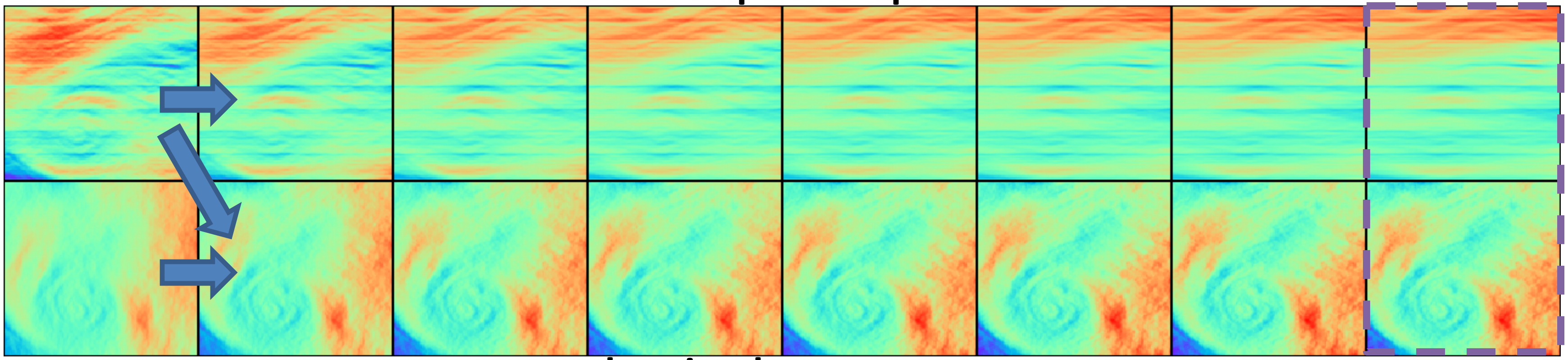

destriped component

Algorithm: M. Bouali, A. Ignatov, *J. Atmos. Oceanic Technol.*, **31**, 150-163 (2014).

Destriping Method: Nonlinear filter

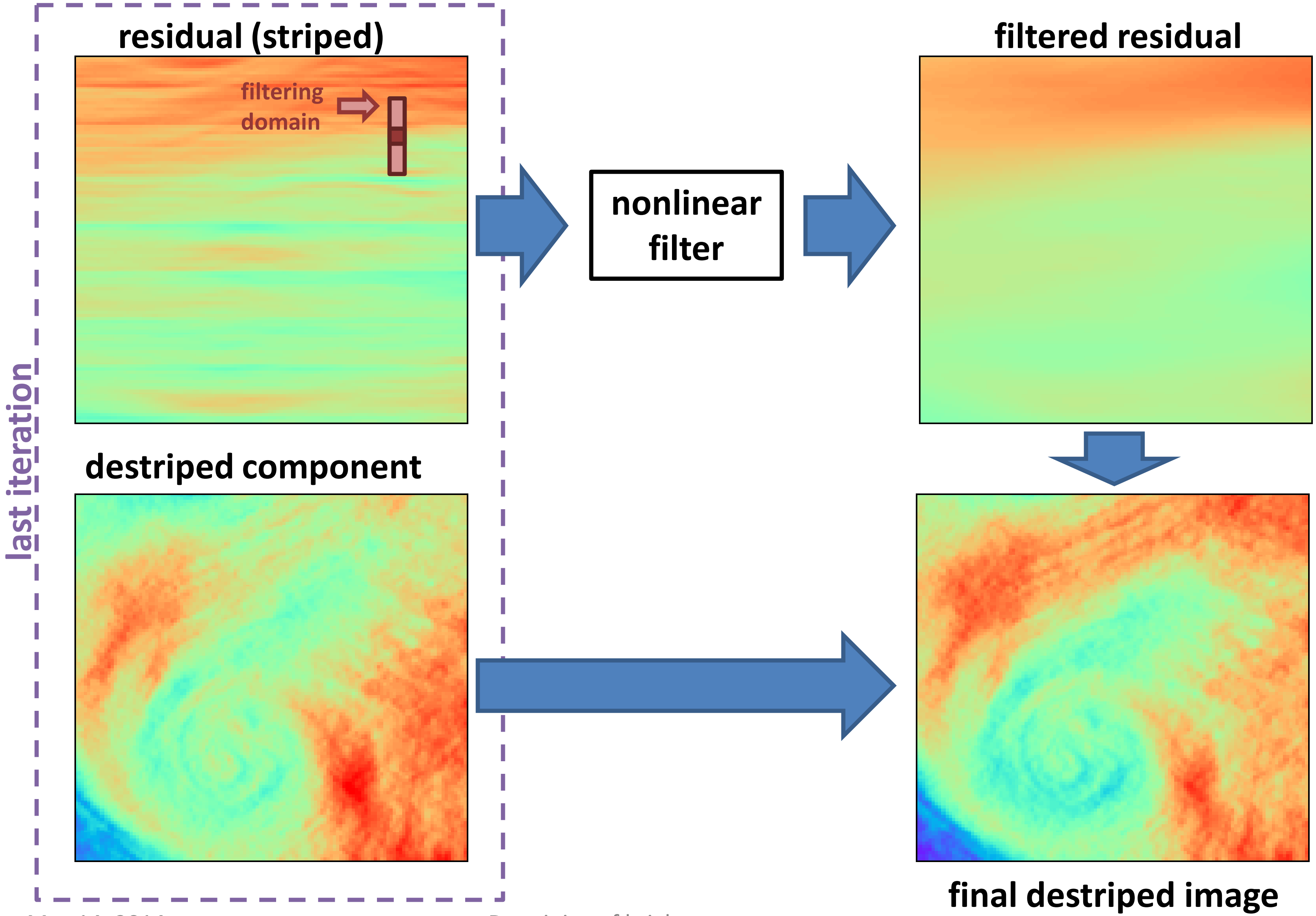

Nighttime

$$T_S = a_0 + (a_1 + a_2 S_\vartheta) T_{3.7} + (a_3 + a_4 S_\vartheta) (T_{11} - T_{12}) + a_5 S_\vartheta$$

$T_{3.7}$, T_{11}, T_{12}	observed BTs in M12, M15, M16
$S_\vartheta = 1/\cos(\vartheta)$	ϑ is view zenith angle
a's	regression coefficients

NIGHT – Original BT in VIIRS band M12 (3.7μm)

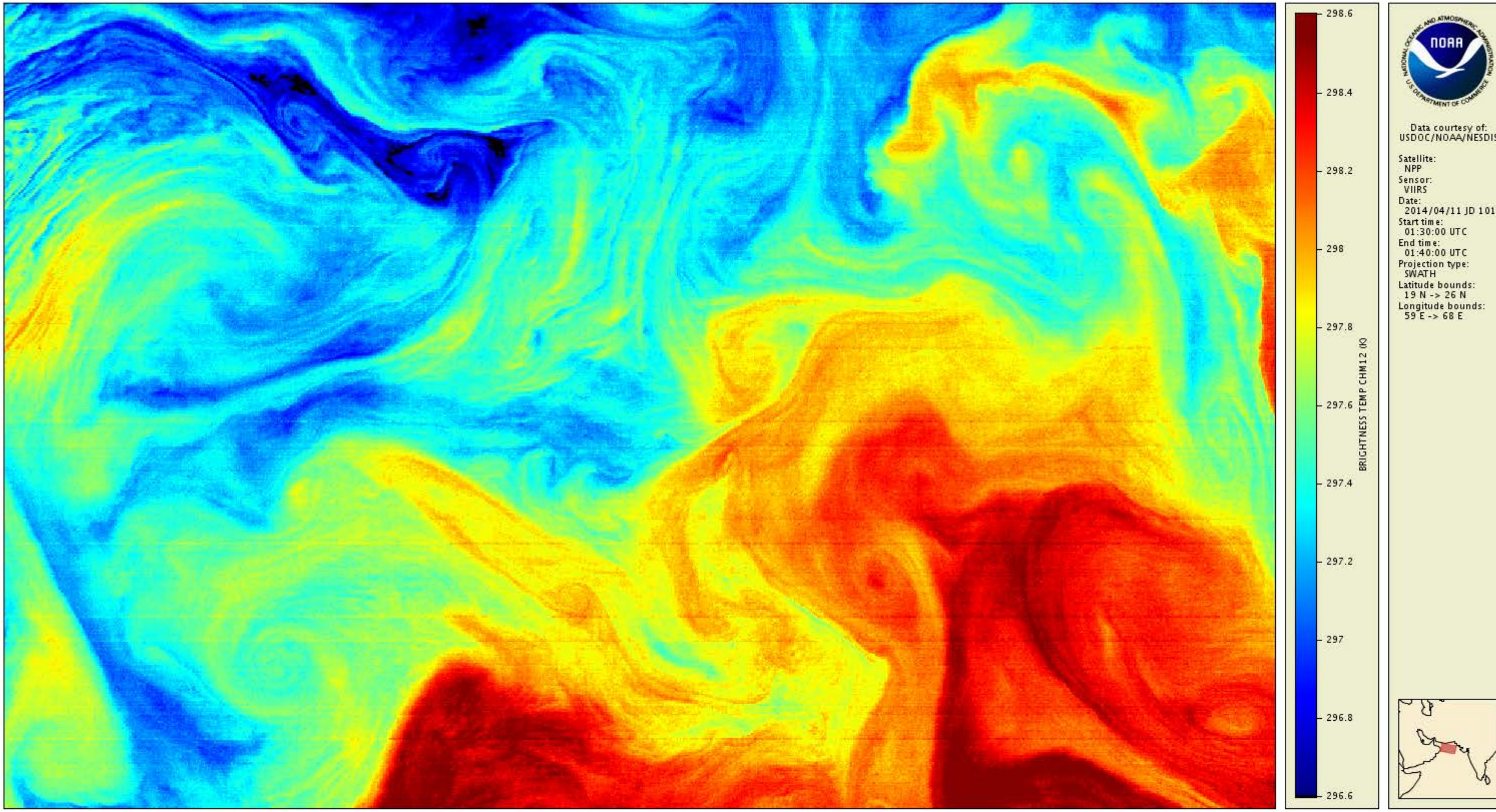

NIGHT – Destriped BT in VIIRS band M12 (3.7μm)

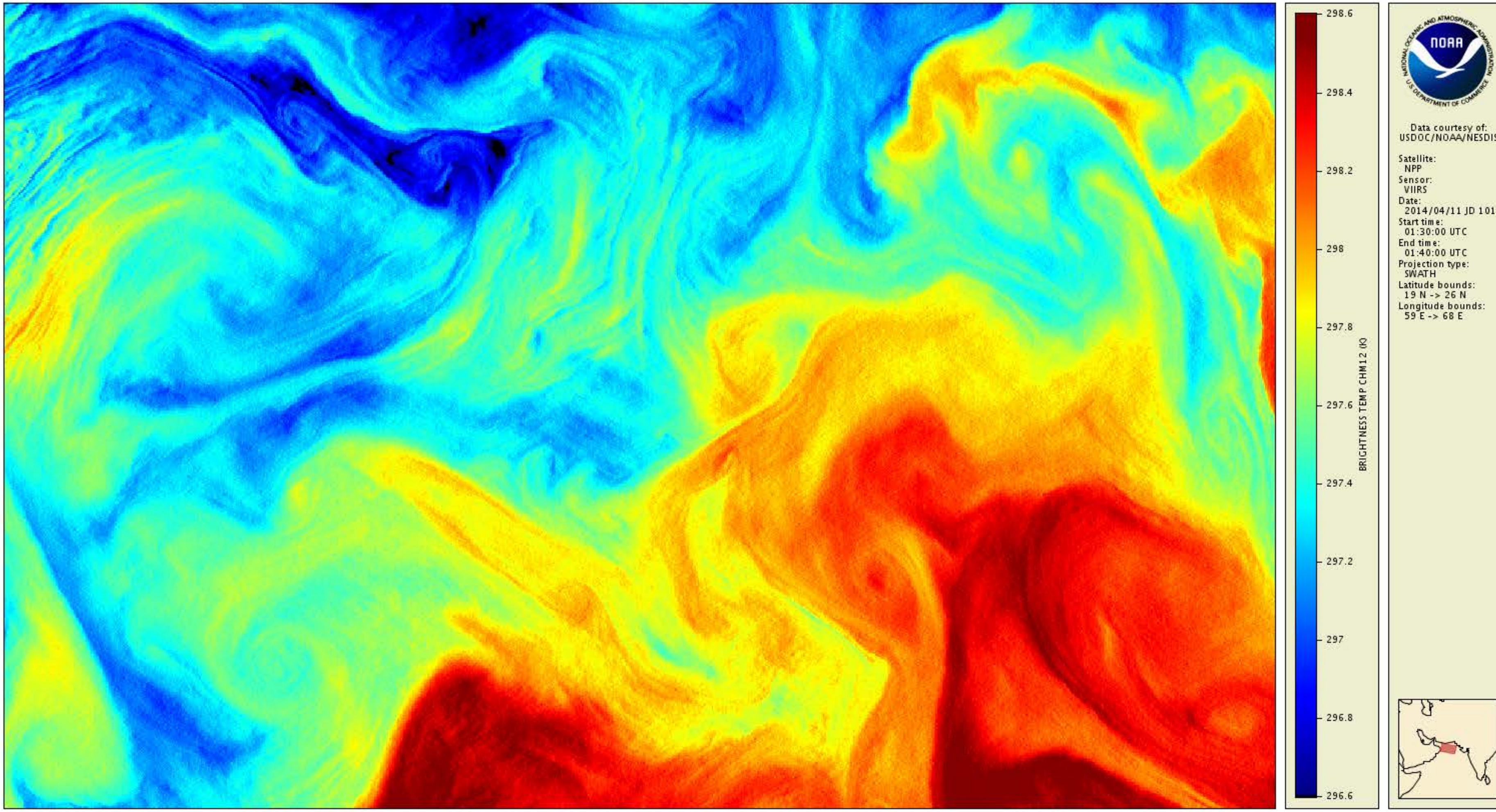

NIGHT – Original BT in VIIRS band M15 (10.8μm)

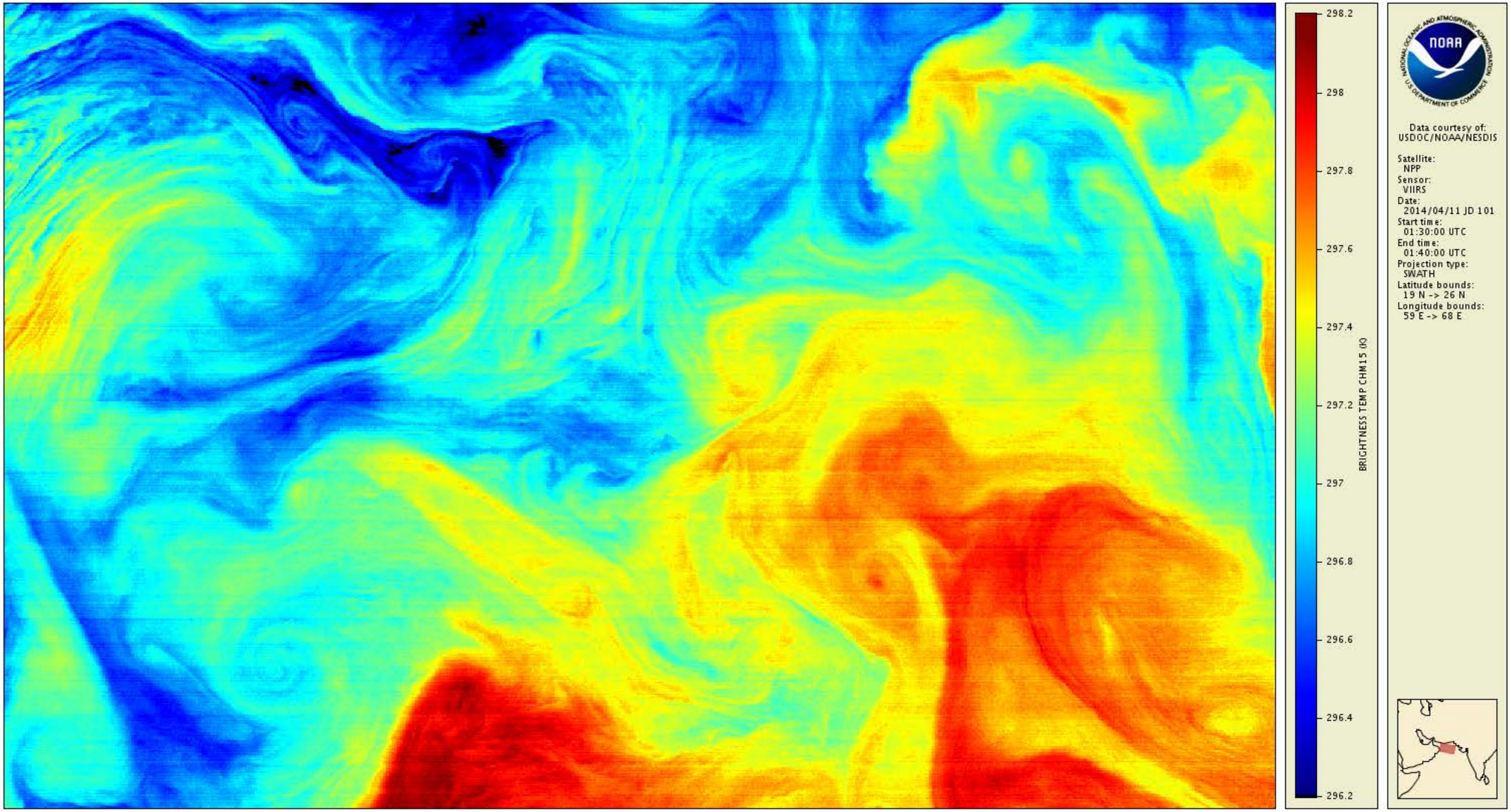

NIGHT – Destriped BT in VIIRS band M15 (10.8μm)

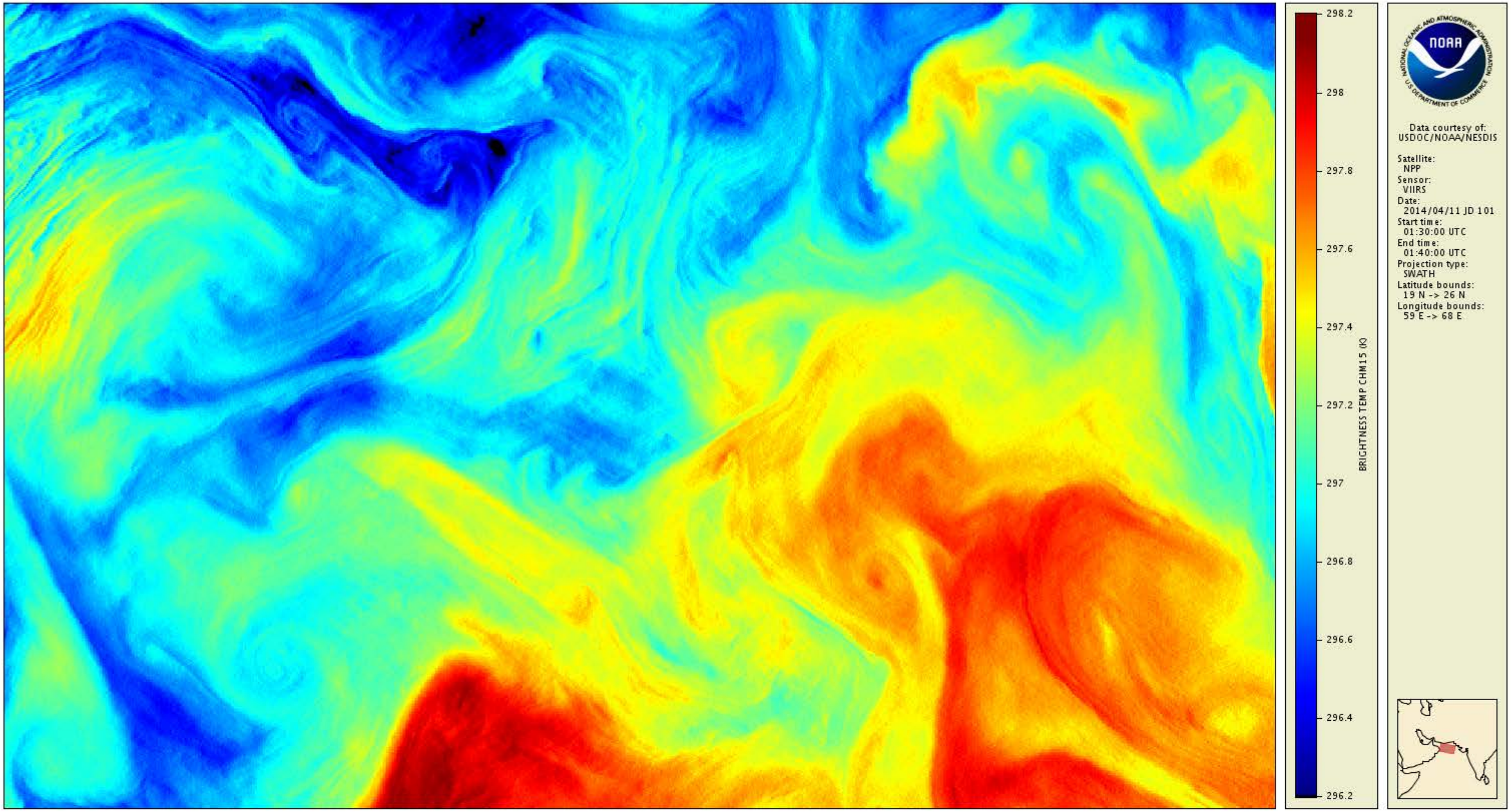

NIGHT – Original BT in VIIRS band M16 (12μm)

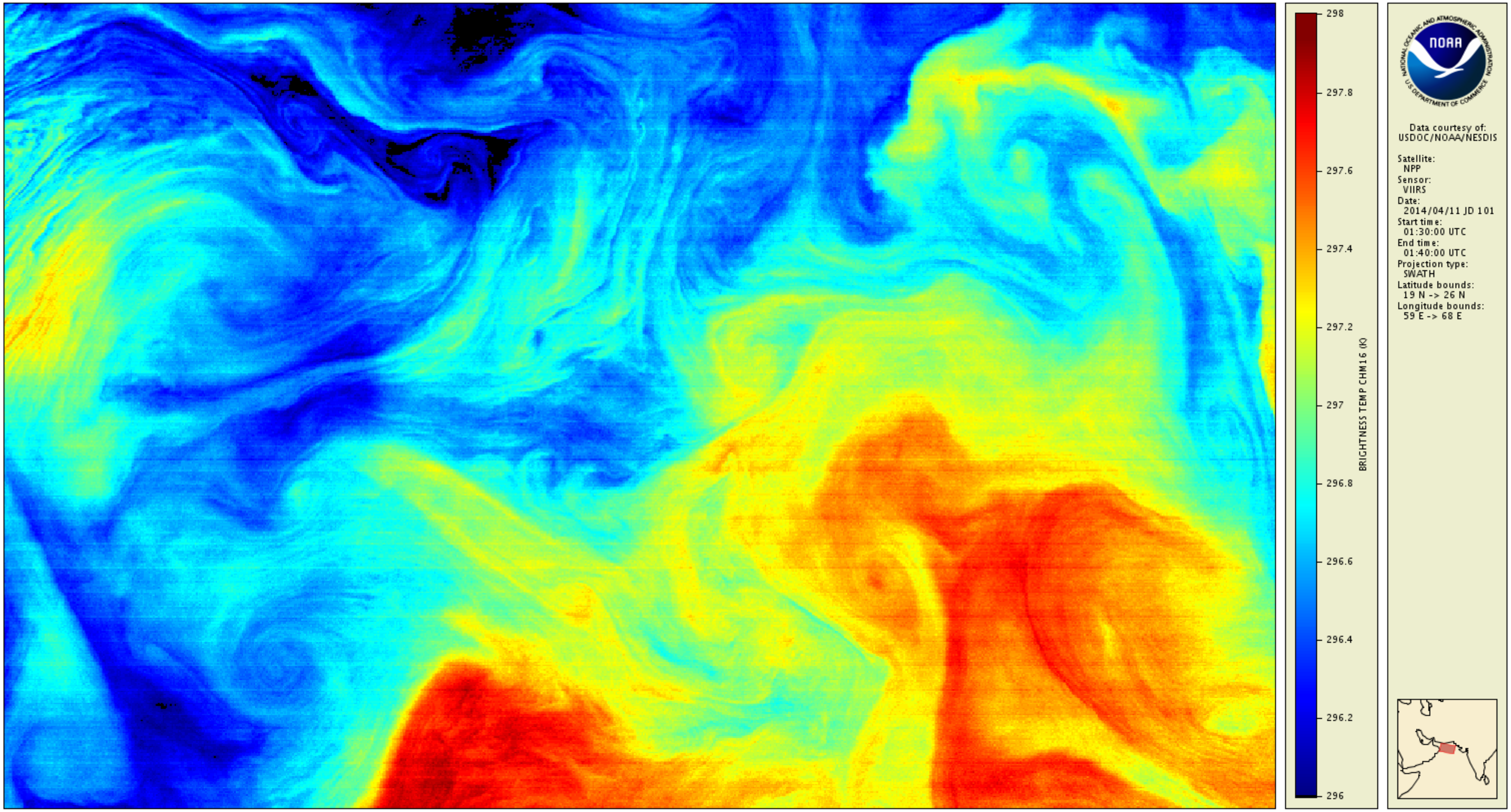

NIGHT – Destriped BT in VIIRS band M16 (12μm)

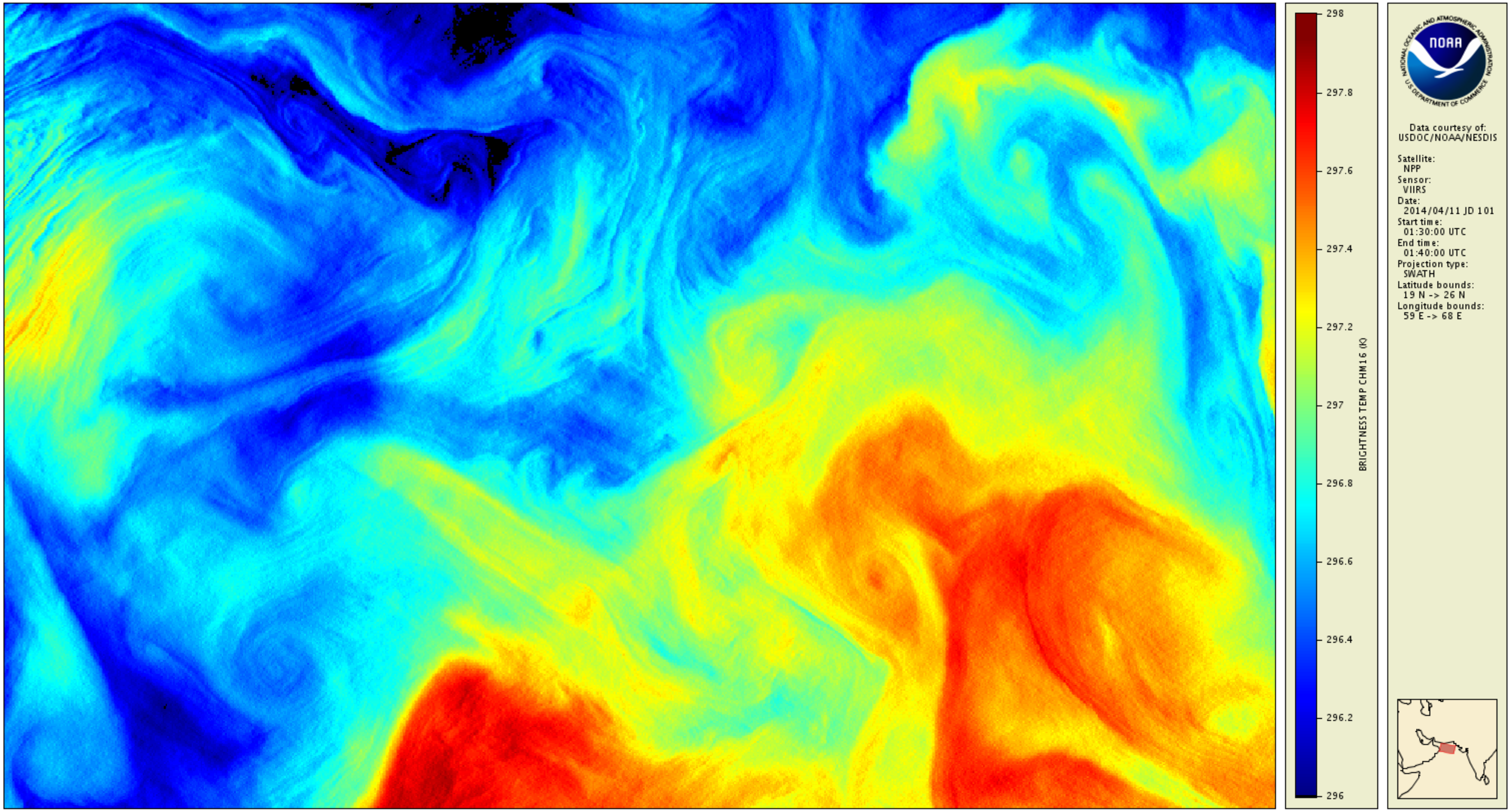

NIGHT – SST from original BTs in M12, M15, M16

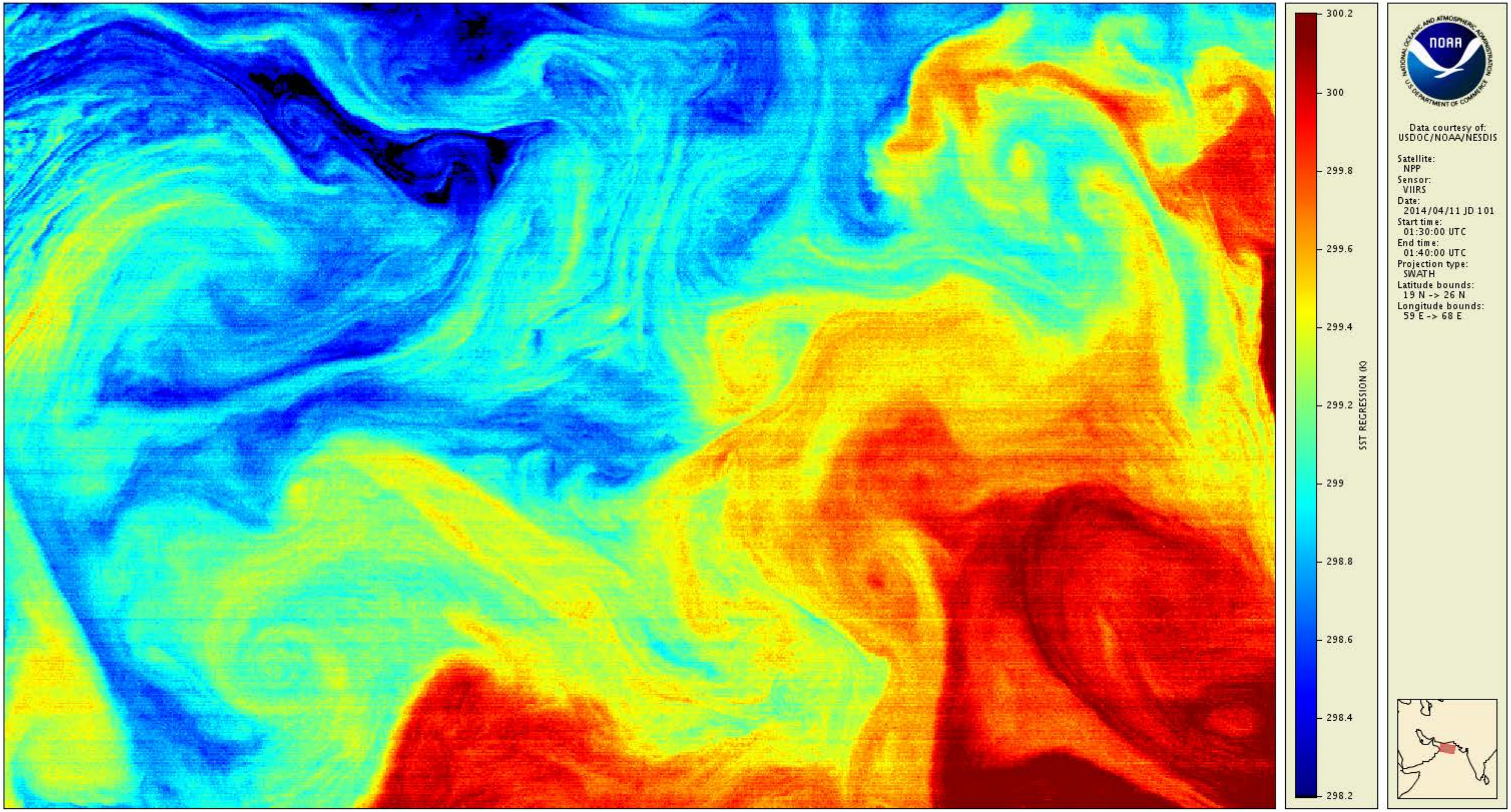

NIGHT – SST from destriped BTs in M12, M15, M16

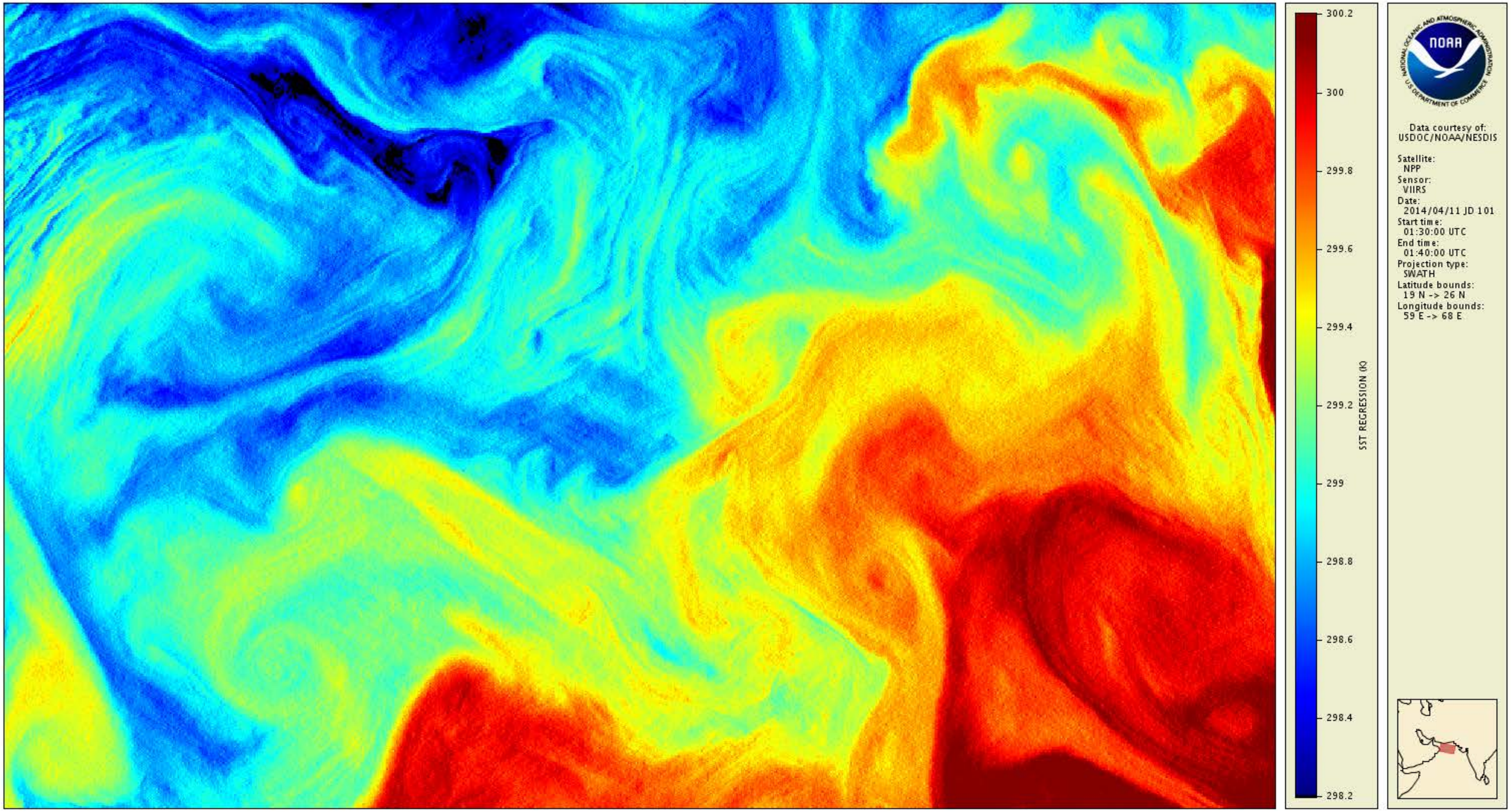

Daytime

$$T_S = a_0 + (a_1 + a_2 S_\vartheta) T_{11} + [a_3 + a_4 T_S^0 + a_5 S_\vartheta] (T_{11} - T_{12}) + a_6 S_\vartheta$$

T_{11}, T_{12}	observed BTs in M15, M16
$S_\vartheta = 1/\cos(\vartheta)$	ϑ is view zenith angle
T_S^0	first guess SST (in °C)
a's	regression coefficients

DAY – Original BT in VIIRS band M15 (10.8μm)

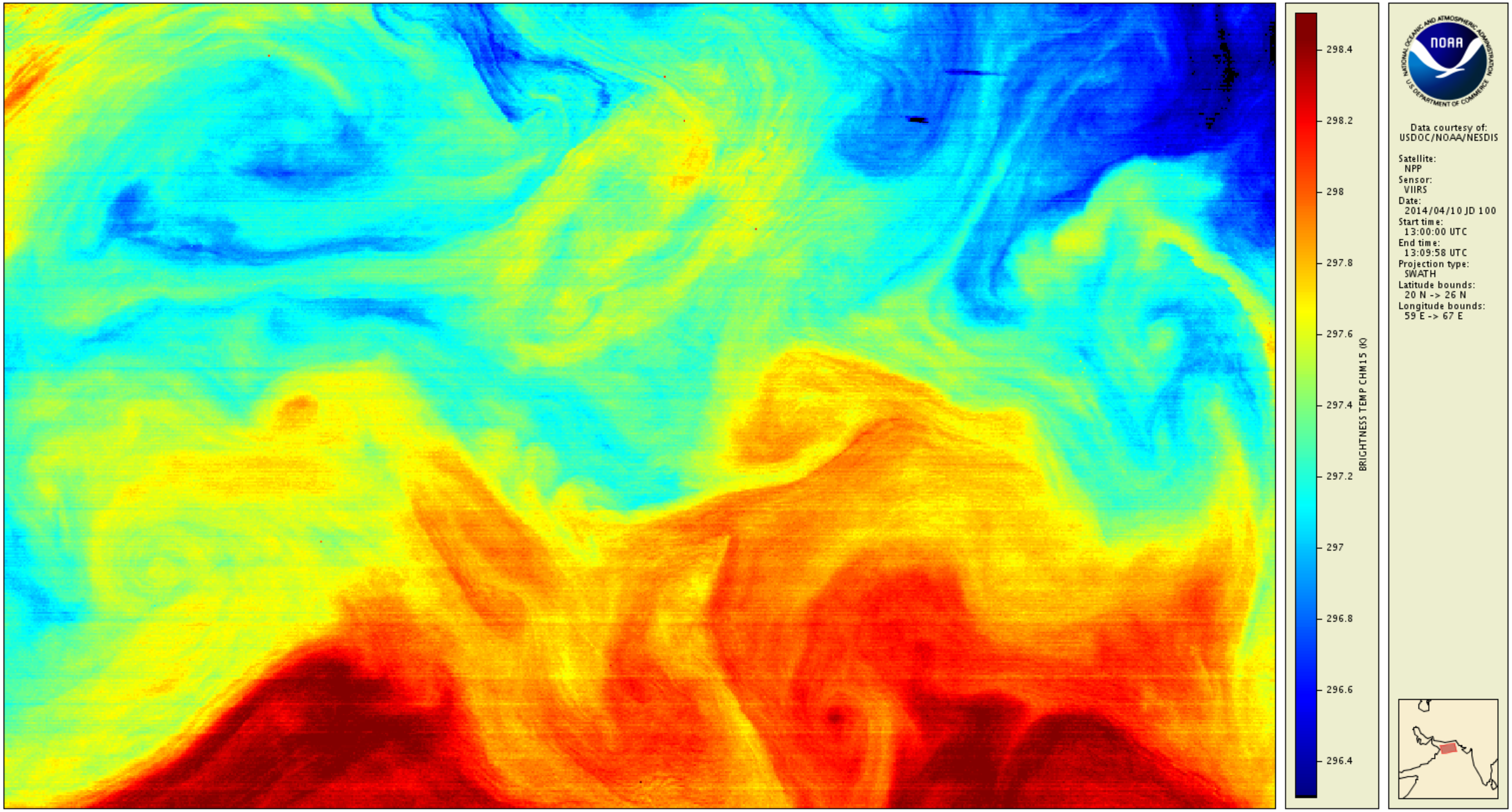

DAY – Destriped BT in VIIRS band M15 (10.8μm)

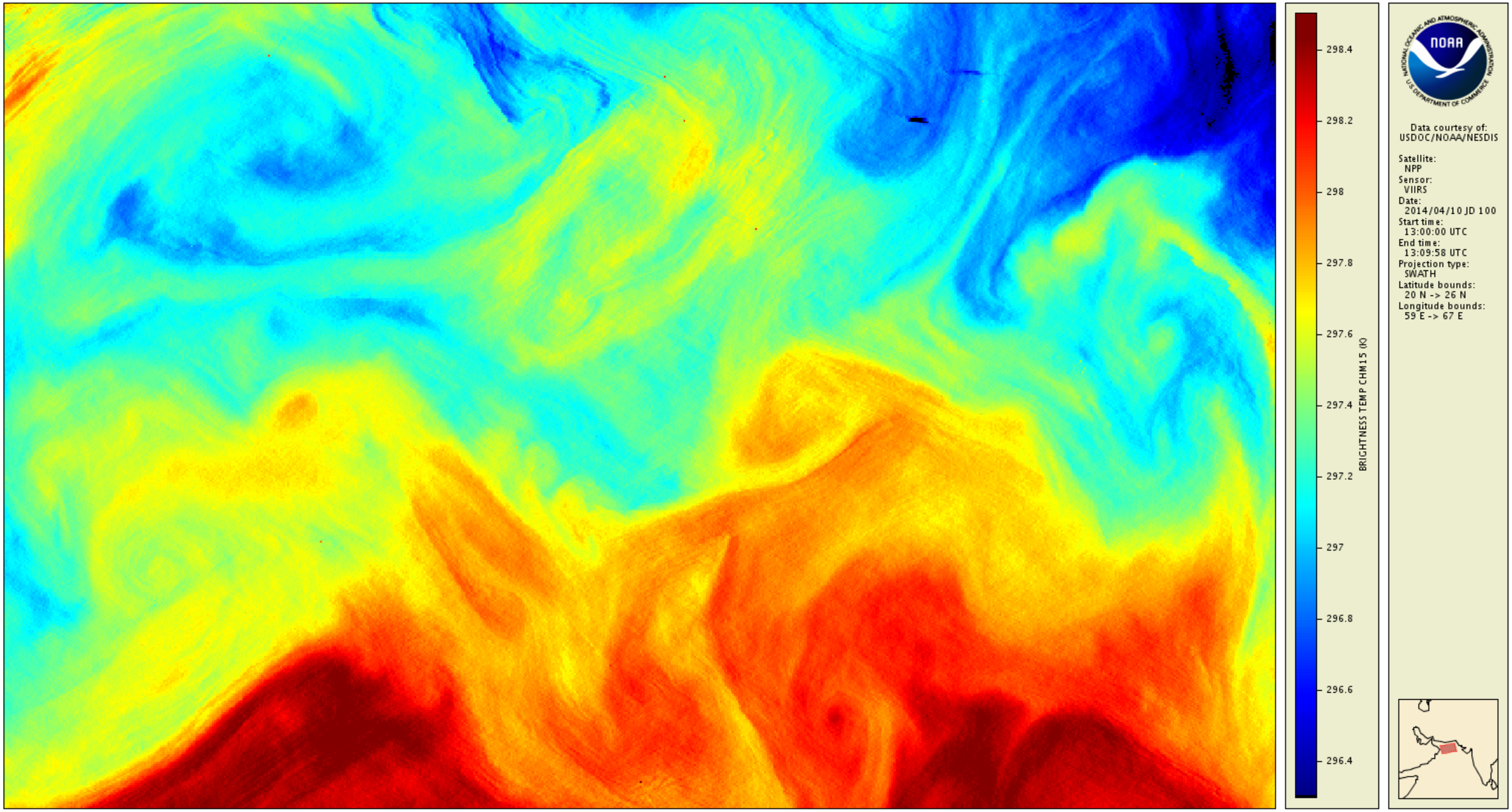

DAY – Original BT in VIIRS band M16 (12μm)

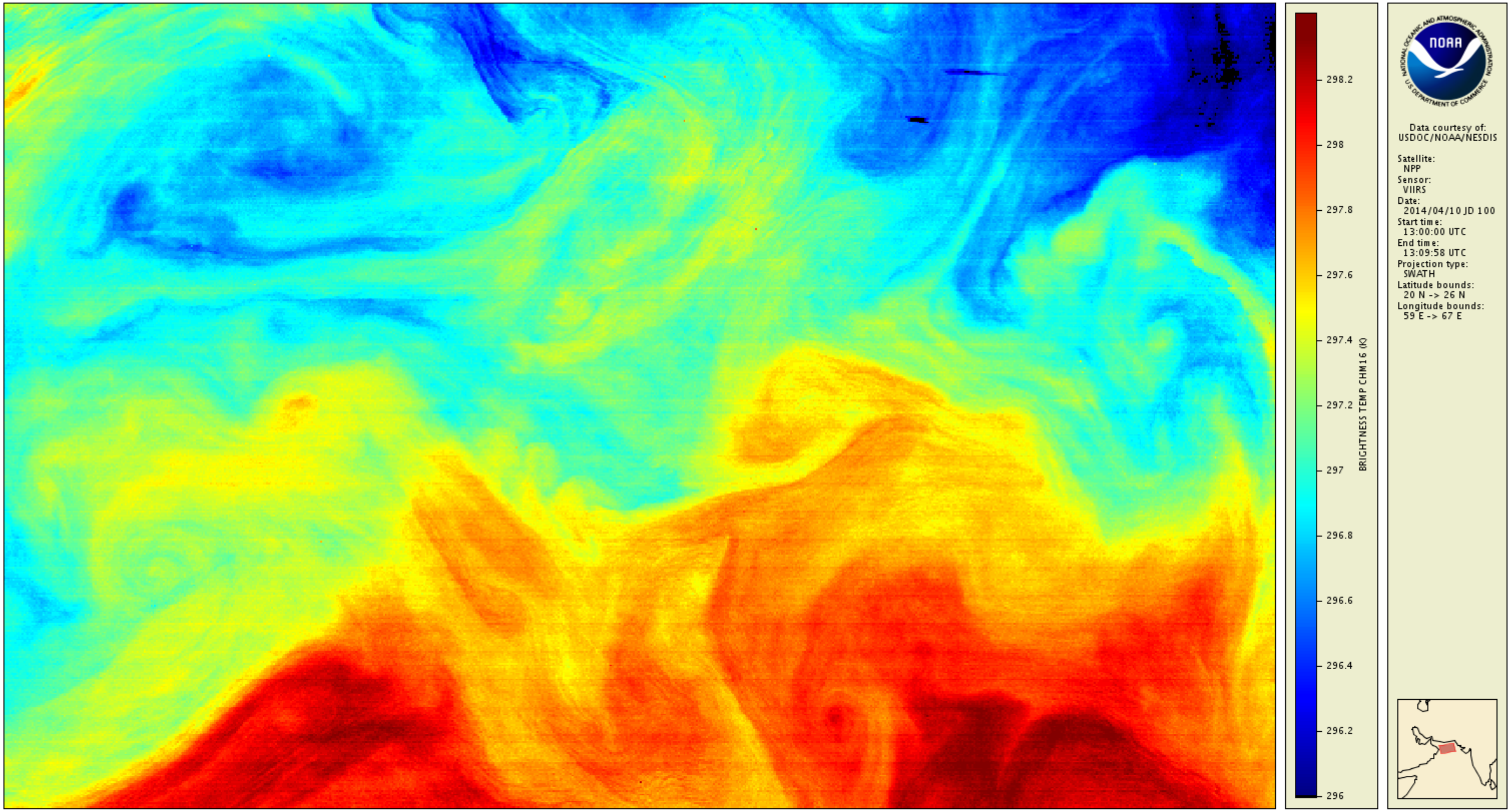

DAY – Destriped BT in VIIRS band M16 (12μm)

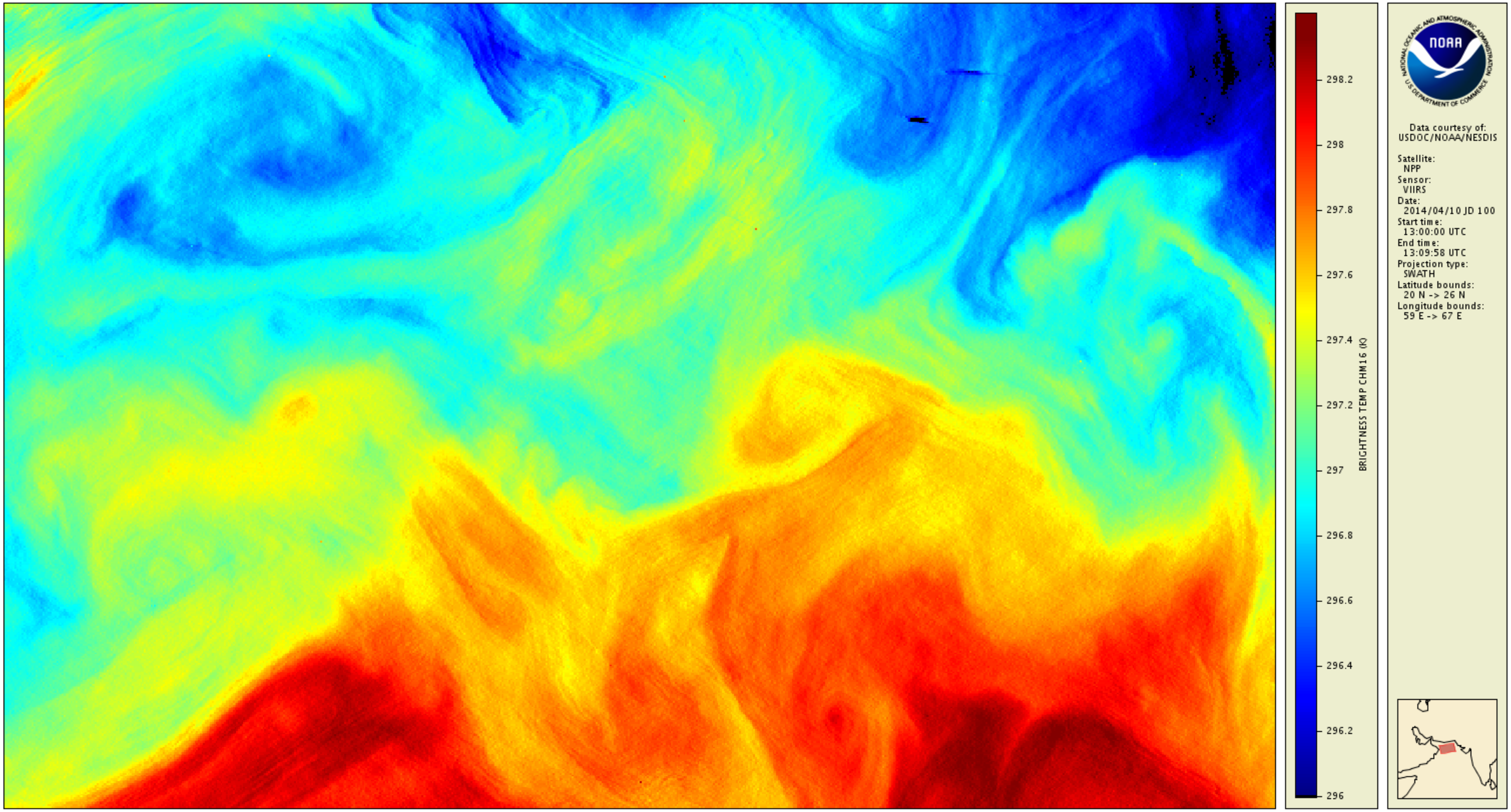

DAY – SST from original BTs in M15 and M16

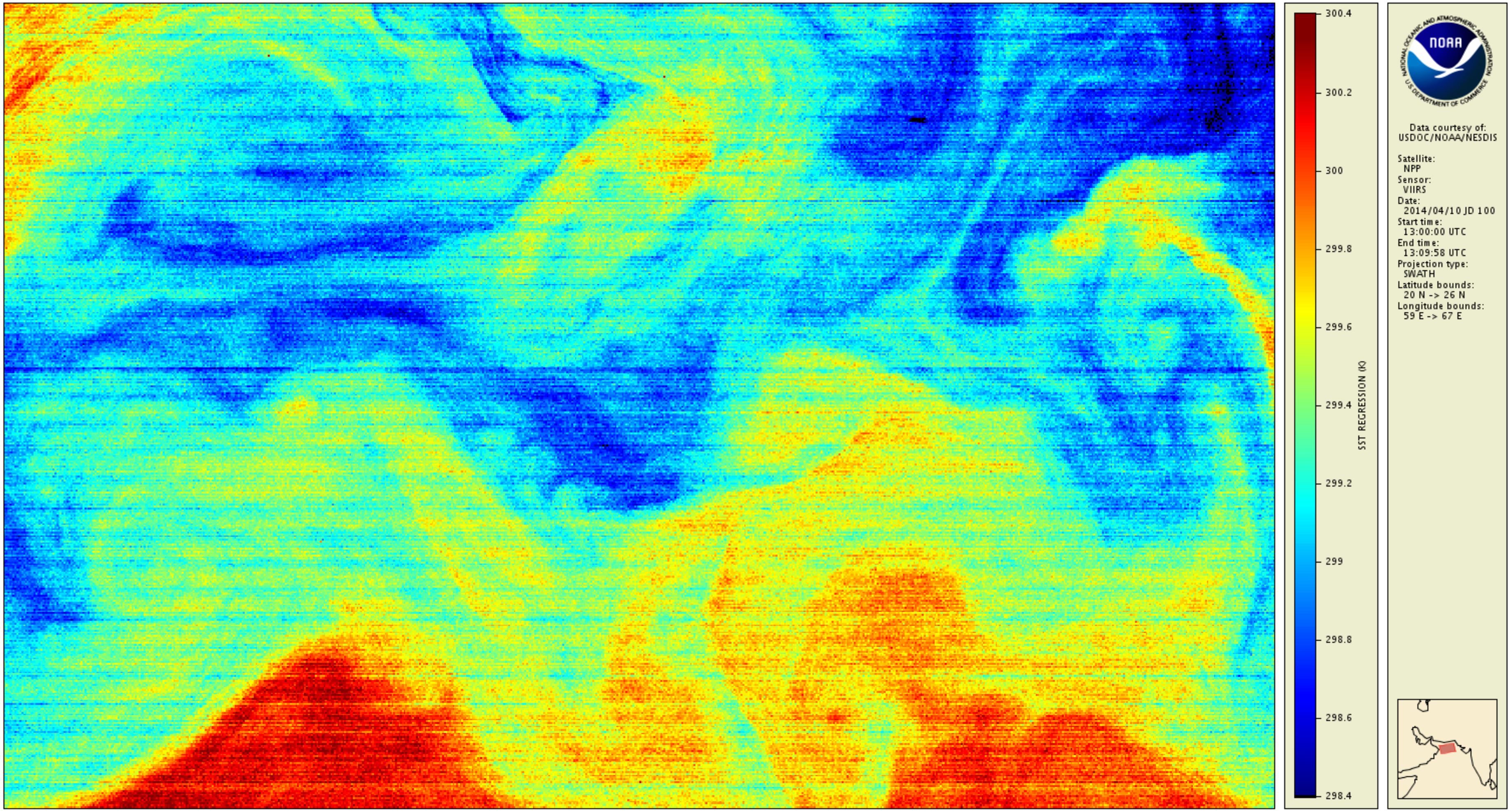

DAY – SST from destriped BTs in M15 and M16

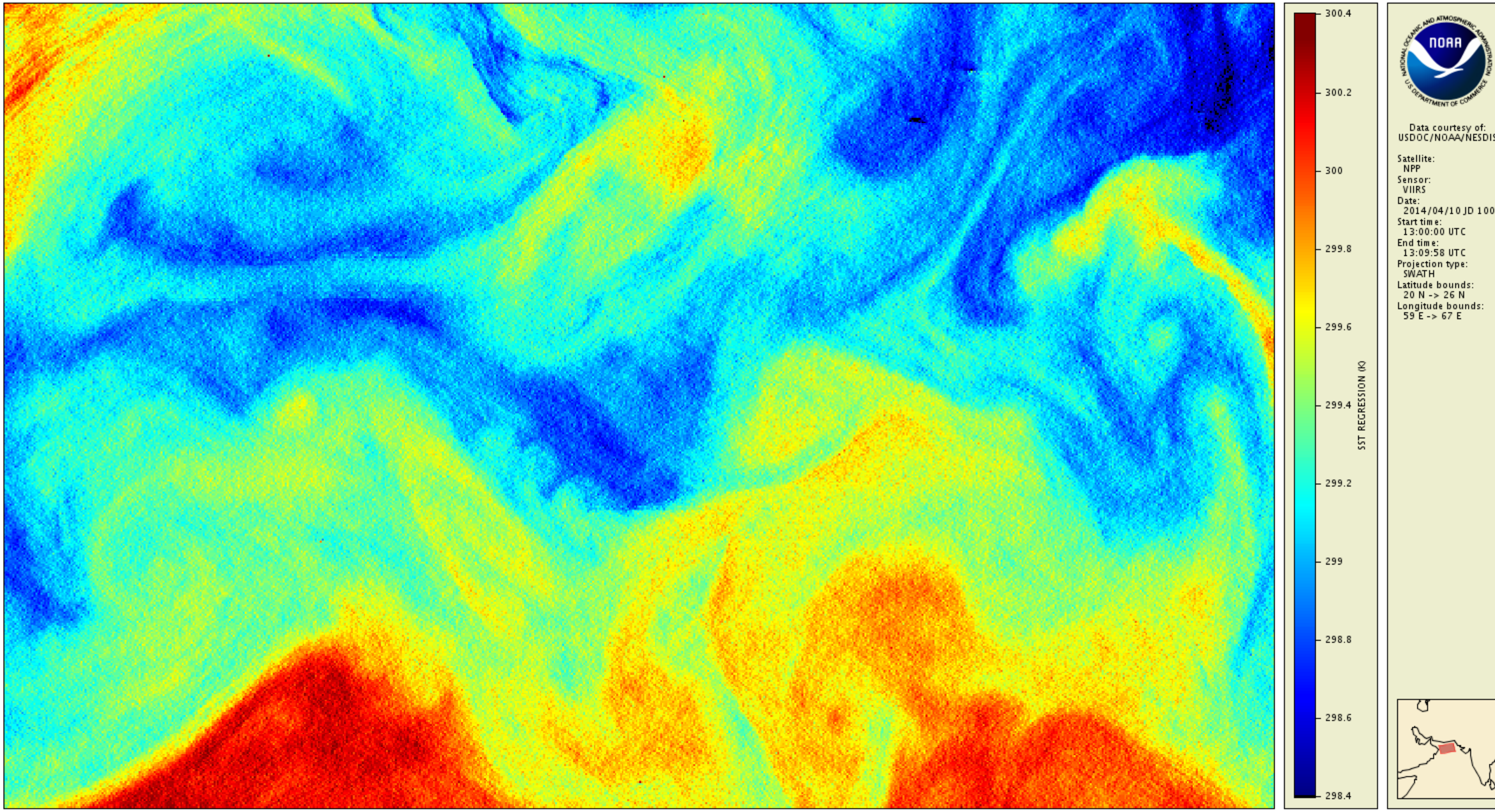

Effect of striping on ACSPO Clear-sky Mask

DAY – SST from original BTs – effect on cloud mask

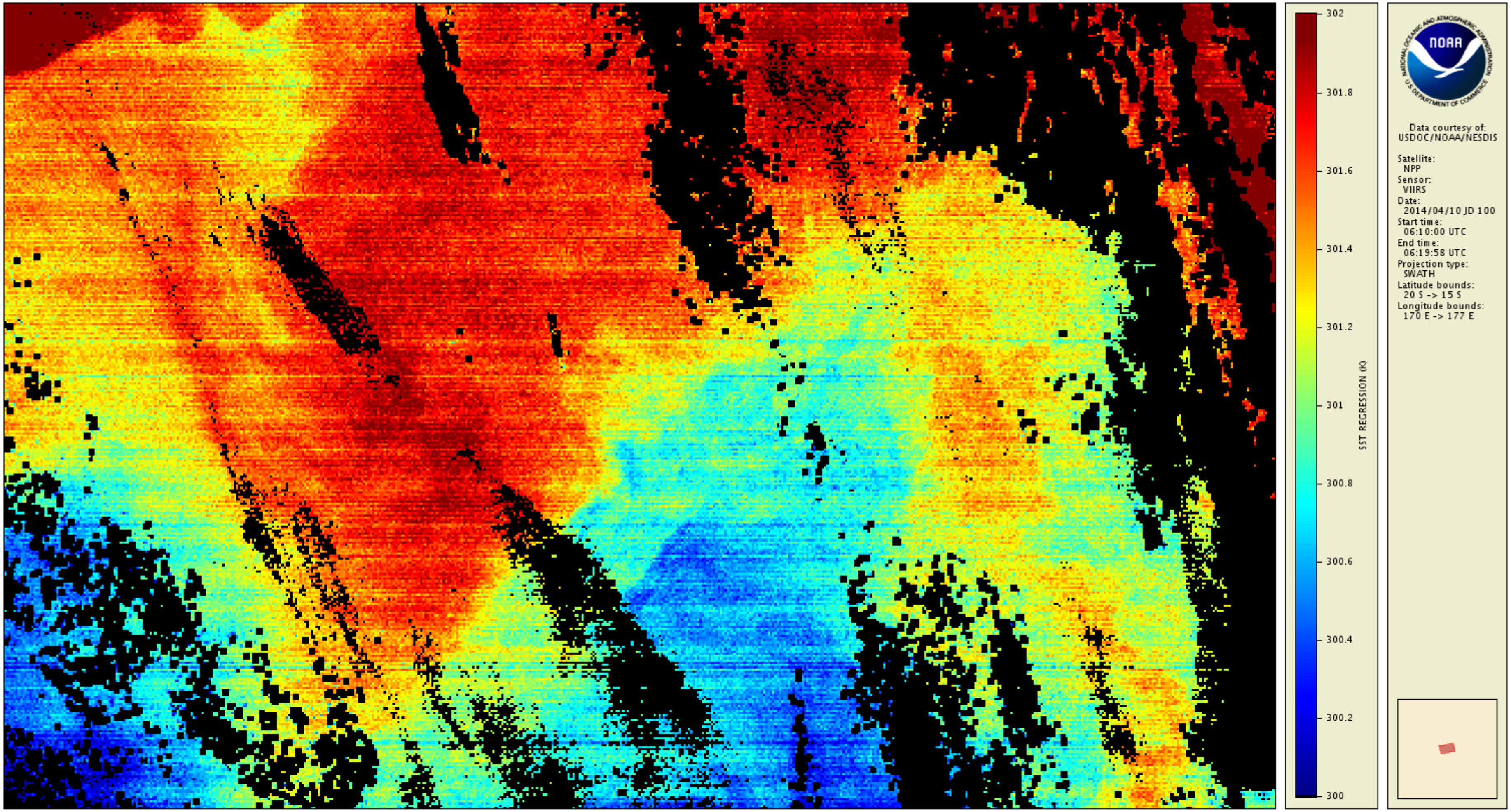

Cloud mask identification affected by striping

DAY – SST from destriped BTs – effect on cloud mask

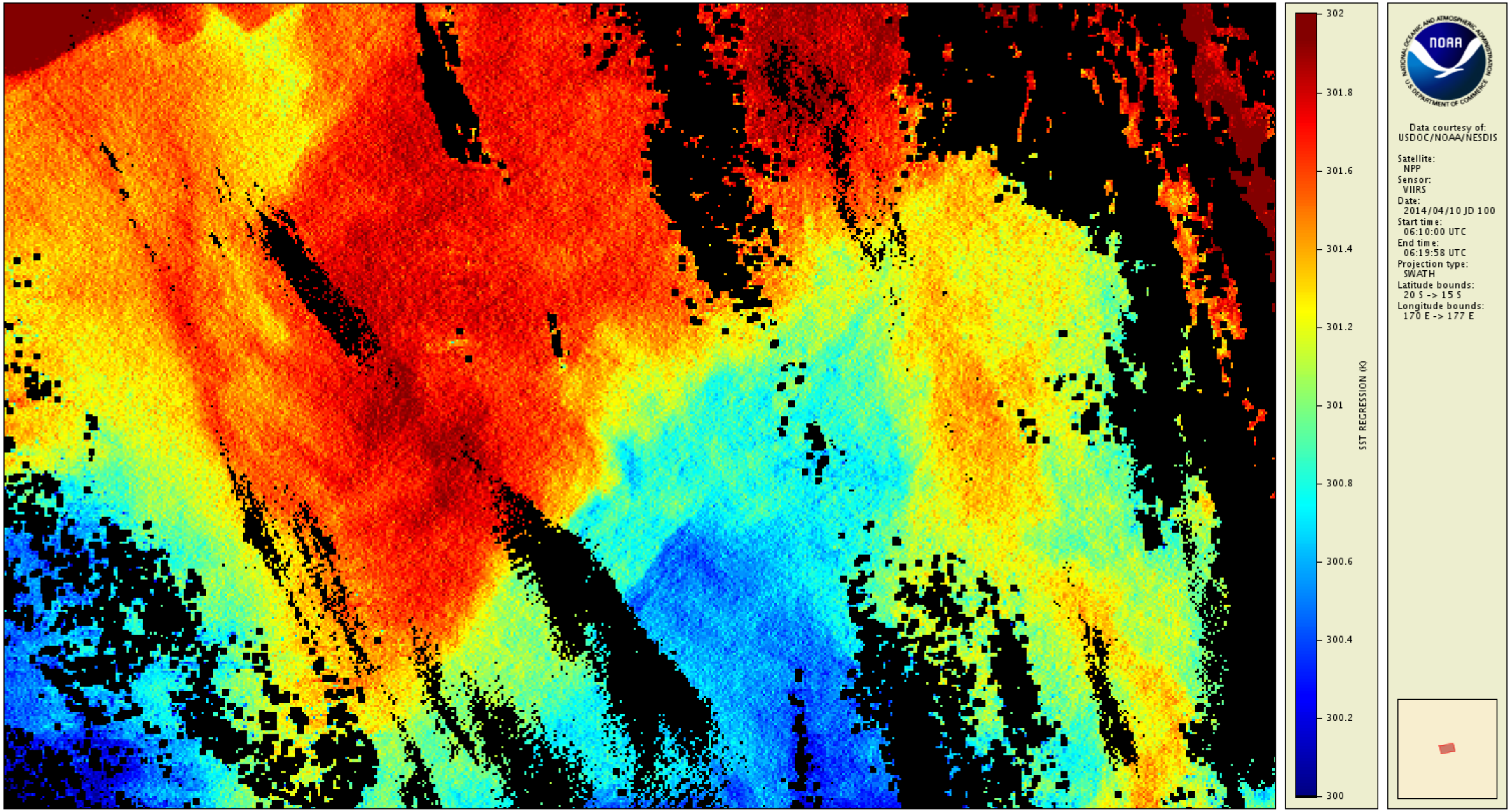

Striped artifacts in cloud mask removed

Performance – IDL vs C

	IDL	C
Test environment	Intel Xeon 3.5 GHz NVIDIA Tesla M2070 GPU gpulib, cuda libraries	Intel Xeon 3.5 GHz 8 threads fftw3, openmp libraries
Running times		
One day of VIIRS (M12, M15, M16)	6 hours	37 min
One day of MODIS (Aqua + Terra) Bands 20, 31, 32	6 hours	83 min
One day of VIIRS (M12, M15, M16) + MODIS (Aqua + Terra) Bands 20, 31, 32	**12 hours**	**2 hours**

- overall, C code is about 6 times faster
- I/O is a significant factor for C version: ≈25% time (VIIRS) and ≈40% time (MODIS)

Summary

1. Fast, operational production ready destriping code developed at NOAA
2. Capable of working with S-NPP VIIRS and Terra/Aqua MODIS
3. Initially prototyped in GPU-IDL (VIIRS: ×0.25; 2.5min/10min granule)
4. Now rewritten into C – 10 times faster than GPU-IDL for VIIRS (×0.025, 15sec/10min granule)
5. Implemented at STAR in experimental mode with Terra/Aqua MODIS – 4.5 times faster than GPU-IDL
6. Brightness temperature & SST imagery, ACSPO cloud mask, and SST gradients significantly improved

Next Steps

Immediate

1. Incorporate destriping code as a preprocessor for ACSPO VIIRS in NDE operations
2. Destripe "optional" IR bands (VIIRS: M13, M14; MODIS: B22, B23, B29)

Near term

1. Destripe solar reflectances for ACSPO Clear-Sky Mask (VIIRS: M6/7; MODIS: B6/7)
2. Address saw-like modulations in glint areas (short wavelength bands, daytime)
3. Further optimize codes for reprocessing of historical VIIRS and MODIS data

Back-Up slides

TERRA

Results – MODIS Terra band 20 (3.75μm)

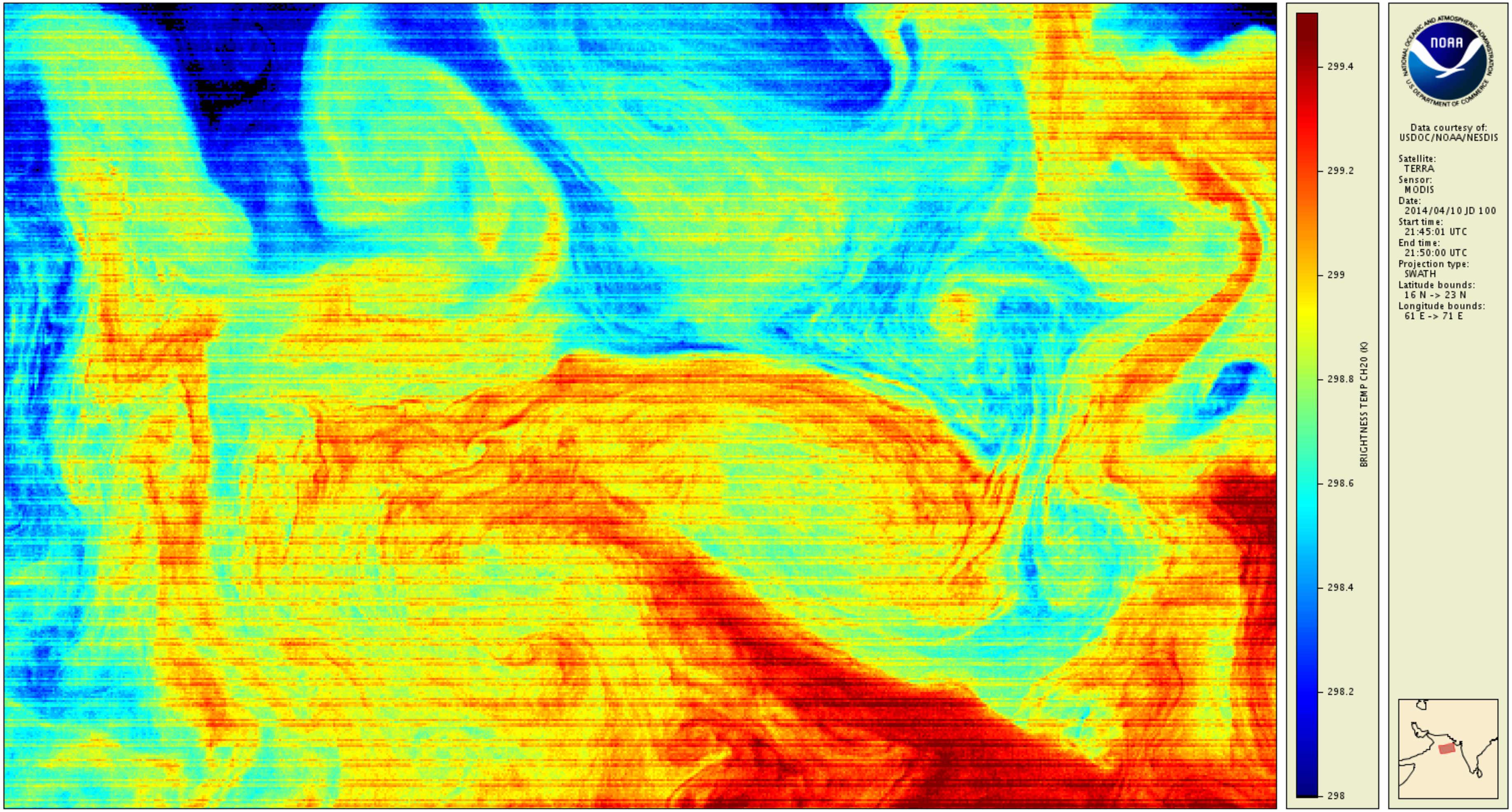

Results – MODIS Terra band 20 (3.75μm)

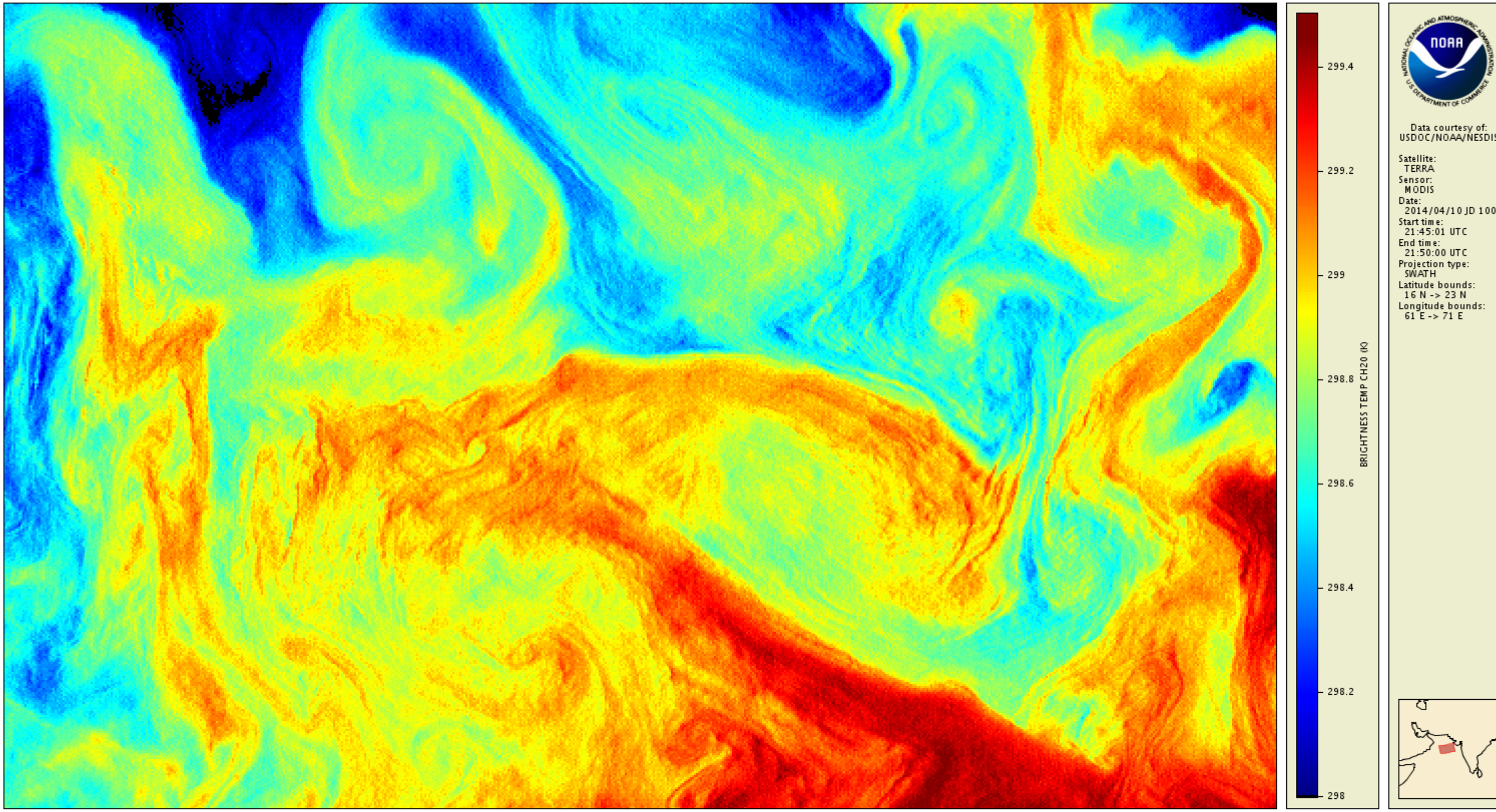

Results – MODIS Terra band 31 (11.0μm)

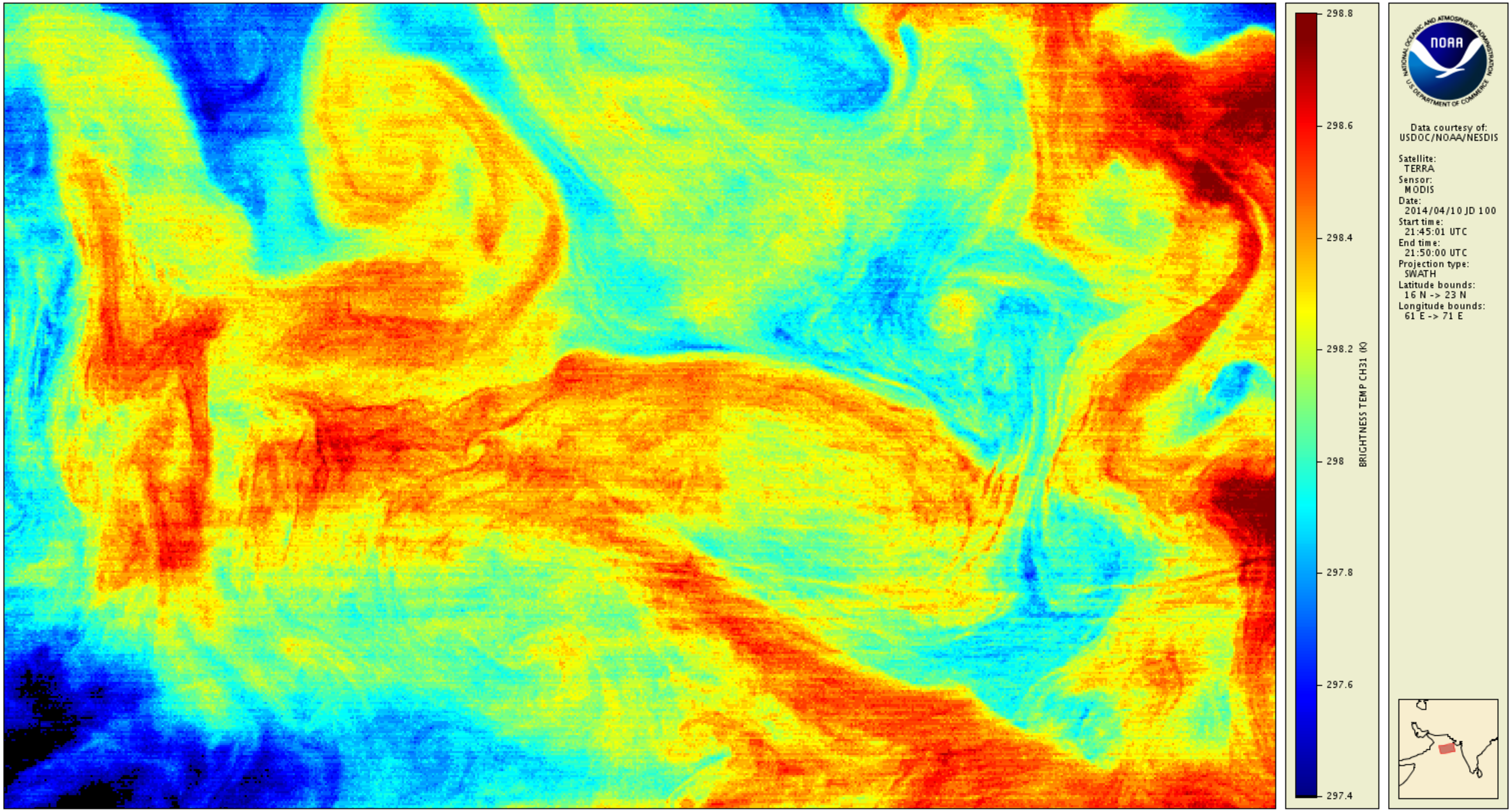

Results – MODIS Terra band 31 (11.0μm)

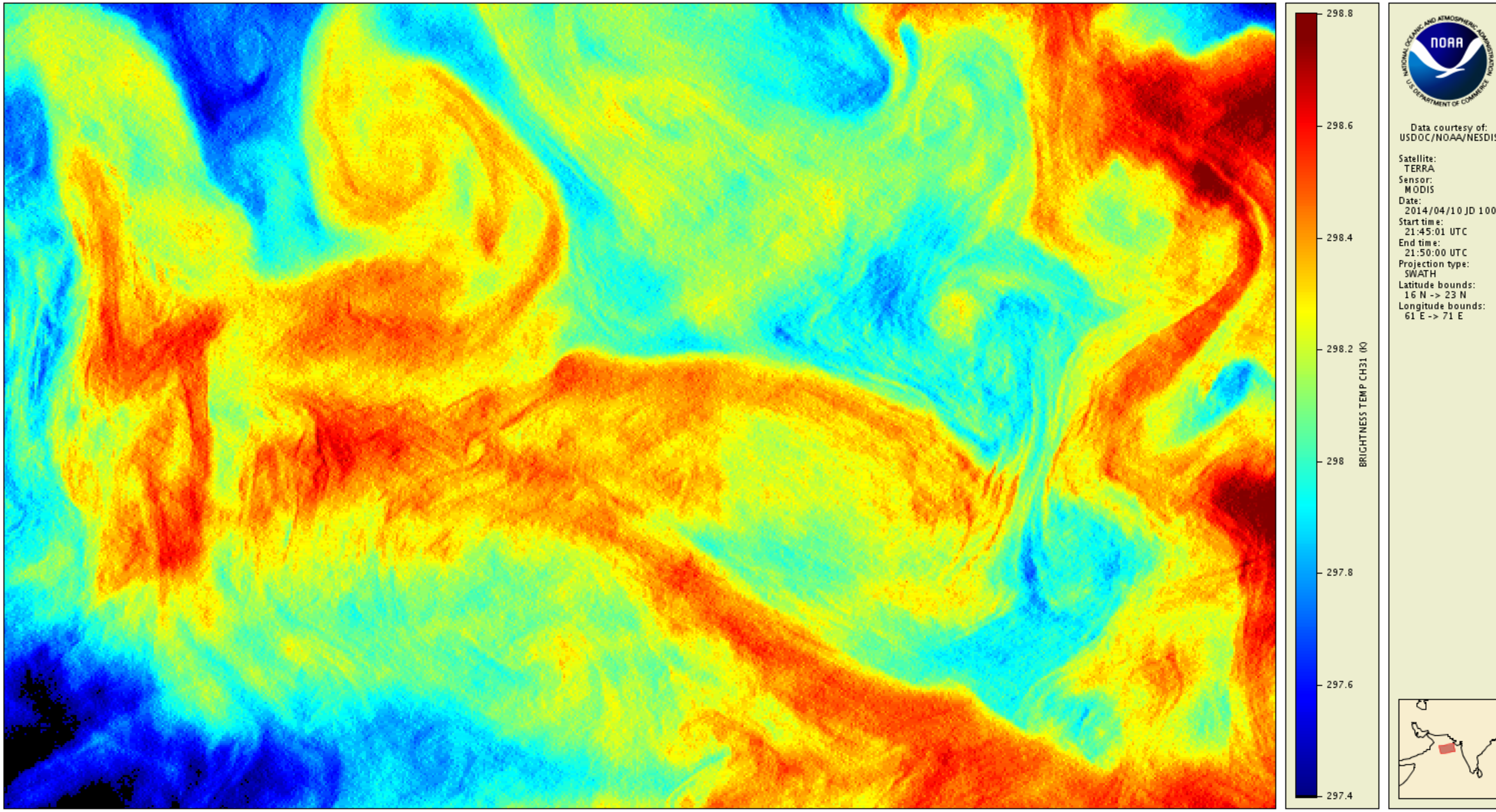

Results – MODIS Terra band 32 (12.0μm)

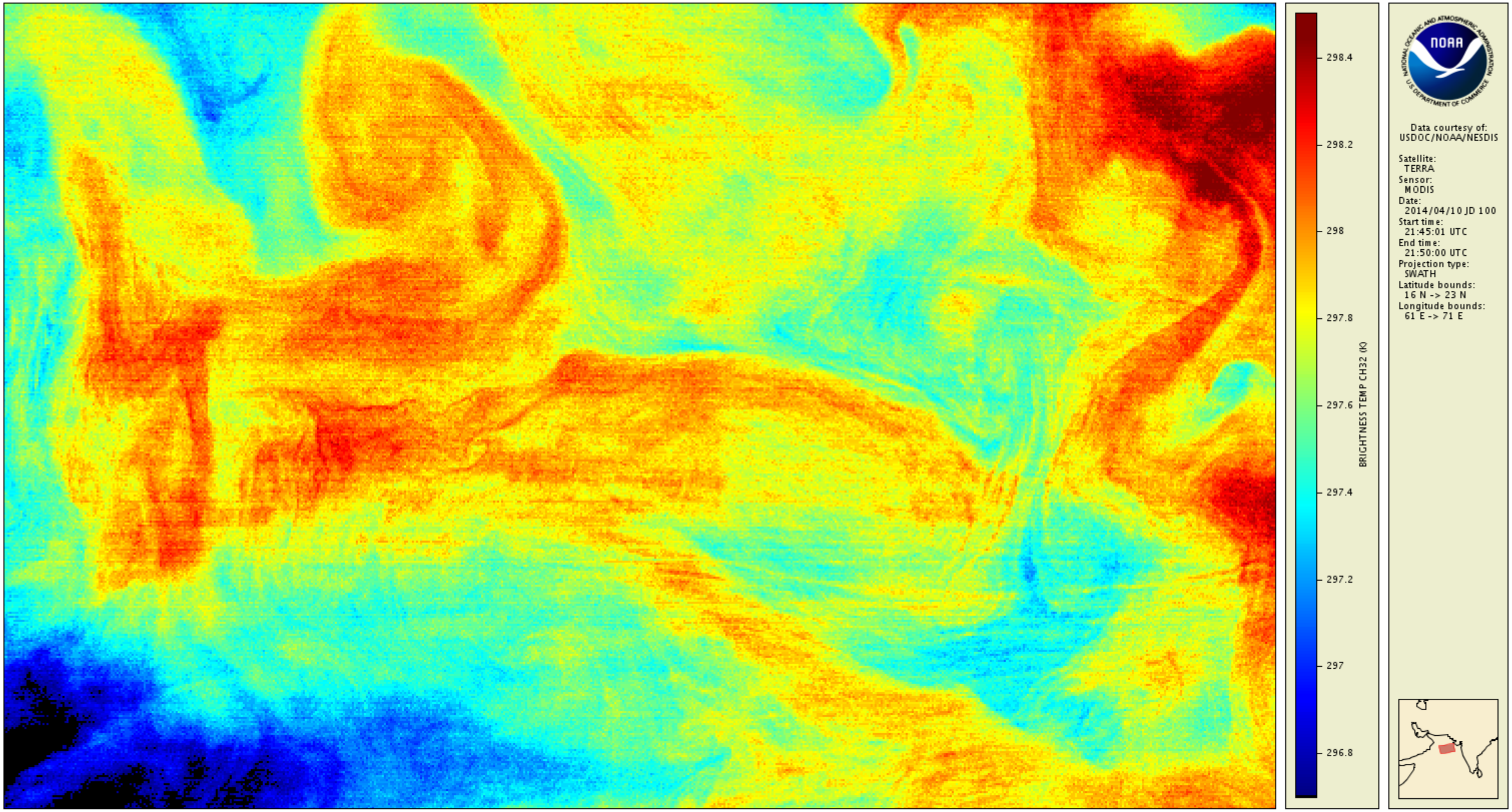

Results – MODIS Terra band 32 (12.0μm)

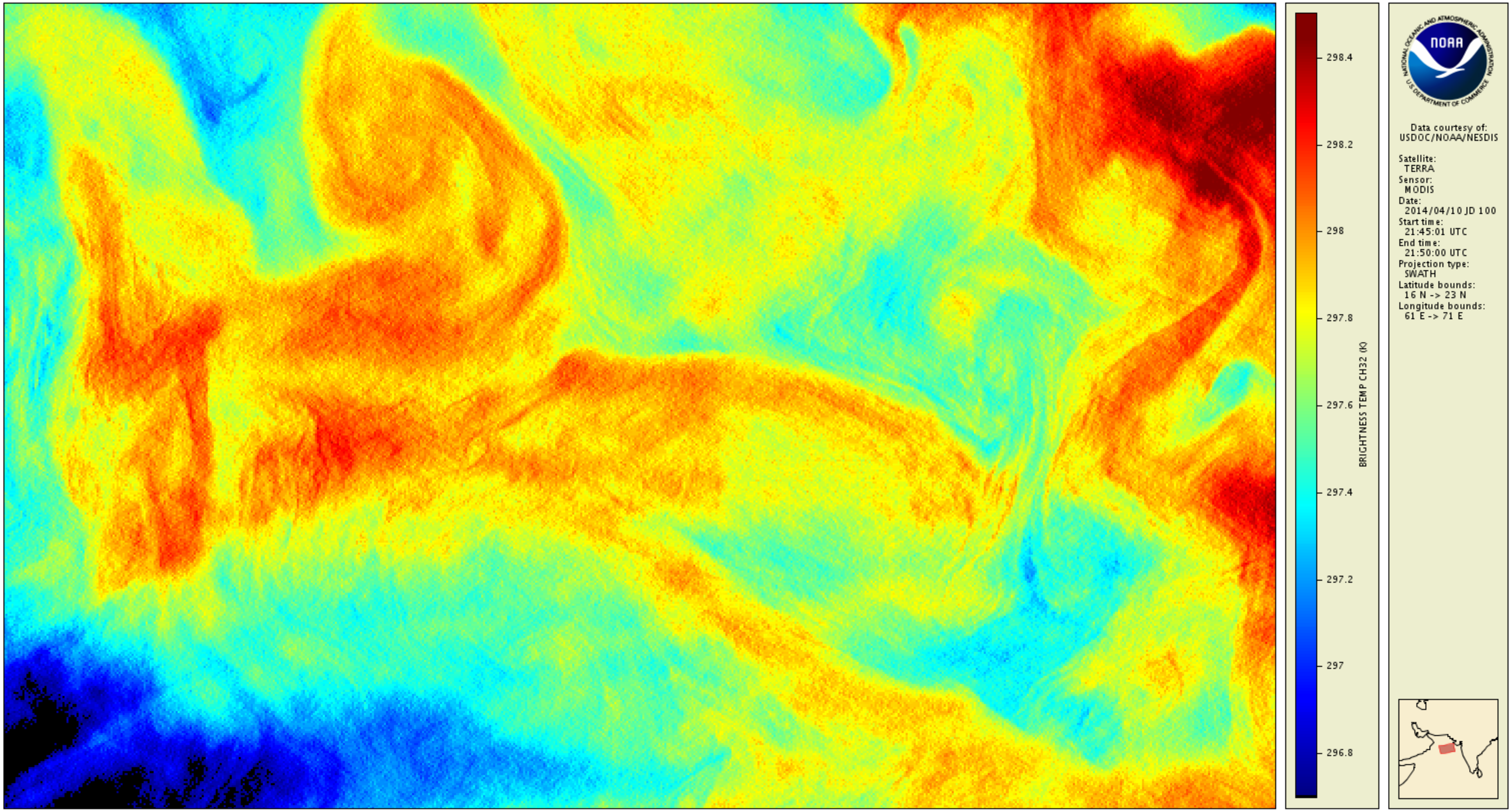

AQUA

Results – MODIS Aqua band 20 (3.75μm)

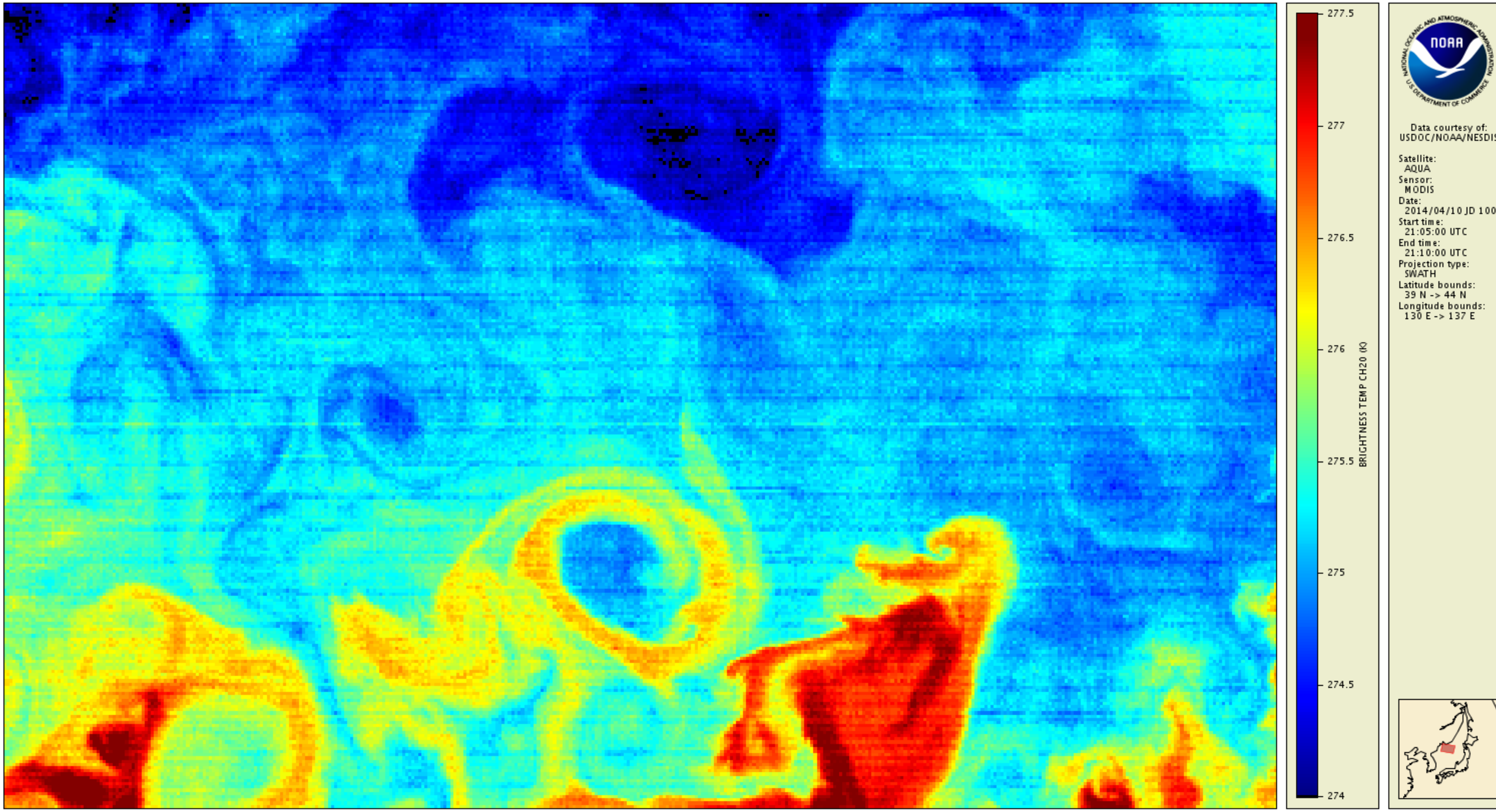

Results – MODIS Aqua band 20 (3.75μm)

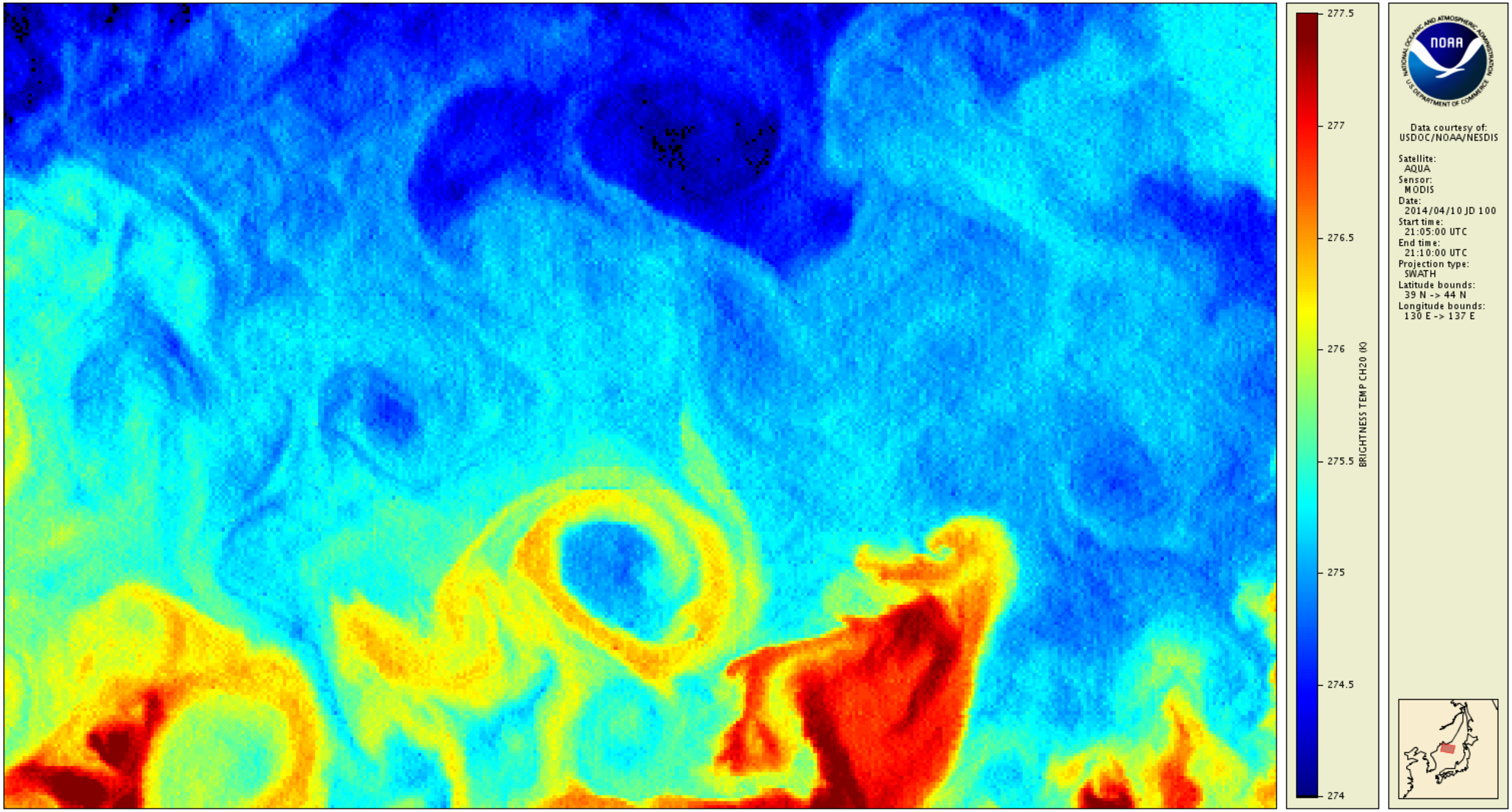

Results – MODIS Aqua band 31 (11.0μm)

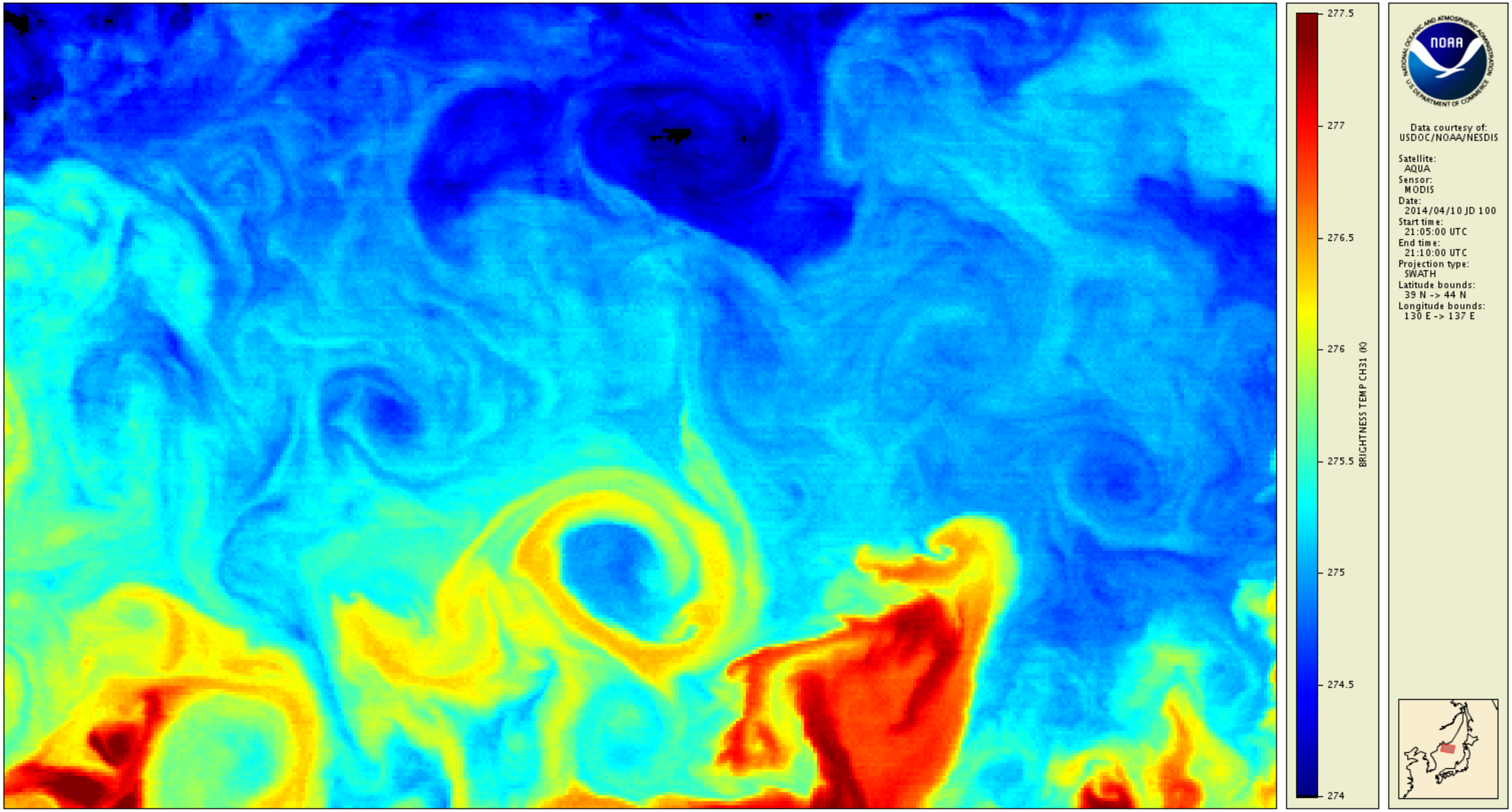

Results – MODIS Aqua band 31 (11.0μm)

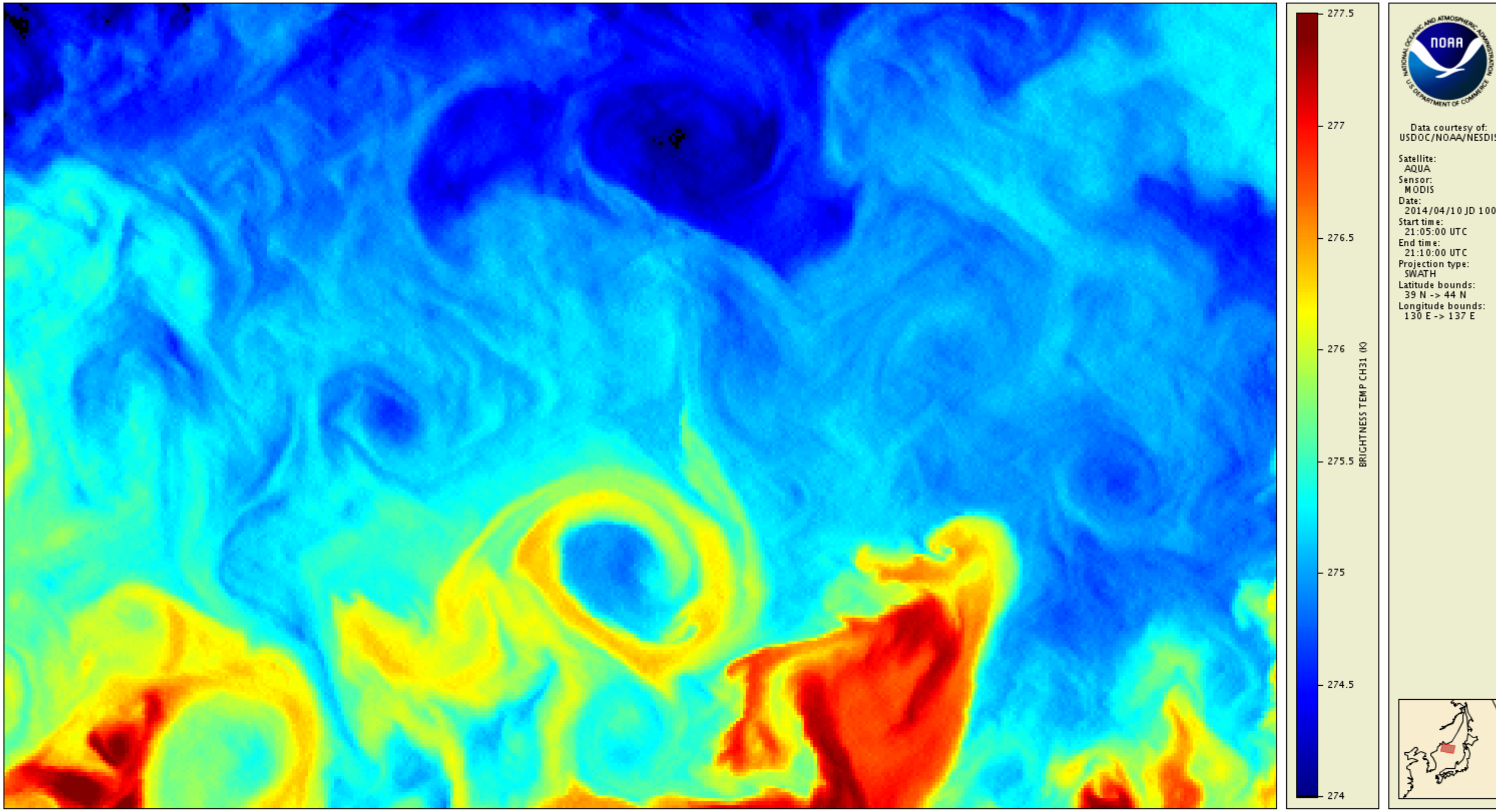

Results – MODIS Aqua band 32 (12.0µm)

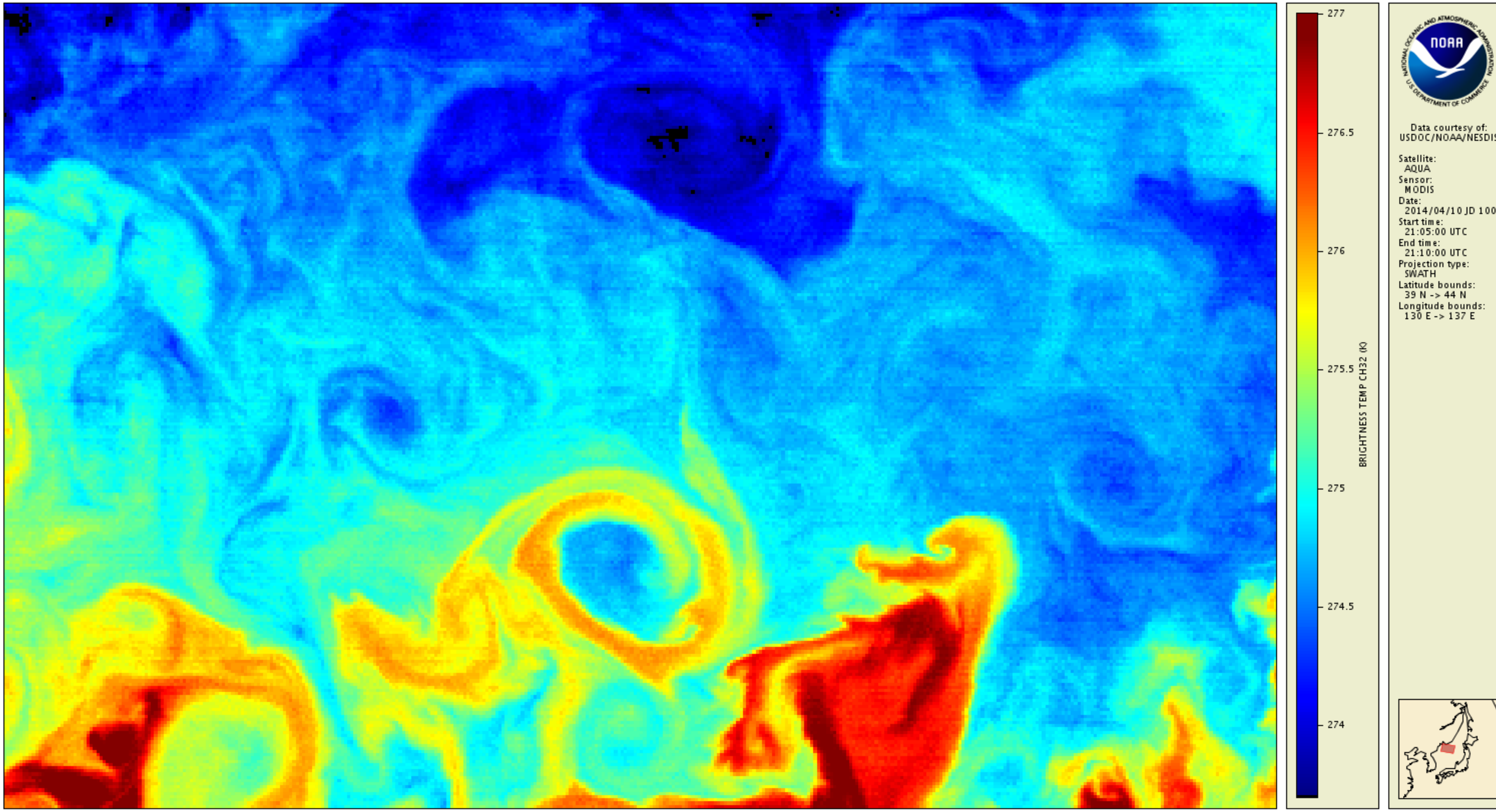

Results – MODIS Aqua band 32 (12.0μm)

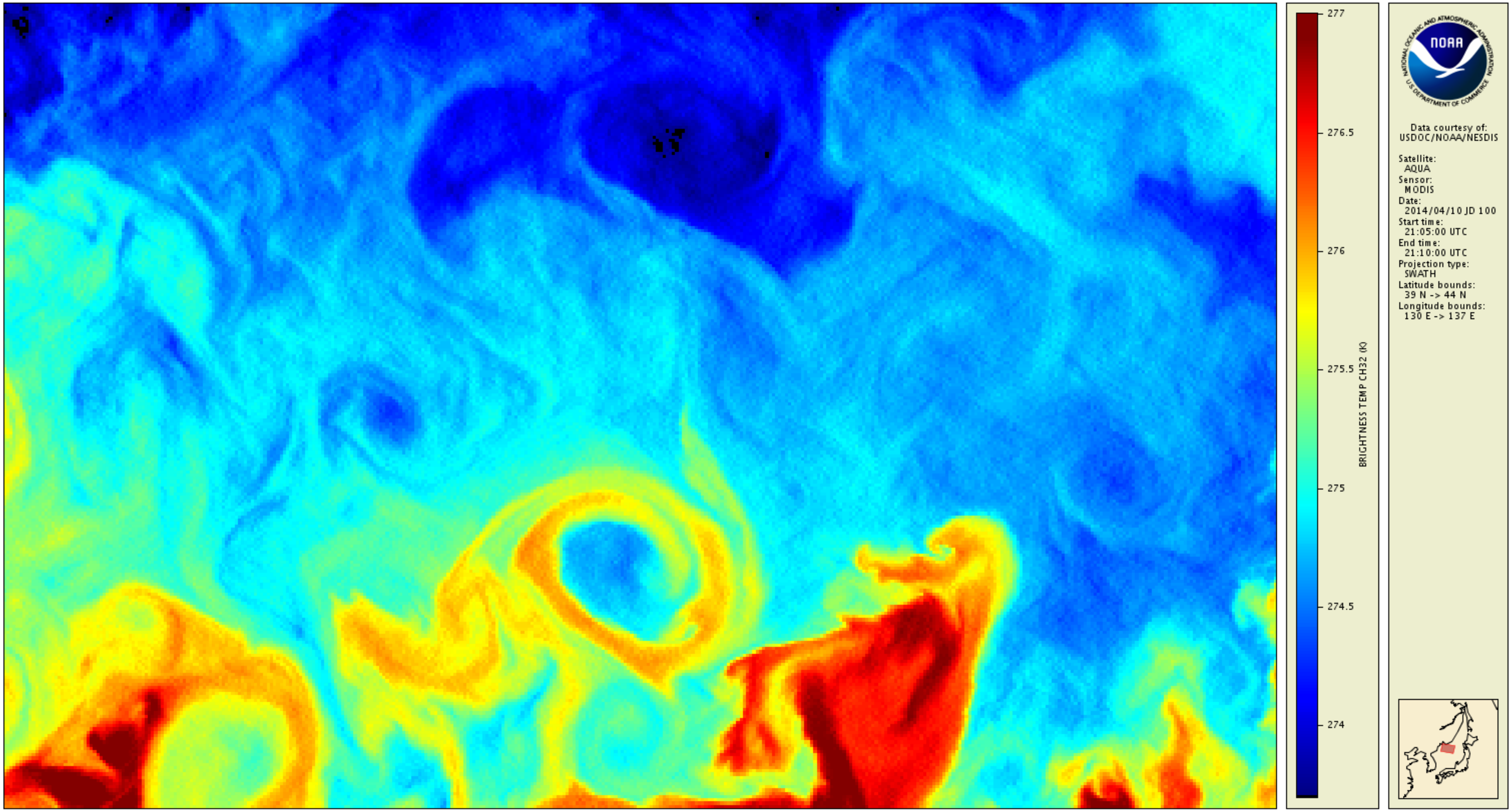

Saw-Like Structure in daytime M12

Results – VIIRS band M12 (3.7μm) – day (glint)

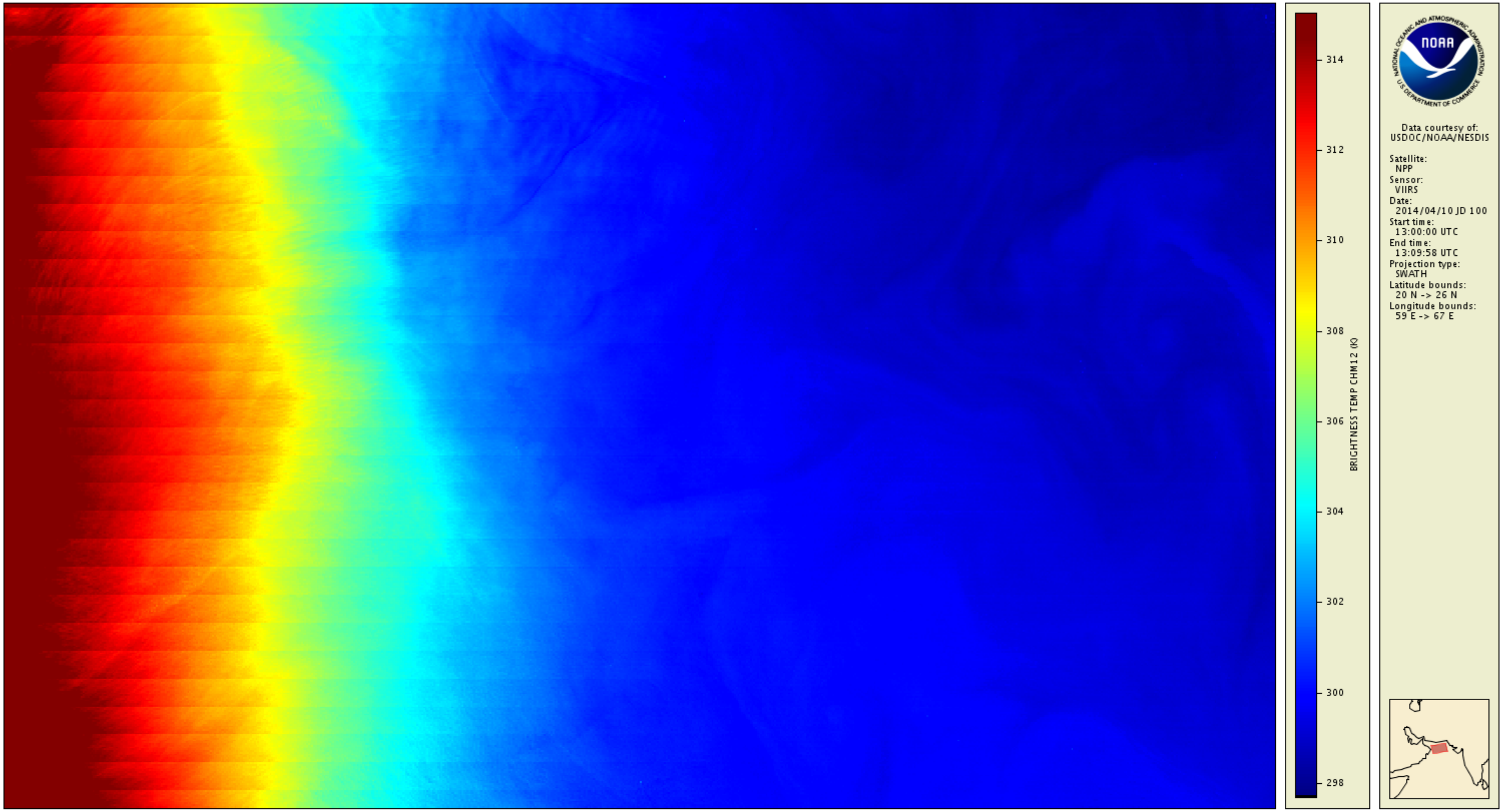

Striping in glint region primarily due to different viewing angle for detectors
Study: Q. Liu, C. Cao, F. Weng, *J. Atmos. Oceanic Technol.*, **30**, 2478-2487 (2013).

Results – VIIRS band M12 (3.7μm) – day (glint)

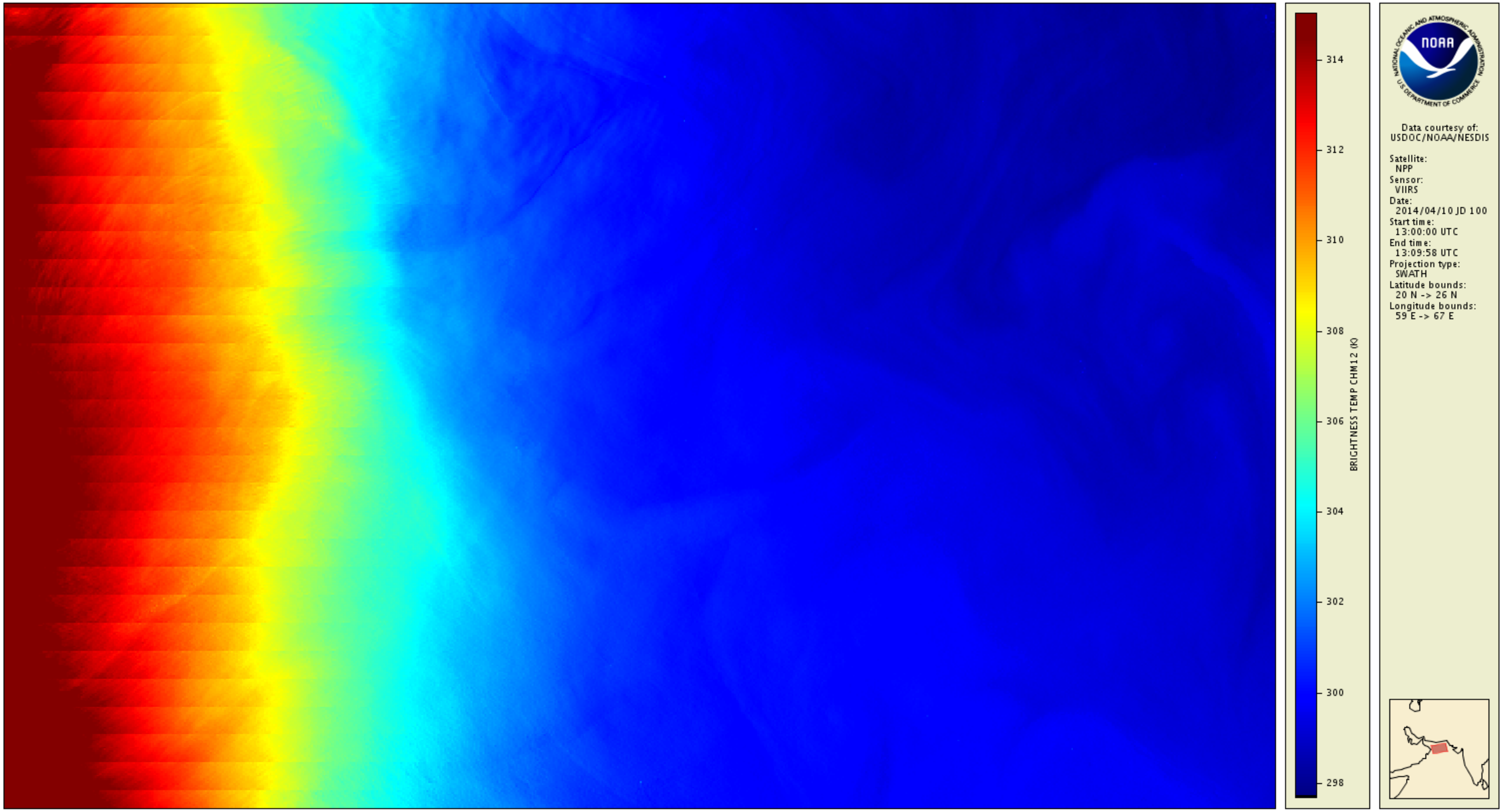

- Areas outside the glint region and onset of glint region are destriped
- High amplitude striping in the center of glint region is not removed

VIIRS Atmospheric Correction Algorithms

Miami V6:

- $SST2b = a_0 + a_1T_{11} + a_2(T_{11} - T_{12})\ T_{sfc} + a_3(T_{11}\text{-}T_{12})\ S_\theta$
- $SST3b = a_0 + a_1T_{11} + a_2(T_{3.7} - T_{12})\ T_{sfc} + a_3\ S_\theta$

Miami V7:

- $SST2b = a_0 + a_1T_{11} + a_2(T_{11} - T_{12})\ T_{sfc} + a_3(T_{11}\text{-}T_{12})\ S_\theta + a_4\ S_\theta + a_5\ S_\theta^{\ \chi}$

$$\chi = \text{fn(lat)}$$

- $SST3b = a_0 + a_1T_{11} + a_2(T_{3.7} - T_{12})\ T_{sfc} + a_3\ S_\theta + a_4\ S_\theta^{\ \chi}$

$$\chi = 0.1 \text{ for } |\text{lat}| \leq 40°;\ 2.0 \text{ for } |\text{lat}| > 40°$$

$$S_\theta = \sec(\theta)\text{-}1$$

UNIVERSITY OF MIAMI
ROSENSTIEL
SCHOOL of MARINE &
ATMOSPHERIC SCIENCE

Simple Global Statistics

Algorithm	N	Mean	Std Dev	Median	Median Abs Diff
Satellite zenith <55^o					
SST - day	92061	-0.089	0.510	-0.085	0.337
SST - night	126174	-0.160	0.436	-0.153	0.331
SST_3 - night	81155	-0.172	0.395	-0.152	0.230
Satellite zenith >55^o					
SST - day	34693	-0.105	0.647	-0.149	0.536
SST - night	29922	-0.193	0.519	-0.206	0.485
SST_3 - night	35982	-0.131	0.489	-0.161	0.355

Statistics of the differences between the VIIRS skin SST retrievals and the subsurface temperatures measured from drifting buoys.

UNIVERSITY OF MIAMI
ROSENSTIEL
SCHOOL of MARINE &
ATMOSPHERIC SCIENCE

Zenith angle dependence

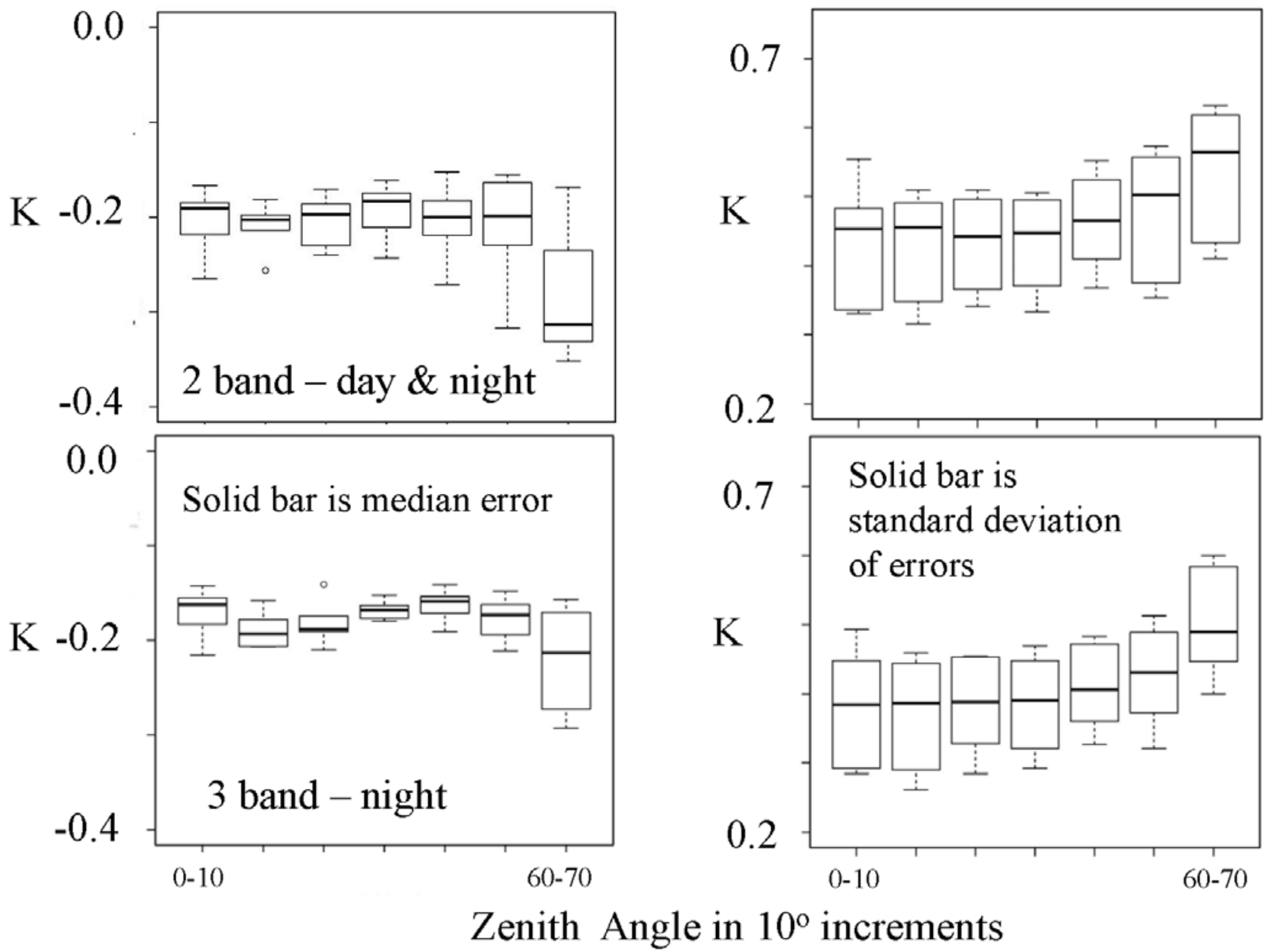

UNIVERSITY OF MIAMI
ROSENSTIEL
SCHOOL of MARINE &
ATMOSPHERIC SCIENCE

Time dependences – in latitude bands

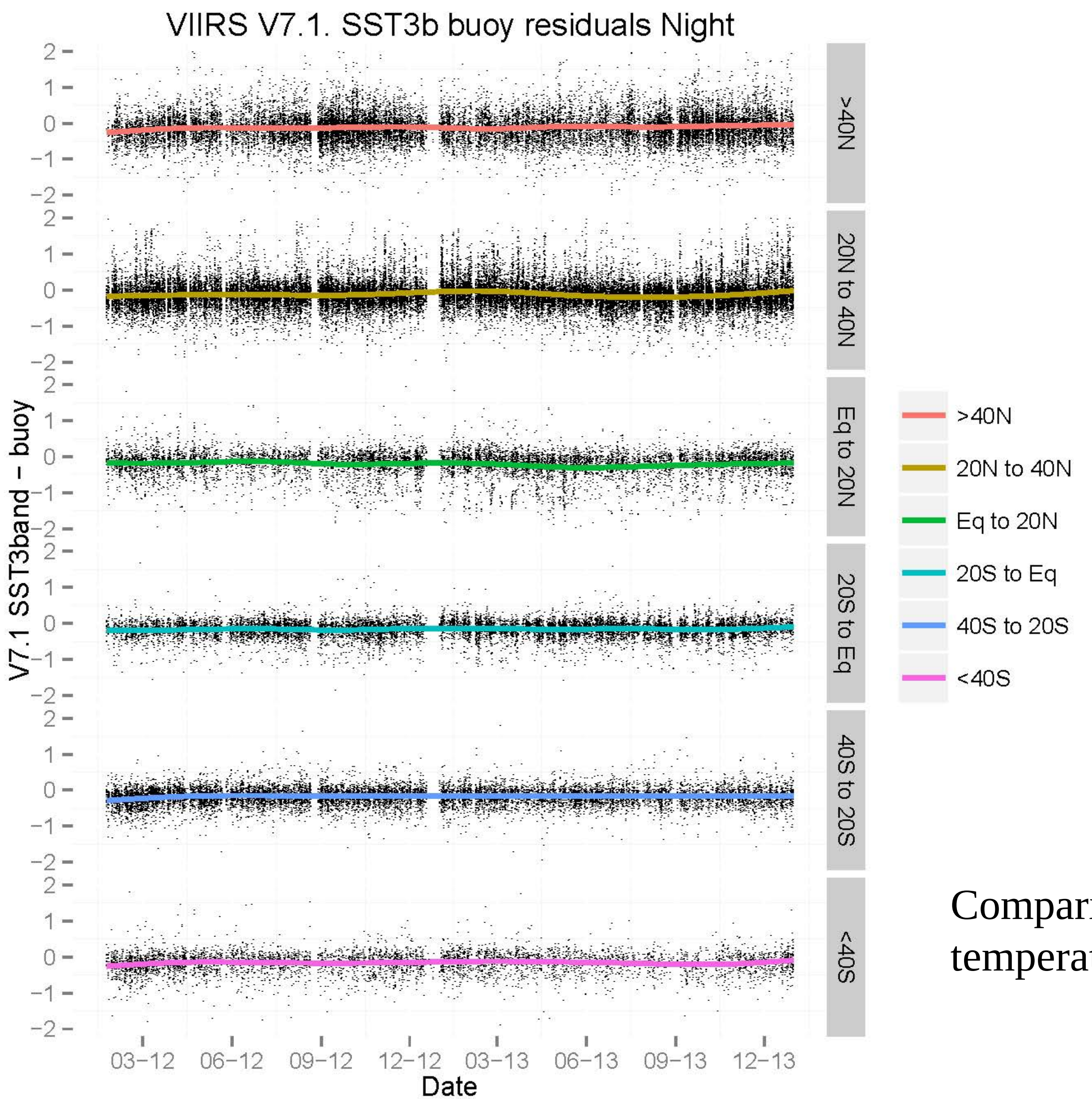

Comparisons to buoy temperatures

UNIVERSITY OF MIAMI
ROSENSTIEL SCHOOL of MARINE & ATMOSPHERIC SCIENCE

VIIRS SST at the Naval Oceanographic Office analyses at NAVO/USM

Jean-François Cayula
QinetiQ North America,inc

Douglas May, Bruce McKenzie, Keith Willis
Naval Oceanographic Office

NAVOCEANO Milestones

- Operational with NPP VIIRS SST: March 2013
- Official Distribution in GDS 2.0 format: September 2013 (first GDS 2.0 SST product on JPL/GDAC)
- Monitoring NAVO SST statistics for over 2 years

NAVOCEANO SST Evaluation

- Statistics for April based on match-up buoys (count)
- NAVO VIIRS SST (Best quality):

	Count	Bias	RMS error
day	19780	-0.06	0.41
night	32470	-0.02	0.37

- NAVO VIIRS SST Statistics have remained stable and within requirements.
- Similar or better than NAVO AVHRR SST

NAVOCEANO SST EDR Evaluation

- For comparison, IDPS SST EDR (Best quality):

	Count	Bias	RMS error
day	8199	0.06	0.50
night	9476	-0.08	0.29

- Much smaller domain because of satellite zenith angle limit can be relaxed with new equations
- Daytime RMS error varies 0.45-0.50°C due to missed aerosol and cloud contamination

Evaluation of Clear Sky determination on SST accuracy

- Accuracy of the VIIRS Cloud Mask (VCM) “cloud-free” SST retrievals
- Comparison with NAVOCEANO Cloud Mask (NCM)

NCM is a good comparison standard as it produces very clean SST for assimilation by oceanographic models.

VCM only handles the detection of clouds and not other contaminants ➡ needs extra tests for a valid comparison.

Evaluation of Clear Sky determination on SST accuracy

- Added contamination tests: Simple tests to be considered as proof of concept
  - Daytime:
    - Reflectance test contingent on field test

  - Nighttime:
    - NCM aerosol test
    - Adjacency to cloud test contingent on field test

Evaluation of Clear Sky determination on SST accuracy

Daytime / February	Buoy matches	RMS error °C
NCM / NCM + test	4967 / 4901	0.51 / 050
VCM / VCM + test	16844 / 14863	0.70 / 0.51

Nighttime / February	Buoy matches	RMS error °C
NCM	6785	0.36
VCM / VCM + tests	21052 / 17171	0.56 / 0.34

- Additional tests mostly flagging adjacent retrievals to detected clouds ➡ cloud leakage w/ original VCM
- VCM with additional tests performs as well as NCM, and allows increased coverage

Example of Clear Sky SST

Daytime SST fields on April 6, 2014 a) for NCM clear, b) for VCM clear, c) for VCM clear with additional test, d) with a tightened additional test to remove remaining cloud leakage

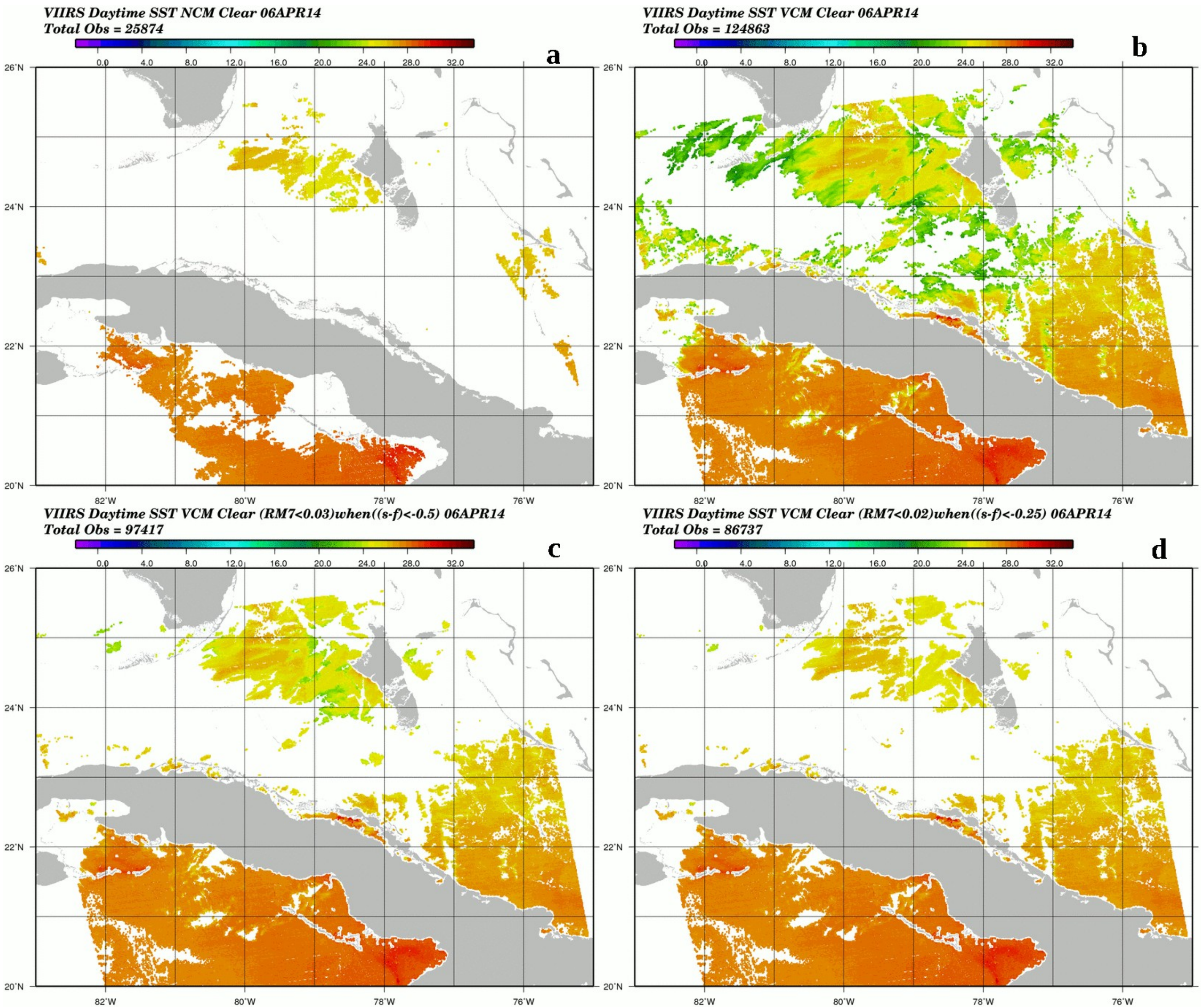

SST analyses with Swath Overlap

- With full swath processing, significant swath overlap even at low latitudes
- The overlap between swath can help evaluate SST equations at higher satellite zenith angle (SZA).
- Three types of equations:
  - Standard Non Linear SST – NL53deg (designed for SZA < 53°)
  - NLSST equation with additional SZA terms – “Non Linéaire Complet” (NLC) which is OSI/SAF daytime equation
  - Miami Lat-band algorithm v6
- For NLC: coefficients from NAVO, STAR, Météo France.

SST field May 14 2013

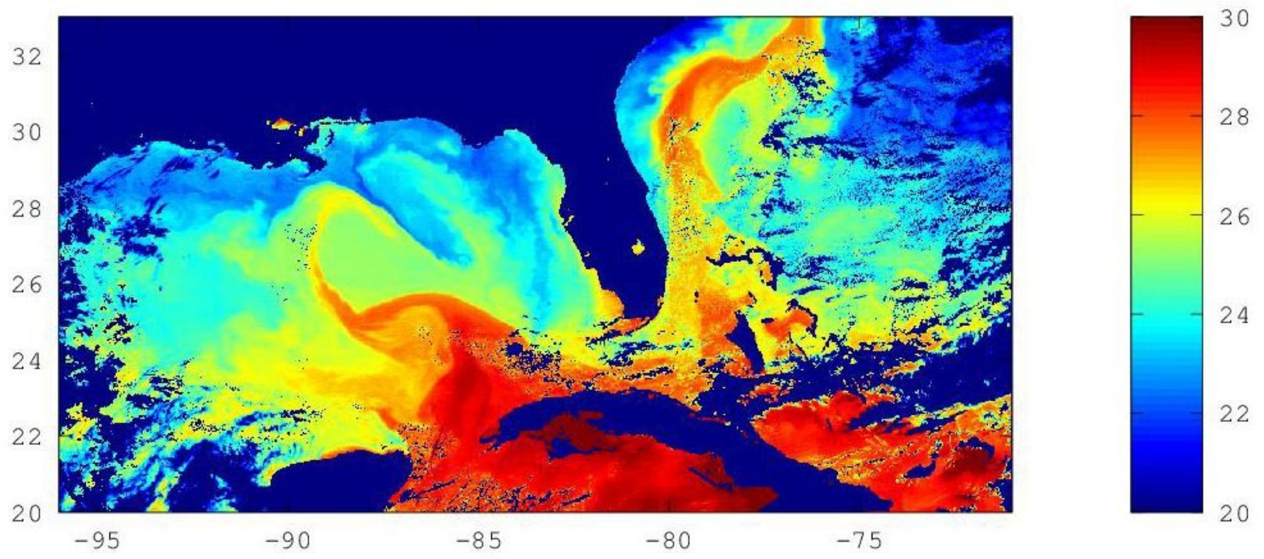

SST analyses with Swath Overlap

- SST field of later orbit is subtracted from that of earlier orbit
- Uncorrected limb darkening effect appears as a cold bias on west side of the overlap region and a warmer bias on the east side

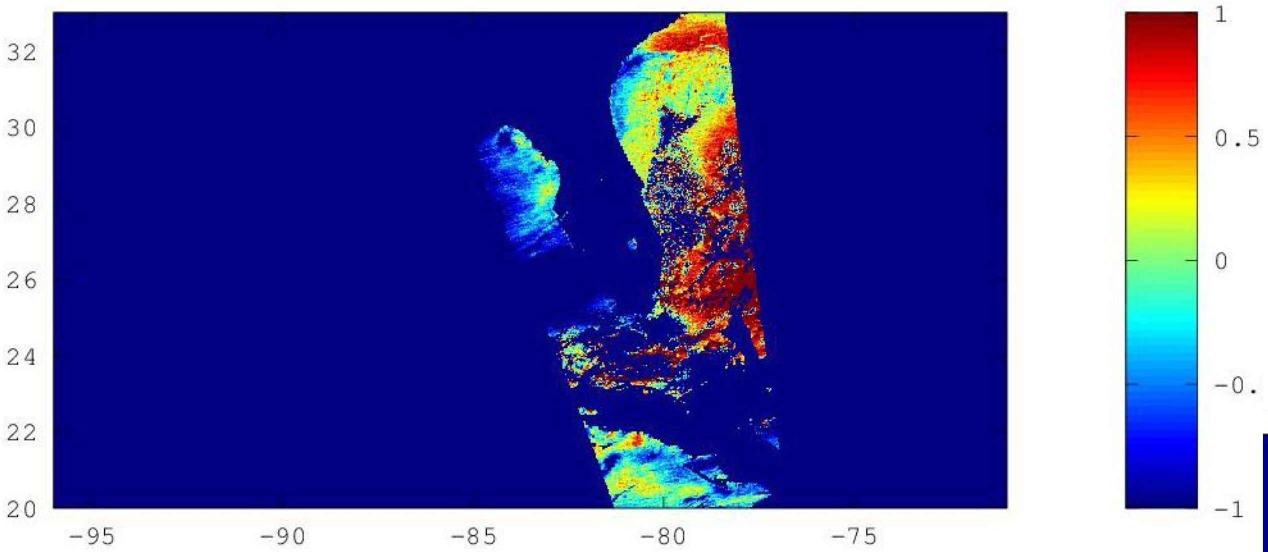

NL53deg

NLC

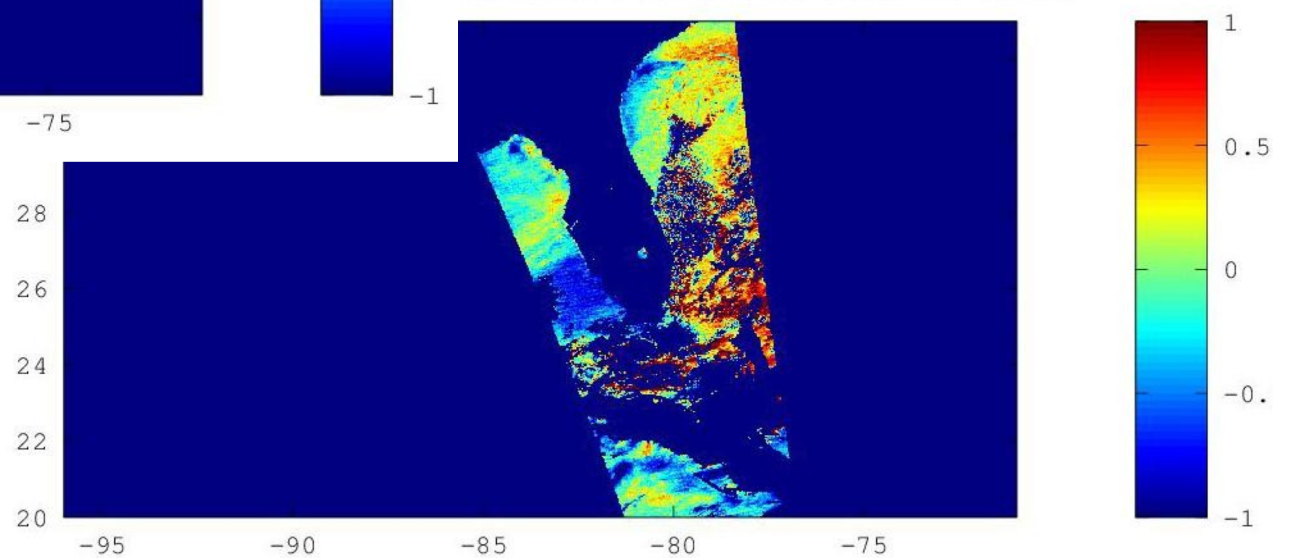

SST analyses with Swath Overlap

- Numerical results for domain shown in previous two slides
- As expected at high satellite zenith angle NL53deg performs significantly worse than NLC.

May 14, 2013	bias °C	mean absolute bias °C
NL53deg	-0.23	0.51
IDPS (old equations)	-0.23	0.52
Miami	-0.15	0.39
NLC (NOAA coefs 10/2013)	-0.12	0.41
NLC (Météo France coefs)	-0.13	0.38
NLC (NAVO coefs)	-0.09	0.27

NAVOCEANO improvements

- NAVOCEANO is investigating the use of VCM or improvements to NCM for SST production
- Example: Recent improvements address coverage and cloud detection artifact issues in nighttime SST

Before April 29, 2013

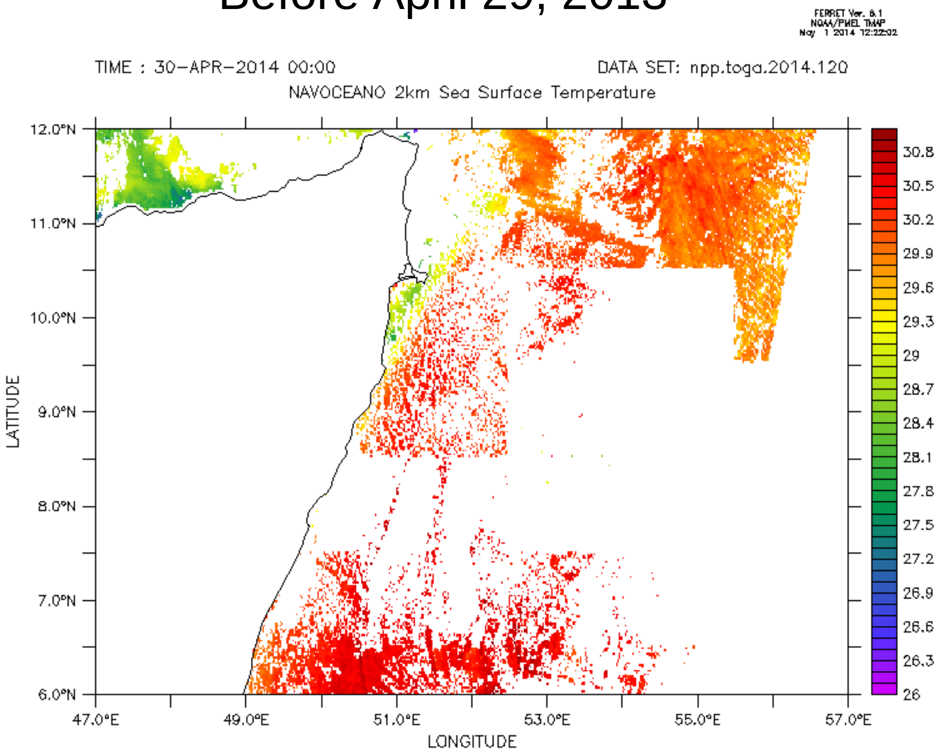

Nighttime Sea Surface Temperature (celsius)

Current operational

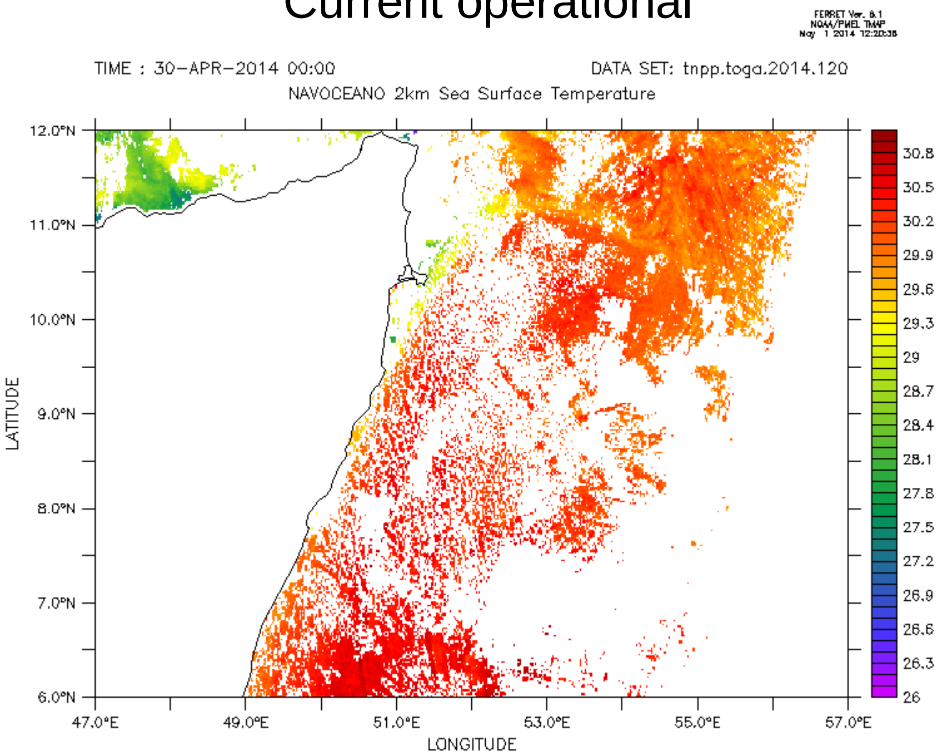

Nighttime Sea Surface Temperature (celsius)

NAVOCEANO improvements

- Example: Proposed modification to address coverage and cloud detection artifact issues in daytime SST

Current operational

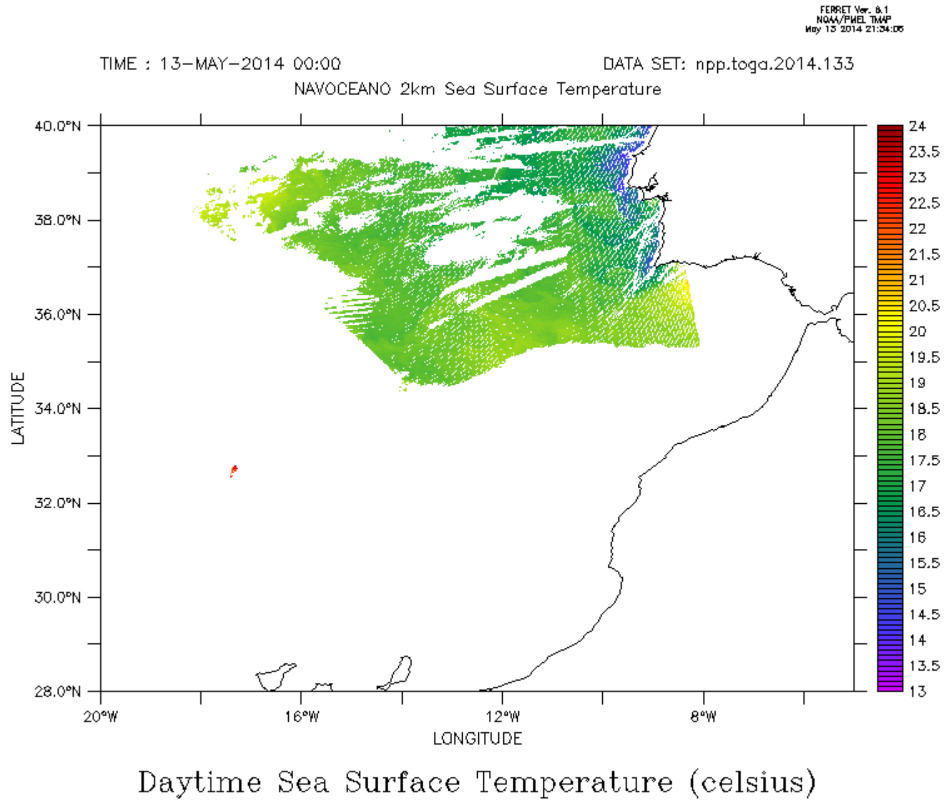

In testing

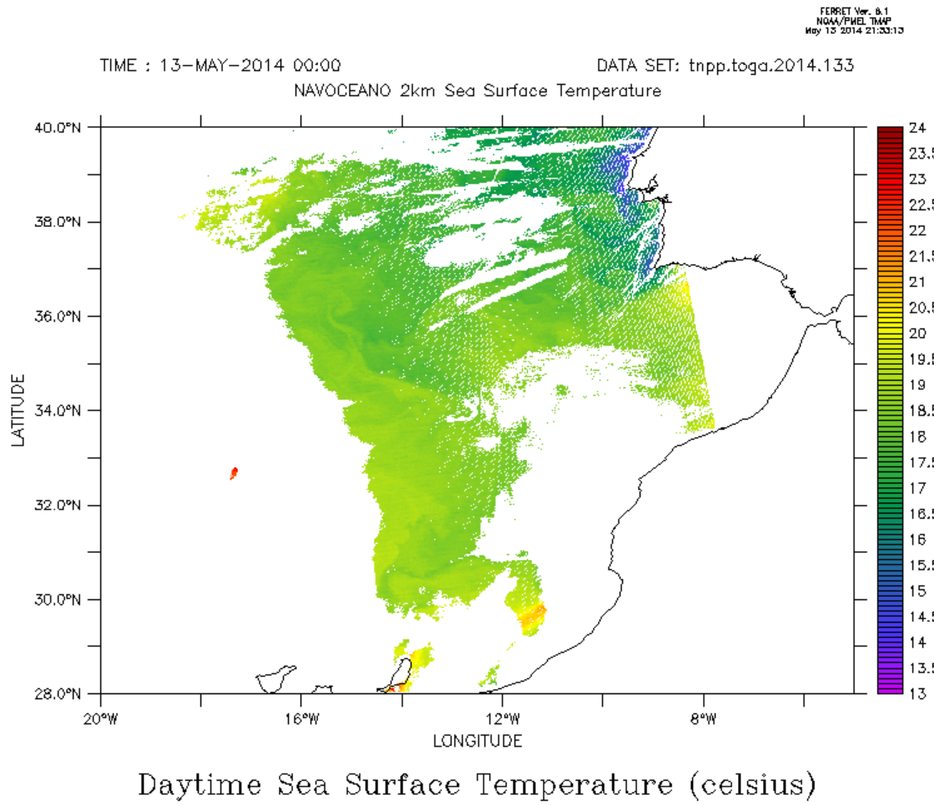

Conclusion

- VIIRS is an excellent sensor which allows the production of quality SST retrievals.
- VCM with additional tests performs well for SST production. VCM would benefit from access to computed SST retrievals and a good previous day SST field.
- Full swath processing allows overlap analyses even at low latitudes but requires the switch to an NLC (NL with extra SZA terms) type equation.

Sea Surface Temperature (University of Southern Miss)

Arnone, Vandermeulen, Fargion,

Objectives: VIIRS Cal Val – SST EDR products

Evaluate SST product performance for operational use and science applications

Evaluate Regional Coast SST products

Updates for IDPS processing and algorithms

Project Accomplishments: Past year

1. **Assembled SST products from IDPS , and OSI_SAF and Miami algorithms in Gulf of Mexico .**
2. **Compared SST products in Coastal Fronts and coastal regions.**
3. **Demonstrated use of the VIIRS orbital overlap for sensor validation. - Poster**
4. **Began SST validation in Coastal areas (Mississippi Sound, Mobile Bay)**
5. **Evaluated the SST assimilation into Ocean Models (NCOM, HYCOM)**

Future Plans –

Paper on SST Cal Val Over lap orbits with J.Cayula and S. Ignatov

Validation SST products in Coastal and estuary areas –

Examine the Detector response on SST retrievals

Sea Surface Temperature (University of Southern Miss)

Regional Studies - Filament Location

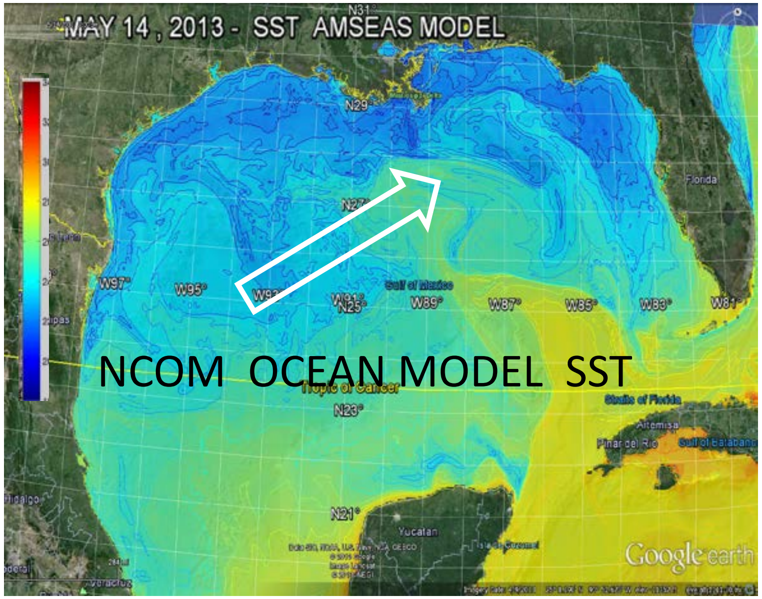

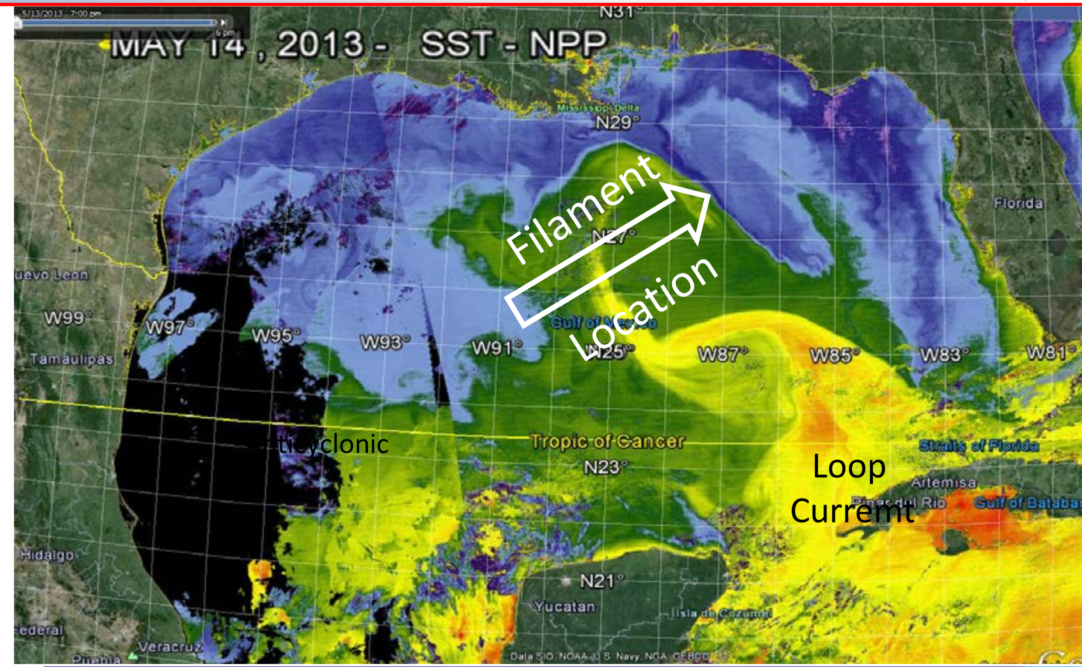

Over compensation in Cloud Mask can impact the Ocean Model SST

Difference in Filament location of Model and SNPP SST - associated with Assimilation and Cloud MASK

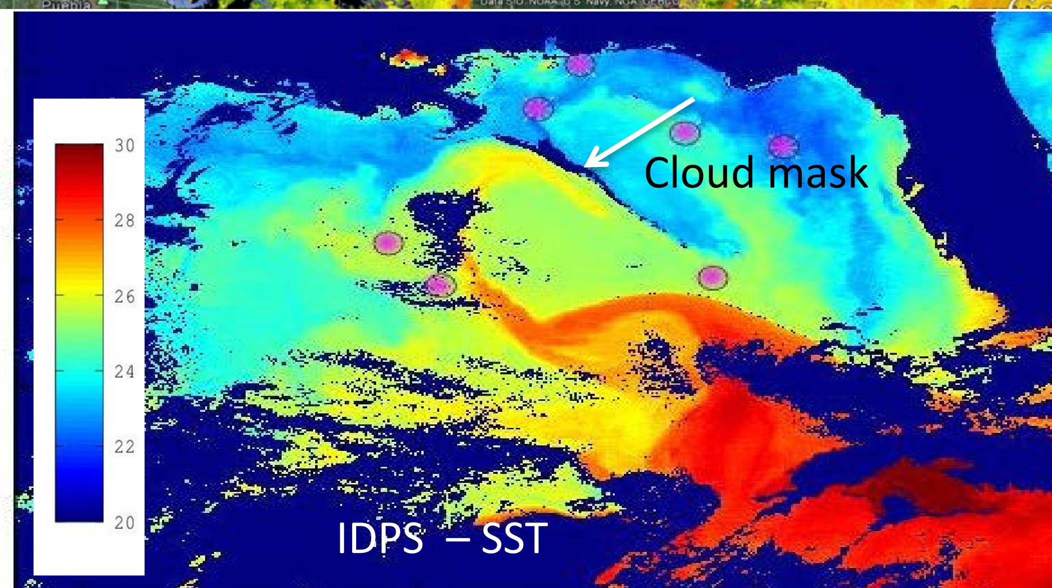

”Why MOBY and why MOBY-Refresh”

UNIVERSITY OF MIAMI

Kenneth Voss, Physics Dept. Univ of Miami

MOBY TEAM (Carol Johnson, NIST, and Mark Yarbrough and many at Moss Landing Marine lab)

5/14/14, NOAA STAR JPSS Science Team Annual Meeting.

1) Review of Vicarious Calibration Needs

2) Current MOBY system

3) MOBY-Refresh

4) Estimated Schedule

The originally announced goal for ocean color sensors:

The uncertainty in the (normalized) water-leaving radiance retrieved from the sensor in oligotrophic waters at 443 nm should not exceed 5%, and uncertainty in Chlorophyll should be < 30%.

Meeting this goal requires the sensor have a calibration uncertainty no more than ~ 0.5% at 443 nm. This is difficult to meet even prelaunch!

In-orbit calibration (vicarious) is required to adjust the pre-launch calibration. Need Accurate data for this!

Because of measurement and atmospheric correction uncertainties and variability's, one measurement is not sufficient.

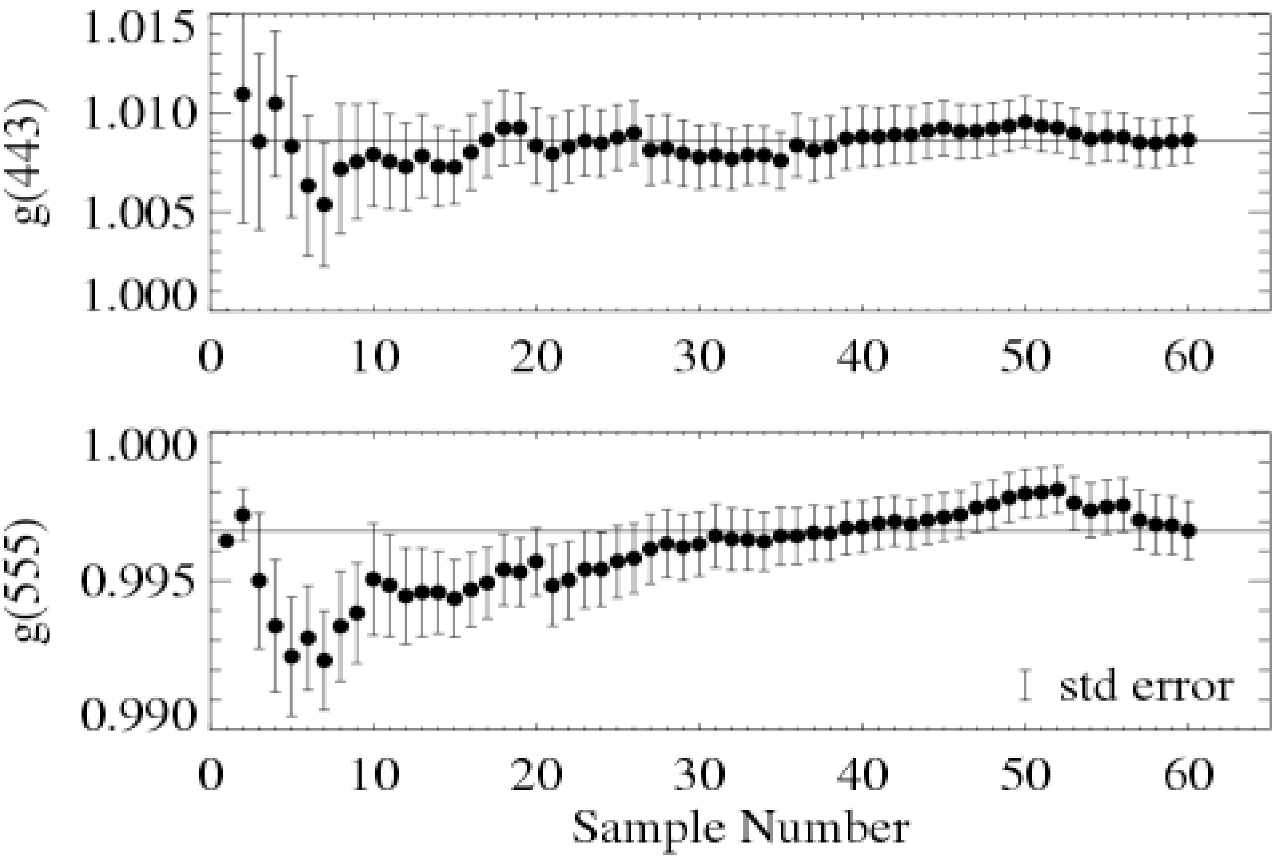

This is the very stable SeaWIFS with frequent lunar looks to keep temporal stability in check.

Shows the need for both an autonomous system and reprocessing of the satellite data.

Werdell et al., 2006, Ocean Optics XVIII,
http://oceancolor.gsfc.nasa.gov/cgi/obpgpubs.cgi

Dennis Clark (NOAA/NESDIS) chose the site shown below off of Lanai, Hawaii and measurements began there in 1997.

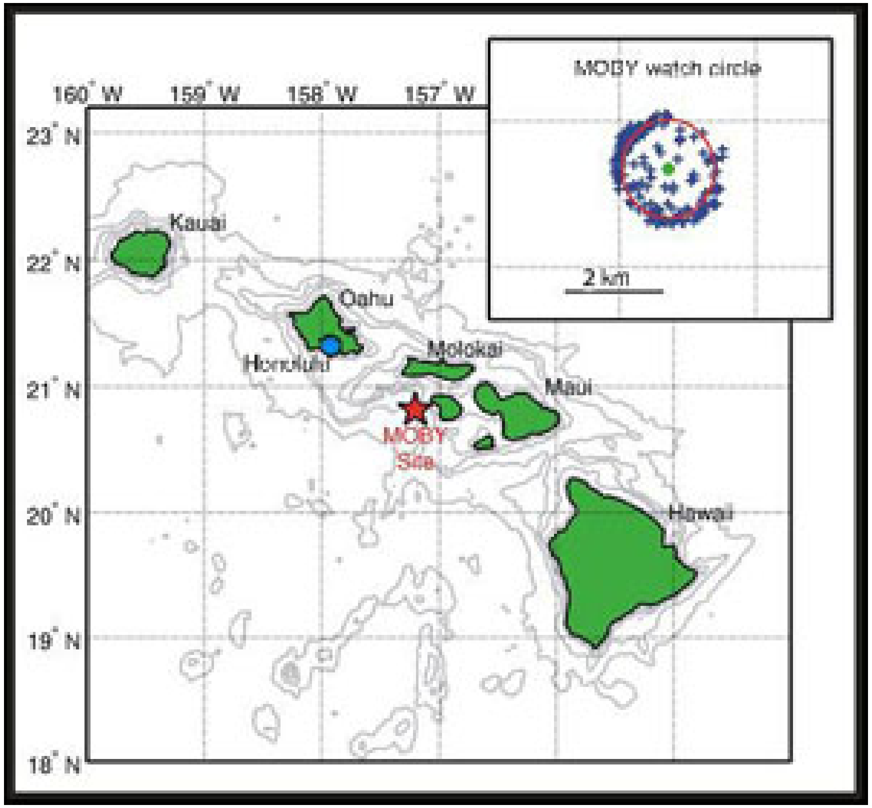

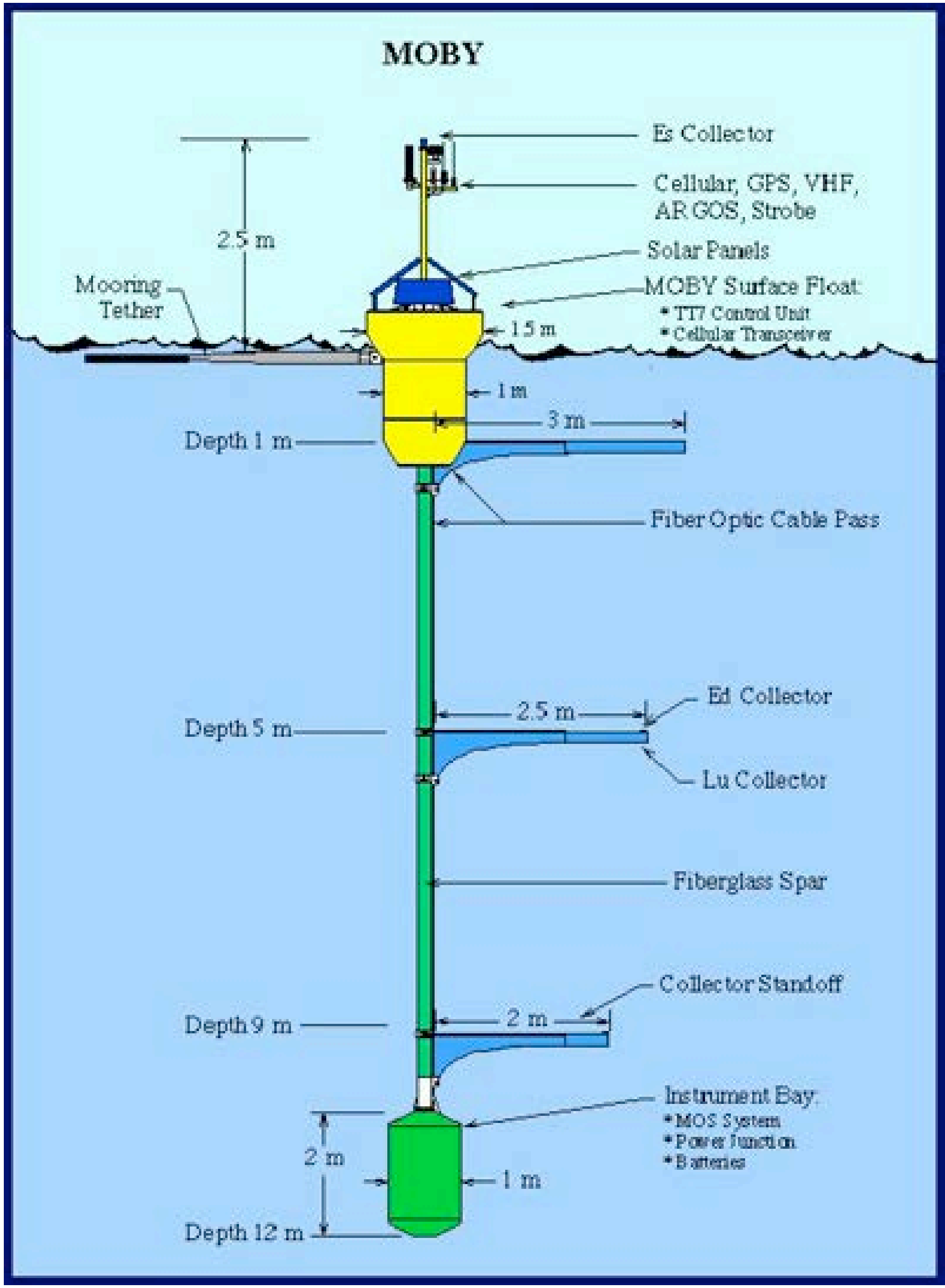

Obtain a time series of Lw, individual measurements used in VC

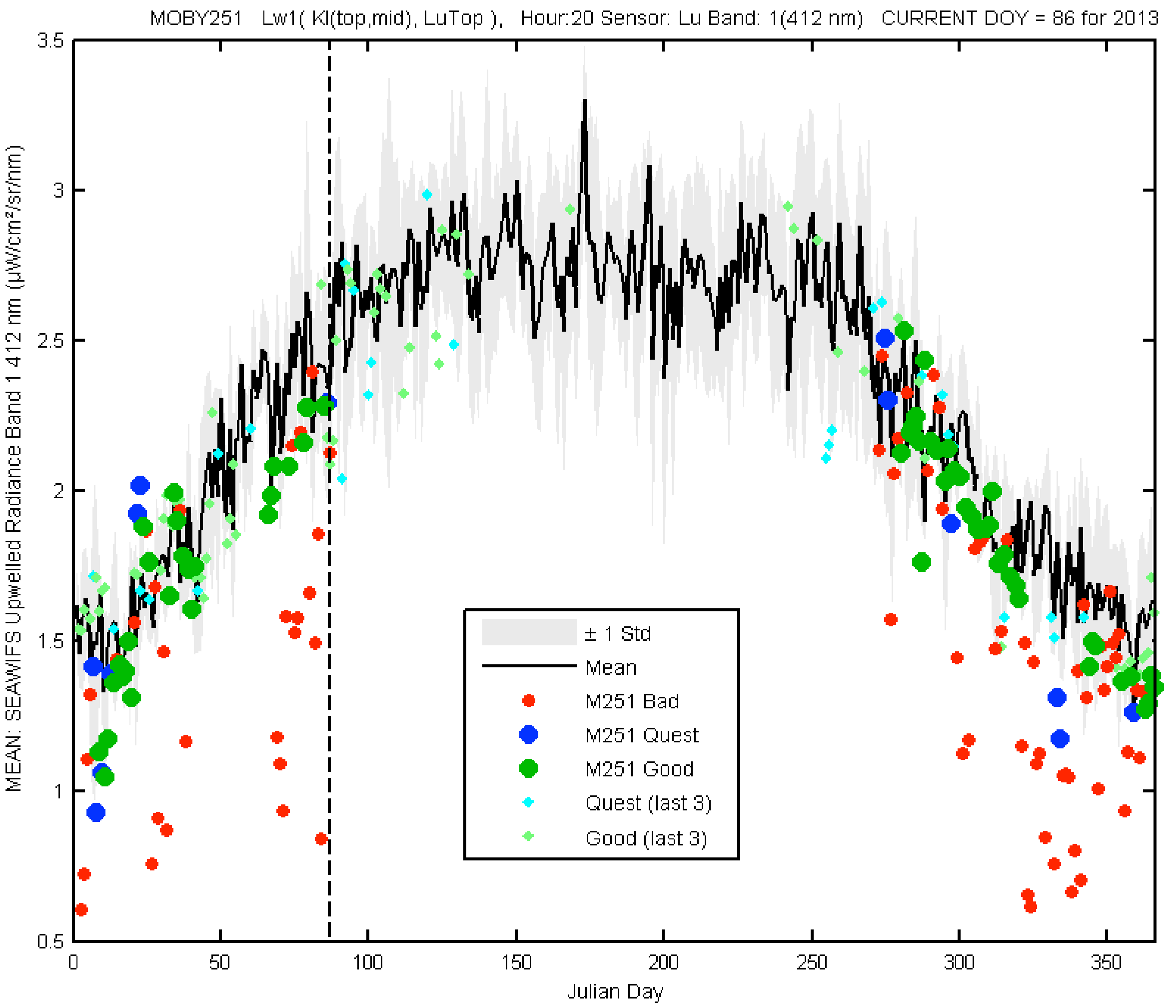

Each good measurement if a corresponding satellite measurement is found, can be be used to generate a gain factor to adjust the calibration of the satellite sensor

Goals of MOBY-Refresh

- Update control electronics (example, TT7 has 68332 processor, 100MByte HD limit).
- Update optics to correct degradation, and improve system above original performance
- Add other systems (UV biofouling, better orientation sensing, better depth sensing) to reduce uncertainties in the final products.

GOALS: Reduce risk of instrument failure and improve measurement variability and uncertainty!

MOBY Refresh

If there is one point that we are using to improve the MOBY Lw uncertainties it is the concept of simultaneity:

Simultaneous acquisition of all Lu, Ed, and Es data (7-8 channels)

Possibility to include calibration inputs at same time (red, blue LED’s, incandescent lamp).

Simultaneous acquisition of other auxiliary measurements: tilt, roll, arm depth.

Reduce measurement uncertainties and variability!

This is a combination of measurement variations and atmospheric correction variations

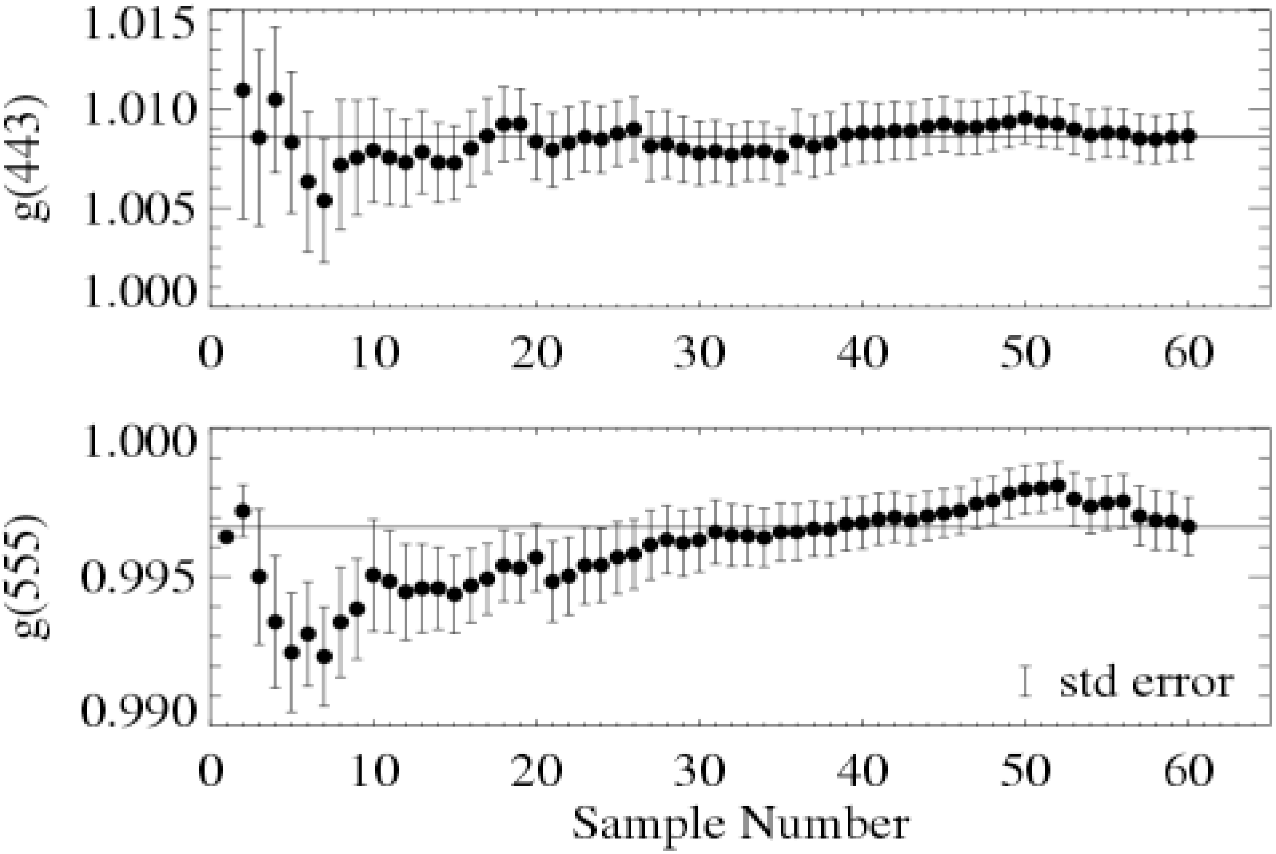

Werdell et al., 2006, Ocean Optics XVIII,
http://oceancolor.gsfc.nasa.gov/cgi/obpgpubs.cgi

MOBY Refresh

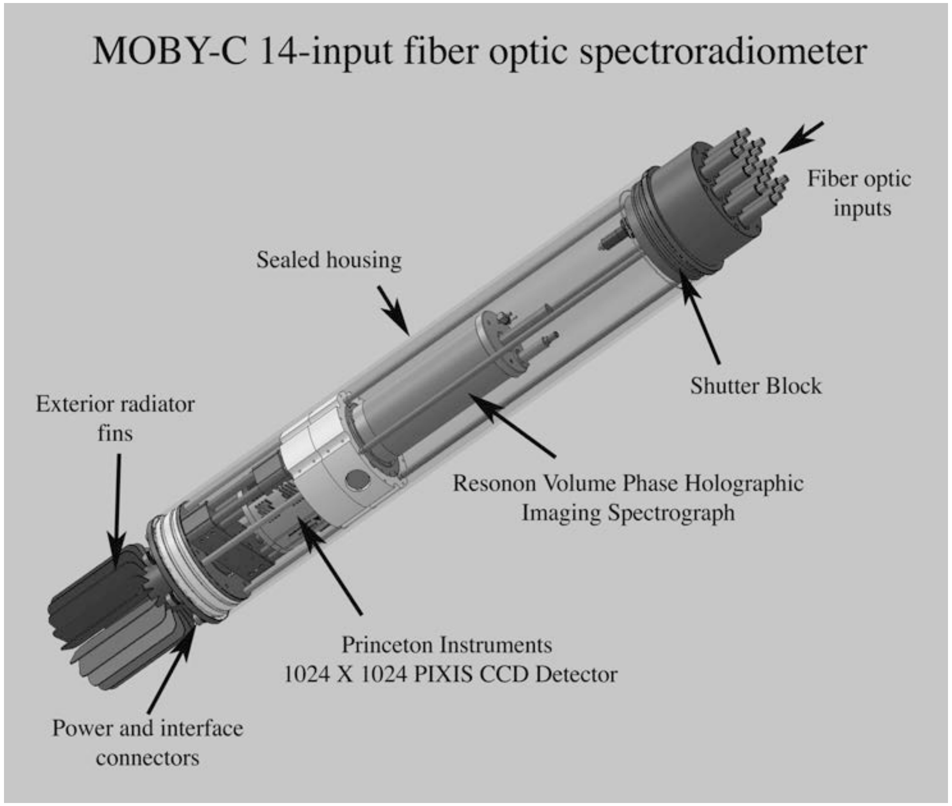

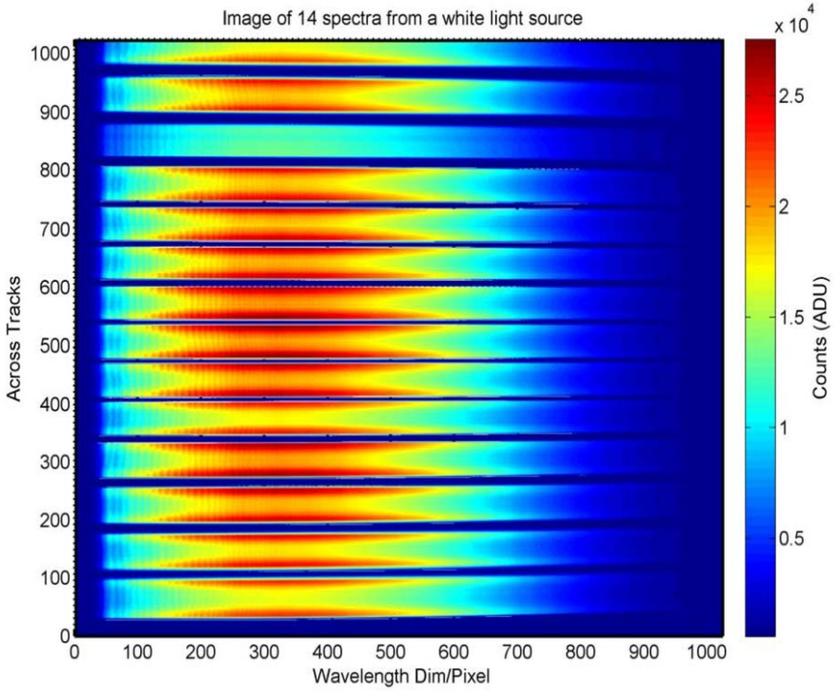

MOBY Refresh

Auxiliary measurements (tilt, roll, compass, depth) currently measured between other measurements now.

With new controllers they will record these values at high frequency while spectrometer shutter is open….will return minimum, maximum, standard deviation, average.

Auxiliary measurements will be more accurate, for example 24-bit high speed pressure transducer for depth.

Schedule

- 6/13-2/14-blue spectrometers have been ordered, control system is assembled and is being programmed, orientation modules in hand.
- 3/14-2/15: Fabricate parts to be able to attach spec to MOBY (along with old optics), develop control software, start characterizing systems
- 3/15-2/16: Finish characterizing systems, start fielding first set of Blue optics on a buoy deployment, continue fabricating other blue systems

Schedule continued

- 3/16-2/17: Start acquisition for Red optical system. Keep Blue system operating side/side with the old system.
- 3/17-2/18: characterize Red optical system, deploy as possible
- 3/18-2/19: phase out old optics, operational deployment with 3 full up buoys with spare part assemblies for another system.

"Calibration uncertainty in ocean color satellite sensors and trends in long-term environmental records"

K.R. Turpie, R.E. Eplee, Jr.,
B. Franz, C. Del Castillo

Suomi National Polar-orbiting Partnership (NPP)
Science Team Meeting
College Park, Maryland
14 May 2014

INTRODUCTION

- **There has been considerable interest in estimating trends in the oceanic phytoplankton activity in response to climate change and anthropogenci forcing.**
- **Observed changes in chlorophyll *a* concentration is a key indicator of change in phytoplankton activity.**
- **Spatial and temporal patterns of chlorophyll *a* concentration in the upper layers of the ocean can be estimated synoptically using remote sensing.**
- **However, before we can make statements about changes or trends in chlorophyll a, we must quantify how much can be attributed to uncorrected variation in the instrument.**
- **This study introduces an initial study connecting residual instrument change on satellite chlorophyll data.**

INTRODUCTION

- Several sources of uncertainty could change with time, and thus could affect trends (or effect spurious trends) in ocean color data products.

  - **Instrument calibration trend uncertainty.**

    - **Extapolation Uncertainty**
    - **Solar Diffuser Stability Monitor**
    - **Relative Spectral Response Change**
    - **Polarization Response Change.**
    - **Counts-to-Radiance Conversion**

INSTRUMENT CALIBRATION TREND UNCERTAINTY

WHAT WE KNOW :

- ❑ Errors in at-sensor measurements stem from calibration and instrument effects (e.g., noise).

- ❑ Measurements of the ocean surface require removal of the atmospheric contribution to at-sensor measurements. The NIR bands assist with this step.

- ❑ Because the atmosphere contributes to ~90% of the measured light, a small error is relatively large to the remaining surface contribution.

- ❑ **Opposite-signed errors between the two NIR bands lead to significant effects in the surface measurements.**

- ❑ **Errors in surface measurements for the blue and green bands lead to errors in the estimate of Chlorophyll *a*.**

- ❑ **Trends in these errors can lead to spurious trends in Chlorophyll *a*.**

Relative Mean Bias for nLw

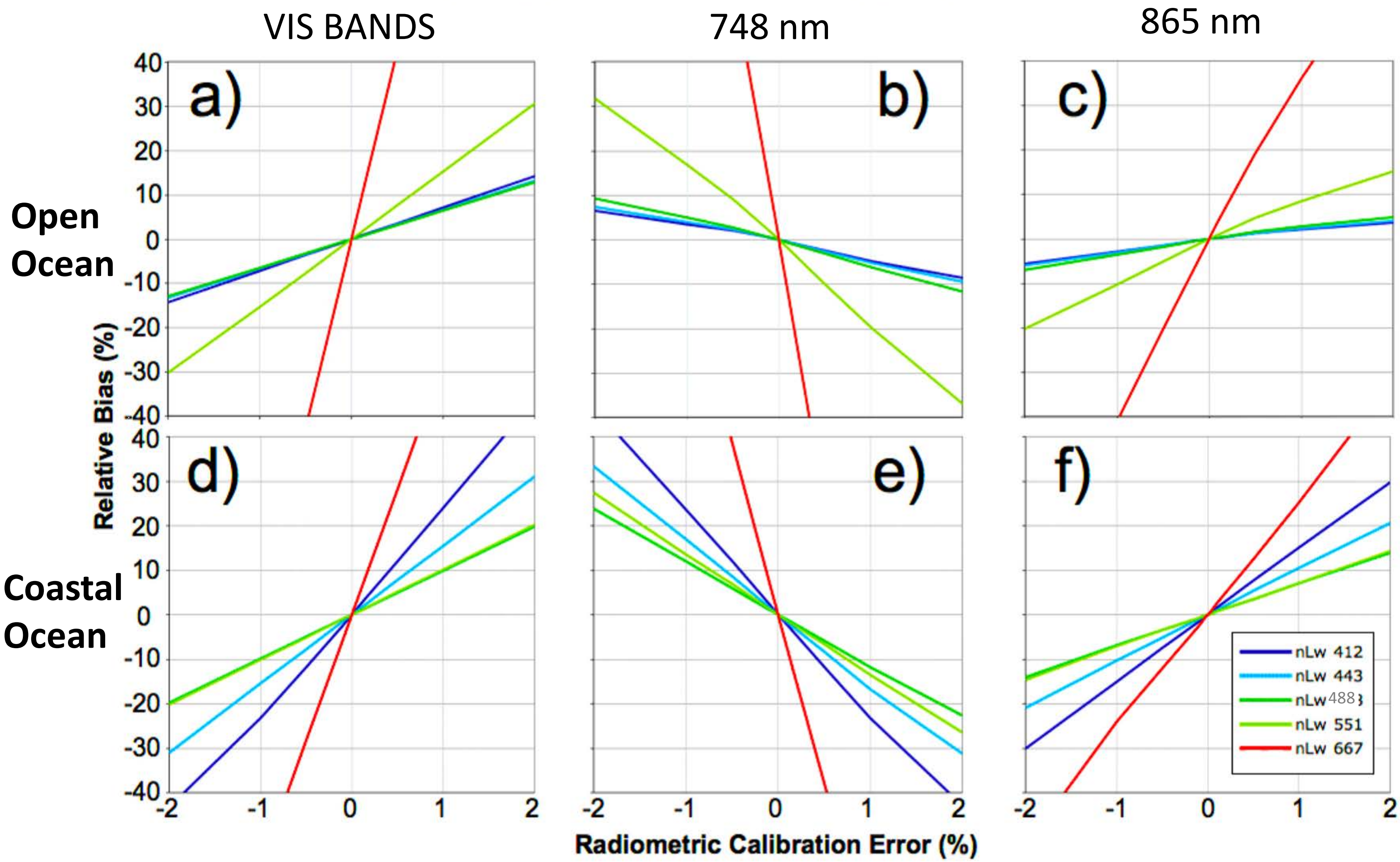

A small relative error in the at-sensor measurement leads to a relative error in the surface measurement that is an order of magnitude larger.

Changes between band pairs can also have effects.

For instance, opposite-signed errors in NIR ratios can cause coastal and open ocean waters to change in opposite directions.

Such changes could suggest false geophysical interpretations.

Affects on Chlorophyll of opposite signed errors in NIR bands of 0.3%

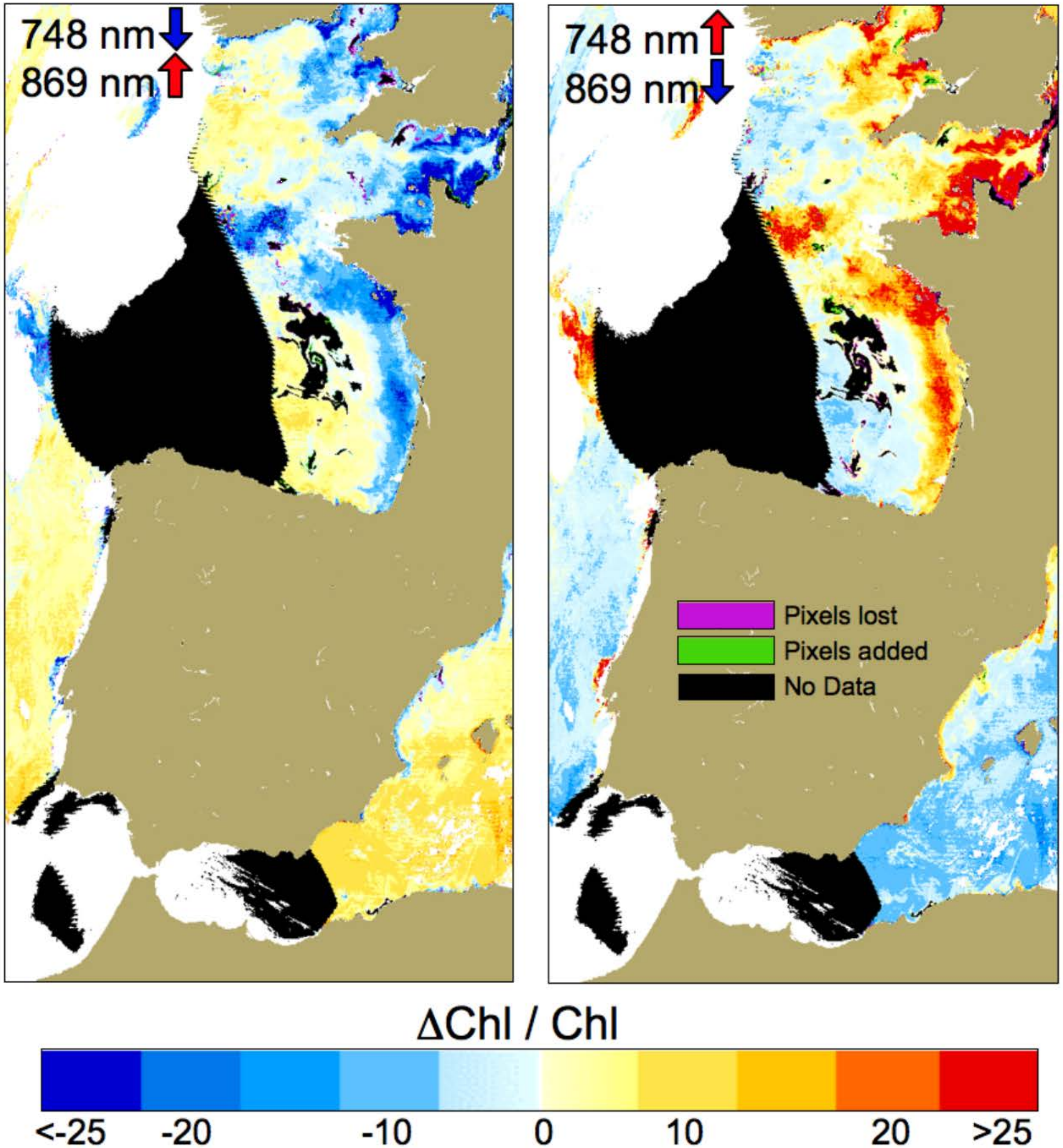

INSTRUMENT CALIBRATION TREND UNCERTAINTY

WHAT WE KNOW :

- ❑ VIIRS (like SeaWiFS or MODIS) experiences changes in responsitivity with time.
- ❑ This change is expecially pronounced for Suomi-NPP VIIRS in the NIR.
- ❑ Measurements of the Solar Diffuser (SD) to track and account for these changes.
- ❑ **Like MODIS, NASA OBPG fits functions to the SD measurement trends and those are used to correct data in the Earth-view measurements.**
- ❑ **Small, residual errors in this process could lead to spurious trend errors in surface measurements.**
- ❑ **This can be assessed with examination of trending residual and a Monte Carlo experiment.**

METHODOLOGY

- Calibration trends are fitted using the same methods used for SeaWiFS and MODIS.
- Nonlinear fit using Levenberg-Marquardt optimization
- For VIIRS, a linear combination of Exponential and Linear terms fit to blue-green band trends.
- Linear combination of two Exponential terms are fit to red-NIR band trends.

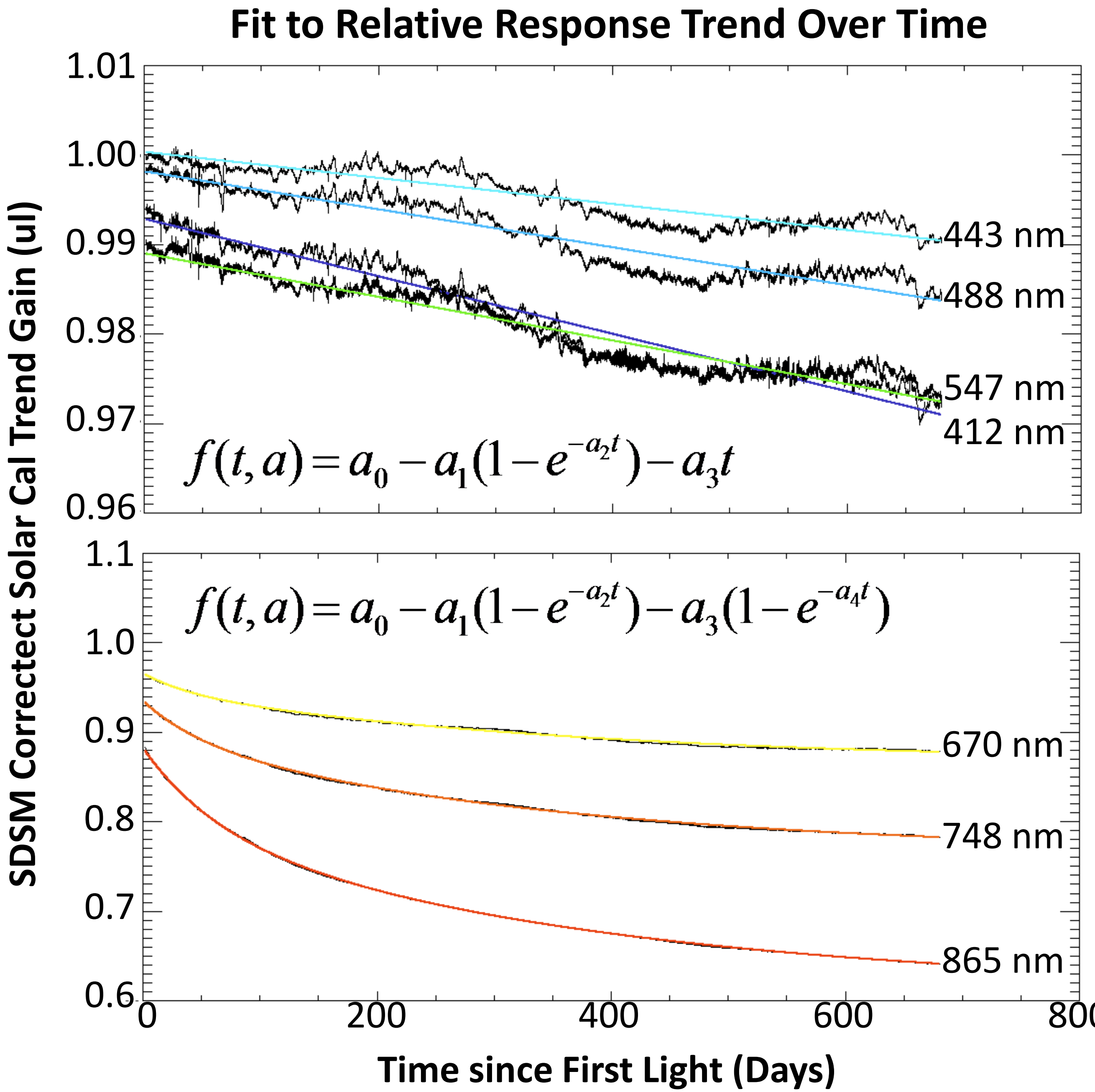

METHODOLOGY

- ❑ Declare the operational fitted functions as the “true” instrument trend.
- ❑ Add a random noise model using Gaussian (white) noise plus a systematic, seasonal signal.
    - Gaussian noise component has a standard deviation of 0.1%, matching the original fit residuals.
    - Systematic effect is given an amplitude of 0.2% matching the original fit residuals.
- ❑ Fit the original trend curve plus the noise model.
- ❑ Take the difference between the original “true” trend and the new fitted curve to get the modeled spurious trend.
- ❑ Compute the root mean squared error (RSME) of the modeled spurious trend.
- ❑ Repeat the process many times, each time collecting RSME of the modeled spurious trend.

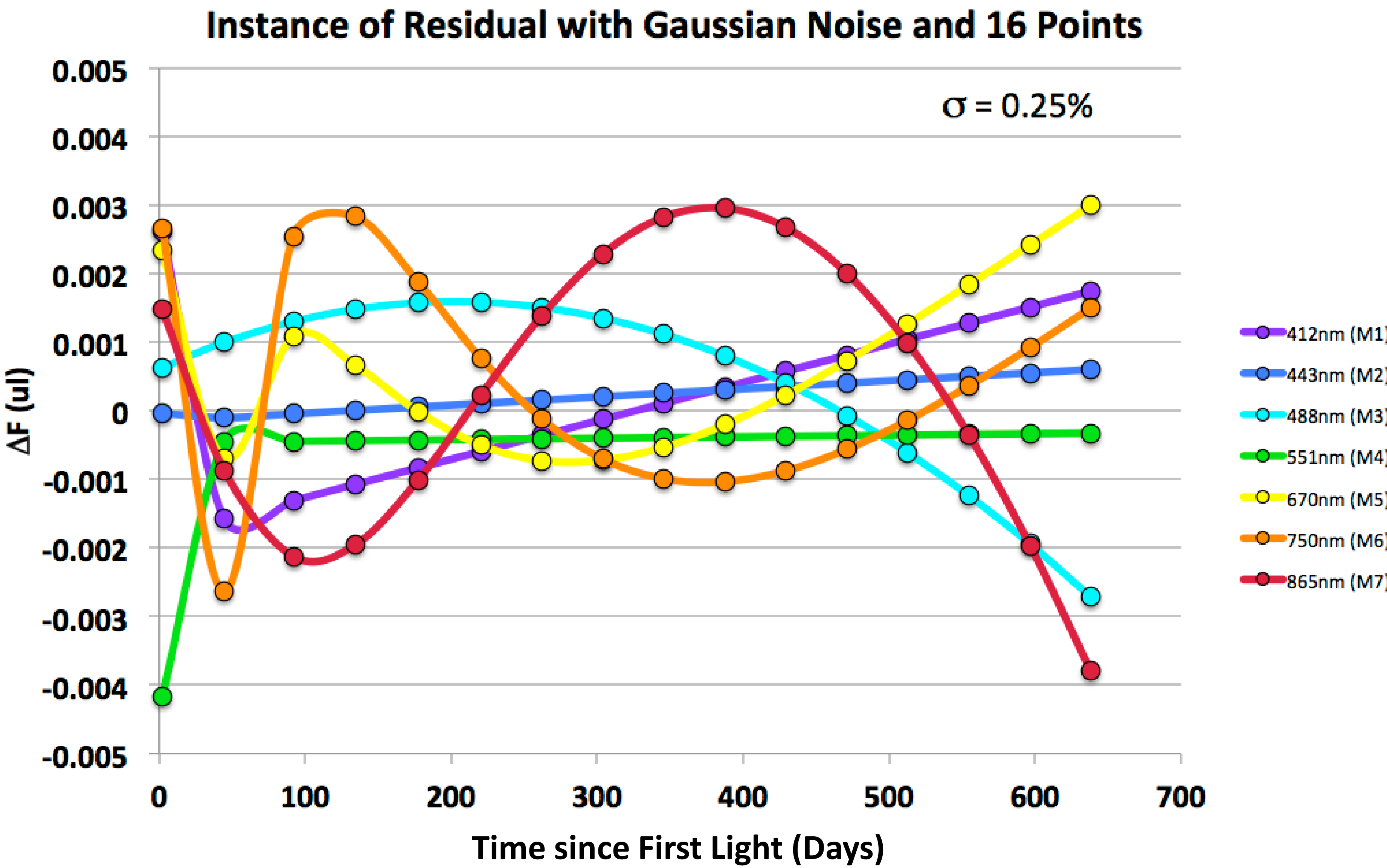

To demonstate what a single trial can look like, one was generate for a noise level of 0.25%. The spurious trends over the two year period are large and, unlike the input noise, strongly autocorrelated (note NIR bands)

ADDITION OF A SYSTEMATIC EFFECT

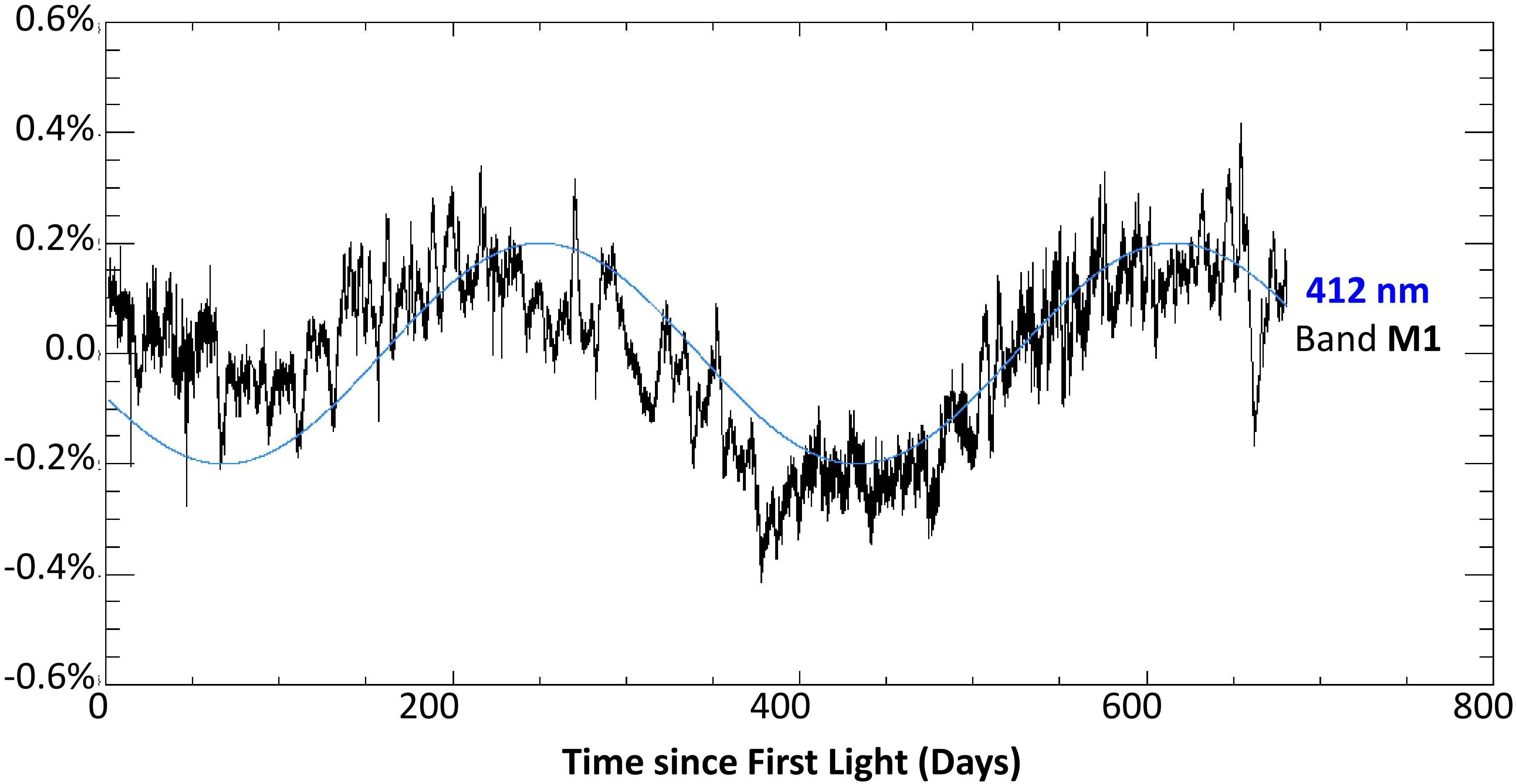

- This is a sinusoidal curve similar to the systematic effect seen in the blue bands.
- The longer wavelength bands are slightly more complex, but about the same amplitude.

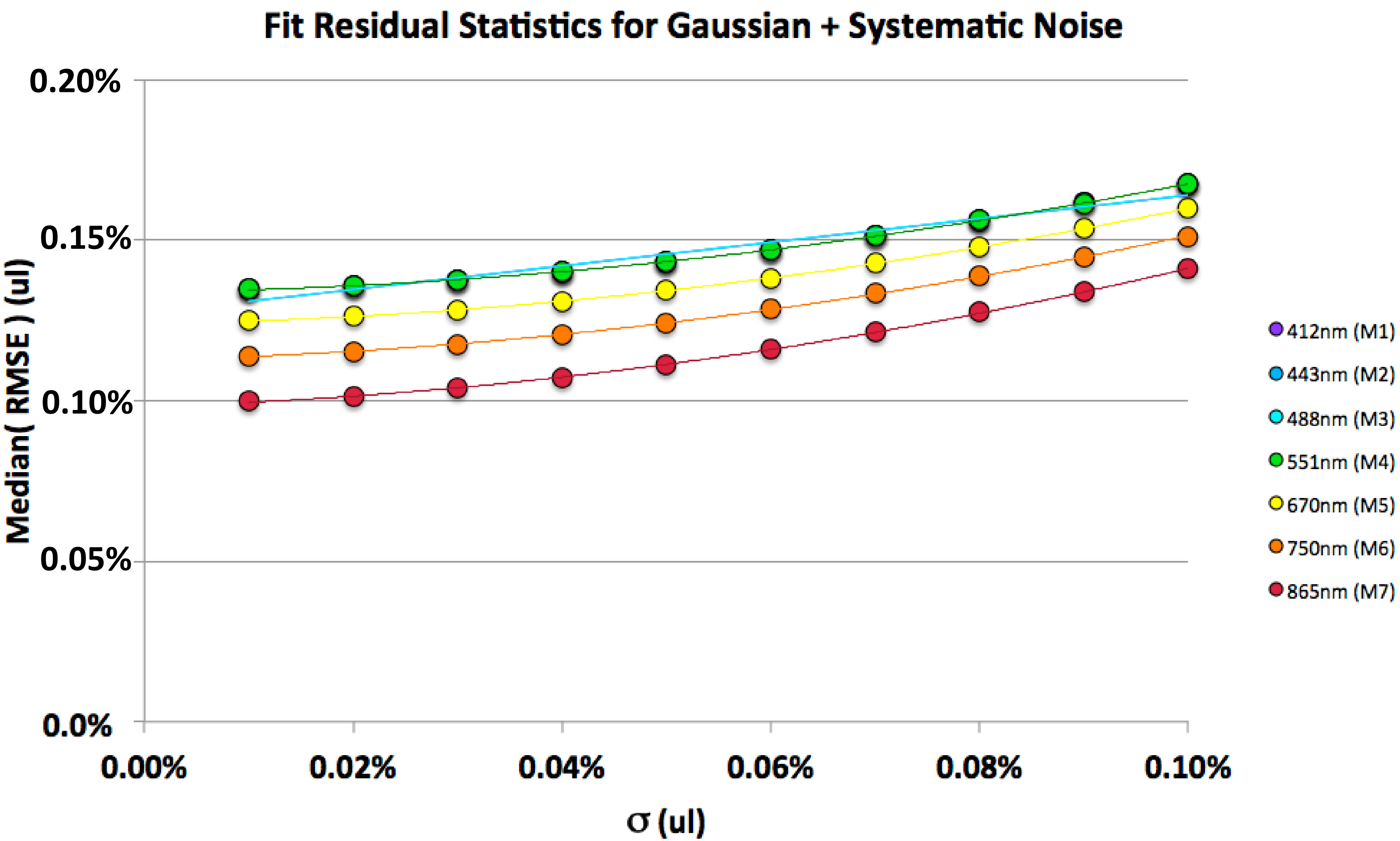

- **Increasing the noise level (σ) from 0.01% to 0.1%.**
- **The 0.2% systematic error effects dominate the residual.**
- **The band wavelength relationship is reversed from the spurious trend.**

RESULTS

- The Monte Carlo experiment was repeated for several Gaussian noise standard deviation ranging from 0.01-0.10%.
- A systematic, seasonal noise component with a 0.2% amplitude as also added.
- Using noise model with a Gaussian noise component alone produced a modeled spurious trend with median RSME that was comparable to the input noise standard deviation.
- Inclusion of a systematic, seasonal noise component of 0.2% caused a ~0.1% median RSME.
- The resulting effect to Chlorophyll *a* trends would be smaller than the 0.3% effect in the example shown, but still significant, especially given the autocorrelation.

CONCLUSIONS

- We cannot know whether the functional form sufficiently describes the underlying SD trend, unless another reference is available.
- Gaussian noise alone is easy to fit through, but produces a spurious trend with slight less amplitude, but strongly autocorrelated.
- Including a 0.2% systematic, seasonal artifact, induces a significant spurious trend comparable in amplitude.
- Resulting trends are highly autocorrelated and can be anti-correlated between bands (exacerbating the effect to derived products).
- These effects could cause apparent “geophysical” trends in Chlorophyll a observations at the few to several percent level.
- Reduction in the systematic artifact (e.g., with new calibration system look-up tables) may greatly reduce most of the trend uncertainty.

RECOMMENDATIONS AND FUTURE WORK

- ❑ **Further modeling should be done for longer time series and for various sampling densities (e.g., densities analogous to lunar data).**

- ❑ **Resulting biases should be directly propagated to ocean surface measurements to confirm/quantify impact.**

- ❑ **Other sources of trend uncertainty should be assessed.**

  - **Extapolation Uncertainty. (soon)**
  - **Solar Diffuser Stability. Monitor (NASA VIIRS Calibratin Support Team)**
  - **Relative Spectral Response Change. (underway)**
  - **Polarization Response Change. (future)**
  - **Counts-to-Radiance Conversion. (future)**

THANK YOU

INITIAL EXPERIMENT: EFFECT OF NOISE ON FIT PARAMETERS

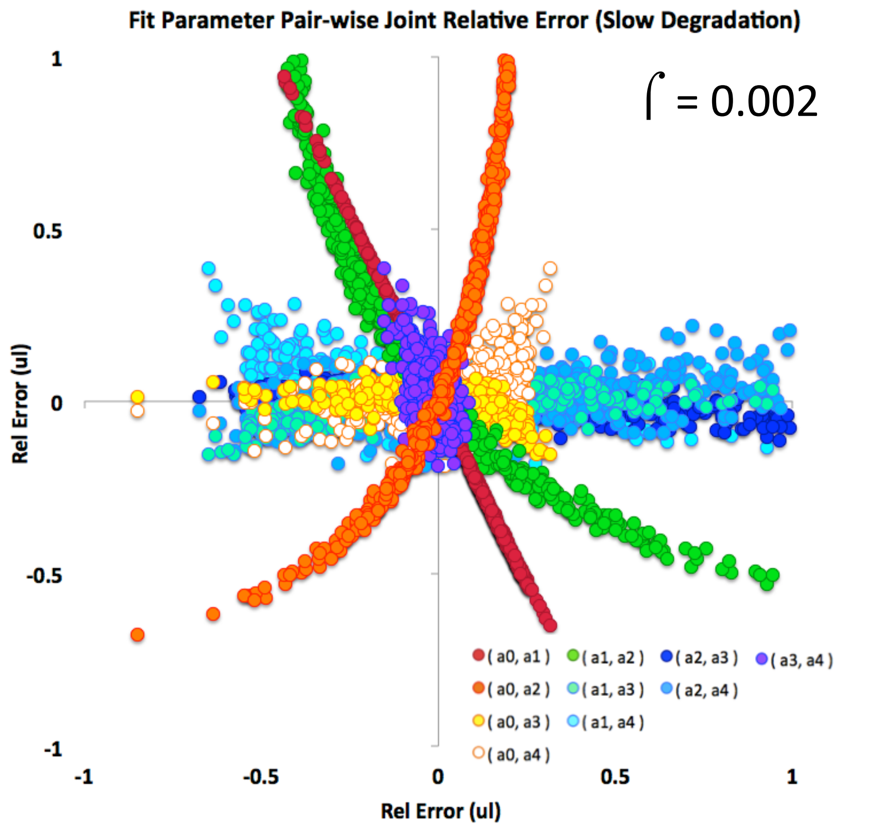

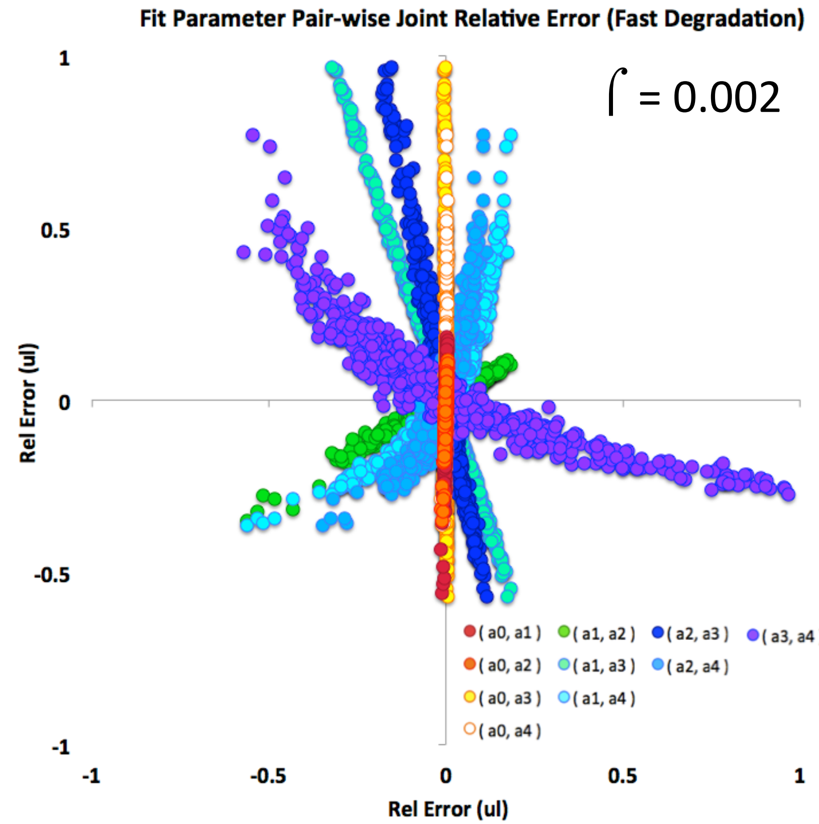

RESULTS

- The fit parameters can change greatly with the random point-to-point variation.
- The parameter variation is highly correlated.
- This suggests that there are multiple or shallow minima in parameter space.
- This is similar to an underdetermined problem.
- However, we are not after the parameters themselves – so this is not a big problem.

Validation of Ocean Color Sensors Using a Profiling Hyperspectral Radiometer

Michael Ondrusek	NOAA NESDIS
- michael.ondrusek@noaa.gov	
Eric Stengel	NOAA NESDIS
Marina Ampollo Rella	NATO NURC
Wesley Goode	Naval Research Laboratory
Sherwin Ladner	Naval Research Laboratory
Michael Feinholz	Moss Landing Marine Laboratory

2014 STAR JPSS Annual Science Team Meeting
NCWCP College Park, MD May 14, 2014

- **Validation of satellite ocean color sensors :**
  - Requires accurate and traceable in situ measurements
  - Hyperspectral to match all sensors
  - Many matchups and water types

- **Satlantic Profiler II (Hyperpro) in-water radiometer:**
  - Hyperspectral
  - Profiling
  - Lu, Ed, and Es

- **Validation capabilities**
  - Lwn/Rrs (in- and above-water)
  - Chlorophyll/pigments
  - Backscatter/Absorption
  - TSM
  - Aerosol Optical Depth

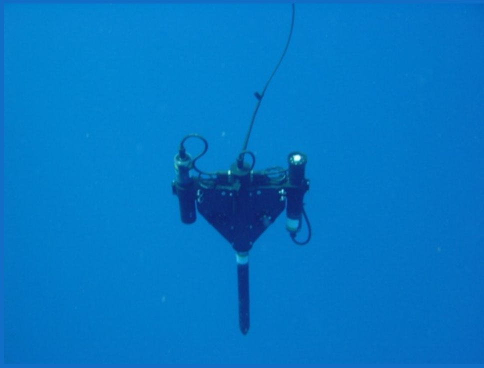

OUTLINE

- Past validations
- Calibration stability
- Inter-calibrations
- Consistency between Hyperpros
- Matchups to MOBY and Boussole
- Comparison to above-water measurements
- Initialization and Validation of JPSS Suomi NPP VIIRS

NOAA has been using a Hyperpro in-water radiometer to validate ocean color sensors and algorithm development since 2006

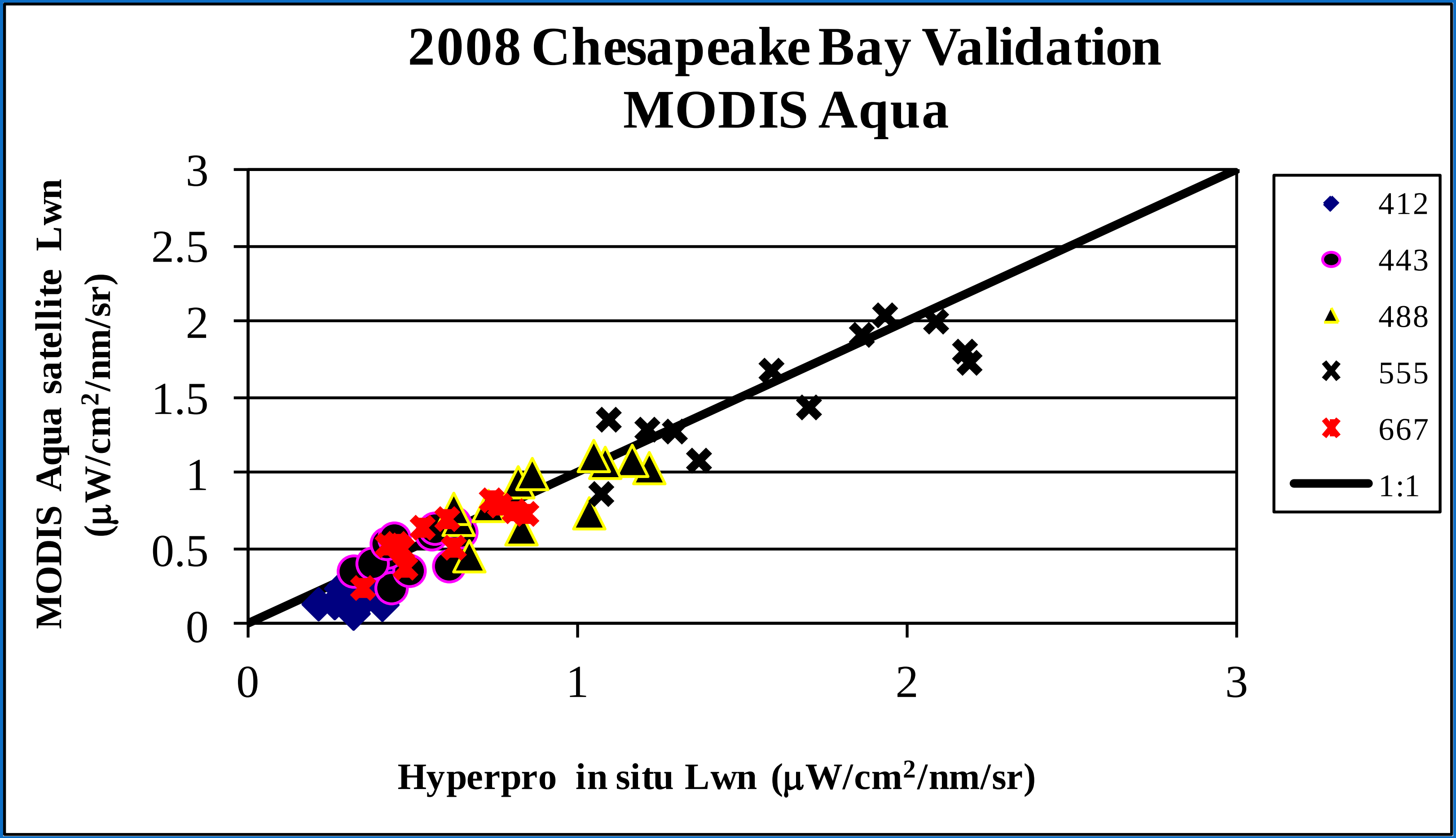

CALIBRATION STABILITY

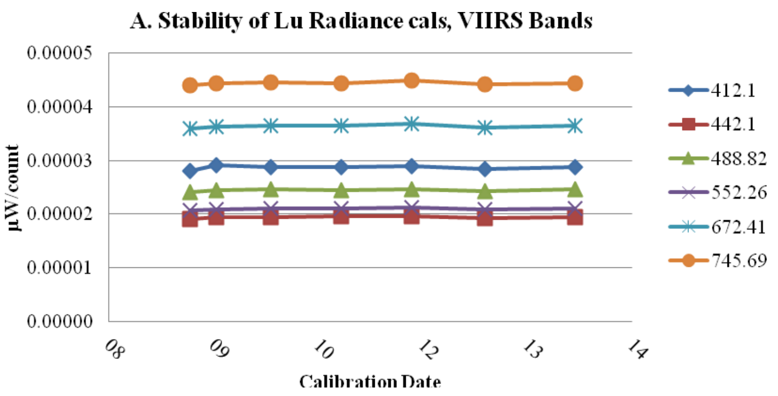

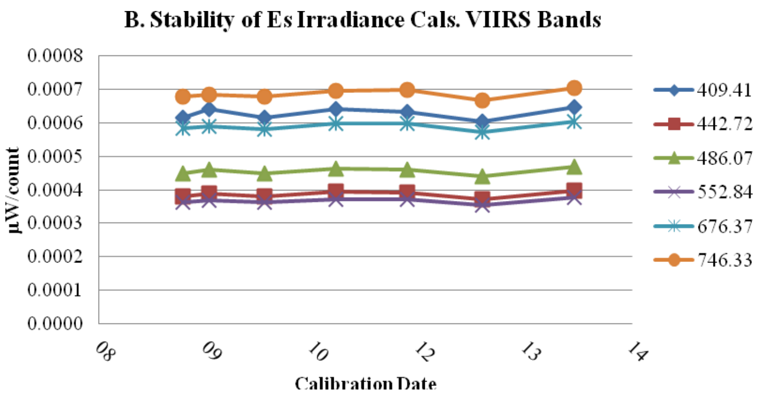

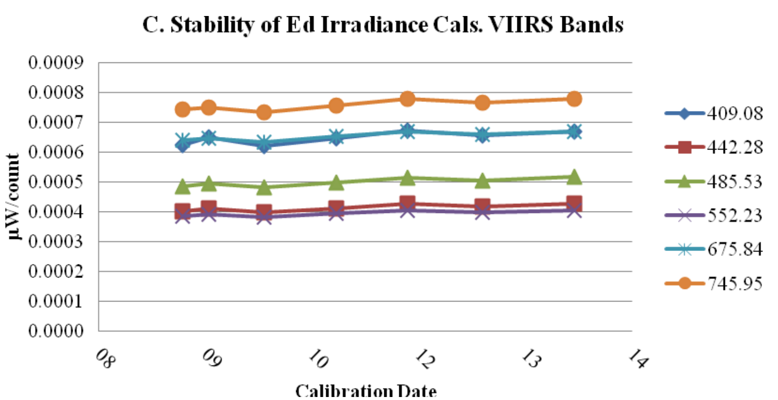

nW/count

A. Lu	412.1	442.1	488.82	552.26	672.41	745.69
3/19/2009	0. 0281	0. 0191	0. 0240	0. 0207	0.0359	0. 0440
7/22/2009	0. 0291	0. 0195	0. 0245	0. 0209	0. 0363	0. 0443
4/7/2010	0. 0288	0. 0195	0. 0246	0. 0211	0. 0365	0. 0445
3/9/2011	0. 0289	0. 0196	0. 0246	0. 0210	0. 0364	0. 0443
2/9/2012	0. 0289	0. 0196	0. 0247	0. 0212	0. 0368	0. 0449
1/24/2013	0. 0284	0. 0193	0. 0242	0. 0208	0. 0361	0. 0441
3/31/2014	0. 0288	0. 0196	0. 0246	0. 0210	0. 0364	0. 0443
Average	0. 0287	0. 0194	0. 0245	0. 0210	0. 0364	0. 0443
Std Dev.	0. 0003	0. 0002	0. 0002	0. 0002	0. 0003	0. 0003

B. Es	409.41	442.72	486.07	552.84	676.37	746.33
3/19/2009	0. 616	0. 381	0. 450	0. 364	0. 583	0. 679
7/22/2009	0. 640	0. 390	0. 459	0. 368	0. 590	0. 685
4/7/2010	0. 614	0. 380	0. 450	0. 363	0. 581	0. 679
3/9/2011	0. 639	0. 393	0. 463	0. 372	0. 597	0. 694
2/9/2012	0. 632	0. 391	0. 461	0. 372	0. 598	0. 699
1/24/2013	0. 605	0. 373	0. 441	0. 355	0. 571	0. 667
3/31/2014	0. 647	0. 398	0.470	0. 377	0. 603	0. 703
Average	0. 628	0. 387	0. 456	0. 367	0. 589	0. 686
Std Dev.	0. 016	0. 009	0. 010	0. 007	0. 011	0. 013

C. Ed	409.08	442.28	485.53	552.23	675.84	745.95
3/19/2009	0. 623	0. 400	0. 486	0. 386	0. 640	0. 744
7/22/2009	0. 649	0. 409	0. 496	0. 390	0. 647	0. 749
4/7/2010	0. 620	0. 397	0. 483	0. 383	0. 632	0. 735
3/9/2011	0. 646	0. 412	0. 499	0. 394	0. 653	0. 757
2/9/2012	0. 672	0. 426	0. 515	0. 405	0. 670	0. 779
1/24/2013	0. 655	0. 416	0. 504	0. 397	0. 659	0. 766
3/31/2014	0. 669	0. 426	0. 516	0. 405	0. 670	0. 777
Average	0. 644	0. 410	0. 497	0. 392	0. 648	0. 755
Std Dev.	0. 018	0. 010	0. 011	0. 008	0. 014	0. 016

Validation of Calibration with MOBY Sources

MOBY CALIBRATION SOURCE 2/25/14

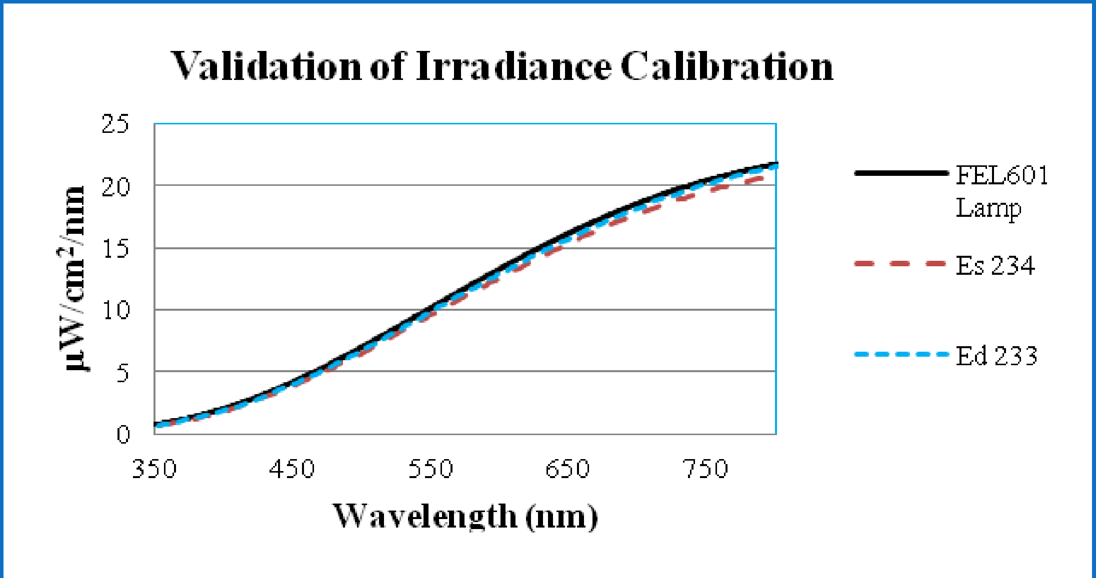

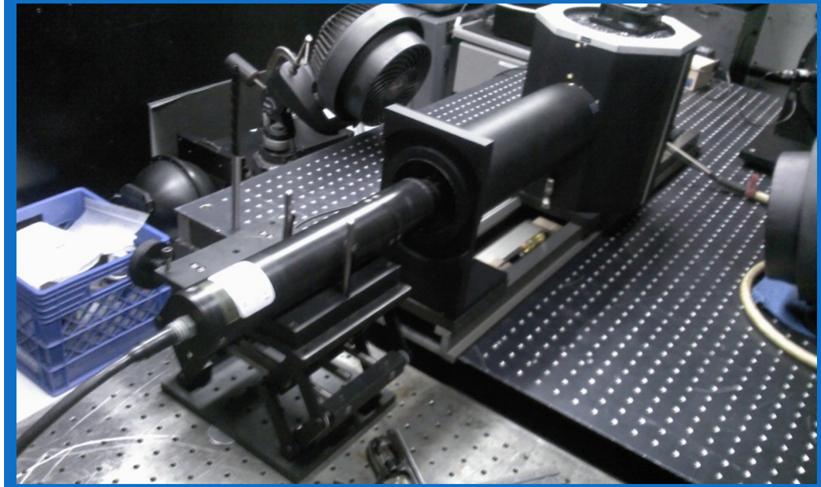

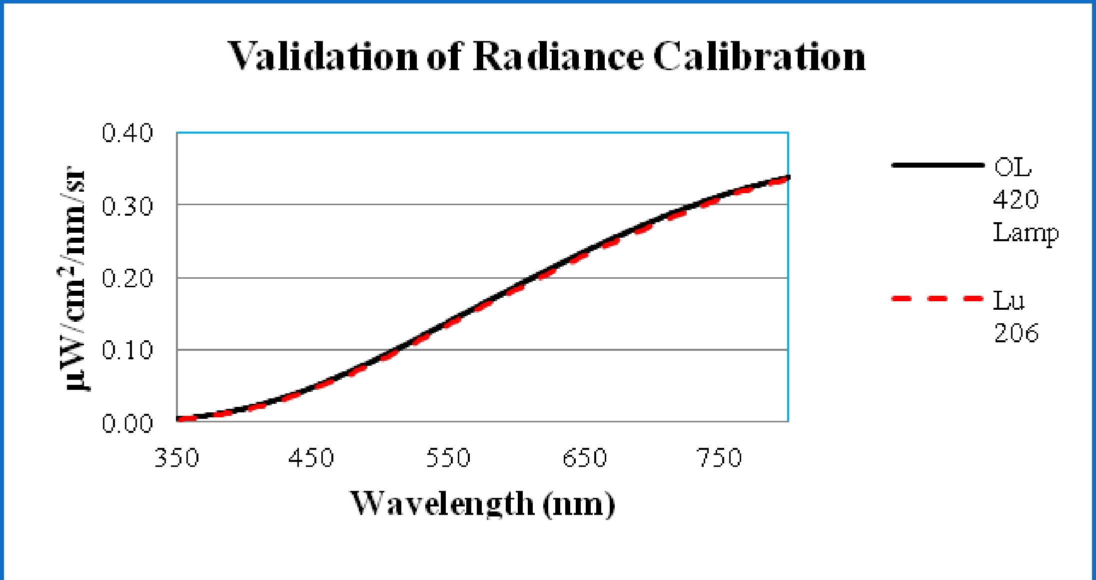

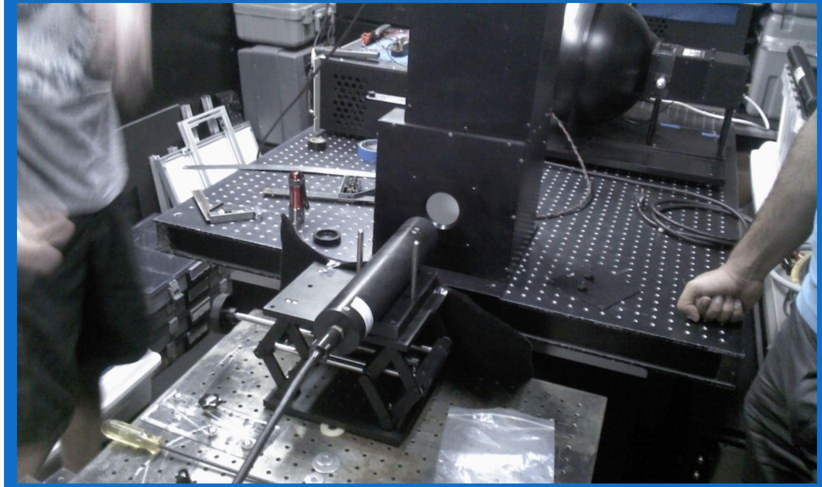

Consistency between Hyperpros, August, 2010 NATO Cruise, 41 Stations with 3 Simultaneous Hyperpro cast to assess variability between instruments.

Lwn plots from different Hyperpro profilers (NOAA dashed line)

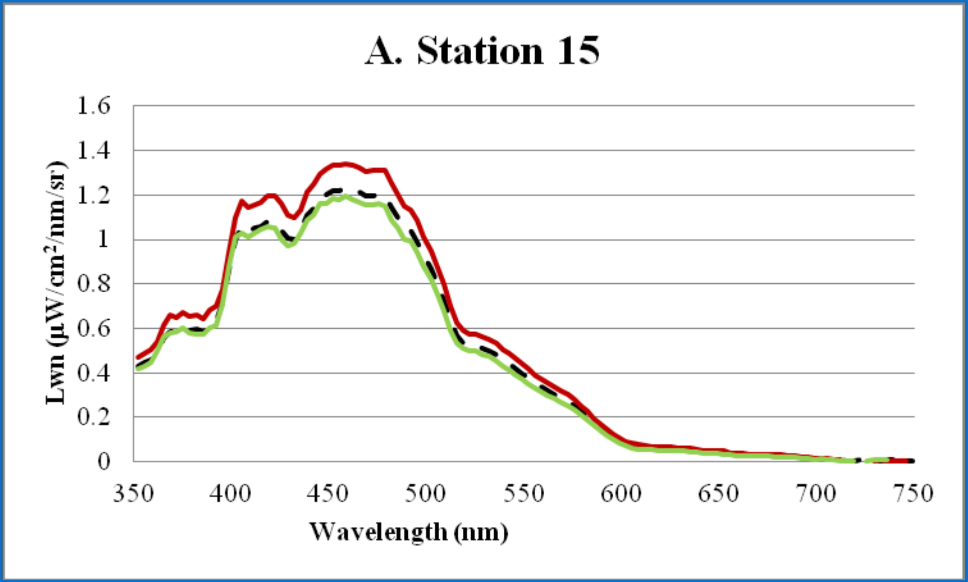

Mean Percent Difference to NOAA Hyperpro

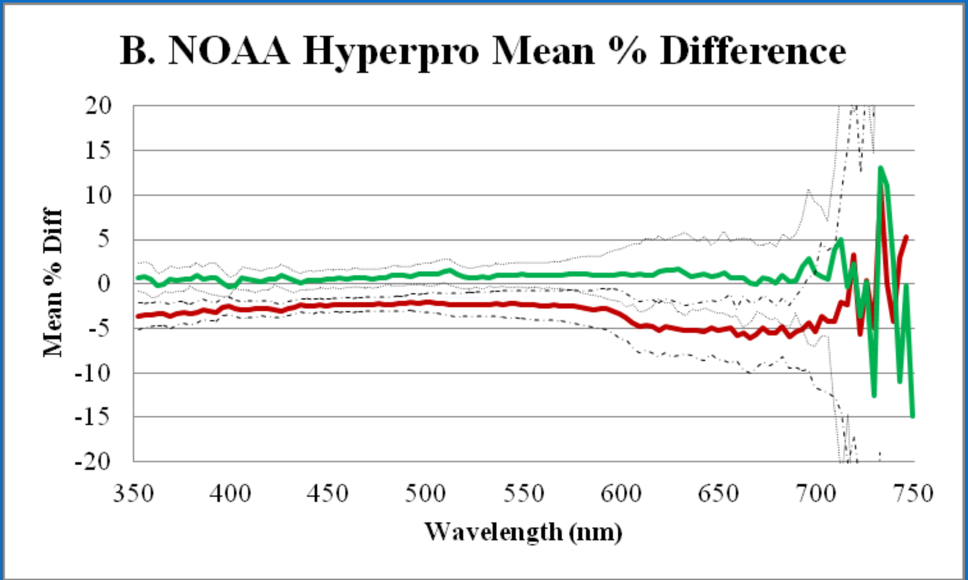

New calibration facility at NCWCP for optical calibrations.

- more frequent calibrations
- inter-calibration of team members.

NIST Spectral Irradiance Standard with Gamma Sci. 5000 Housing

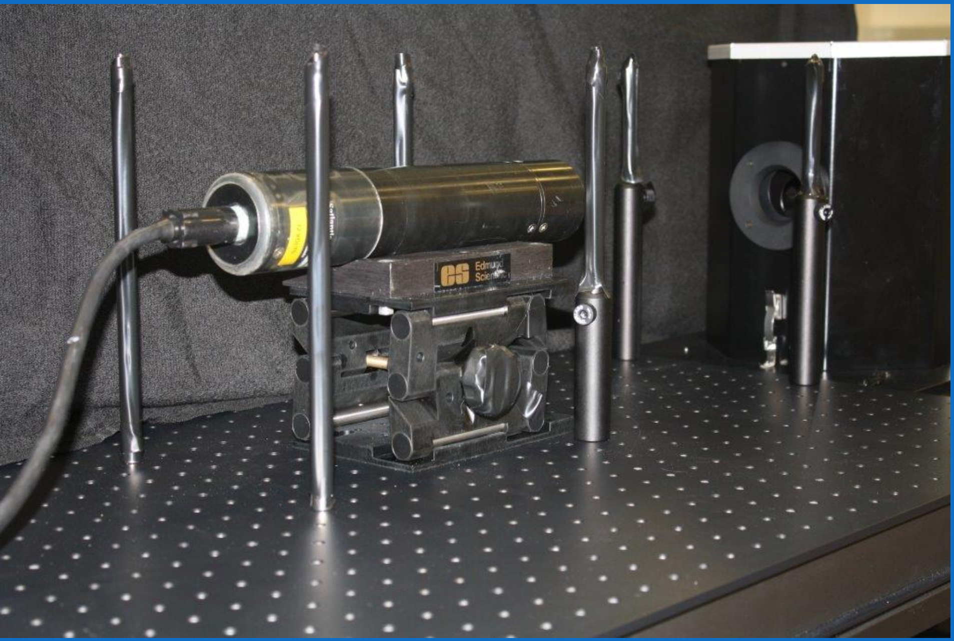

Gooch & Housego OL455 Integrating Sphere Radiance Calibration Source

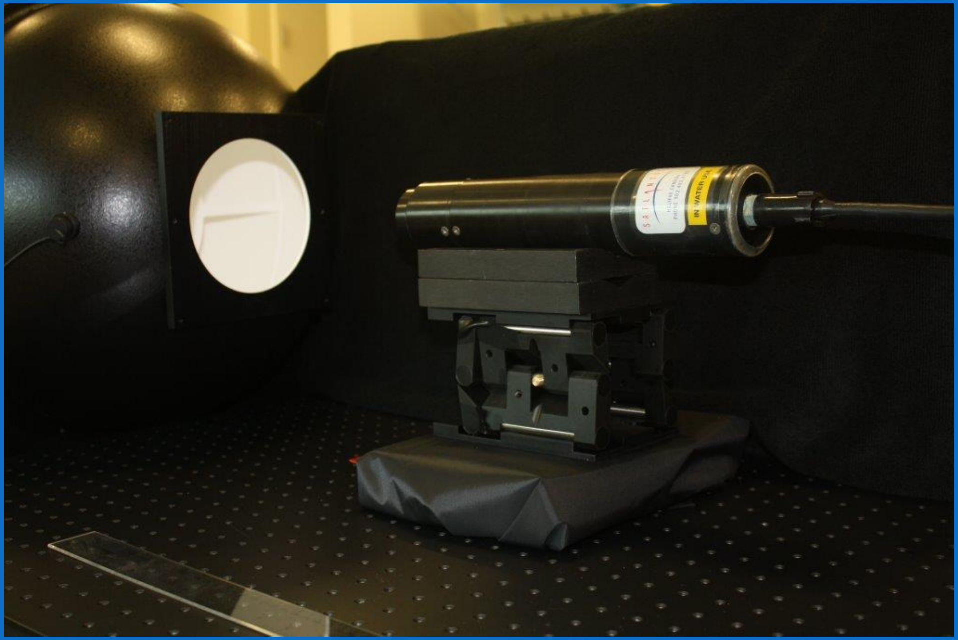

Remote Sensing Reflectances from simultaneous NOAA Hyperpro and Boussole Buoy measured during NATO Cruise, August 30, 2010

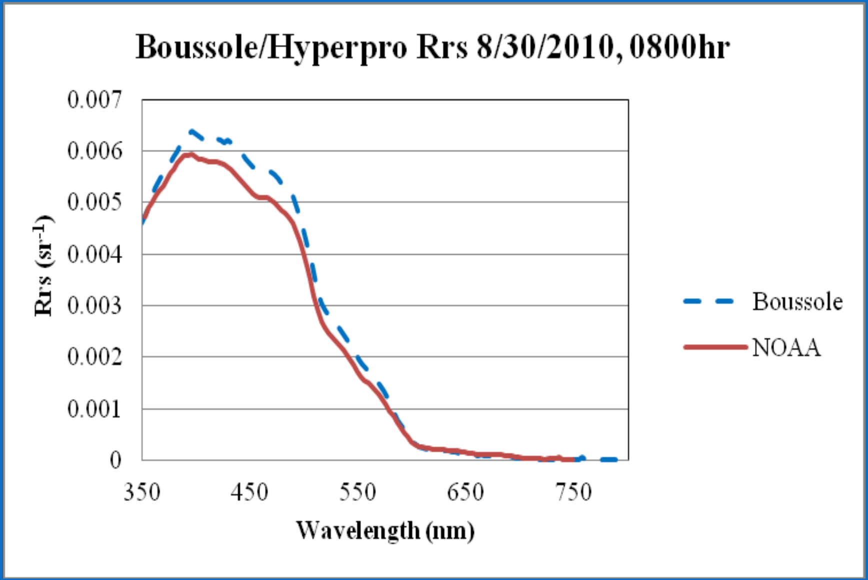

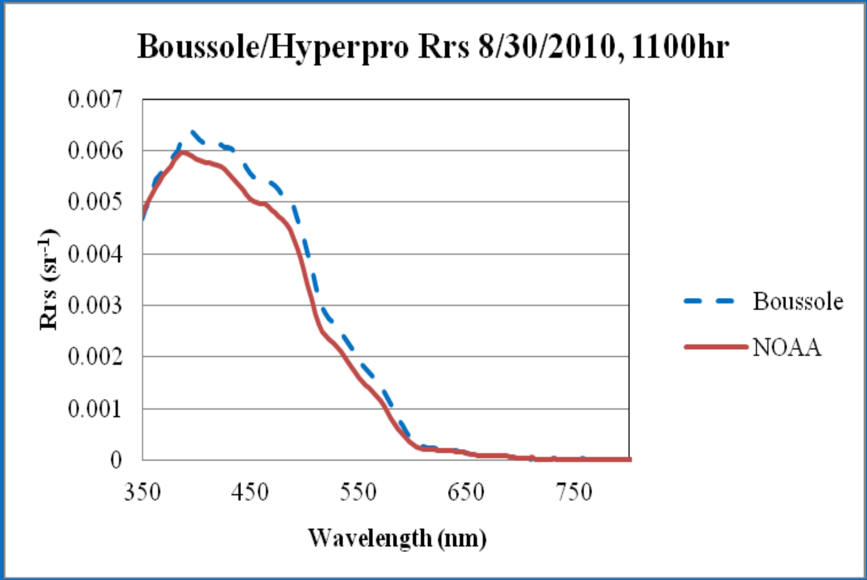

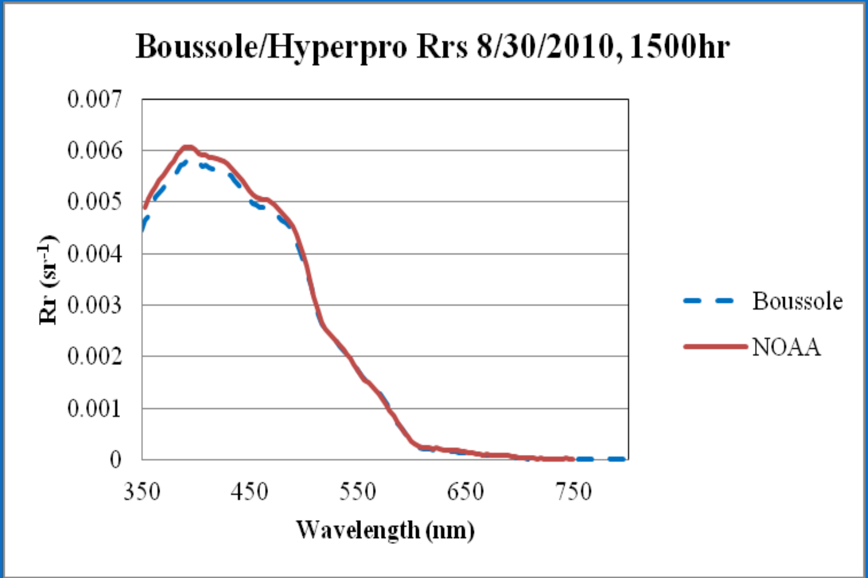

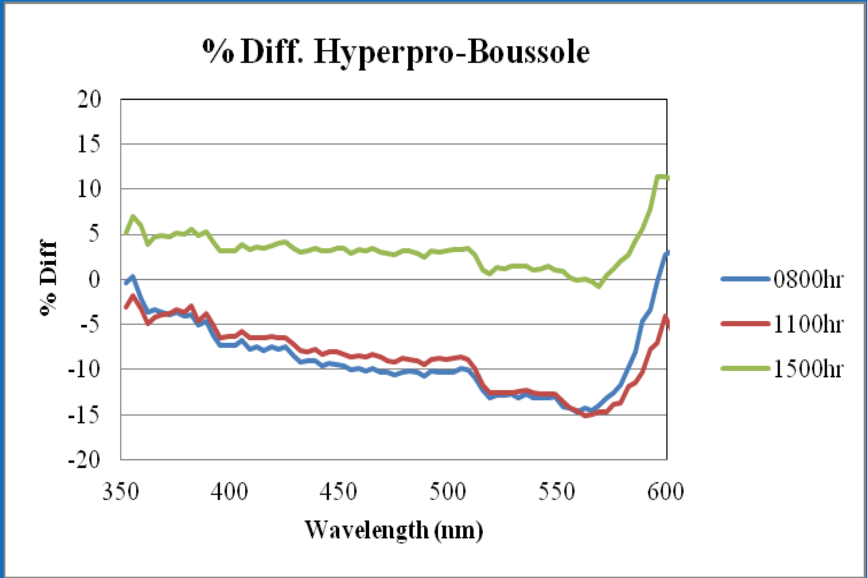

Normalized Water-Leaving Radiances and percent differences from simultaneous NOAA Hyperpro and MOBY Buoy measured during an April 2009 MOBY swapout cruise.

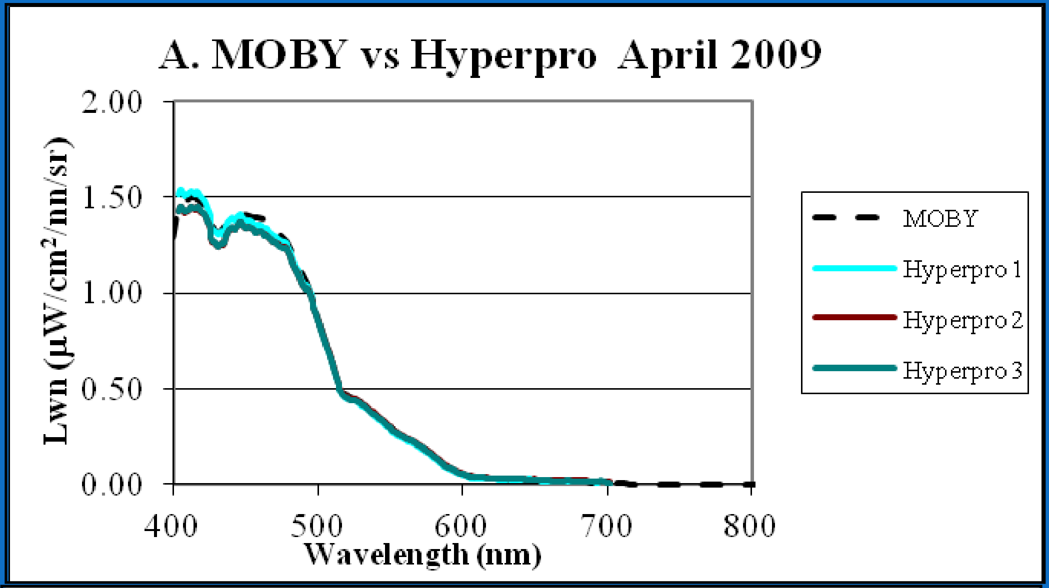

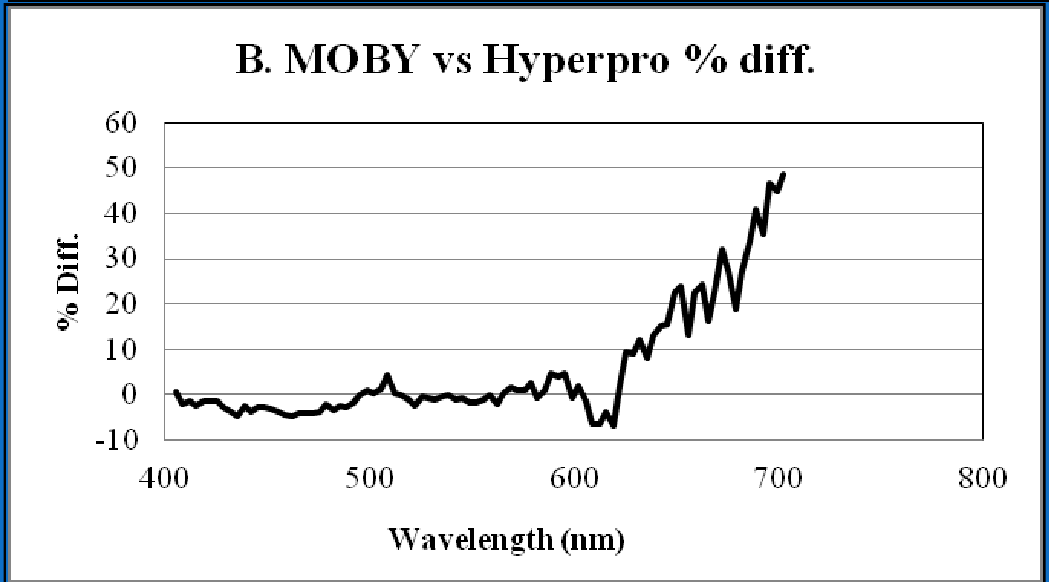

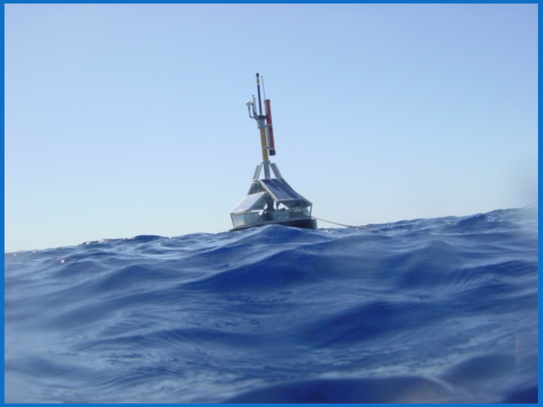

Remote Sensing Reflectance Comparison Between NOAA Hyperpro Profiler and ASD Handheld II above-water radiometer during March 2012 Florida Cruise

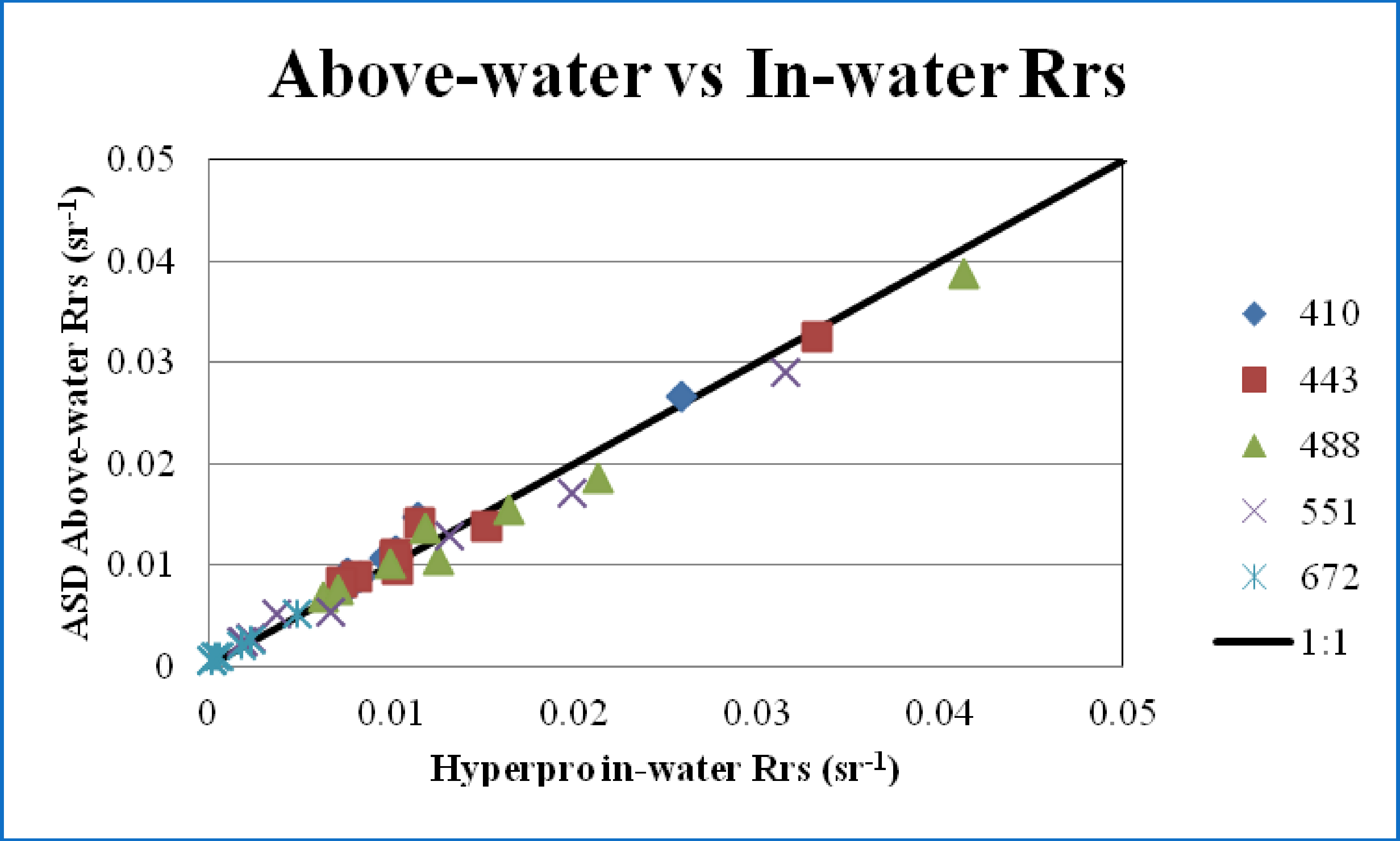

Chesapeake Bay VIIRS Ocean Color Validation: Conducted routine in-water Hyperpro and above-water ASD validation measurements in the Chesapeake Bay 12/1/11, 2/3/12, 3/27/12, 5/11/12, 7/3/12, 10/11/12, 11/2/12, 1/7/13, 1/10/13, 2/14/13, 2/15/13, 4/11/13, 5/1/13, 5/2/13, 5/3/13, 5/30/13, and 5/31/13, 6/21/13 , 7/30/13, 8/12/13, 8/13/13, 8/14/13, 8/15/13, 8/16/13, 8/19/13, 8/20/13, 8/21/13, 8/22/13, 9/25/13 on 10/11/13, 10/21/13, and 12/11/13
Total of 107 Stations in the Bay since Launch of VIIRS.

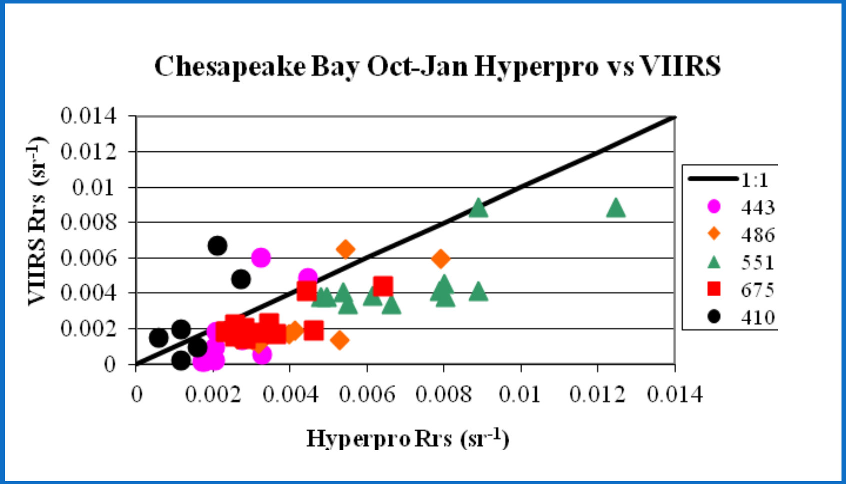

Band (nm)	Avg. % diff. Hyperpro – VIIRS Oct 12-Jan 13	Avg. % diff. Hyperpro – VIIRS Jun 13 - present
410	66	36
443	-50	-24
488	-46	-36
551	-35	-22
671	-33	-28
Average 443 to 671 nm	-41	-27

South Florida Cruise Feb. – Mar. 2012, 16 Hyperpro and ASD Validation Stations.

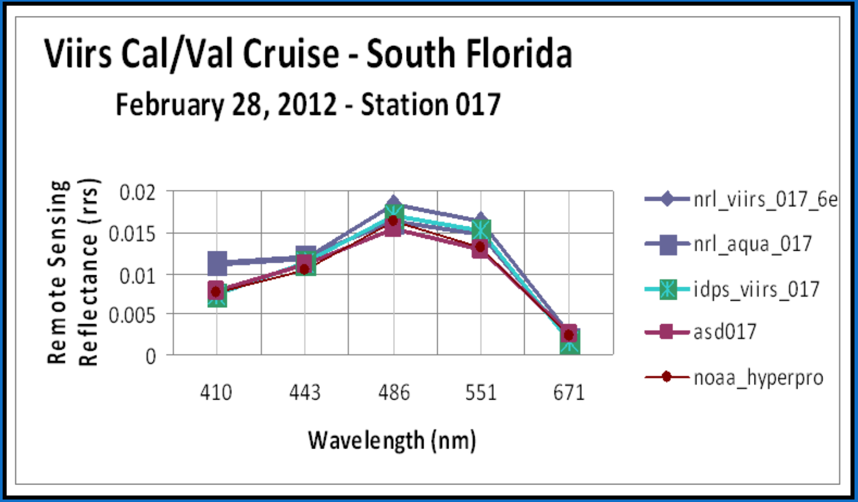

	Hypro vs IDPS		Hypro vs L2GEN		ASD vs L2gen		ASD vs IDPS		ASD vs Aqua		Hyperpro vsAqua	
ch	r2	slope	r2	slope	r2	slope	r2	slope	r2	slope	r2	slope
410	0.8628	0.8752	0.9071	1.0177	0.8414	0.9639	0.8364	0.7994	0.5753	1.2016	0.4575	1.2782
443	0.9848	0.9329	0.9848	0.9058	0.9468	0.9072	0.9766	0.9125	0.9202	0.9692	0.8922	0.9796
488	0.9981	0.9772	0.9964	0.9762	0.9735	1.0503	0.9912	0.9964	0.9888	0.9115	0.9914	0.8727
551	0.9895	0.9603	0.9850	0.9838	0.9635	1.1198	0.9759	1.0767	0.9804	0.9281	0.9779	0.873
671	0.9953	0.7362	0.9959	0.9368	0.8992	1.0056	0.9613	0.7327	0.9712	0.576	0.9792	0.6486

VIIRS validation using in situ Hyperpro measurements off Oahu, Hawaii collected in September, 2012 using NASA and NRL processings. The VIIRS data in the cross plot was processed using NASA data. 21 matchup stations.

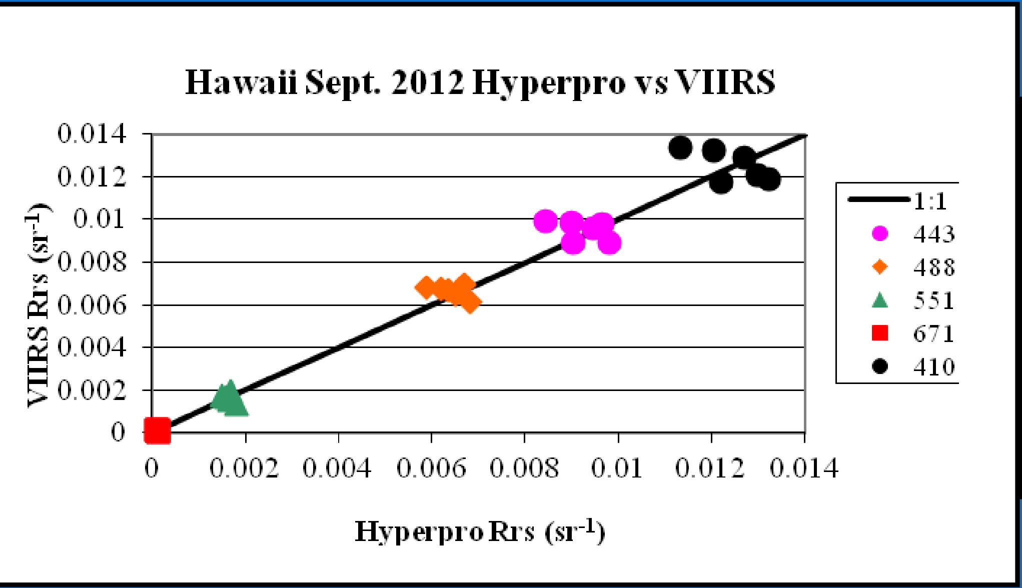

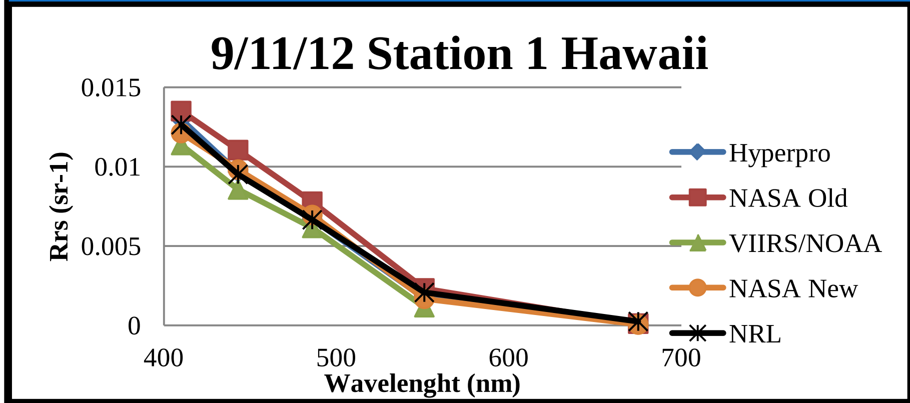

Band	% Diff Hyperpro – NASA	Std Dev of % Diff Hyperpro
410	1.50	3.48
443	3.18	1.05
488	3.93	3.38
551	1.40	36.27
671	-8.81	158.79
Average 410 to 551	2.50	11.05

V2012256235456_chlor_a

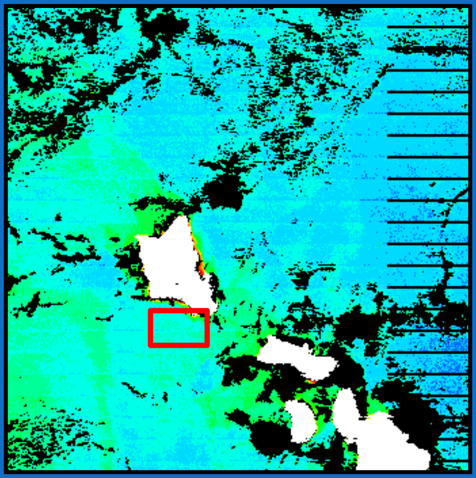

Two week, August 2013 Cruise with CUNY/CREST covering entire Chesapeake Bay. Shown, Day 234, transect up the bay. 42 Stations total

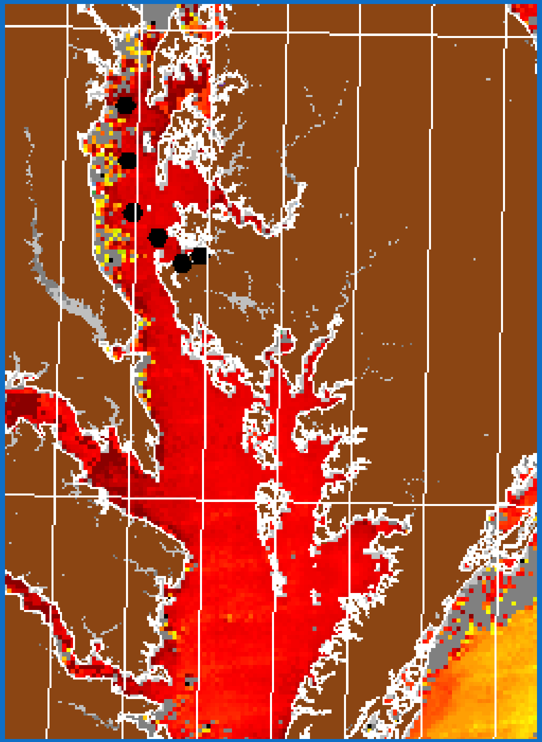

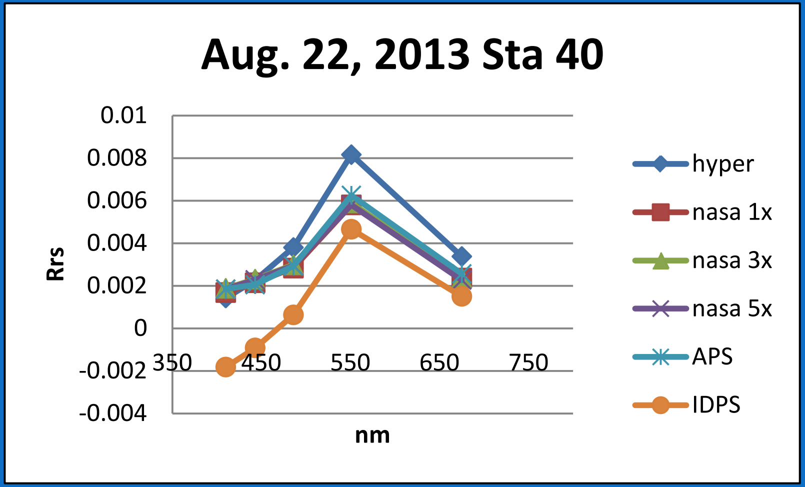

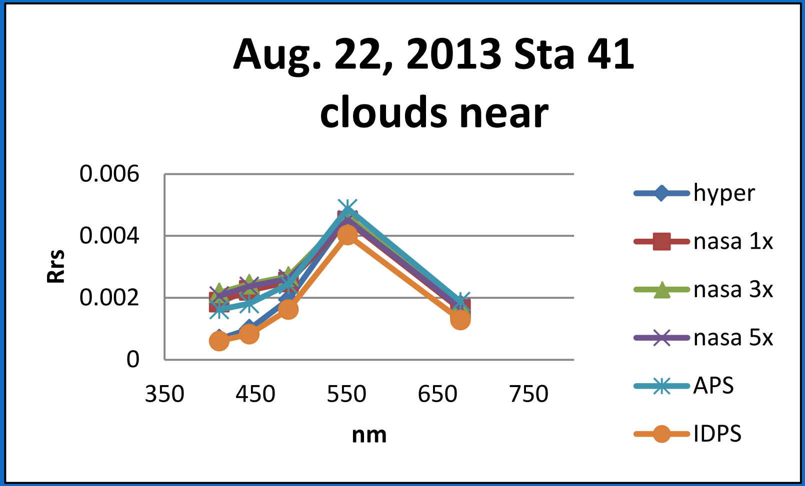

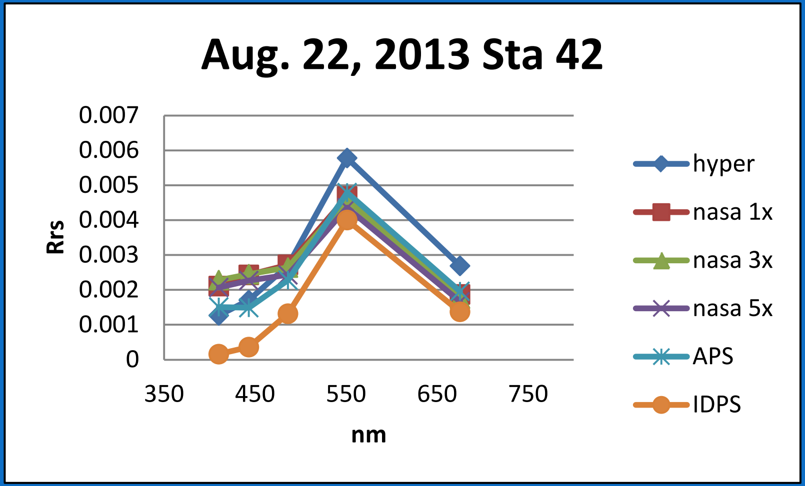

Sept. 2013 Geocape Cruise 112 Stations Rrs Data shown from 9/11, 13, and 14, 2013 and Ecopuc backscatter validations are show in bottom right.

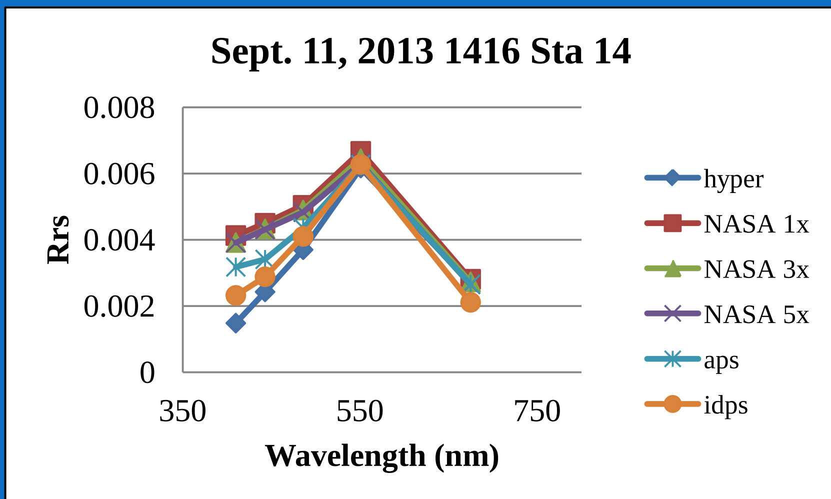

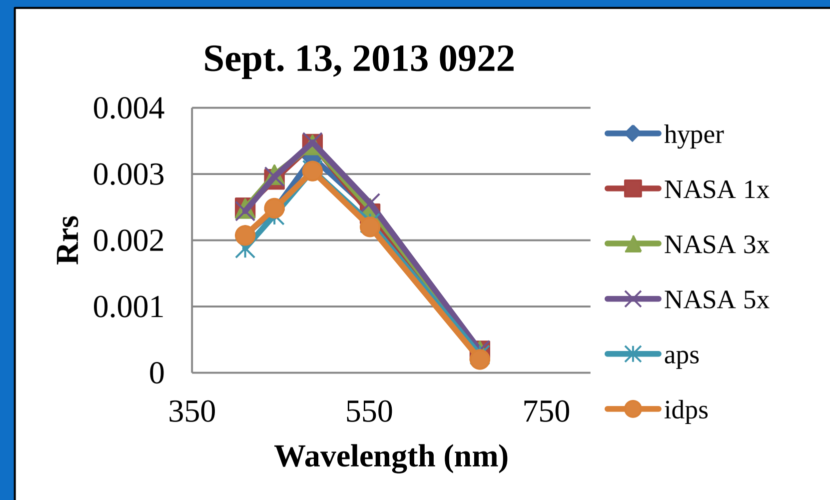

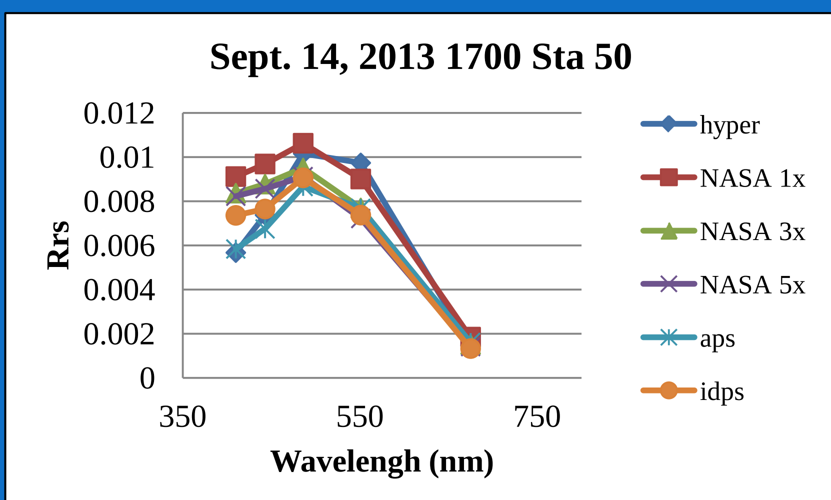

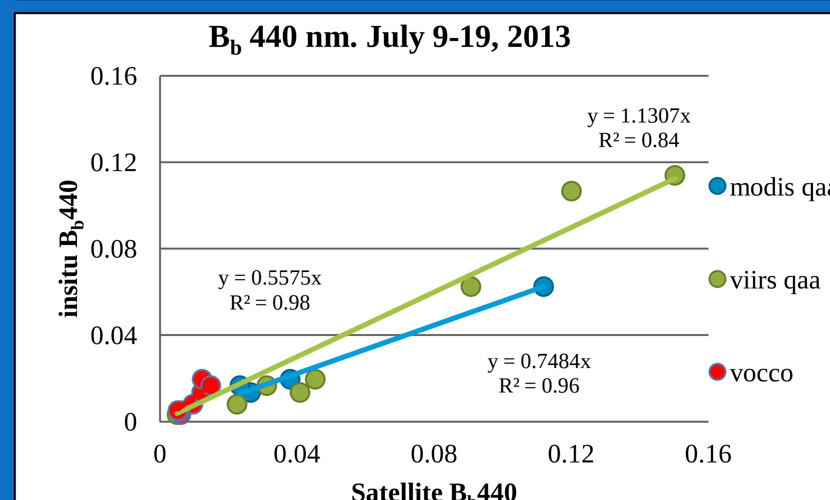

Sept. 25, 2013 VIIRS and *Multiple Altimeter Beam Experimental Lidar* (*MABEL*) Flyover Validations Locations, 5 Stations

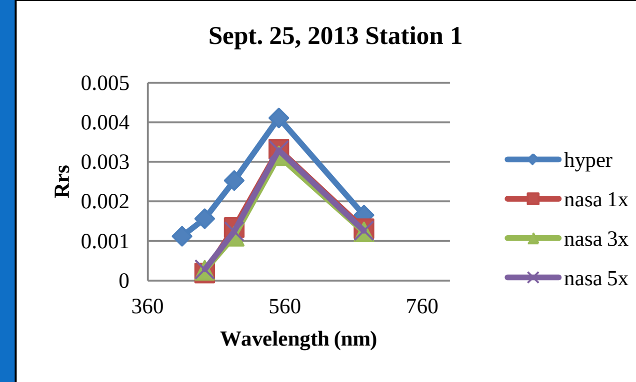

MABEL Track

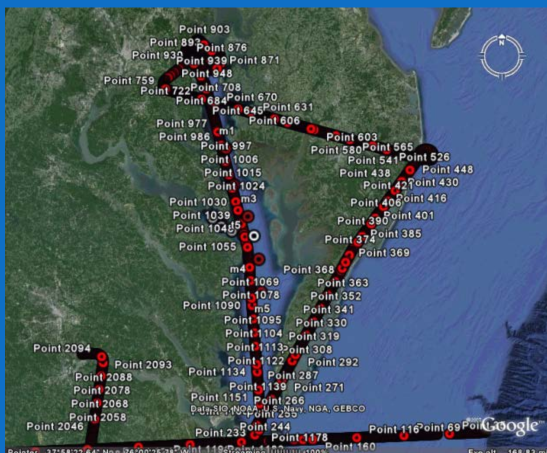

Validation Stations

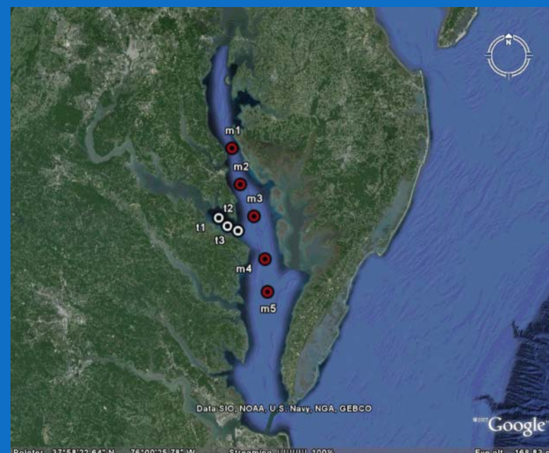

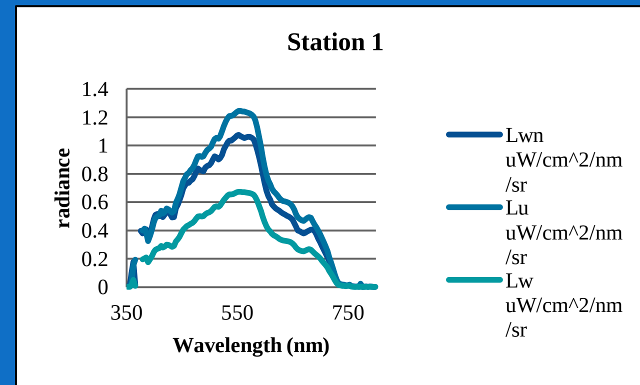

Blue water **VIIRS ocean color validation at MOBY** site in Hawaii. March 2 – 4, 2014: Conducted measurement comparisons between our Hyperpro, MOBY and Dr. Lee's (U. Mass) new skylight blocking radiometer at 12 stations.

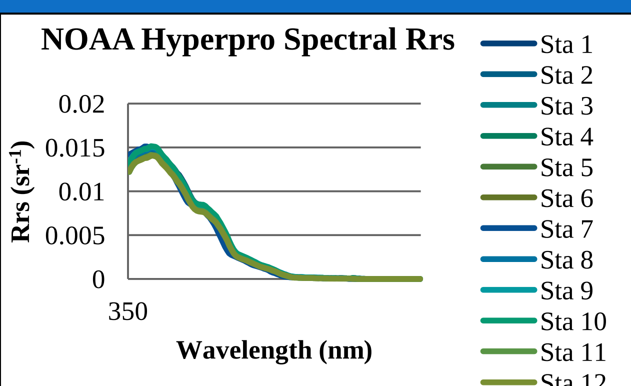

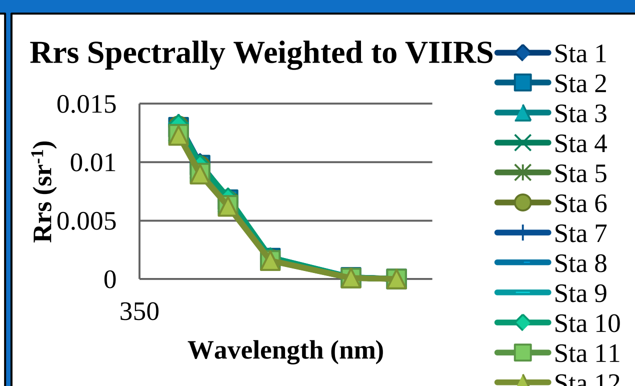

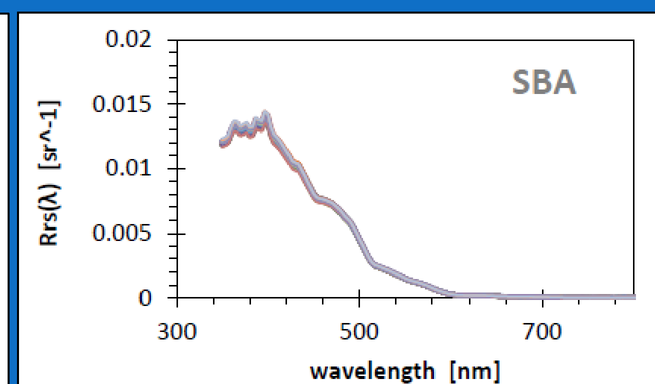

VIIRS/Landsat 8/SBA validation cruise South of Puerto Rico
May 3-5, 2014.   15 Stations

CONCLUSIONS

- With good calibration techniques and careful attention to protocols, Hyperpros can provide accurate traceable validation measurements for ocean color sensors
- Calibrations can be stable for years
- Repeatability and consistency between Hyperpros are very good
- Hyperpros matched MOBY and Boussole well
- Hyperpros compared well to above-water instrument
- Recommend frequent calibrations and inter-calibrations
- Recommend using new multi-cast method and Prosoft Version 8 for collecting and processing data

Effective Band Center Wavelengths for MODIS and VIIRS for Open Ocean Waters

Puneeta Naik[a,b] and **Menghua Wang**[b]

[a]NOAA National Environmental Satellite, Data, and Information Service
Center for Satellite Applications and Research
College Park, MD 20740, USA
[b]CIRA, Colorado State University, Fort Collins, CO 80523, USA

Wednesday, May 14, 2014, College Park, Maryland

Acknowledgements: We thank the MOBY team (IP: Ken Voss) for the MOBY in situ data.

INTRODUCTION

- The in-band and out-of-band responses refer to sensor spectral response contribution from within and outside the spectral bandwidth of the sensor bands, while total-band refers to the contribution from in-band as well as out-of-band regions.

- Most ocean color satellite sensors in addition to an in-band contribution, have a significant contribution from out-of-band region. Although the out-of-band effects can be small, it is not uniform over all bands hence can cause biases in derived biogeochemical variables.

- The out-of-band contributions for Sea-viewing Wide Field-of-view Sensor (SeaWiFS) and Moderate Resolution Imaging Spectroradiometer (MODIS) are relatively well characterized as compared to Visible Infrared Imaging Radiometer Suite (VIIRS).

OBJECTIVES

- Analyze the sensor out-of-band effects for MODIS and VIIRS.
- Determine the effective spectral band center wavelengths for MODIS and VIIRS.

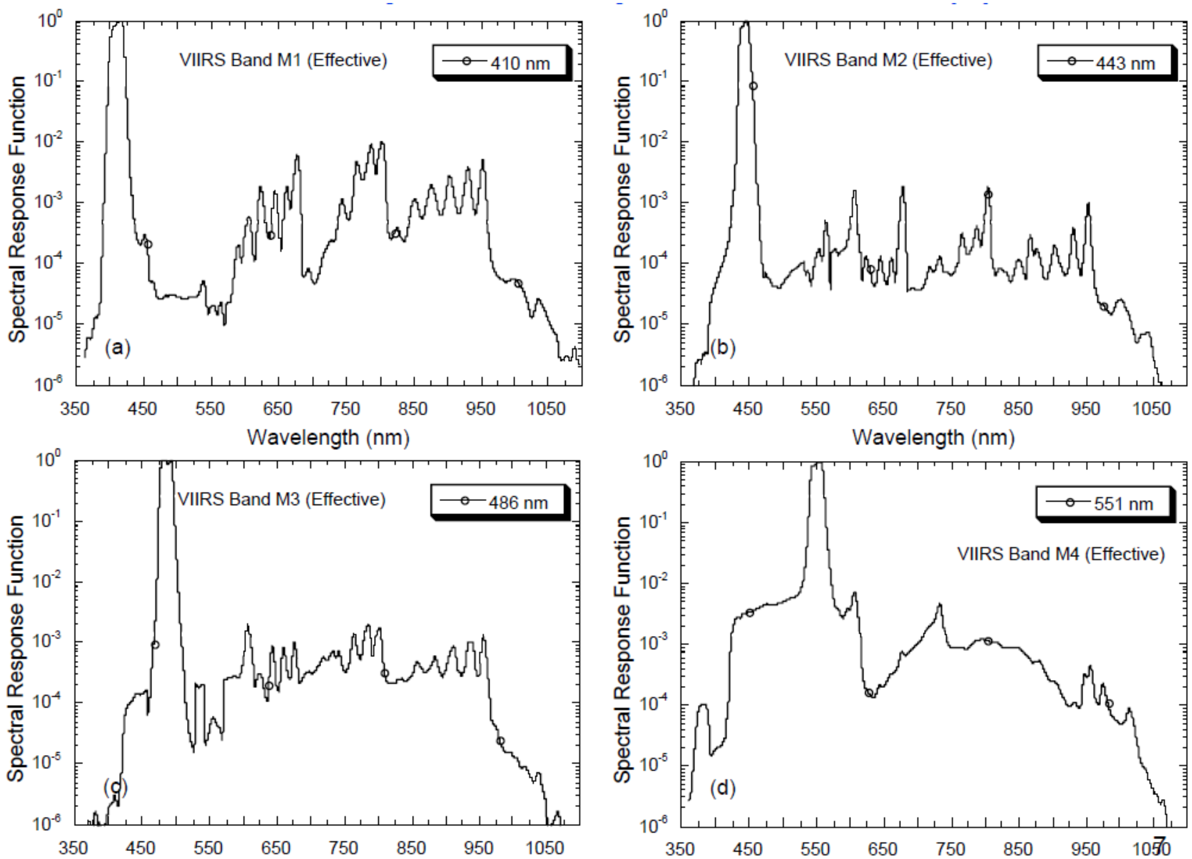

VIIRS Spectral Response Function

http://cioss.coas.oregonstate.edu/CIOSS/workshops/VIIRS_CalVal_Mar_10/VIIRS_Presentations/Wang_Algorithm_Evaluation.pdf

METHODS AND DATA

➢ Convolving normalized water leaving radiance ($nL_w(\lambda)$) with respect to satellite sensor spectral response functions:

Total-band

$$nL_w^{(Total)}(\lambda) = \frac{\int_{\mathrm{All}} nL_w(\lambda) RSR(\lambda)\, d\lambda}{\int_{\mathrm{All}} RSR(\lambda)\, d\lambda}$$

In-band

$$nL_w^{(In\text{-}Band)}(\lambda) = \frac{\int_{\pm 1\%} nL_w(\lambda) RSR(\lambda)\, d\lambda}{\int_{\pm 1\%} RSR(\lambda)\, d\lambda}$$

$RSR(\lambda)$ --- Sensor spectral response function

Sensor Out-of-Band Effects:

$$OOB(\%) = \left(\frac{nL_w^{(Total)}(\lambda)}{nL_w^{(In\text{-}Band)}(\lambda)} - 1 \right) \times 100$$

METHODS AND DATA

- In situ data:

  Marine Optical Buoy (MOBY)
  (http://coastwatch.noaa.gov/moby/)

- MOBY is deployed in clear oligotrophic oceanic waters (chlorophyll-a is in the range of ~0.01–0.1 mg m^{-3}).

- Hyperspectral *nLw(λ)* data from MOBY covers wavelengths range from ~ 340 nm to 750 nm.

- The hyperspectral resolution of *nLw(λ)* from clear oceanic waters makes MOBY an optimum platform to analyze sensor out-of-band effects.

http://moby.mlml.calstate.edu/

RESULTS

Total-band and In-band comparisons for **MODIS**

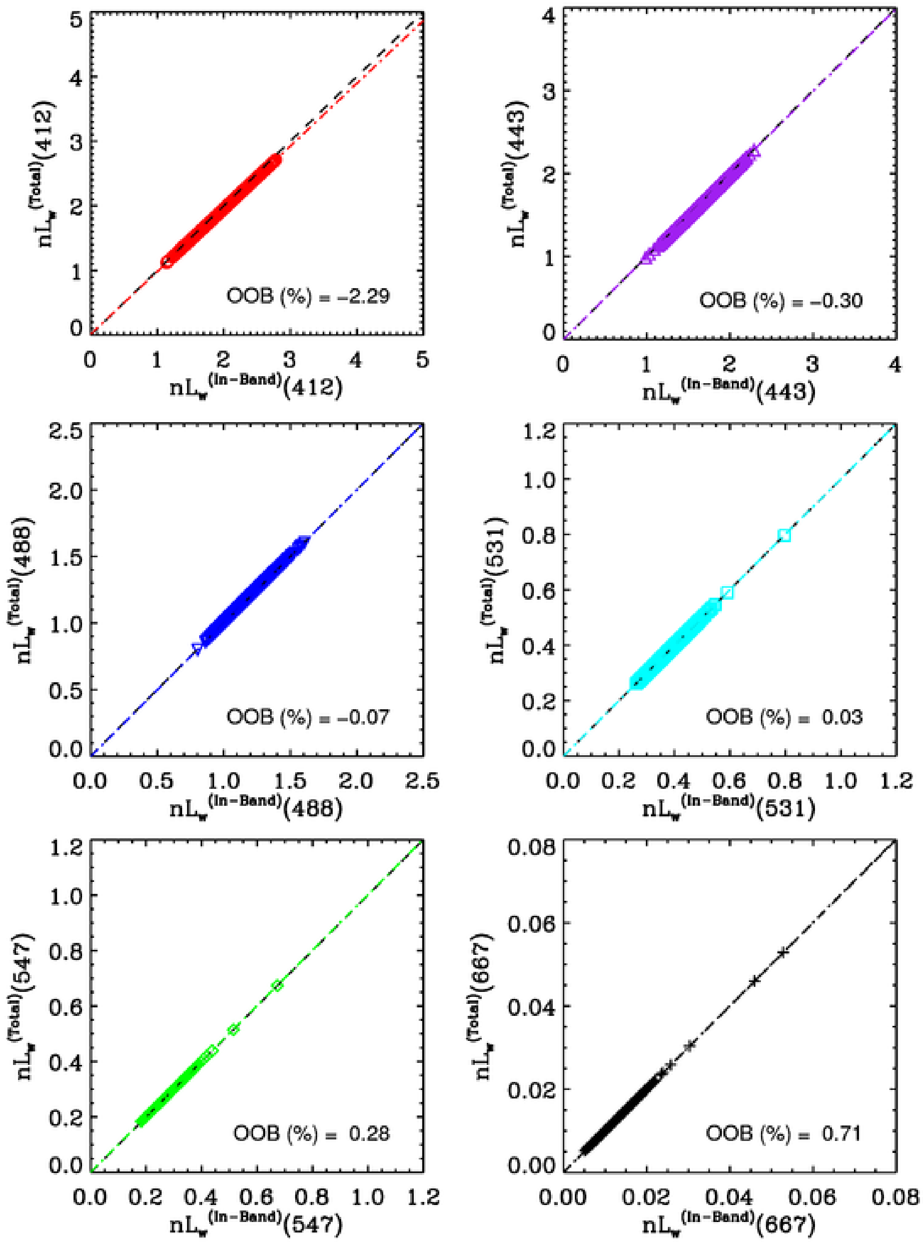

RESULTS

Total-band and In-band comparisons for **VIIRS**

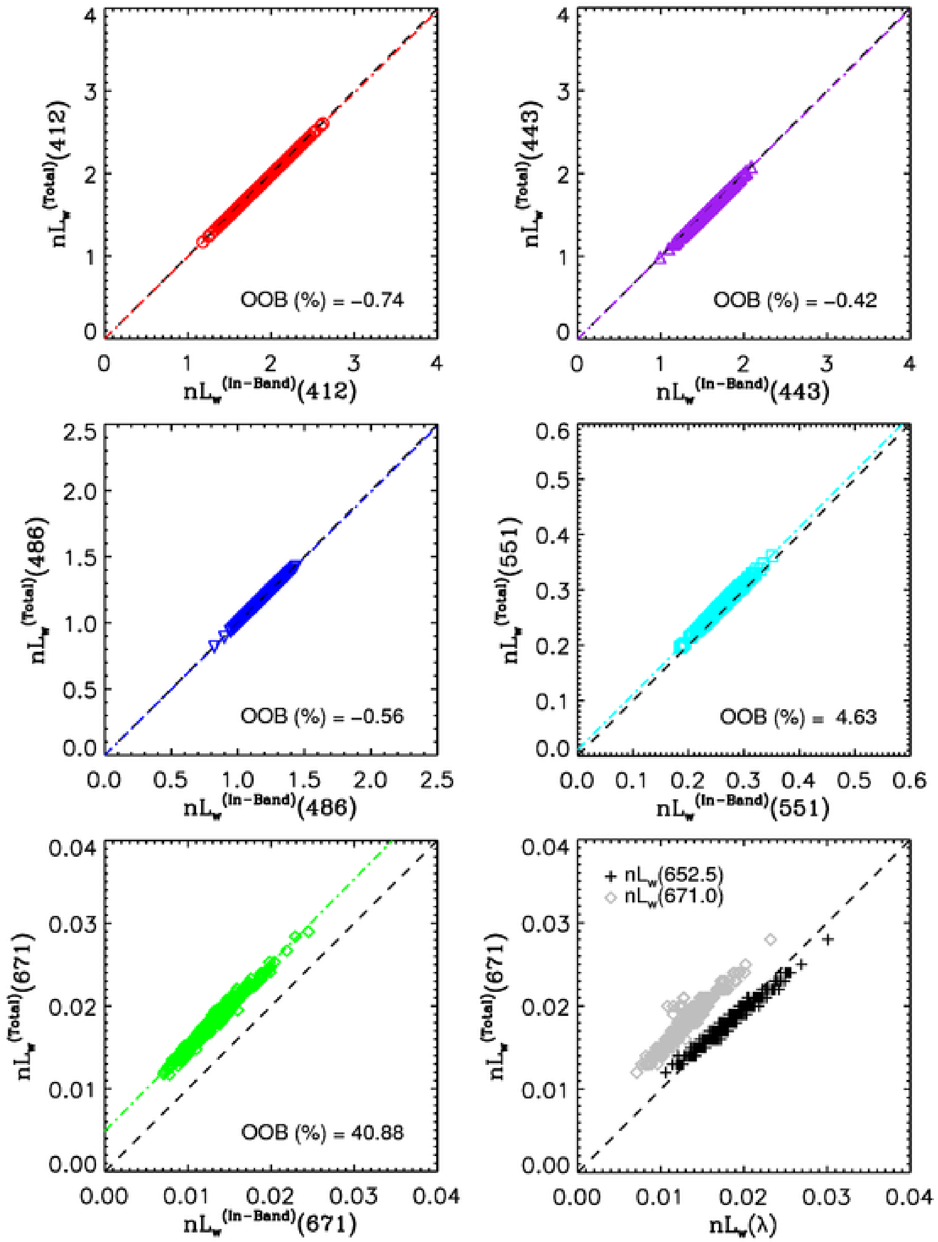

RESULTS

VIIRS Spectral Response function – band M5 (671 nm)

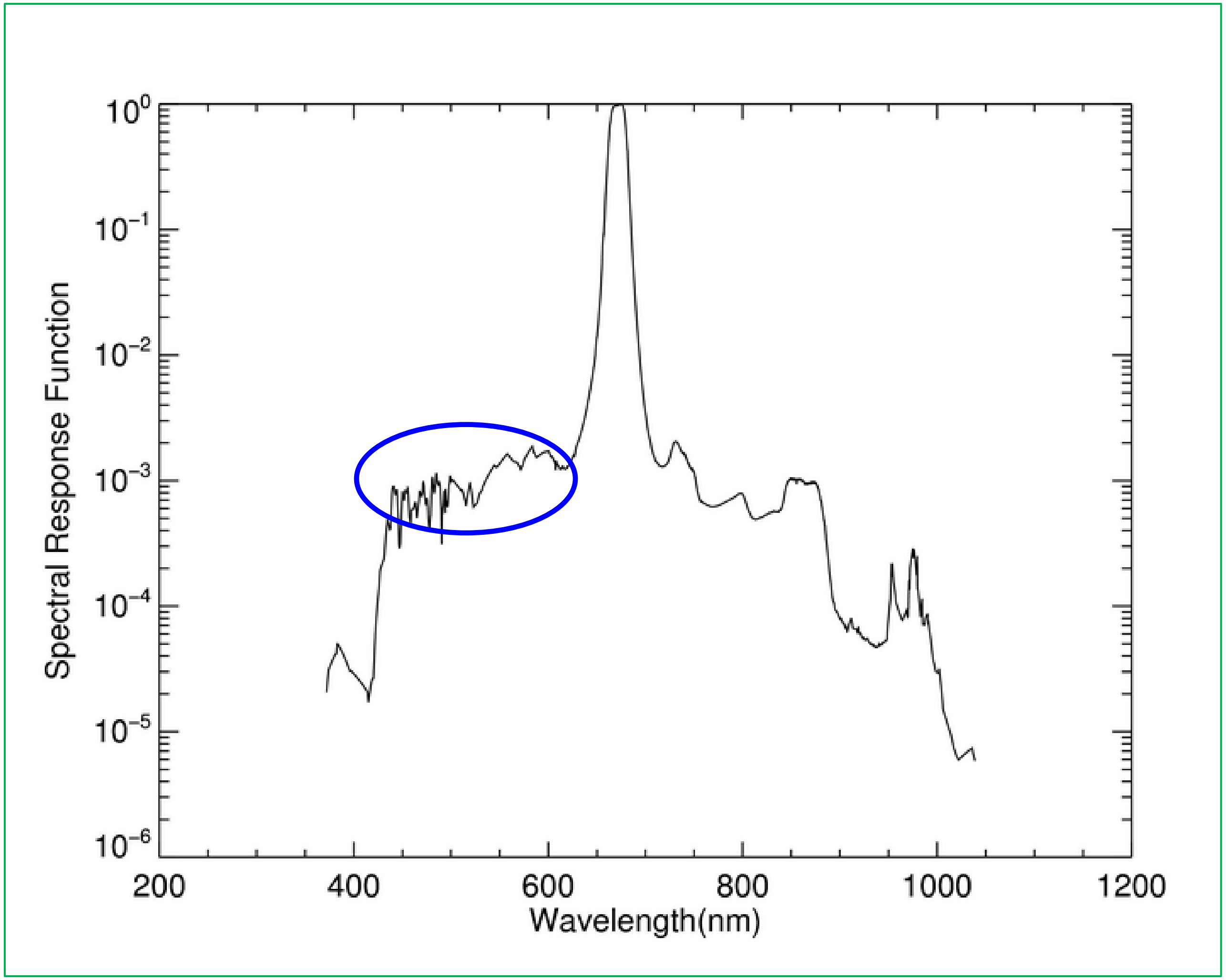

Large Leakage of light from blue region of the spectrum.

RESULTS

Effective band center wavelengths for **MODIS**

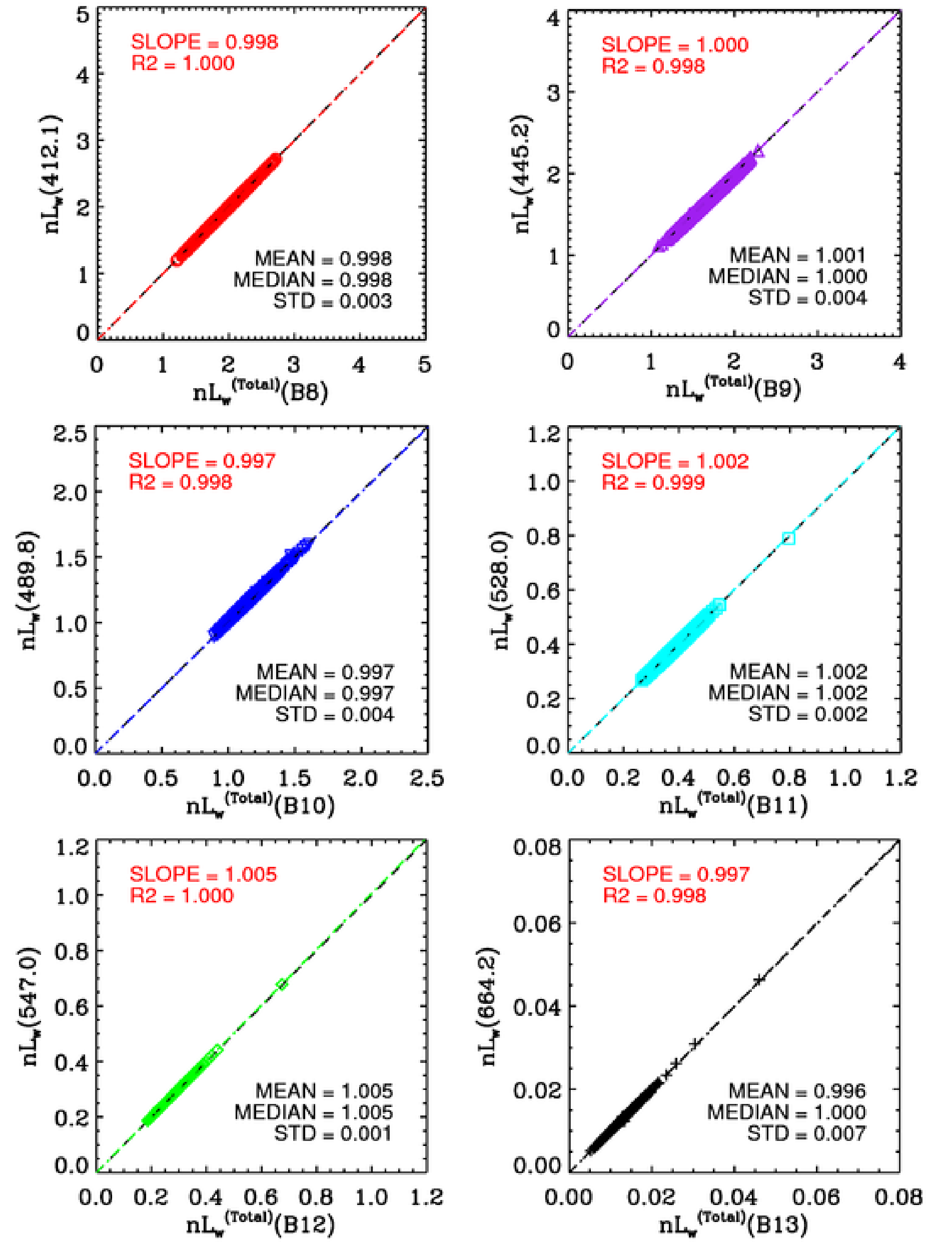

RESULTS

Effective band center wavelengths for **VIIRS**

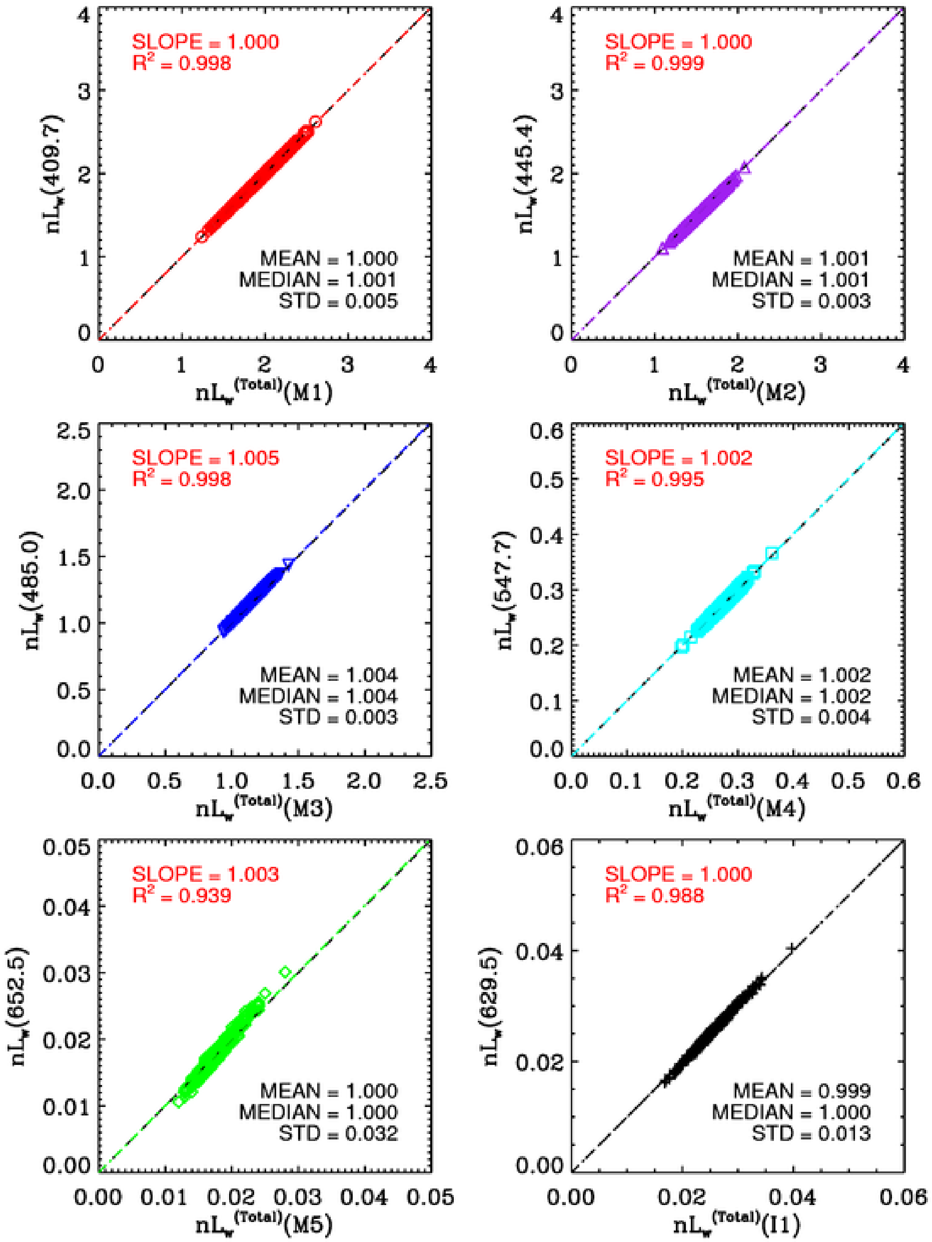

RESULTS

Nominal and effective center wavelengths for MODIS and VIIRS

MODIS			VIIRS		
Nominal Center Wavelength (nm)	nL_w**(nominal)/** nL_w**(Total)**	**Effective Center Wavelength** (nm)	**Nominal Center Wavelength** (nm)	nL_w**(nominal)/** nL_w**(Total)**	**Effective Center Wavelength** (nm)
412 (B8)	0.994	412.1	410 (M1)	1.022	409.7
443 (B9)	1.034	445.0	443 (M2)	0.959	445.4
488 (B10)	0.977	489.8	486 (M3)	1.072	485.0
531 (B11)	1.012	528.0	551 (M4)	1.078	547.7
551 (B12)	1.005	547.0	671 (M5)	1.399	652.5
667 (B13)	0.977	664.2	635 (I1)	1.070	629.5

The effect of the out-of-band response on the derived $nL_w(\lambda)$ at nominal center wavelengths can be evaluated by taking a ratio of the radiance at nominal center wavelength to total-band averaged radiances, i.e., $nL_w(\lambda) / nL_w^{(Total)}(\lambda)$

CONCLUSIONS

- For the MOBY site (open oceans) the out-of-band contribution for MODIS is less than ~3% for the bands we have analyzed. While, for VIIRS, the out-of-band contribution is less than ~5% except for band M5 (671 nm).
- The high out-of-band contribution at the band M5 of VIIRS is due to a large leakage (out-of-band spectral distribution) from the blue region of the spectrum.
- In general, the out-of-band response is greater for VIIRS relative to MODIS, except at the blue band.
- The effective band center wavelengths are within ±6 nm of the nominal center wavelengths for both MODIS and VIIRS, except for the VIIRS M5 band.
- It is noted that the effective band center wavelengths represent the center band wavelengths of MODIS and VIIRS-measured $nL_w(\lambda)$ for open ocean waters.

THANK YOU